USC
UNIVERSIDADE DE SANTIAGO DE COMPOSTELA

ESCUELA DE DOCTORADO
INTERNACIONAL DE LA USC

Ana
Castro Balado

Tesis doctoral

# Pharmaceutical compounding and drug repositioning from hospital pharmacy in situations of therapeutic gap

Santiago de Compostela, 2023

Programa de doctorado en Investigación y Desarrollo de Medicamentos

USC
UNIVERSIDADE
DE SANTIAGO
DE COMPOSTELA

TESE DE DOUTORAMENTO

# PHARMACEUTICAL COMPOUNDING AND DRUG REPOSITIONING FROM HOSPITAL PHARMACY IN SITUATIONS OF THERAPEUTIC GAP

Ana Castro Balado

**ESCUELA DE DOCTORADO INTERNACIONAL DE
LA UNIVERSIDAD DE SANTIAGO DE COMPOSTELA**

**PROGRAMA DE DOUTORAMENTO EN
INVESTIGACIÓN E DESENVOLVEMENTO DE MEDICAMENTOS**

SANTIAGO DE COMPOSTELA
2023

USC
UNIVERSIDADE
DE SANTIAGO
DE COMPOSTELA

# DECLARACIÓN DO AUTOR DA TESE

## Pharmaceutical compounding and drug repositioning from hospital pharmacy in situations of therapeutic gap

D.ª Ana Castro Balado,

Presento a miña tese seguindo o procedemento axeitado ao Regulamento e declaro que:

1) A miña tese abarca os resultados da elaboración do meu traballo.
2) De selo caso, na tese faise referencia ás colaboracións que tivo este traballo.
3) A tese é a versión definitiva presentada para a súa defensa e coincide coa versión enviada en formato electrónico.
4) Confirmo que a tese non incorre en ningún tipo de plaxio doutros autores nin de traballos presentados por min para a obtención doutros títulos.

En Santiago de Compostela, a 17 de Febreiro de 2023

Asdo. Ana Castro Balado

USC
UNIVERSIDADE
DE SANTIAGO
DE COMPOSTELA

# AUTORIZACIÓN DOS DIRECTORES

## Pharmaceutical compounding and drug repositioning from hospital pharmacy in situations of therapeutic gap

D. Francisco Javier Otero Espinar

D. Anxo Fernández Ferreiro

D. Miguel González Barcia

INFORMAN:

Que a presente tese, se corresponde co traballo realizado por D.ª Ana Castro Balado, baixo a nosa dirección/titorización, e autorizamos a súa presentación considerando que reúne os requisitos esixidos no Regulamento de Estudos de Doutoramento da USC, e que como directores desta non incorre nas causas de abstención establecidas na Lei 40/2015.

De acordo co indicado no Regulamento de Estudos de Doutoramento, declaran tamén que a presente tese de doutoramento é idónea para ser defendida en base á modalidade de Monográfica con reprodución de publicacións, nos que a participación do doutorando foi decisiva para a súa elaboración e as publicacións se axustan ao Plan de Investigación.

En Santiago de Compostela, a 17 de Febreiro de 2023

Asdo. Francisco J. Otero Espinar

Asdo. Anxo Fernández Ferreiro

Asdo. Miguel González Barcia

USC
UNIVERSIDADE
DE SANTIAGO
DE COMPOSTELA

# AGRADECIMIENTOS

USC
UNIVERSIDADE
DE SANTIAGO
DE COMPOSTELA

USC
UNIVERSIDADE
DE SANTIAGO
DE COMPOSTELA

# AGRADECIMIENTOS

A lo largo de esta Tesis, muchas personas me han ofrecido su ayuda y apoyo inestimables, tanto de forma directa como indirecta. Gracias a ellos el camino ha resultado mucho más fácil y, sin ellos, nunca haría llegado hasta el final. A través de estas líneas quiero expresarles mi más sincera gratitud.

En primer lugar, quería agradecer a mis tres directores de Tesis, Fran, Anxo y Miguel, los primeros en animarme, confiar en mí y guiarme durante todo el camino.

A **Fran**, por tu dedicación, empeño y apoyo. Gracias por tu amabilidad y empatía, por estar siempre disponible y con una sonrisa, por ayudarme a mejorar y por todos los consejos y enseñanzas que me has transmitido durante todos estos años.

A **Miguel**, por animarme a adentrarme en la investigación desde siempre. Por tu interés constante, templanza ante las adversidades y por todas tus sabias ideas. Sin tus conocimientos esta tesis nunca habría llegado a término. Gracias por aconsejarme, guiarme y apoyarme desde entré en la farmacia.

A **Anxo**, por la pasión, optimismo y entusiasmo desbordantes que contagias. Por empujarme y convencerme a seguir tus ideas locas, animarme y enseñarme cómo llevarlas a cabo. Por apoyarme cuando la confianza flaqueaba, por saber llevarme en los momentos de crisis y por celebrar los éxitos conmigo. Gracias por creer en mí y por todas las oportunidades que me has brindado desde entonces.

Gracias a **Irene Zarra**, por tu dedicación, confianza, apoyo para la realización de este trabajo y por permitirme crecer como investigadora y como farmacéutica hospitalaria durante estos años.

A todos los integrantes del **servicio farmacia**. Atravesar sus puertas en mi primer día de prácticas me cambió la vida y fascinó a partes iguales. Gracias por todas las horas, días, guardias, meriendas, alegrías y celebraciones. **Técnicos**, **auxiliares** y **personal de enfermería**, con vosotros el camino se ha hecho infinitamente más llevadero. Gracias en especial a Magda, Vero y Soraya, por cuidarme tan bien.

También quería darles las gracias en particular a mis compañeros farmacéuticos, y más concretamente a aquellos que pasaron a ser amigos, **Teresa**, **Chema**, **Roi**,

USC UNIVERSIDADE DE SANTIAGO DE COMPOSTELA

**Helena**, **Teshita**, **Ana H.**, **Pedro**, **Alba L.** y **Alba M.** A mis compañeros de residencia **Sara**, **Iria**, **Manuel B.**, **Fran**, **María** y **Álvaro**, no pude haber tenido más suerte con vosotros. A **Manolito**, por tu fantástico humor y las risas infinitas compartidas, y a **Bea**, por haber sido y ser desde el primer día y siempre una inspiración. Gracias a los dos por ser un hogar para mí y mi familia en momentos hostiles. A **Jaime**, por escucharme y comprenderme sin necesidad de muchas palabras, y por guiarme desde que te conozco. Sin tu apoyo incondicional no me hubiera atrevido a dar los pasos más importantes de mi vida profesional.

Gracias también a mis compañeros de la Unidad de Investigación e Innovación del servicio de farmacia, **Kiko, Jesús y Lorena**, por todos vuestros consejos. Al festival de bromas del Laboratorio 8, **Gonzalo** y **Andrea**, gracias por las horas de esfuerzo invertidas juntos, peleas con la cisteamina, cafés, risas y todo el apoyo y cariño que me habéis dado en momentos complicados. A **Cristina**, por acogerme en el mundo de la investigación con calidez y una enorme sonrisa, aconsejarme, orientarme y apoyarme, tanto a nivel profesional pero, sobre todo, personal. Gracias a **Kike**, por haber peleado juntos en muchas batallas (aunque enfrentados en aquellas que fueron culinarias), por soportar mis taras, celebrar mis logros y empujarme todas las veces que no confié en mí. A **Laura**, por haber hecho de madre, de hermana y hasta de mí misma. Gracias por los viajes, los planes, las risas, la complicidad y por cuidarme siempre. Gran parte de esta tesis es tuya.

A mis doctoras de confianza, **Lucía Barrera** y **Cris Pou**, por las confidencias y desdichas compartidas durante la residencia. Siempre acabarán ganando los buenos momentos.

Gracias a **Raquel**, por acompañarnos en el camino desde que tenemos uso de razón. A **Laura**, por haber compartido más de media vida juntas, gracias por estar y acogerme siempre como una hermana. A **Tatiana**, mi compañera de pupitre, por confiar en mí, animarme, apoyarme y aguantarme cuando ni yo me soportaba. A **Cris A. Asteinza**, por empezar juntas esta andadura de la Farmacia, y por los ánimos que siempre me has dado en cada una de sus fases.

Pero sobre todo,

A **mi familia**, por animarme, alentarme y, principalmente, aguantarme durante todo el camino, que no es cosa fácil. Gracias por estar siempre pendientes, por cuidarme, comprenderme y apoyarme en todo lo que me he ido proponiendo en estos años. Gracias a mi **hermana**, a mi **abuela**, a **Titú** y **Keco** y, en especial, gracias a **mis padres, Miguel** y **Rosa**. Por habérmelo dado todo, por compartir mis alegrías, sobrellevar mis angustias, y por tener una paciencia infinita conmigo como sólo vosotros sabríais tener. Esta tesis es vuestra.

USC
UNIVERSIDADE DE SANTIAGO DE COMPOSTELA

# SUMMARY

USC
UNIVERSIDADE
DE SANTIAGO
DE COMPOSTELA

USC
UNIVERSIDADE
DE SANTIAGO
DE COMPOSTELA

# SUMMARY

The **pharmaceutical compounding sections** of hospital pharmacy departments are responsible for the elaboration of compounded formulations adapted to the needs and characteristics of patients, being one of the areas with the greatest workload and constituting one of the classic, fundamental, and inherent pillars of hospital pharmacy. Despite this, it is still an area where insufficient resources are allocated to allow its adequate modernization and adaptation to current healthcare demands. To achieve this objective, it is necessary to make a definite commitment to research in the field of pharmaceutical compounding since, to date, drug development is not a priority line of research among those usually addressed by hospital pharmacy.

This commitment to **research** in each of the areas covered by hospital pharmacy is vital to achieve advances that will make it possible to accomplish excellence in health care. One of the possible strategies to pursue for galenic research is to become a key tool to boost innovation in the development and characterization of new compounded formulations to cover the existing therapeutic gaps. There are several scenarios in daily clinical practice in which there are no therapeutic options, or they are not available for the treatment of certain pathologies. These circumstances arise in the case of rare diseases, that do not have marketed drugs or they are sometimes difficult for patients to access; and in emerging diseases, such as the outbreak of the SARS-CoV-2 pandemic, for which there were no previous effective treatments.

**Rare diseases** affect fewer than 5 people per 10,000 inhabitants. Due to their low prevalence, there are considerable knowledge gaps concerning their etiology, diagnostic methods, management, and treatment. For this reason, diagnosis is often delayed or never made, making it difficult to adopt preventive or therapeutic measures. In addition, research in this field is scarce and is usually very dispersed among different working groups, to which must be added the limited interest of the industry in investing in the development of drugs for the treatment of these diseases due to their low profitability and high cost of research and marketing. Also, commercial orphan drugs, intended to treat rare diseases, are often not available in most countries due to the mandatory evaluation and authorization procedures. One clarifying example of rare disease in which these circumstances occur is the case of cystinosis.



USC UNIVERSIDADE DE SANTIAGO DE COMPOSTELA

**Cystinosis** is a lysosomal disorder in which there is an accumulation of crystals of the amino acid cystine inside the lysosomes, causing detrimental effects in various tissues such as the kidney, pancreas, and cornea, among others. Currently the only approved treatment is cysteamine, which is available as an orphan drug in oral form in many countries. Because the eye has a complex anatomical structure, the ophthalmic bioavailability of oral cysteamine is insufficient to produce the desired effect. Although its topical ophthalmic instillation is the treatment of choice in ocular cystinosis to prevent the occurrence of photophobia, corneal erosions, keratopathies, visual impairment and finally blindness, commercial ophthalmic presentations of cysteamine are not always available, so its preparation as a **compounded formulation** by pharmacy departments is a therapeutic alternative for those patients who do not have access to the treatment.

On the other hand, the violent outbreak of **SARS-CoV-2 infection** hit the world in the early 2020s, causing a pandemic with devastating consequences. Since then, major efforts have been made in various fields to deal with the spread of the infection and to prevent the progression of the already established disease. To this end, the scientific community began research against the clock in order to offer effective vaccines and treatments. After three years of pandemic, the optimal therapeutic approach for COVID-19 is still in the process of being positioned with the evidence that are still being generated. To date, and based on its pathogenesis, therapeutic strategies in the early stages of infection have been directed **against the virus** using antivirals, passive immunity, and interferons, while **modulation of the immune response** has been shown to be more effective in advanced stages of the disease. One of the strategies implemented to offer treatment alternatives quickly and safely has been **drug repositioning**, which consists of identifying new therapeutic indications for approved drugs. This approach is faster and more cost-effective than *de novo* drug discovery, since pharmacokinetic, toxicological and safety data are already available. This has facilitated the approval by regulatory agencies such as the US Food and Drug Administration (FDA) or the European Medicines Agency (EMA) of the indication for SARS-CoV-2 treatment for some of the drugs that make up the therapeutic arsenal against COVID-19.

Molecular characterization of SARS-CoV and MERS-CoV suggested, in early days of the pandemic that SARS-CoV-2 is susceptible to **antiseptics** such as ethanol, as it has demonstrated activity against enveloped viruses. Because viral replication in the early stages of infection takes place in the upper respiratory tract, administration of **ethanol** early at the disease onset could reduce viremia and prevent progression to more severe stages. Ethanol had previously been used as a compounded formulation in hospital pharmacy departments for other indications, but its application as an inhaled antiseptic had not been studied before.



USC UNIVERSIDADE DE SANTIAGO DE COMPOSTELA

In both situations, cystinosis and COVID-19 infection, **research from hospital pharmacy** in the field of drug development could be positioned as an opportunity to offer therapeutic alternatives such as an ophthalmic compounded formulation of cysteamine for the treatment of ocular cystinosis and a compounded formulation of inhaled ethanol against COVID-19 infection in early stages of the disease. The transversal position of hospital pharmacy, the mastery of pharmacology and drug development, together with the use of strategies such as drug repositioning would favor the adequate translation of the results to clinical practice. For this, it is necessary to correctly develop and thoroughly characterize formulations through chemical, physical, microbiological, and pharmacokinetic stability studies, as well as to evaluate their efficacy and safety.

**Chapter 1** includes a review that aims to give an overview of recent developments in the field of molecular imaging in relation to preclinical studies of ocular biodistribution. The aim of this work is to find the best imaging tool that can be applicable and transferable to the ophthalmic developments that will be studied later in this Doctoral Thesis. These techniques provide pharmacokinetic data in a non-invasive manner and in real time, without the need to sacrifice animals, saving costs and avoiding the redistribution of the compound by dissection methods. There is no perfect modality that presents at the same time high sensitivity, specificity, temporal and spatial resolution; however, biological procedures can be studied successfully when the information provided by some of them is combined. Through this kind of studies, it is possible to improve the biopermanence of ophthalmic drugs at their site of action and thus optimize their dosage.

Initially, positron emission tomography (PET) and single photon emission computed tomography (SPECT) techniques, used in topical ocular biodistribution studies of radiolabeled drugs and vehicles, as well as in intraocular administration studies, are described. Both provide a quantifiable signal of the pharmacokinetic profile of the administered radiopharmaceutical, so that it is possible to obtain a signal in the eye after instillation, with subsequent signal detection in the nasolacrimal duct and nasal cavity. They are highly sensitive and are usually combined with morphological techniques such as computed tomography (CT) and magnetic resonance imaging (MRI), which allow adequate anatomical localization of the radioactive signal. PET and SPECT disadvantages are their low resolution and the possible alteration that radiolabeling can produce in the properties of small molecules, although those of larger molecular size are not affected. Other techniques such as fluorescence are successfully used in the pharmacokinetic study of macromolecules. On the other hand, an excellent resolution is provided by MRI. Finally, further technologies that have been less explored in the field of research up to the present time, such as ultrasonography and optical coherence tomography, are described.



USC UNIVERSIDADE DE SANTIAGO DE COMPOSTELA

**Chapter 2** comprises a review of the most recent research in ocular cystinosis. First, an overview of the epidemiology, pathogenesis, treatment, and evolution of the commercial presentations of cysteamine as orphan drugs approved in recent years by the FDA and the EMA is presented. In turn, reference is also made to the difficulties encountered by patients diagnosed with cystinosis in accessing this type of treatment, and the reasons why the development of new formulations for topical ophthalmic administration is necessary. Then, up-to-date advances in cysteamine ocular delivery systems to provide greater ocular bioavailability and to avoid cumbersome dosing are described and analyzed. Within these delivery systems, the latest advances and advantages of cysteamine-loaded hydrogels, nanowafers and contact lenses are described.

Subsequently, cysteamine structure and chemical characteristics are outlined. Cysteamine is an extreme instable molecule that transforms by rapid oxidation to cystamine, which is ineffective in the treatment of cystinosis. This reaction is favored by the presence of light and temperature, this being one of the main drawbacks when developing new ophthalmic formulations. In addition, several techniques are described to avoid cysteamine oxidation and increase its stability. Another challenge related to the development of formulations with cysteamine is its detection and quantification together with cystamine. For this reason, multiple methods for its determination, such as high-performance liquid chromatography (HPLC), enzymatic assays, gas chromatography or electrochemical detection, are also described in the literature even though none of them can be considered a gold standard.

Finally, the review focuses on new lines of research for the treatment of cystinosis, such as the use of genetically modified hematopoietic stem cells isolated from cystinosis patients. Other therapeutic approaches were the use of microvesicles with functional cystinosin and the combined therapy of cysteamine with everolimus, as demonstrated by the study of human induced pluripotent stem cell (iPSC) and renal organoid models of cystinosis. Additionally, reference is made to new discoveries related to the pathogenesis of the disease, such as the hypothesis on the role that cystinosin could have as a component of the mTORC1 pathway, as well as transporting cystine out of the lysosome. This section also critically discusses the results reported so far from clinical trials with cysteamine, allowing us to establish and structure an experimental phase to respond to the gaps found in this field.

**Chapter 3** is based on the development and characterization of a topical ophthalmic compounded formulation of cysteamine prepared with hyaluronic acid and packaged in innovative single-dose systems for the treatment of ocular cystinosis. Commercial presentations of ophthalmic cysteamine are orphan drugs that are not always available in all countries, so hospital pharmacies could play an essential role



USC UNIVERSIDADE DE SANTIAGO DE COMPOSTELA

in offering treatment alternatives. Cysteamine is a highly oxidizable compound, so we have sought to increase its stability by packaging it in single-dose systems that would allow them to be kept in the refrigerator/freezer for a long period of time, and the use of one container per day for later disposal. Additionally, to increase the ocular residence time, the formulation was prepared using a commercial presentation of hyaluronic acid (Aquoral®) as a vehicle.

The effect of two different storage temperatures (refrigerator and freezer) and the presence/absence of nitrogen on the physicochemical stability of the formulation and its packaging was studied until the optimum storage conditions were found. The results showed that the 0.55% cysteamine formulation is stable for 30 days when stored at -20 °C with concentrations around 98% of active ingredient, although it does not exceed 7 days of chemical stability when stored at 2-8 °C, with active ingredient concentrations close to 88%. The presence of nitrogen did not provide differences in the oxidation of cysteamine. In addition, opening the vials every 4 h at room temperature after 30 days of freezing maintained the cysteamine concentration for up to 16 h, allowing the use of a single-dose container daily, except for sleeping hours. The pH and osmolarity values were within the ranges required for ophthalmic administration, and no microbial growth was detected.

The viscosity provided by hyaluronic acid was maintained after 30 days in the refrigerator but decreased in the freezer. Because of this, *in vivo* ocular biopermanence studies were performed using molecular imaging with the radiolabeled formulation, concluding that this drop in viscosity did not impact ocular residence time, with a half-life of 31.11 min for the hyaluronic acid formulation stored for 30 days at -20 °C, compared to 14.63 min for the 0.9% sodium chloride control eye drops. Likewise, storage at low temperatures did not affect the mechanical properties of the single-dose containers used in this study. These results favor transfer to clinical practice, without complex production processes such as nitrogen saturation as well as saving patients numerous visits to the hospital to pick up the formulation by increasing its stability, which will facilitate better therapeutic adherence of patients to treatment.

**Chapter 4** focuses on the development and characterization of the inhaled ethanol compounded formulation prior to its use in the Phase II clinical trial. In the initial phases of the pandemic there were no approved effective treatments, so hospital pharmacy proposed the use of ethanol as a compounded formulation for inhaled administration as an antiseptic in elderly patients. Many of the treatments used in the early stages of the pandemic were contraindicated in this population.

A 65° inhaled ethanol formulation was developed and characterized, which proved to be stable at room temperature and protected from light for 15 days, maintaining



USC UNIVERSIDADE DE SANTIAGO DE COMPOSTELA

its physicochemical and microbiological properties. The optimum oxygen flow necessary for an adequate administration 3 times a day, for a total of 15 minutes per inhalation, was studied. For this purpose, flow rates of 2 and 3 L/min were tested using an automated headspace gas chromatographic analysis technique (HS-GC-MS). At 2 L/min, the mean ethanol concentrations emitted were 51.5 ± 4.5 mg/L, compared to those observed at 3 L/min, which were found to be 39.9 ± 5.7 mg/L during the 45 min of treatment. Considering the respiratory volume per minute of 5 L/min for human adults, and the inhalation:exhalation ratio of 1:2, the estimated mean amounts of inhaled ethanol were 33.6 ± 3.6 mg/min and 40.0 ± 5.7 mg/min at 2 L/min and 3 L/min, respectively. With this a greater amount of ethanol is emitted in grams with the 3 L/min flow, although the concentration is higher and more stable at 2 L/min, this being the flow finally selected in the subsequent clinical trial.

Additionally, a preclinical toxicological safety study was carried out in rats, where the formulation was administered for a total of 5 days. Subsequently samples of respiratory tract and lungs were analyzed, demonstrating the absence of histological damage at this level. On the other hand, ethanol was radiolabeled and administered in rats through endotracheal insufflations to study its pharmacokinetics by PET/CT. With this it was possible to visualize an initial localization of ethanol in the respiratory tract and lungs, to achieve later a greater signal at the hepatic level, the main ethanol metabolizing organ. Finally, a preliminary clinical study was carried out on six healthy volunteers divided into two groups (1:1), who were subjected to ethanol administration during 15 minutes of oxygen therapy at 2 L/min and 3 L/min through a Ventimask® face mask, with no alterations observed in heart rate, blood pressure, or oxygen saturation.

After the development and characterization of the inhaled ethanol compounded formulation, administrative procedures were initiated to determine its efficacy and safety throughout a clinical trial.

The results of the ALCOVID-19 Phase II clinical trial (EudraCT: 2020-001760-29) are reported in **Chapter 5**. This is a randomized, triple-blind, placebo-controlled study in COVID-19 positive elderly patients institutionalized in a nursing home for infection control, conducted between October 2020 and March 2021, that is, in the second wave of the pandemic. Patients had to be in the early phase of the disease, with < 7 days of symptoms, absence of dyspnea and pneumonia, room air oxygen saturation > 93% or oxygen partial pressure > 70 mmHg and respiratory rate < 25 per minute.

A total of 75 patients were included who received treatment (1:1) with 65° ethanol inhaled via Ventimask® using oxygen flow at 2 L/min every 8 hours, at 15 minutes per inhalation, for a total of 5 days in the experimental group, while distilled water



USC UNIVERSIDADE DE SANTIAGO DE COMPOSTELA

was administered in the placebo group. Concomitantly, the treatment recommended at the time by the Ministry of Health for COVID-19 was administered. The overall objective was to assess progression to more severe stages using the World Health Organization (WHO) Clinical Progression Scale. The specific efficacy objectives were evolution of body temperature, the use of antipyretics, oxygen saturation, viral load assessed by cycling threshold (Ct) in real-time polymerase chain reaction (RT-PCR), biochemical markers of progression, and use of antibiotics or corticosteroids. Specific safety objectives were the absence of plasma ethanol and electrocardiographic, analytical or respiratory alterations.

After 28 days of follow-up, no differences in disease progression were observed at any of the study visits in the intention-to-treat population. A total of 7 patients (19.4%) in the ethanol group and 6 (16.7%) in the placebo group required hospital admission for a median of 10.5 (SD: 7.1) days in the ethanol group and 8.5 (SD: 8.5) in the placebo group. The median time from inclusion in the study to hospitalization was 6 days (RIQ: 3.0-9.0) and 6.5 days (RIQ: 4.0-7.0), respectively. None of these differences were significant. Two patients died in each group. The values obtained for body temperature, antipyretic use and oxygen saturation were similar in both groups.

Viral load decreased over the course of the study in both groups, both in the pooled analysis of the N, E and RdRP genes, and also if the N gene, the most conserved one, was considered individually. Mean Ct values were numerically higher in the ethanol group (lower viral load) in most of the visits, reaching a value above 33 only in the ethanol group on day 14, the cutoff above which patients are considered non-infectious. Creatinine kinase was reduced to a greater extent in the ethanol group (36.08% versus 11.65% ($p$ = 0.0020)), while C-reactive protein increased only in the placebo group (50% ($p$ = 0.0379)). The use of corticosteroids and antibiotics was similar in both groups. Inhaled ethanol proved to be safe since no plasma levels were detected and no electrocardiographic, analytical, or respiratory alterations occurred.

Further studies are needed to obtain conclusive data and to evaluate the long-term efficacy and safety of inhaled ethanol for SARS-CoV-2 infection. Even so, its non-specific mechanism of action could open the door to the evaluation of its use in other infectious respiratory pathologies, as it has shown to be a safe treatment.

In **conclusion**, this Doctoral Thesis proposes two different compounded formulations to address situations of therapeutic gap. On the one hand, the developed cysteamine 0.55% formulation in hyaluronic acid and packaged in innovative single-dose systems aims to respond to the absence of treatment in ocular cystinosis, and on the other, the developed 65° inhaled ethanol formulation

USC UNIVERSIDADE DE SANTIAGO DE COMPOSTELA

seeks to offer to offer a therapeutic alternative in a rapidly emerging contagious disease for which there was no previous treatment, as was the case of COVID-19. Both compounded formulations represent the capacity of hospital pharmacy to contribute to the fight against each of these pathologies, generating scientific evidence, favoring access to treatment in patients who do not have therapeutic options, and all this in an efficient, practical, and easily transferable way to clinical practice.



USC UNIVERSIDADE DE SANTIAGO DE COMPOSTELA

# RESUMO

As seccións de **farmacotecnia** dos servizos de farmacia hospitalaria ocúpanse da elaboración de formulacións maxistrais adaptadas ás necesidades e características dos pacientes, sendo unha das áreas con maior carga de traballo e constituíndo un dos piares clásicos, fundamentais e inherentes da farmacia hospitalaria. A pesar disto, segue sendo unha área á que non se destinan os recursos suficientes que permitan a súa adecuada modernización e adaptación ás demandas asistenciais actuais. Para alcanzar este obxectivo é necesario apostar pola investigación neste campo de forma definitiva xa que, a día de hoxe, a elaboración de medicamentos non é unha liña de investigación prioritaria entre as habitualmente abordadas pola farmacia hospitalaria.

Esta aposta pola **investigación** en cada unha das áreas que abarca a farmacia hospitalaria é vital para conseguir avances que permitan lograr a excelencia asistencial. Unha das posibles estratexias a seguir para que a investigación en galénica se postule como unha arma clave para favorecer e impulsar o proceso de renovación nesta área é o desenvolvemento e caracterización de novas formulacións maxistrais destinadas a cubrir situacións de baleiro terapéutico. Son diversos os escenarios na práctica clínica cotiá nos que non existen opcións terapéuticas ou ben non se atopan dispoñibles para o tratamento de determinadas patoloxías. Estas circunstancias preséntanse no caso das enfermidades raras, para as cales non existen medicamentos comercializados, ou ben resultan en ocasións ser dificilmente accesibles para os pacientes; e en enfermidades emerxentes, como foi a irrupción da pandemia por SARS-CoV-2, para a cal non existían tratamentos eficaces previos.

As **enfermidades raras** afectan a menos de 5 persoas por cada 10.000 habitantes. Debido en parte á súa escasa prevalencia, existen considerables lagoas de coñecemento relativas á súa etioloxía, métodos diagnósticos, manexo e tratamento. Por este motivo, é frecuente que o diagnóstico se atrase ou nunca chegue a producirse, dificultando a adopción de medidas preventivas ou terapéuticas. Ademais, a investigación neste ámbito é escasa e adoita estar moi dispersa entre distintos grupos de traballo, ao cal se suma o escaso interese da industria por investir no desenvolvemento de fármacos para o tratamento destas enfermidades pola súa baixa rendibilidade e elevado custo de investigación e comercialización. A isto súmase que en moitas ocasións os medicamentos orfos comerciais, destinados ao tratamento de enfermidades raras, non están dispoñibles na maioría dos países



USC UNIVERSIDADE DE SANTIAGO DE COMPOSTELA

debido aos procedementos de avaliación e autorizacións necesarios. Unha das enfermidades raras nas que se dan estas circunstancias é a **cistinose**.

A **cistinose** é un trastorno no que se produce a acumulación de cristais do aminoácido cistina nos lisosomas de diversos tecidos como o ril, páncreas e a córnea, entre outros. Actualmente o único tratamento aprobado para a súa abordaxe é a **cisteamina**, dispoñible como medicamento orfo en forma de presentación oral en moitos países. Debido a que o ollo presenta unha complexa estrutura anatómica, a biodisponibilidade oftálmica da cisteamina resulta insuficiente para producir o efecto desexado. Aínda que a súa instilación tópica oftálmica é o tratamento de elección na cistinose ocular para evitar a aparición de fotofobia, erosións corneais, queratopatías, discapacidade visual e finalmente cegueira, as presentacións oftálmicas comerciais de cisteamina non sempre se atopan dispoñibles, polo que a súa elaboración como **formulación maxistral** desde os servizos de farmacia supón unha alternativa terapéutica para aqueles pacientes que non teñen acceso ao tratamento.

Doutra banda, a violenta irrupción da **infección por SARS-CoV-2** azoutou ao mundo a partir de principios do 2020, provocando unha pandemia con consecuencias devastadoras. Grandes esforzos realizáronse desde entón partindo de diversos ámbitos para facer fronte ao avance dos contaxios e evitar a progresión da enfermidade xa instaurada. Para iso, a comunidade científica comezou unha investigación a contrarreloxo para poder ofrecer vacinas e tratamentos efectivos. Tras tres anos de pandemia, o enfoque terapéutico óptimo para a COVID-19 aínda se atopa en vías de posicionamento cos datos que se seguen xerando. Ata hoxe, en base á súa patoxénese, as estratexias terapéuticas nas fases iniciais da infección diríxense **fronte ao propio virus** mediante o emprego de antivirais, inmunidade pasiva e interferóns, mentres que a **modulación da resposta inmunitaria** mostrou ser máis eficaz en fases avanzadas da enfermidade. Unha das estratexias levadas a cabo para poder ofrecer alternativas de tratamento de forma rápida e segura foi o **reposicionamento de fármacos**, que consiste na identificación de novas indicacións terapéuticas para medicamentos xa aprobados. Este enfoque resulta máis rápido e custo-efectivo que o descubrimento de fármacos *de novo*, xa que os datos farmacocinéticos, toxicolóxicos e de seguridade atópanse previamente dispoñibles. Isto facilitou a aprobación por parte de axencias reguladoras como a US Food and Drug Administration (FDA) ou a European Medicines Agency (EMA) desta nova indicación nalgúns dos fármacos que forman parte do arsenal terapéutico fronte á COVID-19.

A caracterización molecular de SARS-CoV e MERS-CoV suxeriu desde os momentos iniciais da pandemia que o SARS-CoV-2 é susceptible aos **antisépticos** que demostraron actividade contra os virus con envoltura, como é o caso do etanol.



USC UNIVERSIDADE DE SANTIAGO DE COMPOSTELA

Debido a que nas fases temperás da infección a replicación viral ten lugar nas vías respiratorias altas, a súa administración na etapa inicial da enfermidade podería reducir a viremia e evitar a progresión a estadios de maior gravidade. O **etanol** fora empregado con anterioridade como formulación maxistral nos servizos de farmacia hospitalaria para outras indicacións, pero o seu uso como antiséptico inhalado non fora estudado con anterioridade.

En ambas as situacións, na cistinose e na infección por COVID-19, a **investigación dende a farmacia hospitalaria** no campo de elaboración de medicamentos podería posicionarse como unha oportunidade de ofrecer alternativas terapéuticas como é o caso dunha formulación maxistral oftálmica de cisteamina para o tratamento da cistinose ocular e unha formulación maxistral de etanol inhalado fronte á infección por COVID-19 en estadios iniciais da enfermidade. A posición transversal da farmacia hospitalaria, o dominio da farmacoloxía e a tecnoloxía farmacéutica, xunto co emprego de estratexias como o reposicionamento de fármacos favorecería a adecuada translación dos resultados á práctica clínica. Para iso, é necesario un correcto desenvolvemento e caracterización exhaustiva previos das formulacións mediante estudos de estabilidade químicos, físicos, microbiolóxicos e farmacocinéticos, así como unha avaliación da súa eficacia e seguridade.

O **capítulo 1** engloba unha revisión bibliográfica que pretende dar unha perspectiva global dos recentes desenvolvementos que se produciron no campo da imaxe molecular en relación aos estudos preclínicos de biodistribución ocular. O obxectivo desta é dar coa mellor ferramenta de imaxe que poida ser aplicable e trasladable aos desenvolvementos oftálmicos que se levarán a cabo posteriormente nesta Tese Doutoral. Estas técnicas proporcionan datos farmacocinéticos de forma non invasiva e a tempo real, sen a necesidade de sacrificar aos animais, aforrando custos e evitando a redistribución do composto producida polos métodos de disección. Non existe unha modalidade perfecta que presente ao mesmo tempo alta sensibilidade, especificidade, resolución temporal e espacial; con todo, pódense estudar satisfactoriamente os procedementos biolóxicos cando se combina a información proporcionada por varias delas. Mediante este tipo de estudos, é posible mellorar a biopermanencia dos medicamentos oftálmicos no seu lugar de acción e optimizar deste xeito a súa dosificación.

Inicialmente descríbense as técnicas de tomografía por emisión de positróns (PET) e a tomografía computarizada por emisión de fotón único (SPECT), empregadas en estudos de biodistribución tópica ocular de fármacos e vehículos radiomarcados, así como en estudos de administración intraocular. Ambas proporcionan un sinal cuantificable do perfil farmacocinético do radiofármaco administrado, de forma que é posible obter un sinal no ollo tras a instilación, cunha posterior detección de sinal no conduto nasolagrimal e na cavidade nasal. Presentan unha gran sensibilidade e



USC UNIVERSIDADE DE SANTIAGO DE COMPOSTELA

adoitan combinarse con técnicas morfolóxicas como a tomografía computarizada (TC) e a resonancia magnética (RM), que permiten unha adecuada localización anatómica do sinal radioactivo. Teñen como desvantaxe a súa baixa resolución e a posible alteración que o radiomarcaxe pode producir nas propiedades de moléculas pequenas, aínda que aquelas de maior tamaño molecular non se ven afectadas. Outras técnicas como a fluorescencia son empregadas con éxito no estudo farmacocinético de macromoléculas. Doutra banda, faise referencia á excelente resolución que proporciona RM e aos diversos estudos nos que foi empregada. Finalmente descríbense tecnoloxías menos exploradas no campo da investigación ata o momento actual, como son a ultrasonografía e a tomografía de coherencia óptica.

O **capítulo 2** comprende unha revisión bibliográfica sobre a investigación máis recente relativa á cistinose ocular. En primeiro lugar, exponse unha descrición xeral da epidemioloxía, patoxénese, tratamento e evolución das presentacións comerciais de cisteamina como medicamentos orfos aprobadas nos últimos anos pola FDA e a EMA. Á súa vez, tamén se fai referencia ás dificultades que presentan os pacientes diagnosticados de cistinose para acceder a este tipo de tratamentos, e os motivos polos cales é necesario o desenvolvemento de novas formulacións de administración tópica oftálmica. Despois, descríbense e analízanse os máis novidosos avances en sistemas de administración ocular de cisteamina co obxectivo proporcionar unha maior biodisponibilidade ocular para evitar incómodas posoloxías. Dentro destes sistemas de administración faise referencia ós últimos avances e vantaxes dos hidroxeis, nanowafers e lentes de contacto cargadas con cisteamina.

Posteriormente, faise referencia á estrutura e características químicas das cisteamina, xunto coa súa extrema inestabilidade debida á súa rápida oxidación a cistamina, inefectiva no tratamento da cistinose ocular. Esta reacción está favorecida pola presenza de luz e temperatura, sendo este un dos principais inconvenientes á hora de desenvolver novas formulacións oftálmicas. Así mesmo, descríbense diversas técnicas para evitar esta oxidación e incrementar a súa estabilidade. Outro dos retos relativos ao desenvolvemento de formulacións con cisteamina é a súa detección e cuantificación xunto coa cistamina, sen estar definida una metodoloxía *gold standard*. Por iso, recóllense tamén os múltiples métodos descritos para a súa determinación na bibliografía, como é o caso da cromatografía líquida de alto rendemento (HPLC), os ensaios enzimáticos, a cromatografía de gases ou a detección electroquímica.

Por último, a revisión céntrase en novas liñas de investigación para o tratamento da cistinose, como é o emprego de células nai hematopoéticas modificadas xeneticamente illadas de pacientes afectados de cistinose. Outras aproximacións



USC UNIVERSIDADE DE SANTIAGO DE COMPOSTELA

terapéuticas estudadas foron o emprego de microvesículas con cistinosina funcional e a terapia combinada de cisteamina con everolimus, como se puido demostrar mediante o estudo de modelos de células nai humanas pluripotentes inducidas (iPSC) e organoides renais de cistinose. Ademais, faise referencia novos descubrimentos relativos á patoxénese da enfermidade, como é a hipótese sobre o papel que podería ter a cistinosina como compoñente da vía mTORC1, ademais de transportar cistina fóra do lisosoma. Neste apartado discútense tamén de forma crítica os resultados reportados ata o momento a partir de ensaios clínicos con cisteamina, permitíndonos todo isto establecer e estruturar unha fase experimental para dar resposta aos baleiros atopados neste campo.

O **capítulo 3** baséase no desenvolvemento e caracterización dunha formulación maxistral oftálmica tópica de cisteamina preparada con ácido hialurónico e envasada en innovadores sistemas monodosis destinada ao tratamento da cistinose ocular. As presentacións comerciais de cisteamina oftálmica son medicamentos orfos que non sempre están dispoñibles en todos os países, polo que a farmacia hospitalaria podería ter un papel esencial á hora de ofrecer alternativas de tratamento. A cisteamina é un composto moi oxidable, polo que se buscou incrementar a súa estabilidade mediante o envasado en sistemas monodosis que permitise a súa conservación en neveira/conxelador durante un longo período de tempo, e que permitise empregar un envase por día para posteriormente refugalo. Ademais, para incrementar o tempo de residencia ocular, a formulación elaborouse empregando unha presentación comercial de ácido hialurónico (Aquoral®) como vehículo.

Estudouse o efecto de dúas temperaturas diferentes de almacenamento (neveira e conxelador) e presencia/ausencia de nitróxeno sobre a estabilidade fisicoquímica da formulación e o seu envase, ata dar coas condicións óptimas de almacenamento. Os resultados mostraron que a formulación de cisteamina ao 0,55% é estable durante 30 días se se almacena a -20 °C con concentracións en torno ao 98% de principio activo, aínda que non supera os 7 días de estabilidade química cando é almacenada entre 2-8 °C, sendo as concentracións de principio activo próximas ao 88%. A presenza de nitróxeno non proporcionou diferenzas na oxidación da cisteamina. Ademais, a apertura dos viais cada 4 h a temperatura ambiente tras 30 días de conxelación mantén a concentración de cisteamina ata 16 h, permitindo o uso dun envase monodosis diario, fóra das horas de soño. Os valores de pH e osmolaridade atopáronse dentro dos rangos requiridos para a administración oftálmica, e non se detectou crecemento microbiano.

A viscosidade proporcionada polo ácido hialurónico mantívose tras 30 días en neveira, pero reduciuse en conxelador. Debido a isto, realizáronse estudos de biopermanencia ocular *in vivo* mediante o emprego de imaxe molecular coa



USC UNIVERSIDADE DE SANTIAGO DE COMPOSTELA

formulación radiomarcada, concluíndo que esta caída en viscosidade non repercute no tempo de residencia ocular, cunha vida media de 31,11 minutos para a formulación de ácido hialurónico almacenada durante 30 días a -20 °C, fronte aos 14,63 minutos do colirio control de cloruro sódico ao 0,9%. Así mesmo, a conservación a baixas temperaturas non afectou ás propiedades mecánicas dos envases monodosis empregados. Estes resultados favorecen a transferencia á práctica clínica, prescindindo de complexos procesos de produción como a saturación de nitróxeno e evitando aos pacientes numerosas visitas ao hospital para recoller a formulación ao incrementar a estabilidade da mesma, o que facilitará unha mellor adherencia terapéutica dos pacientes ao tratamento.

O **capítulo 4** céntrase no desenvolvemento e caracterización da formulación maxistral de etanol inhalado previo ao seu uso no ensaio clínico fase II. Nos momentos iniciais da pandemia non existían tratamentos eficaces aprobados, por iso desde a farmacia hospitalaria propúxose o emprego do etanol elaborado como formulación maxistral para a súa administración inhalada como antiséptico en pacientes maiores, para os cales moitos dos tratamentos empregados en fases iniciais da pandemia estaban contraindicados.

Desenvólvese e caracterízase unha formulación de etanol 65° inhalado, que demostrou ser estable a temperatura ambiente e protexida da luz durante 15 días, mantendo as súas propiedades fisicoquímicas e microbiolóxicas. Ademais, estudouse cal sería o seu fluxo de osíxeno óptimo necesario para unha adecuada administración de 3 veces ao día, durante un total de 15 minutos por inhalación. Para iso ensaiáronse os fluxos de 2 e 3 L/min mediante unha técnica automatizada de análise cromatográfico de gases en espazo de cabeza (HS-GC-MS). A 2 L/min, as concentracións medias de etanol emitidas foron de 51,5 ± 4,5 mg/L, fronte ás observadas a 3 L/min, que resultaron ser de 39,9 ± 5,7 mg/L durante os 45 min de tratamento. Tendo en conta o volumen respiratorio por minuto de 5 L/min para humanos adultos, e a relación inhalación:exhalación de 1:2, as cantidades medias estimadas de etanol inhalado foron de 33,6 ± 3,6 mg/min e 40,0 ± 5,7 mg/min a 2 L/min e 3 L/min, respectivamente. Con isto dedúcese que se emite unha maior cantidade de etanol en gramos co fluxo de 3 L/min, aínda que as concentracións son maiores e máis estables a 2 L/min, sendo este o fluxo finalmente seleccionado no ensaio clínico.

Ademais, realizouse un estudo preclínico de seguridade toxicolóxica en ratas, onde se administrou a formulación durante un total de 5 días, analizando posteriormente mostras de vías respiratorias e pulmóns, a partir do cal se demostrou a ausencia de danos histolóxicos a este nivel. Por outra banda, se radiomarcou o etanol e procedeuse á súa administración a través de insuflacións endotraqueais para o estudo da súa farmacocinética en ratas mediante PET/TC. Con iso foi posible



USC UNIVERSIDADE DE SANTIAGO DE COMPOSTELA

visualizar unha localización inicial do etanol en vías respiratorias e pulmóns, para alcanzar posteriormente un maior sinal a nivel hepático, principal órgano metabolizador do etanol. Por último, levouse a cabo un estudo clínico preliminar en seis voluntarios sans divididos en dous grupos (1:1), que foron sometidos á administración do etanol durante 15 minutos de osixenoterapia a 2 L/min e 3 L/min a través dunha máscara facial Ventimask®, a partir do cal non se observaron alteracións na frecuencia cardíaca, presión arterial nin saturación de osíxeno.

Tras o desenvolvemento e caracterización da formulación maxistral de etanol inhalado, iniciáronse os trámites para caracterizar a súa eficacia e seguridade mediante a realización dun ensaio clínico.

Os resultados do ensaio clínico fase II ALCOVID-19 (EudraCT: 2020-001760-29) recóllense no **capítulo 5**. Trátase dun estudo aleatorizado, triplo cego e controlado con placebo en pacientes maiores COVID-19 positivo institucionalizados nun centro destinado ao control da infección en residencias sociosanitarias, levado a cabo entre outubro de 2020 e marzo de 2021, é dicir, na segunda onda da pandemia. Os pacientes debían atoparse na fase inicial da enfermidade, con < 7 días de síntomas, ausencia de disnea e pneumonía, saturación de osíxeno en aire ambiente > 93% ou presión parcial de osíxeno > 70 mmHg e frecuencia respiratoria < 25 por minuto.

Incluíronse a un total de 75 pacientes que recibiron tratamento (1:1) con etanol 65° por vía inhalada a través de Ventimask® mediante un fluxo de osíxeno a 2 L/min cada 8 horas, a 15 minutos por inhalación, durante un total de 5 días no grupo experimental, mentres que no grupo placebo administrouse auga destilada. De forma concomitante administrouse o tratamento recomendado nese momento polo Ministerio de Sanidade para a COVID-19. O obxectivo xeral foi avaliar a progresión a estadios de maior gravidade mediante a Escala de Progresión Clínica da Organización Mundial da Saúde (OMS). Os obxectivos específicos de eficacia foron a evolución da temperatura corporal, uso de antipiréticos, saturación de osíxeno, carga viral avaliada polo limiar de ciclo (Ct) na reacción en cadea da polimerasa en tempo real (RT-PCR), marcadores bioquímicos de progresión e o uso de antibióticos ou corticoides. Os obxectivos específicos de seguridade foron a ausencia de etanol en plasma e de alteracións electrocardiográficas, analíticas ou respiratorias.

Tras 28 días de seguimento, non se observaron diferenzas relativas á progresión da enfermidade en ningunha das visitas de estudo na poboación por intención de tratar. Un total de 7 pacientes (19,4%) do grupo etanol e 6 (16,7%) do grupo placebo precisaron ingreso hospitalario durante unha media de 10,5 (DE: 7,1) días no grupo etanol e 8,5 (DE: 8,5) no grupo placebo. A mediana de tempo desde a inclusión no estudo ata a hospitalización foi de 6 días (RIQ: 3,0-9,0) e 6,5 días (RIQ: 4,0-7,0), respectivamente. Ningunha destas diferenzas foi significativa. Dous pacientes



USC UNIVERSIDADE DE SANTIAGO DE COMPOSTELA

faleceron en cada grupo. Os valores obtidos de temperatura corporal, uso de antipiréticos e saturación de osíxeno foron similares en ambos os grupos.

A carga viral diminuíu ao longo do transcurso do estudo en ambos os grupos, tanto na análise conxunta dos xenes N, E e RdRP como tendo en conta o xene N, o máis conservado, de forma individual. Os valores medios de Ct foron numericamente superiores no grupo do etanol (menor carga viral) na maioría das visitas, alcanzándose un valor superior a 33 só no grupo etanol o día 14, corte por encima do cal os pacientes se consideran non infecciosos. A creatinina quinasa reduciuse en maior medida no grupo etanol (36.08% versus 11.65% ($p$ = 0.0020)), mentres que a proteína C reactiva incrementouse unicamente no grupo placebo (50% ($p$ = 0.0379)). O uso de corticoides e antibióticos foi similar en ambos os grupos. O etanol inhalado demostrou ser seguro xa que non se detectaron niveis plasmáticos e non se produciron alteracións electrocardiográficas, analíticas nin respiratorias.

Necesítanse máis estudos para obter datos concluíntes e avaliar a eficacia e seguridade a longo prazo do etanol inhalado para a infección por SARS-CoV-2. Aínda así, o seu mecanismo de acción inespecífico podería abrir a porta á avaliación do seu uso noutras patoloxías respiratorias infecciosas, tras demostrar ser un tratamento seguro.

En **conclusión**, nesta Tese Doutoral propóñense dúas formulacións maxistrais diferentes para abordar situacións de baleiro terapéutico. Por unha banda, a formulación desenvolvida de cisteamina ao 0,55% en ácido hialurónico e envasada en innovadores sistemas monodosis pretende dar resposta á ausencia de tratamento na cistinosis ocular, e por outro, a formulación desenvolvida de etanol inhalado ao 65° pretende ofrecer unha alternativa terapéutica nunha enfermidade contaxiosa de rápida aparición para a que non existía tratamento previo, como foi o caso da COVID-19. Ambas representan a capacidade da farmacia hospitalaria na contribución á loita fronte a cada unha destas patoloxías, xerando evidencia científica, favorecendo o acceso a tratamento en pacientes que non dispoñen de opcións terapéuticas e todo iso dunha forma eficiente, práctica, e facilmente trasladable á práctica clínica.



USC UNIVERSIDADE DE SANTIAGO DE COMPOSTELA

# RESUMEN

Las secciones de **farmacotecnia** de los servicios de farmacia hospitalaria se ocupan de la elaboración de formulaciones magistrales adaptadas a las necesidades y características de los pacientes, siendo una de las áreas con mayor carga de trabajo y constituyendo uno de los pilares clásicos, fundamentales e inherentes de la farmacia hospitalaria. A pesar de esto, sigue siendo un área a la que no se destinan los recursos suficientes que permitan su adecuada modernización y adaptación a las demandas asistenciales actuales. Para alcanzar este objetivo es necesario apostar por la investigación en este campo de forma definitiva ya que, a día de hoy, la elaboración de medicamentos no es una línea de investigación prioritaria entre las habitualmente abordadas por la farmacia hospitalaria.

Esta apuesta por la **investigación** en cada una de las áreas que abarca la farmacia hospitalaria es vital para conseguir avances que permitan lograr la excelencia asistencial. Una de las posibles estrategias a seguir para que la investigación en galénica se postule como un arma clave para favorecer e impulsar el proceso de renovación en esta área es el desarrollo y caracterización de nuevas formulaciones magistrales destinadas a cubrir situaciones de **vacío terapéutico**. Son diversos los escenarios en la práctica clínica cotidiana en los que no existen opciones terapéuticas o bien no se encuentran disponibles para el tratamiento de determinadas patologías. Estas circunstancias se presentan en el caso de las enfermedades raras, para las cuales no existen medicamentos comercializados, o bien resultan en ocasiones ser difícilmente accesibles para los pacientes; y en enfermedades emergentes, como ha sido la irrupción de la pandemia por SARS-CoV-2, para la cual no existían tratamientos eficaces previos.

Las **enfermedades raras** afectan a menos de 5 personas por cada 10.000 habitantes. Debido en parte a su escasa prevalencia, existen considerables lagunas de conocimiento relativas a su etiología, métodos diagnósticos, manejo y tratamiento. Por este motivo, es frecuente que el diagnóstico se retrase o nunca llegue a producirse, dificultando la adopción de medidas preventivas o terapéuticas. Además, la investigación en este ámbito es escasa y suele estar muy dispersa entre distintos grupos de trabajo, a lo cual se suma el escaso interés de la industria por invertir en el desarrollo de fármacos para el tratamiento de estas enfermedades por su baja rentabilidad y elevado coste de investigación y comercialización. A esto se suma que en muchas ocasiones los medicamentos huérfanos comerciales,



USC UNIVERSIDADE DE SANTIAGO DE COMPOSTELA

destinados al tratamiento de enfermedades raras, no están disponibles en la mayoría de los países debido a los procedimientos de evaluación y autorizaciones necesarios. Una de las enfermedades raras en la que se dan estas circunstancias es el caso de la cistinosis.

La **cistinosis** es un trastorno lisosomal en el que se produce la acumulación de cristales del aminoácido cistina en diversos tejidos como el riñón, páncreas y la córnea, entre otros. Actualmente el único tratamiento aprobado es la **cisteamina**, disponible como medicamento huérfano en forma de presentación oral en muchos países. Debido a que el ojo presenta una estructura anatómica compleja, la biodisponibilidad oftálmica de la cisteamina resulta insuficiente para producir el efecto deseado. Aunque, su instilación tópica oftálmica es el tratamiento de elección en la cistinosis ocular para evitar la aparición de fotofobia, erosiones corneales, queratopatías, discapacidad visual y finalmente ceguera, las presentaciones oftálmicas comerciales de cisteamina no siempre se encuentran disponibles, por lo que su elaboración como **formulación magistral** desde los servicios de farmacia supone una alternativa terapéutica para aquellos pacientes que no tienen acceso al tratamiento.

Por otro lado, la violenta irrupción de la **infección por SARS-CoV-2** azotó al mundo a partir de principios del 2020, provocando una pandemia con consecuencias devastadoras. Grandes esfuerzos se han realizado desde entonces partiendo de diversos ámbitos para hacer frente al avance de los contagios y evitar la progresión de la enfermedad ya instaurada. Para ello, la comunidad científica comenzó una investigación a contrarreloj para poder ofrecer vacunas y tratamientos efectivos. Tras tres años de pandemia, el enfoque terapéutico óptimo para la COVID-19 aún se encuentra en vías de posicionamiento con los datos que se siguen generando. Hasta hoy, en base a su patogénesis, las estrategias terapéuticas en las fases iniciales de la infección se han dirigido **frente al propio virus** mediante el empleo de antivirales, inmunidad pasiva e interferones, mientras que la **modulación la respuesta inmunitaria** se ha mostrado más eficaz en fases más avanzadas de la enfermedad. Una de las estrategias llevadas a cabo para poder ofrecer alternativas de tratamiento de forma rápida y segura ha sido el **reposicionamiento de fármacos**, que consiste en la identificación de nuevas indicaciones terapéuticas para medicamentos ya aprobados. Este enfoque resulta más rápido y coste-efectivo que el descubrimiento de fármacos *de novo*, ya que los datos farmacocinéticos, toxicológicos y de seguridad se encuentran previamente disponibles. Esto ha facilitado la aprobación por parte de agencias reguladoras como la US Food and Drug Administration (FDA) o la European Medicines Agency (EMA) de esta nueva indicación en algunos de los fármacos que forman parte de del arsenal terapéutico frente a la COVID-19.



USC UNIVERSIDADE DE SANTIAGO DE COMPOSTELA

La caracterización molecular de SARS-CoV y MERS-CoV sugirió desde los momentos iniciales de la pandemia que el SARS-CoV-2 es susceptible a los **antisépticos** que han demostrado actividad contra los virus con envoltura, como es el caso del etanol. Debido a que en las fases tempranas de la infección la replicación viral tiene lugar en las vías respiratorias altas, su administración en la etapa inicial de la enfermedad podría reducir la viremia y evitar la progresión a estadios de mayor gravedad. El **etanol** había sido empleado con anterioridad como formulación magistral en los servicios de farmacia hospitalaria para otras indicaciones, pero su uso como antiséptico inhalado no había sido estudiado con anterioridad.

En ambas situaciones, en la cistinosis y en la infección por SARS-CoV-2, la **investigación desde la farmacia hospitalaria** en el campo de elaboración de medicamentos podría posicionarse como una oportunidad de ofrecer alternativas terapéuticas como es el caso de una formulación magistral oftálmica de cisteamina para el tratamiento de la cistinosis ocular y una formulación magistral de etanol inhalado frente a la infección por COVID-19 en estadios iniciales de la enfermedad. La posición transversal de la farmacia hospitalaria, el dominio de la farmacología y la tecnología farmacéutica, junto con el empleo de estrategias como el reposicionamiento de fármacos favorecería la adecuada traslación de los resultados a la práctica clínica. Para ello, es necesario un correcto desarrollo y caracterización exhaustiva previos de las formulaciones mediante estudios de estabilidad químicos, físicos, microbiológicos y farmacocinéticos, así como una evaluación de su eficacia y seguridad.

El **capítulo 1** engloba una revisión bibliográfica que pretende dar una perspectiva global de los recientes desarrollos que se han producido en el campo de la imagen molecular en relación a los estudios preclínicos de biodistribución ocular. El objetivo de esta es dar con la mejor herramienta de imagen que pueda ser aplicable y trasladable a los desarrollos oftálmicos que se llevarán a cabo posteriormente en esta Tesis Doctoral. Estas técnicas proporcionan datos farmacocinéticos de forma no invasiva y a tiempo real, sin la necesidad de sacrificar a los animales, ahorrando costes y evitando la redistribución del compuesto producida por los métodos de disección. No existe una modalidad perfecta que presente al mismo tiempo alta sensibilidad, especificidad, resolución temporal y espacial; sin embargo, se pueden estudiar los procedimientos biológicos satisfactoriamente cuando se combina la información proporcionada por varias de ellas. Mediante este tipo de estudios, es posible mejorar la biopermanencia de los medicamentos oftálmicos en su lugar de acción y optimizar de este modo su dosificación.

Inicialmente se describen las técnicas de tomografía por emisión de positrones (PET) y la tomografía computarizada por emisión de fotón único (SPECT), empleadas en

USC UNIVERSIDADE DE SANTIAGO DE COMPOSTELA

estudios de biodistribución tópica ocular de fármacos y vehículos radiomarcados, así como en estudios de administración intraocular. Ambas proporcionan una señal cuantificable del perfil farmacocinético del radiofármaco administrado, de forma que es posible obtener una señal en el ojo tras la instilación, con una posterior detección de señal en el conducto nasolagrimal y en la cavidad nasal. Presentan una gran sensibilidad y suelen combinarse con técnicas morfológicas como la tomografía computarizada (TC) y la resonancia magnética (RM), que permiten una adecuada localización anatómica de la señal radiactiva. Tienen como desventaja su baja resolución y la posible alteración que el radiomarcaje puede producir en las propiedades de moléculas pequeñas, si bien aquellas de mayor tamaño molecular no se ven afectadas. Otras técnicas como la fluorescencia son empleadas con éxito en el estudio farmacocinético de macromoléculas. Por otro lado, se hace referencia a la excelente resolución que proporciona RM y a los diversos estudios en los que ha sido empleada. Finalmente se describen tecnologías menos exploradas en el campo de la investigación hasta el momento actual, como son la ultrasonografía y la tomografía de coherencia óptica.

El **capítulo 2** comprende una revisión bibliográfica sobre la investigación más reciente relativa a la cistinosis ocular. En primer lugar, se expone una descripción general de la epidemiología, patogénesis, tratamiento y evolución de las presentaciones comerciales de cisteamina como medicamentos huérfanos aprobadas en los últimos años por la FDA y la EMA. A su vez, también se hace referencia a las dificultades que presentan los pacientes diagnosticados de cistinosis para acceder a este tipo de tratamientos, y los motivos por los cuales es necesario el desarrollo de nuevas formulaciones de administración tópica oftálmica. Después, se describen y analizan los más novedosos avances en sistemas de administración ocular de cisteamina con el objetivo proporcionar una mayor biodisponibilidad ocular para evitar incómodas posologías. Dentro de estos sistemas de administración se exponen los últimos avances y ventajas de los hidrogeles, nanowafers y lentes de contacto cargados con cisteamina.

Posteriormente, se hace referencia a la estructura y características químicas de las cisteamina, junto con su extrema inestabilidad debida a su rápida oxidación a cistamina, inefectiva en el tratamiento de la cistinosis ocular. Esta reacción está favorecida por la presencia de luz y temperatura, siendo este uno de los principales inconvenientes a la hora de desarrollar nuevas formulaciones oftálmicas. Asimismo, se describen diversas técnicas para evitar esta oxidación e incrementar su estabilidad. Otro de los retos relativos al desarrollo de formulaciones con cisteamina es su detección y cuantificación junto con la cistamina, sin estar definida una metodología *gold standard*. Por ello, se recogen los múltiples métodos descritos en la bibliografía, como es el caso de la cromatografía líquida de alto rendimiento



USC UNIVERSIDADE DE SANTIAGO DE COMPOSTELA

(HPLC), los ensayos enzimáticos, la cromatografía de gases o la detección electroquímica.

Por último, la revisión se centra en nuevas líneas de investigación para el tratamiento de la cistinosis, como es el empleo de células madre hematopoyéticas modificadas genéticamente aisladas de pacientes afectados de cistinosis. Otras aproximaciones terapéuticas estudiadas fueron el empleo de microvesículas con cistinosina funcional y la terapia combinada de cisteamina con everolimus, como se ha podido demostrar mediante el estudio de modelos de células madre humanas pluripotentes inducidas (iPSC) y organoides renales de cistinosis. Además, se hace referencia nuevos descubrimientos relativos a la patogénesis de la enfermedad, como es la hipótesis sobre el papel que podría tener la cistinosina como componente de la vía mTORC1, además de transportar cistina fuera del lisosoma. En este apartado se discuten también de forma crítica los resultados reportados hasta el momento a partir de ensayos clínicos con cisteamina, permitiéndonos todo ello establecer y estructurar una fase experimental para dar respuesta a los vacíos encontrados en este campo.

El **capítulo 3** se basa en el desarrollo y caracterización de una formulación magistral oftálmica tópica de cisteamina preparada con ácido hialurónico y envasada en innovadores sistemas monodosis destinada al tratamiento de la cistinosis ocular. Las presentaciones comerciales de cisteamina oftálmica son medicamentos huérfanos que no siempre están disponibles en todos los países, por lo que la farmacia hospitalaria podría tener un papel esencial a la hora de ofrecer alternativas de tratamiento. La cisteamina es un compuesto muy oxidable, por lo que se ha buscado incrementar su estabilidad mediante el envasado en sistemas monodosis que permitiera su conservación en nevera/congelador durante un largo periodo de tiempo, y que permitiera emplear un envase por día para posteriormente desecharlo. Además, para incrementar el tiempo de residencia ocular, la formulación se elaboró empleando una presentación comercial de ácido hialurónico (Aquoral®) como vehículo.

Se estudió el efecto de dos temperaturas diferentes de almacenamiento (nevera y congelador) y la presencia/ausencia de nitrógeno sobre la estabilidad fisicoquímica de la formulación y su envase, hasta dar con las condiciones óptimas de almacenamiento. Los resultados mostraron que la formulación de cisteamina al 0,55% es estable durante 30 días si se almacena a -20 °C con concentraciones en torno al 98% de principio activo, aunque no supera los 7 días de estabilidad química cuando es almacenada entre 2-8 °C, siendo las concentraciones de principio activo cercanas al 88%. La presencia de nitrógeno no proporcionó diferencias en la oxidación de la cisteamina. Además, la apertura de los viales cada 4 h a temperatura



USC UNIVERSIDADE DE SANTIAGO DE COMPOSTELA

ambiente tras 30 días de congelación mantiene la concentración de cisteamina hasta 16 h, permitiendo el uso de un envase monodosis diario, a excepción de las horas de sueño. Los valores de pH y osmolaridad se encontraron dentro de los rangos requeridos para la administración oftálmica, y no se detectó crecimiento microbiano.

La viscosidad proporcionada por el ácido hialurónico se mantuvo tras 30 días en nevera, pero se redujo en congelador. Debido a esto, se realizaron estudios de biopermanencia ocular *in vivo* mediante el empleo de imagen molecular con la formulación radiomarcada, concluyendo que esta caída en viscosidad no repercute en el tiempo de residencia ocular, con una vida media de 31,11 min para la formulación de ácido hialurónico almacenada durante 30 días a -20 °C, frente a los 14,63 min del colirio control de cloruro sódico al 0,9%. Asimismo, la conservación a bajas temperaturas no afectó a las propiedades mecánicas de los envases monodosis empleados. Estos resultados favorecen la transferencia a la práctica clínica, prescindiendo de complejos procesos de producción como la saturación de nitrógeno y evitando a los pacientes numerosas visitas al hospital para recoger la formulación al incrementar la estabilidad de la misma, lo que facilitará una mejor adherencia terapéutica de los pacientes al tratamiento.

El **capítulo 4** se centra en el desarrollo y caracterización de la formulación magistral de etanol inhalado previo a su uso en el ensayo clínico fase II. En los momentos iniciales de la pandemia no existían tratamientos eficaces aprobados, por ello desde la farmacia hospitalaria se propuso el empleo del etanol elaborado como formulación magistral para su administración inhalada como antiséptico en pacientes mayores, para los cuales muchos de los tratamientos empleados en fases iniciales de la pandemia estaban contraindicados.

Se desarrolla y caracteriza una formulación de etanol 65° inhalado, que demostró ser estable a temperatura ambiente y protegida de la luz durante 15 días, manteniendo sus propiedades fisicoquímicas y microbiológicas. Además, se estudió cuál sería su flujo de oxígeno óptimo necesario para una adecuada administración de 3 veces al día, durante un total de 15 minutos por inhalación. Para ello se ensayaron los flujos de 2 y 3 L/min mediante una técnica automatizada de análisis cromatográfico de gases en espacio de cabeza (HS-GC-MS). A 2 L/min, las concentraciones medias de etanol emitidas fueron de 51,5 ± 4,5 mg/L, frente a las observadas a 3 L/min, que resultaron ser de 39,9 ± 5,7 mg/L durante los 45 min de tratamiento. Teniendo en cuenta el volumen respiratorio por minuto de 5 L/min para humanos adultos, y la relación inhalación:exhalación de 1:2, las cantidades medias estimadas de etanol inhalado fueron de 33,6 ± 3,6 mg/min y 40,0 ± 5,7 mg/min a 2 L/min y 3 L/min, respectivamente. Con esto se deduce que se emite una



USC UNIVERSIDADE DE SANTIAGO DE COMPOSTELA

mayor cantidad de etanol en gramos con el flujo de 3 L/min, aunque las concentraciones son mayores y más estables a 2 L/min, siendo este el flujo finalmente seleccionado en el ensayo clínico.

Además, se realizó un estudio preclínico de seguridad toxicológica en ratas, donde se administró la formulación durante un total de 5 días, analizando posteriormente muestras de vías respiratorias y pulmones, a partir de lo cual se demostró la ausencia de daños histológicos a este nivel. Por otra parte, se radiomarcó el etanol y se procedió a su administración mediante insuflaciones endotraqueales para el estudio de su farmacocinética en ratas mediante PET/TC. Con ello fue posible visualizar una localización inicial del etanol en vías respiratorias y pulmones, para alcanzar posteriormente una mayor señal a nivel hepático, principal órgano metabolizador del etanol. Por último, se llevó a cabo un estudio clínico preliminar en seis voluntarios sanos divididos en dos grupos (1:1), que fueron sometidos a la administración del etanol durante 15 minutos de oxigenoterapia a 2 L/min y 3 L/min a través de una mascarilla facial Ventimask®, a partir del cual no se observaron alteraciones en la frecuencia cardiaca, presión arterial ni saturación de oxígeno.

Tras el desarrollo y caracterización de la formulación magistral de etanol inhalado, se iniciaron los trámites para caracterizar su eficacia y seguridad mediante la realización de un ensayo clínico.

Los resultados del ensayo clínico fase II ALCOVID-19 (EudraCT: 2020-001760-29) se recogen en el **capítulo 5**. Se trata de un estudio aleatorizado, triple ciego y controlado con placebo en pacientes mayores COVID-19 positivo institucionalizados en un centro destinado al control de la infección en residencias sociosanitarias, llevado a cabo entre octubre de 2020 y marzo de 2021, es decir, en la segunda ola de la pandemia. Los pacientes debían encontrarse en la fase inicial de la enfermedad, con < 7 días de síntomas, ausencia de disnea y neumonía, saturación de oxígeno en aire ambiente > 93% o presión parcial de oxígeno > 70 mmHg y frecuencia respiratoria < 25 por minuto.

Se incluyeron a un total de 75 pacientes que recibieron tratamiento (1:1) con etanol 65° por vía inhalada a través de Ventimask® mediante un flujo de oxígeno a 2 L/min cada 8 horas, a 15 minutos por inhalación, durante un total de 5 días en el grupo experimental, mientras que en el grupo placebo se administró agua destilada. De forma concomitante se administró el tratamiento recomendado en ese momento por el Ministerio de Sanidad para la COVID-19. El objetivo general fue evaluar la progresión a estadios de mayor gravedad mediante la Escala de Progresión Clínica de la Organización Mundial de la Salud (OMS). Los objetivos específicos de eficacia fueron la evolución de la temperatura corporal, uso de antipiréticos, saturación de oxígeno, carga viral evaluada por el umbral de ciclo (Ct) en la reacción en cadena



USC UNIVERSIDADE DE SANTIAGO DE COMPOSTELA

de la polimerasa en tiempo real (RT-PCR), marcadores bioquímicos de progresión y el uso de antibióticos o corticoides. Los objetivos específicos de seguridad fueron la ausencia de etanol en plasma y de alteraciones electrocardiográficas, analíticas o respiratorias.

Tras 28 días de seguimiento, no se observaron diferencias relativas a la progresión de la enfermedad en ninguna de las visitas de estudio en la población por intención de tratar. Un total de 7 pacientes (19,4%) del grupo etanol y 6 (16,7%) del grupo placebo precisaron ingreso hospitalario durante una media de 10,5 (DE: 7,1) días en el grupo etanol y 8,5 (DE: 8,5) en el grupo placebo. La mediana de tiempo desde la inclusión en el estudio hasta la hospitalización fue de 6 días (RIQ: 3,0-9,0) y 6,5 días (RIQ: 4,0-7,0), respectivamente. Ninguna de estas diferencias fue significativa. Dos pacientes fallecieron en cada grupo. Los valores obtenidos de temperatura corporal, uso de antipiréticos y saturación de oxígeno fueron similares en ambos grupos.

La carga viral disminuyó a lo largo del transcurso del estudio en ambos grupos, tanto en el análisis conjunto de los genes N, E y RdRP como teniendo en cuenta el gen N, el más conservado, de forma individual. Los valores medios de Ct fueron numéricamente superiores en el grupo del etanol (menor carga viral) en la mayoría de las visitas, alcanzándose un valor superior a 33 sólo en el grupo etanol el día 14, corte por encima del cual los pacientes se consideran no infecciosos. La creatinina quinasa se redujo en mayor medida en el grupo etanol (36.08% versus 11.65% ($p$ = 0.0020)), mientras que la proteína C reactiva se incrementó únicamente en el grupo placebo (50% ($p$ = 0.0379)). El uso de corticoides y antibióticos fue similar en ambos grupos. El etanol inhalado demostró ser seguro ya que no se detectaron niveles plasmáticos y no se produjeron alteraciones electrocardiográficas, analíticas ni respiratorias.

Se necesitan más estudios para obtener datos concluyentes y evaluar la eficacia y seguridad a largo plazo del etanol inhalado para la infección por SARS-CoV-2. Aún así, su mecanismo de acción inespecífico podría abrir la puerta a la evaluación de su uso en otras patologías respiratorias infecciosas, tras haber demostrado ser un tratamiento seguro.

En **conclusión**, en esta Tesis Doctoral se proponen dos formulaciones magistrales diferentes para abordar situaciones de vacío terapéutico. Por un lado, la formulación desarrollada de cisteamina al 0,55% en ácido hialurónico y envasada en innovadores sistemas monodosis pretende dar respuesta a la ausencia de tratamiento en la cistinosis ocular, y por otro, la formulación desarrollada de etanol inhalado al 65° pretende ofrecer una alternativa terapéutica en una enfermedad contagiosa de rápida aparición para la que no existía tratamiento previo, como fue el caso del COVID-19. Ambas representan la capacidad de la farmacia hospitalaria



USC UNIVERSIDADE DE SANTIAGO DE COMPOSTELA

en la contribución a la lucha frente a cada una de estas patologías, generando evidencia científica, favoreciendo el acceso a tratamiento en pacientes que no disponen de opciones terapéuticas y todo ello de una forma eficiente, práctica, y fácilmente trasladable a la práctica clínica.



USC UNIVERSIDADE DE SANTIAGO DE COMPOSTELA

USC
UNIVERSIDADE
DE SANTIAGO
DE COMPOSTELA

# INDEX

USC
UNIVERSIDADE
DE SANTIAGO
DE COMPOSTELA

USC
UNIVERSIDADE
DE SANTIAGO
DE COMPOSTELA

# INDEX

**OBJECTIVES AND ORGANIZATION ..... 1**

STATEMENT OF THE PROBLEM ..... 1

OBJECTIVES ..... 2

ORGANIZATION ..... 3

**INTRODUCTION ..... 7**

RESEARCH IN PHARMACEUTICAL COMPOUNDING ..... 7

CYSTINOSIS ..... 11

Treatment of cistinosis ..... 12
Cysteamine stability ..... 13
Cysteamine ophthalmic delivery systems ..... 14

SARS-CoV-2 INFECTION ..... 14

SARS-CoV-2 treatment and drug repurposing ..... 17
Inhaled ethanol treatment ..... 19

CONCLUDING REMARKS ..... 21

REFERENCES ..... 22

**CHAPTER 1 OCULAR BIODISTRIBUTION STUDIES USING MOLECULAR IMAGING ..... 37**

1. INTRODUCTION ..... 38

2. MOLECULAR IMAGING MODALITIES IN OPHTHALMIC DRUG DELIVERY STUDIES ..... 39

3. POSITRON EMISSION TOMOGRAPHY ..... 39

4. SPECT ..... 43

5. FLUORESCENCE ..... 47

6. MAGNETIC RESONANCE IMAGING ..... 48

7. OTHER IMAGING TECHNIQUES ..... 51

7.1. Ultrasonography ..... 51
7.2. Optical Coherence Tomography and Computed Tomography ..... 51

8. CONCLUSIONS ..... 53

9. REFERENCES ..... 53



USC UNIVERSIDADE DE SANTIAGO DE COMPOSTELA

**CHAPTER 2 RECENT RESEARCH IN OCULAR CYSTINOSIS: DRUG DELIVERY SYSTEMS, CYSTEAMINE DETECTION METHODS AND FUTURE PERSPECTIVES ..... 69**

1. INTRODUCTION ..... 70

2. DRUG DELIVERY SYSTEMS (DDSs) ..... 72

2.1. Hydrogels ..... 73
2.1.1. Synthetic Hydrogels ..... 73
2.1.2. Natural Hydrogels ..... 74
2.2. Nanowafers ..... 76
2.3. Contact Lenses ..... 76
2.3.1. Contact Lenses as Drug Delivery Systems ..... 76
2.3.2. Modified Contact Lenses ..... 77

3. STABILITY AND ANALYTICAL DETERMINATION METHODS ..... 80

3.1. Cysteamine Structure and Stability Properties ..... 80
3.2. Cysteamine Analytical Determination Methods ..... 81
3.2.1. High-Performance Liquid Chromatography (HPLC) ..... 81
3.2.2. Ion-Exchange Column Chromatography ..... 83
3.2.3. Enzymatic Essay ..... 83
3.2.4. Gas Chromatography ..... 83
3.2.5. Electrochemical Detection ..... 84

4. CURRENT SITUATION AND FUTURE PERSPECTIVES ..... 86

5. CONCLUSIONS ..... 88

6. REFERENCES ..... 89

**CHAPTER 3 CYSTEAMINE EYE DROPS IN HYALURONIC ACID PACKAGED IN INNOVATIVE SINGLE-DOSE SYSTEMS: STABILITY AND OCULAR BIOPERMANENCE ..... 103**

1. INTRODUCTION ..... 104

2. MATERIALS AND METHODS ..... 106

2.1. Materials ..... 106
2.2. Elaboration and Packaging of Cysteamine Hydrochloride Sterile Solutions ..... 106
2.3. Cysteamine and Cystamine Quantification ..... 107
2.4. Storage Stability Study ..... 108
2.4.1. Determination of pH and Osmolarity ..... 108
2.4.2. Viscosity Tests ..... 108
2.4.3. Microbiological Stability ..... 108
2.4.4. Statistical Analysis ..... 108
2.4.5. Elasticity of Single-Dose Containers ..... 109
2.5. In-Use Stability Study ..... 109
2.6. In Vivo Evaluation of the Residence Time on the Ocular Surface ..... 109

3. RESULTS ..... 110

3.1. Cysteamine and Cystamine Quantification ..... 110



USC UNIVERSIDADE DE SANTIAGO DE COMPOSTELA

3.2. Storage Stability Study ..... 111
3.2.1. pH and Osmolality ..... 112
3.2.2. Viscosity tests ..... 113
3.2.3. Microbiological Stability ..... 114
3.2.4. Elasticity of Single-Dose Containers ..... 114
3.3. In-Use Stability Study ..... 115
3.4. In Vivo Evaluation of the Residence Time on the Ocular Surface ..... 115
4. DISCUSSION ..... 118
5. CONCLUSIONS ..... 122
6. REFERENCES ..... 123
7. SUPPLEMENTARY MATERIAL ..... 131

**CHAPTER 4 DEVELOPMENT AND CHARACTERIZATION OF INHALED ETHANOL AS A NOVEL PHARMACOLOGICAL STRATEGY CURRENTLY EVALUATED IN A PHASE II CLINICAL TRIAL FOR EARLY-STAGE SARS-COV-2 INFECTION ..... 137**

1. INTRODUCTION ..... 138
2. MATERIALS AND METHODS ..... 140
2.1. Preparation of the 65° Ethanol Solution and Stability Determination in Disposable Humidifying Bottles ..... 140
2.2. Determination of Ethanol in the Administered Oxygen Flow ..... 141
2.3. Preclinical Studies ..... 142
2.3.1. Ethanol Exposure Toxicological Studies and Immunohistochemical Analysis ..... 142
2.3.2. Preclinical Pharmacokinetics ..... 143
3. RESULTS ..... 145
3.1. Stability of the 65° Ethanol Pharmaceutical Compounding and Flow Oxygen Effect ..... 145
3.2. Preclinical Studies ..... 149
3.2.1. Ethanol Exposure Toxicological Studies and Immunohistochemical Analysis ..... 149
3.2.2. Pharmacokinetics ..... 150
4. DISCUSSION ..... 152
5. CONCLUSIONS ..... 155
6. REFERENCES ..... 155
7. SUPPLEMENTARY MATERIAL ..... 161

**CHAPTER 5 EFFICACY AND SAFETY OF INHALED ETHANOL IN EARLY-STAGE SARS-COV-2 INFECTION IN OLDER ADULTS: A PHASE II RANDOMIZED CLINICAL TRIAL ..... 165**

1. INTRODUCTION ..... 166
2. MATERIALS AND METHODS ..... 166



USC UNIVERSIDADE DE SANTIAGO DE COMPOSTELA

2.1. Trial Design ..... 166
2.2. Trial Patients ..... 167
2.3. Randomization and Intervention ..... 167
2.4 Data Collection ..... 168
2.5 Trial End Points ..... 169
2.5.1. General Outcome ..... 169
2.5.2. Specific Effectiveness Outcomes ..... 169
2.5.3. Specific Safety Outcomes ..... 169
2.6. Early Trial Termination ..... 170
2.7. Statistical Analysis ..... 170

3. RESULTS ..... 170

3.1. Trial Population ..... 170
3.2. General Outcome ..... 172
3.3. Specific Effectiveness Outcomes ..... 173
3.3.1. Oxygen Saturation, Temperature, and Antipyretic Treatment Administration ..... 173
3.3.2. Evolution of Viral Load ..... 173
3.3.3. Biomarkers Associated with COVID-19 Disease Progression ..... 174
3.3.4. Use of Corticosteroids and Antibiotics ..... 175
3.4. Specific Safety Outcomes ..... 175
3.4.1. Determination of Systemic Absorption of Ethanol ..... 175
3.4.2. Electrocardiogram and Ethanol toxicity Biomarkers ..... 175
3.4.3. Occurrence of Adverse Effects ..... 175

4. DISCUSSION ..... 176

5. REFERENCES ..... 178

6. SUPPLEMENTARY MATERIAL ..... 183

**CONCLUSIONS ..... 195**

**APPENDIX ..... 209**

CONFLICT OF INTEREST ..... 209

ANIMAL EXPERIMENTS ..... 209

CLINICAL STUDY ..... 209

FUNDING AND ACKNOWLEDGEMENTS ..... 210

ARTICLES DERIVED FROM THIS THESIS ..... 210

FIGURES AUTHORSHIP ..... 214

RESOLUCIÓN DE AUTORIZACIÓN DE PROXECTOS DE EXPERIMENTACIÓN ANIMAL ..... 215

DICTAMEN DEL COMITÉ DE ÉTICA DE LA INVESTIGACIÓN CON MEDICAMENTOS DE GALICIA ..... 217

RESOLUCIÓN DE LA SOLICITUD DE AUTORIZACIÓN DE UN ENSAYO CLÍNICO ..... 221



USC UNIVERSIDADE DE SANTIAGO DE COMPOSTELA

# OBJECTIVES AND ORGANIZATION

USC
UNIVERSIDADE DE SANTIAGO DE COMPOSTELA

USC
UNIVERSIDADE
DE SANTIAGO
DE COMPOSTELA

# OBJECTIVES AND ORGANIZATION

## STATEMENT OF THE PROBLEM

There are scenarios in daily clinical practice in which patients do not have adequate treatments for the management of their pathologies, or these are not easily accessible. In these situations, hospital pharmacy has a very important role to play in offering therapeutic alternatives as pharmaceutical compounding. These situations occur in the case of diseases such as ocular cystinosis and SARS-CoV-2 infection.

The first part of this Thesis was focused on the development of a compounded formulation intended for the treatment of cystinosis, a rare disease in which cystine crystals are deposited in the cornea. The current and only treatment that has proven to be effective for its management is the instillation of cysteamine eye drops. However, commercial presentations are not always available in most countries, since they are marketed as orphan drugs, requiring a demanding evaluation process and complex administrative procedures. In the development of new cysteamine ophthalmic formulations, it is important to consider several factors, such as preventing oxidation of the active ingredient and avoiding the uncomfortable dosing schedules that a low ocular biopermanence would require. The use of new marketed monodose packaging systems would allow to store the formulation at low temperatures for longer periods of time, using only one single-dose container per day. In this way, it would be possible to dispense treatment for longer periods from the hospital pharmacy departments, avoiding frequent visits to the hospital. In addition, the use of vehicles that increase ocular residence time, would extend the dosing interval evading the use of cumbersome posologies that would compromise patient adherence and reduce disease progression.

While experimental work was being carried out, the SARS-CoV-2 pandemic broke out. A new line of research was initiated from hospital pharmacy in order to contribute to disease research and provide a therapeutic alternative, representing the second part of this Thesis. Exploring and studying the potential of a new compounded formulation that would allow a rapid, practical, and effective translation to clinical practice, could offer an alternative treatment to deal with the infection in those patients for whom there were no available treatments. One group of patients with few therapeutic options during the second pandemic wave were



USC UNIVERSIDADE DE SANTIAGO DE COMPOSTELA

elderly patients, for whom there were contraindications for most of the drugs used at that time. In addition to this therapeutic scarcity, there were a high morbidity and mortality rate in this population, for whom COVID-19 infection in the early stages of the pandemic, when vaccines had not yet been developed, caused devastating effects.

## OBJECTIVES

With these considerations in mind, the general objective of this Thesis is to offer treatment alternatives using pharmaceutical compounding to cover therapeutic gaps, as in the case of ocular cystinosis and early-stage SARS-CoV-2 infection.

In order to achieve these purposes, specific objectives linked to these lines of research were set, including:

1. To develop a new cysteamine ophthalmic compounded formulation for the treatment of ocular cystinosis.
    1.1. To understand the applicability of molecular imaging techniques in ocular biodistribution studies prior to its use for the development of a cysteamine ophthalmic formulation.
    1.2. To identify the main factors affecting cysteamine stability and quantification, the latest developments in cysteamine delivery systems and new research lines in cystinosis.
    1.3. To design, optimize, and characterize physiochemically an ophthalmic compounded formulation of 0.55% cysteamine.
    1.4. To characterize the stability of the formulation preserved at two different temperatures, with and without nitrogen saturation, as well as its stability in use.
    1.5. To evaluate the residence time *in vivo* on the ocular surface of the cysteamine ophthalmic formulation.
2. To develop a new inhaled ethanol compounded formulation intended for the treatment of early-stage SARS-CoV-2 infection.
    2.1. To design, optimize, and characterize physiochemically of an inhaled compounded formulation of 65° ethanol at two different oxygen flows.
    2.2. To characterize the stability of the developed formulation.
    2.3. To evaluate the histological toxicity and the pharmacokinetics *in vivo* of the developed formulation.



USC UNIVERSIDADE DE SANTIAGO DE COMPOSTELA

2.4. To evaluate the clinical efficacy and safety of the inhaled ethanol compounded formulation in SARS-CoV-2-infected patients through a phase II clinical trial.

**ORGANIZATION**

According to the established objectives, this Doctoral Thesis is presented as a reproduction of publications consisting of three original papers and two review articles arranged as chapters. The organization of this Doctoral Thesis complies with the regulations of the International Doctorate School at the University of Santiago de Compostela (Spain) regarding the structure of the work, language, and ethics and intellectual property rights.

The present Doctoral Thesis is divided into two main sections corresponding to the development and characterization of the two proposed compounded formulations.

**The first section** focuses on the development and characterization of an ophthalmic compounded formulation of cysteamine for the treatment of ocular cystinosis. It is divided into three chapters, from Chapter 1 to Chapter 3.

**Chapter 1** aims to provide an overview of ocular biodistribution studies using molecular imaging techniques published to date, prior to their application in pharmaceutical compounding development. These techniques provide reliable pharmacokinetic data on the administration of drugs and vehicles through the different ocular routes of administration.

**Chapter 2** comprises a bibliographic review prior to the cysteamine compounded formulation development, highlighting the etiology of the disease, the limitations related to stability and methods of cysteamine and cystamine determination, cysteamine already marketed formulations and alternative formulations under investigation, as well as future perspectives regarding the treatment of the disease.

**Chapter 3** is based on the design, elaboration, and characterization of a cysteamine ophthalmic compounded formulation in hyaluronic acid packaged in innovative single-dose systems. Two storage temperature conditions have been compared, refrigerator and freezer, as well as nitrogen saturation. Chemical stability, microbiological stability, pH, osmolality, viscosity, and package elasticity tests were made. Stability in-use with vial opening at room temperature was also studied and *in vivo* residence time on the ocular surface was evaluated.



USC UNIVERSIDADE DE SANTIAGO DE COMPOSTELA

**The second section** of the present Thesis focuses on the study of an alternative therapeutic option for the treatment of COVID-19 in the early stages of the pandemic, with the use of inhaled ethanol in initial mild disease. It is divided in two chapters, Chapter 4 and Chapter 5.

**Chapter 4** was aimed to develop, optimize, and characterize an inhaled ethanol 65° compounded formulation intended for the treatment of SARS-CoV-2 infection. Its physicochemical and microbiological stability data are accompanied by the study of its administration at two different oxygen flow rates. These results are accompanied by toxicological and pharmacokinetic preclinical data.

**Chapter 5** is based on the ALCOVID-19 phase II clinical trial, which aimed to evaluate the safety and efficacy of inhaled ethanol in elderly patients with mild COVID-19. The general endpoint was disease progression, while specific efficacy outcomes were evolution of body temperature, oxygen saturation, viral load, analytical biomarkers, and the use of antibiotic or corticosteroid treatments. Specific safety outcomes were the absence of ethanol in plasma, electrographic, analytical, or respiratory alterations.



USC UNIVERSIDADE DE SANTIAGO DE COMPOSTELA

# INTRODUCTION

USC
UNIVERSIDADE
DE SANTIAGO
DE COMPOSTELA

USC
UNIVERSIDADE
DE SANTIAGO
DE COMPOSTELA

# INTRODUCTION

## RESEARCH IN PHARMACEUTICAL COMPOUNDING

Up to 80% of the hospital pharmacy departments (HPD) prepare **individualized drugs** adapted to the characteristics of each patient on a daily basis (Fig. 1). This is one of the areas with the greatest health care burden in HPD and must therefore be modernized and adapted to current health care demands. To achieve this goal, it is necessary to maintain an appropriate balance between innovation, the translation of research results to health care, and regulation [1,2].

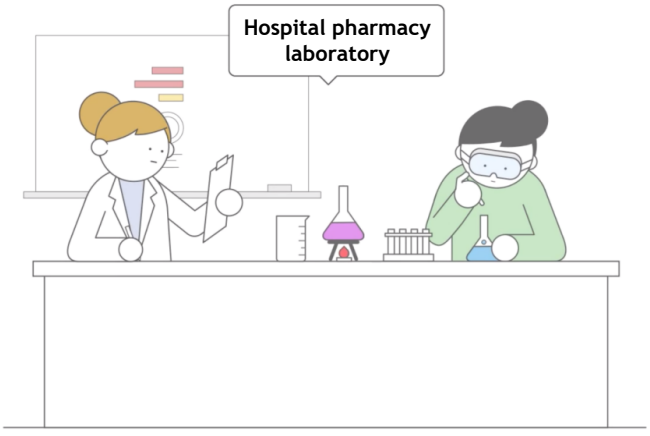



**Figure 1.** Drug compounding in hospital pharmacy departments.

One of the scenarios in which galenic research would have a special role to play is in the development of drugs to fill therapeutic gaps. A **compounded formulation** (CF) is defined as a drug prescribed by a physician for an individualized patient, prepared by or under the direction of the pharmacist, expressly to fulfill a prescription and dispensed in a pharmacy or pharmacy deportment [3]. This strategy would offer treatment alternatives to patients who are in a situation of a **therapeutic gap**, for whom there are no effective, available, or approved treatments. These circumstances occur relatively often, as in the case of **rare diseases** and pathologies whose **incidence shoots up abruptly** with no previously approved therapies, in which CF would facilitate their treatment.



USC UNIVERSIDADE DE SANTIAGO DE COMPOSTELA

**Rare diseases** (RD) affect fewer than 5 people per 10,000 inhabitants, with up to 7,000 different diseases described [4]. Scientifically, these conditions are often poorly characterized pathophysiologically and lack a clear understanding of their biological pathways. Research in RD is scarce and is widely dispersed among research teams that are not always well coordinated. For this reason, diagnosis is sometimes delayed, or patients are never diagnosed, making it difficult to adopt preventive or therapeutic measures. A patient with a RD waits an average of 4 years for a diagnosis, in 20% of cases it takes 10 or more years to get a proper diagnosis. While diagnosis is delayed, the patient receives no support or treatment (29.37% of the cases), has received inadequate treatment (17.9% of the cases) or sees how his disease has worsened (31.26% of the cases) [4,5].

**Orphan drugs** are the therapeutic basis for RD and are regulated by Regulation (EC) No 141/2000 of the European Parliament and of the Council of 16 December 1999 on orphan medicinal products. This designation allows pharmaceutical companies to enjoy several incentives, such as the following: assistance with the protocol (scientific advice for designated orphan drugs) at a reduced price, commercial exclusivity for 10 years once marketing authorization is granted (other companies cannot market a similar drug for a period of 10 years after authorization), a reduced fee applied for marketing authorization applications, and the possibility of accessing support from EU and Member State programs and initiatives for research and development [6].

Despite these incentives, the **industry** is still reluctant to invest in drug development for the treatment of RD due to their **low profitability and high cost** of research and marketing. Innovative treatments are often unevenly available due to high cost, limited availability of reimbursement, lack of experience of treating physicians and lack of consensus treatment recommendations [7]. Only 15% of patients with RD use orphan drugs, while 51% of families have difficulty accessing these drugs [4]. This limited therapeutic options in many countries positions HPDs and their ability to elaborate CFs as a possible alternative that facilitates access to treatment for a significant number of patients and thus improve their quality of life.

**Ocular cystinosis** is one of these RD that can benefit from this strategy and thus offer a more accessible therapeutic alternative for patients when approved commercial treatments are not available. Cystinosis is a rare lysosomal disorder in which amino acid cystine crystals accumulate in tissues such as the cornea. To address its treatment, cysteamine eye drops are instilled, but commercial preparations are not available in most countries as access is sometimes delayed due to required procedures and licensing. In this case, HPDs are responsible for the elaboration of ophthalmic cysteamine compounded formulations as an alternative treatment [8].



USC UNIVERSIDADE DE SANTIAGO DE COMPOSTELA

Another scenario in which therapeutic alternatives are also scarce is the case of the emergence of a disease for which there were previously no approved treatments, as was the case of the **COVID-19 pandemic** outbreak. Its high rate of infection at initial stages of the pandemic, the threat of collapse of the healthcare system and the economic impact have led to research against the clock [9]. Science and innovation have attempted to provide a comprehensive response to COVID-19 from different approaches. In the field of **research**, trials, and programs to learn about the virus, investigation on the immune response, studies on the biology and behavior of the virus, search for possible drugs, stratification of patients according to the prognosis of the disease and exploration for new public health solutions to improve control of the pandemic stand out. In addition, **business projects** have also been promoted to develop products to prevent and alleviate COVID-19 [10]. The limited therapeutic arsenal in the initial stages of the pandemic, the scarcity of evidence on the treatments, and the urgent need for new effective drugs have resulted in the adoption of novel measures to facilitate and accelerate the **clinical trial authorization process** and classification of observational studies [11].

One of the approaches scientists and clinicians contemplated in COVID-19 research was **drug repositioning**, which is the identification of new therapeutic indications for already approved drugs. This strategy is gaining increasing interest compared to the traditional "de novo" drug discovery process and has several advantages. A repurposed drug has been shown to be safe enough in preclinical models and in humans that when early studies are completed, it is unlikely to fail in subsequent studies, at least from a safety standpoint. Second, the time to drug development can be shortened because most of the preclinical testing, safety assessments and, in some cases, formulation development are already done. Third, less investment is required, although this will vary widely depending on the stage and development process of the candidate [12,13]. This strategy, together with CF, would open a door to offer a treatment opportunity to those patients in a situation of therapeutic gap.

Prior to the development these compounded formulations, several factors must be considered. In clinical practice, it is frequent to elaborate a new compounded formulation based on **bibliographic data**, but sometimes there is not enough homogeneity in the elaboration process and stability studies are not always carried out. Usually, when there is no information available on a particular formulation, it is necessary to resort to the “Spanish Guidelines for Good Compounding Practices in Hospital Pharmacy” to assign the expiration date [14]. Several factors like preparation process, route of administration, number of units prepared and susceptibility to microbiological contamination, among others, are considered to establish the period of validity. Even so, these guidelines **do not contemplate the nature of the active ingredient**, so that it is still necessary to perform appropriate stability studies for a correct characterization of its chemical, physical and



USC UNIVERSIDADE DE SANTIAGO DE COMPOSTELA

microbiological parameters, both of the active ingredient and of the excipients and packaging materials [15].

In addition to these classical galenic assays, a complete characterization of the new formulations would be achieved by **reliable pharmacokinetic data**. To this end, new methods and technologies must be developed that allow us to obtain this information in systems as complex as the eyeball (Fig. 2), or with routes of administration that are difficult to sample, such as the inhaled route. In recent years, **molecular imaging techniques** have become a turning point for drug development and characterization because they are non-invasive and allow real-time quantitative determination of the distribution of compounds through *in vivo* studies [16]. This technology is currently applied in healthcare practice for diagnosis and treatment, with enormous potential in the field of research [17]. On this basis, molecular imaging techniques have been developed in our research group, from which the pharmacokinetics of topical ophthalmic [18,19], intravitreal [20,21], rectal [22], and vaginal [23] formulations, among others, have been successfully characterized through preclinical studies.

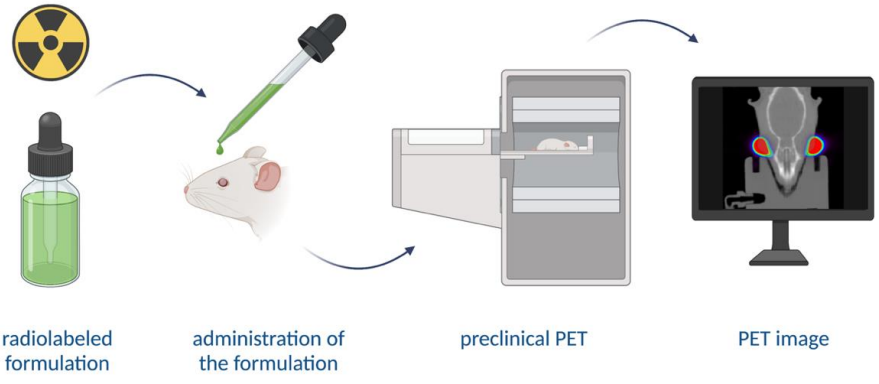



**Figure 2.** Administration of the radiolabeled formulation in rats for subsequent positron emission tomography (PET) study to determine its ocular pharmacokinetics. Created with BioRender.com.

The **role of hospital pharmacy in research** was often limited to coordinating the distribution of investigational drugs for clinical trials. However, in recent years, many hospital pharmacists have become more directly involved in research, as principal or co-investigators for pharmacokinetic studies, drug-drug interaction studies, real-world studies, randomized clinical trials, stability studies and drug development [24]. Despite increasing growth in recent years, compounded formulation has not played a major role within the lines of research of the hospital



USC UNIVERSIDADE DE SANTIAGO DE COMPOSTELA

pharmacy departments. This situation is reflected with the number of papers published in the *Farmacia Hospitalaria* journal that fall under the topic of "drug development", which a counted for 9 out of a total of 99 publications between 2020 and 2021 [25]. Fortunately, recent efforts have been made in research in this field in recent years, allowing the consideration of the compounding formulation as a therapeutic alternative in situations of therapeutic gap, such as ocular cystinosis or SARS-CoV-2 respiratory infection.

## CYSTINOSIS

Cystinosis is considered a **rare autosomal recessive lysosomal disorder** affecting approximately 100,000–200,000 individuals in the general population [26,27]. It is caused by a defect in cystine externalization, with the consequent cystine crystals accumulation in lysosomes. Cystine is the disulfide of the amino acid cysteine, with low solubility in water. This accumulation process is caused by mutations in the *CTNS* (17p13) gene, which encodes cystinosin, the carrier that transports cystine out of lysosomes [28,29]. The presence of cystine crystals in various tissues can lead to progressive damage and dysfunction of multiple organs including pancreas, brain, thyroid, kidneys and eyes [30].

There are three different forms of cystinosis, which differ in age at manifestation and severity of the symptoms: **infantile nephropathic** cystinosis, the most common and severe form; **juvenile nephropathic** cystinosis, with later onset of symptoms and slower progression; and **non-nephropathic** cystinosis, with a mainly ocular manifestation, also known as adult form. The first symptoms in the infantile nephropathic form usually appear between 3 and 6 months of age, with polyuric-polydipsic syndrome and marked growth retardation due to generalized proximal tubular dysfunction accompanied by renal Fanconi syndrome. Juvenile cystinosis (<5% of patients) typically debut around 6-8 years of age with a milder form of proximal tubulopathy and/or proteinuria accompanied by nephrotic syndrome. Progression to renal failure occurs later than in the infantile form. In the absence of specific treatment, the disease progresses to end-stage renal failure before the age of 10 years [27,29].

**Ocular involvement** usually appears after the age of 3 years, while adults may usually remain asymptomatic and manifest only photophobia. The most reported ocular manifestation is the deposition of cystine crystals in the cornea, leading to blepharospasm, photophobia, corneal erosions, superficial punctuate keratopathy, and band keratopathy, but it can also affect other ocular structures, causing visual impairment and eventually blindness [29,31,32]. Early diagnosis and treatment of



USC UNIVERSIDADE DE SANTIAGO DE COMPOSTELA

ocular manifestations in children is critical. Thus, early onset and adherence to topical therapy have a significant impact on the progression.

### *Treatment of cistinosis*

Even though other treatment pathways are being studied, the aminothiol **cysteamine** remains the only approved drug for cystinosis treatment. It lowers intracellular levels of cystine by forming a cysteamine–cysteine mixed disulfide, which resembles lysine and leaves the lysosome using alternative cationic transporters (Fig. 3) [33,34].

The 2012 US Food and Drug Administration (FDA) approval of oral cysteamine (Cystagon®), followed by an extended-release formulation (Procysbi®) a few years later, revolutionized the treatment and prognosis of cystinosis [35–37]. However, systemic cysteamine has low bioavailability in the eye due to lack of corneal vascularization and must therefore be administered by ophthalmic route. Cystaran® 0.44% eye drops received FDA approval in 2012 as an orphan drug, requiring one drop in each eye every waking hour [38], complicating patient compliance. To improve this aspect, Cystadrops® 0.55% was subsequently approved by the European Medicines Agency (EMA) and FDA in 2017 and 2021 respectively [39,40], requiring a more convenient dosage, with an administration every 4 hours.

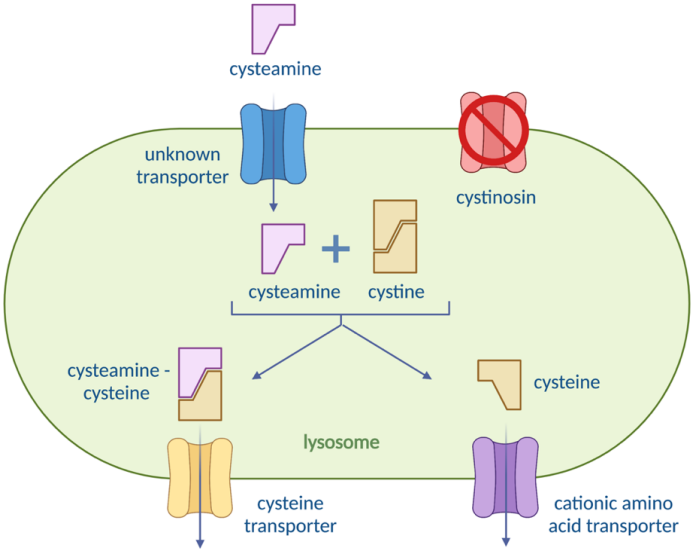



**Figure 3.** Mechanism of action of cysteamine after entry into lysosomes. Created with BioRender.com.



USC UNIVERSIDADE DE SANTIAGO DE COMPOSTELA

These commercial cysteamine eye drops are not available in most countries as access is sometimes delayed due to required procedures and licensing. In this case, the HPD is responsible for the production of ophthalmic cysteamine preparations as an alternative treatment [8]. For their elaboration it is necessary to take into account a series of characteristics and work methodology that make them suitable for their instillation in the eye, allowing them to achieve the desired purpose without causing damage [41,42]. In addition to these mandatory requirements, cysteamine formulations need to be developed with appropriate galenic properties studies before they can be transferred to clinical practice, being its extreme instability the main problem for its proper development [15,43].

### *Cysteamine stability*

Cysteamine is a readily oxidizable molecule and its air shelf life is shortened because the thiol functional group immediately reacts with oxygen to form a disulfide called cysteamine, which is ineffective in the treatment of cystinosis (Fig. 4) [15,26,44]. This process occurs rapidly in air and in solution [45]. Cysteamine instability is especially important to consider when developing new ophthalmic formulations, as it is essential to have a good determination method that allows its qualitative and quantitative detection, as well as the distinction of its major oxidative metabolite, cystamine.

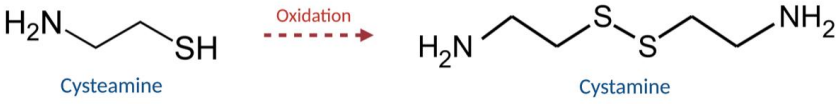



**Figure 4.** Oxidation reaction of cysteamine to the disulfide cystamine. Created with BioRender.com.

It has been shown that oxygen removal or addition of ascorbic acid can increase the stability of the cysteamine solution by filling it under nitrogen. However, this technique is less effective than chelating agents such as edetate disodium [46,47]. Also, it is important to consider the container, preferably using materials that prevent the passage of oxygen. Other strategies to increase stability have been used, such as lowering the pH (between 4.1 and 4.5) and freezing [48].

When developing new compounded formulations of ophthalmic cysteamine, it is necessary to consider in addition to excipients and physical conditions that increase stability, an adequate **biopermanence** that favors a comfortable posology and, therefore, patient adherence. For this purpose, suitable excipients that increase the



USC UNIVERSIDADE DE SANTIAGO DE COMPOSTELA

residence time of cysteamine on the ocular surface, without altering its stability, should be sought [8]. In this sense, the use of techniques that allow the study of ocular biodistribution and biopermanence, as is the case of **molecular imaging**, gains special relevance. For this purpose, an **exhaustive review of ocular biodistribution studies by molecular imaging** has been compiled to subsequently perform PET studies on the formulations under study.

*Cysteamine ophthalmic delivery systems*

Difficulties related to cysteamine stability, combined with the fact that cystinosis is a rare disease, mean that the development of cysteamine ophthalmic delivery systems is more limited than for other eye diseases. In addition to preventing cysteamine oxidation, new methods to **reformulate cysteamine** into corneal drug delivery systems to improve its stability and ocular bioavailability have been investigated. This would make dosing regimens more convenient and facilitate patient compliance. Over the past few decades, several research groups have focused on developing an optimal delivery system, and several strategies have been proposed to date.

The elaboration of the cysteamine formulation using different **hydrogels**, both synthetic and natural, have been described [8,32,49,49–52]. Transparent bioadhesive hydrogels showed to be highly desirable for topical ophthalmic application, facilitating controlled drug release and reducing administration frequency and, consequently, increasing therapeutic compliance [32]. Another explored alternative was the use of **contact lenses** as a drug delivery system. When placed over the eye, a thin layer of fluid is formed between the lens and the cornea, extending the time of contact between the drug and the cornea. The main limitation of this strategy is that polymers that make up the lenses and drugs have low affinity, leading to insufficient drug loading and too rapid delivery [53–56]. Another less explored alternative to achieve sustained cysteamine release was the use of **nanowafers** [57]. All these systems are described in more detail in **Chapter 2** of this Doctoral Thesis.

## SARS-CoV-2 INFECTION

The emergence of severe acute respiratory syndrome coronavirus 2 (SARS-CoV-2) triggered a devastating pandemic. In December 2019, SARS-CoV-2 was identified in Wuhan, China. Three months later, the World Health Organization (WHO) classified the outbreak as a pandemic. As of January 2023, three years after its first identification, it has officially and globally caused more than 650 million confirmed cases and 6,6 million deaths [58].



USC UNIVERSIDADE DE SANTIAGO DE COMPOSTELA

Coronavirus belongs to the subfamily *Coronavirinae* in the family of Coronaviridae. **Viral structure** knowledge is critical for the development of novel treatments and vaccines. The genome of CoVs (27–32 kb) is a single-stranded positive-sense RNA which is larger than any other RNA viruses. The nucleocapsid protein (N) forms a capsid outside the genome, which is further packed by an envelope associated with three structural proteins: the membrane protein (M), the spike protein (S), and the envelope protein (E) (Fig. 5) [59].

In the first step of the **SARS-CoV-2 life cycle**, the S protein on the outer surface is responsible for binding to host receptors or receptors attached to the cell membrane, followed by fusion of the virus with the host cell membrane, releasing viral genomic RNA into the cell. The host ribosome is then hijacked to produce two viral replicase polyproteins that can assemble into replication and transcription complexes to initiate viral RNA replication and transcription. Genomic RNA and structural proteins are then assembled into mature progeny virions, which are subsequently released by exocytosis, initiating another round of infection. Viral proteins may play important physiological roles individually, constitute viral protein machinery for specific fundamental events in the viral life cycle, or broadly interact with cellular factors in host immune responses and pathogenesis [60,61].

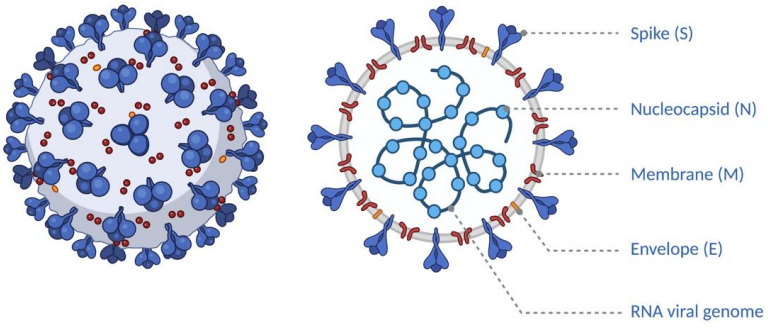



**Figure 5.** SARS-CoV-2 structure. Created with BioRender.com.

SARS-CoV-2 is **transmitted** by aerosols and droplets in unprotected close contact between infected and uninfected individuals, being symptomatic and asymptomatic patients the main source of infection. Droplets containing the virus access to the respiratory tract or contaminate the hands, and then people contact the mucous membranes of the mouth, nose and eyes and cause infection (Fig. 6), although transmission of SARS-CoV-2 is not limited to the respiratory tract [62]. The median incubation period is 4–5 days before symptom onset [63].

Most people infected with SARS-CoV-2 develop mild to moderate disease in which viral replication is primarily confined to the upper respiratory tract, experiencing



USC UNIVERSIDADE DE SANTIAGO DE COMPOSTELA

cough, fever, headache, myalgia, and diarrhea. Some patients develop **life-threatening pneumonia**, which usually begins approximately 1 week after symptom onset. In severe disease, the most common symptom is dyspnea followed by progressive respiratory failure and acute respiratory distress syndrome, defined as severe hypoxemia and bilateral radiographic opacities. In addition to respiratory disease, COVID-19 disease can also cause myocardial damage and arrhythmic complications, neurological complications such as myalgia, headache, dizziness, disturbance of consciousness, intracranial hemorrhage, loss of taste and smell and even stroke. Cases of asymptomatic infection have also been reported, but most asymptomatic patients have been ill since the date of diagnosis [62,64].

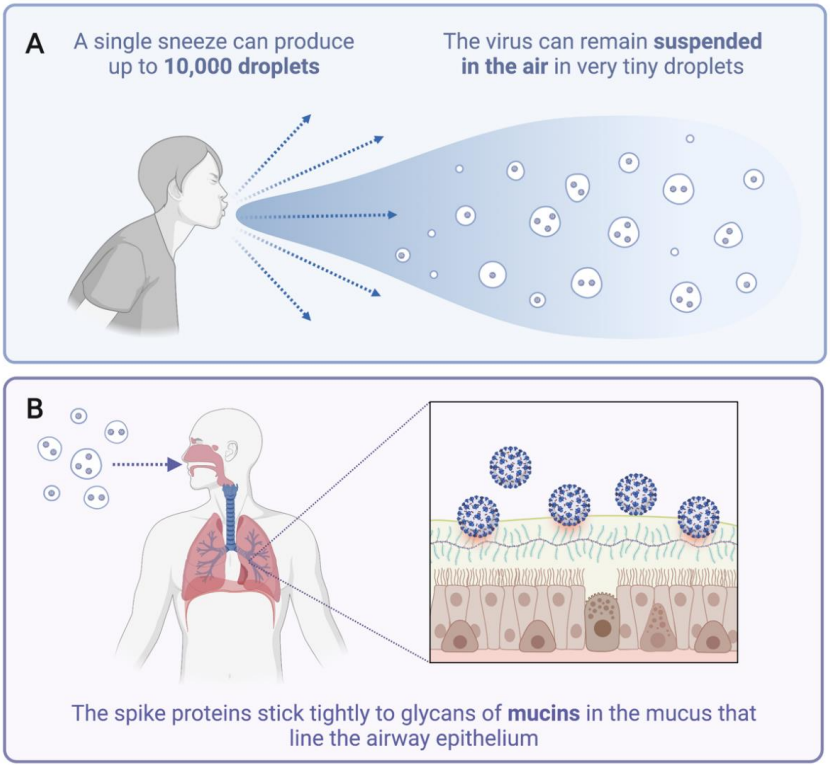



**Figure 6. A)** Airborne transmission of SARS-CoV-2 between individuals via droplets; **B)** Entry through the airways and adhesion to the respiratory epithelium. Created with BioRender.com.

Older age, obesity, and male sex are known **risk factors** for developing severe COVID-19. Common comorbidities include hypertension, heart failure, cardiac arrhythmias, diabetes, renal failure, and chronic lung disease. In addition, there is a genetic predisposition to develop severe COVID-19, which is instructive for understanding SARS-CoV-2 pathophysiology [60,62,64].



USC UNIVERSIDADE DE SANTIAGO DE COMPOSTELA

### *SARS-CoV-2 treatment and drug repurposing*

In the early stages of the COVID-19 pandemic outbreak, rapid spread and high mortality have forced the scientific community to **research against the clock** [11]. Compliance of control measures have restricted the transmission, even so, these actions have not been implemented uniformly, and have not shown to be enough to prevent the spread of the virus [65]. Serious efforts were made worldwide to provide therapeutic strategies to address established disease, many of them with little therapeutic success. In some cases, they have been the result of original research and, in others, a consequence of the repositioning of drugs designed for other indications [66,67], but only the rapid development of effective vaccines has been responsible for the paradigm shift of disease [68].

The **optimal approach** to treatment of COVID-19 is still evolving. Unlike the early days of the pandemic, when management decisions were based on extrapolation from *in vitro* data, case reports, and case series, clinicians today have a collection of therapies based on high-quality evidence. For patients with mild disease who are usually treated on an outpatient basis, the goal is to prevent progression and hospitalization. For hospitalized patients, the goal is to speed recovery and prevent complications and death. From the research conducted during these years of the pandemic it has been possible to conclude that, based on its pathogenesis, approaches that **target the virus** itself (e.g., antivirals, passive immunity, interferons) are more likely to work early in the course of infection, whereas strategies that **modulate the immune response** may have more impact later in the disease course (Fig. 7).

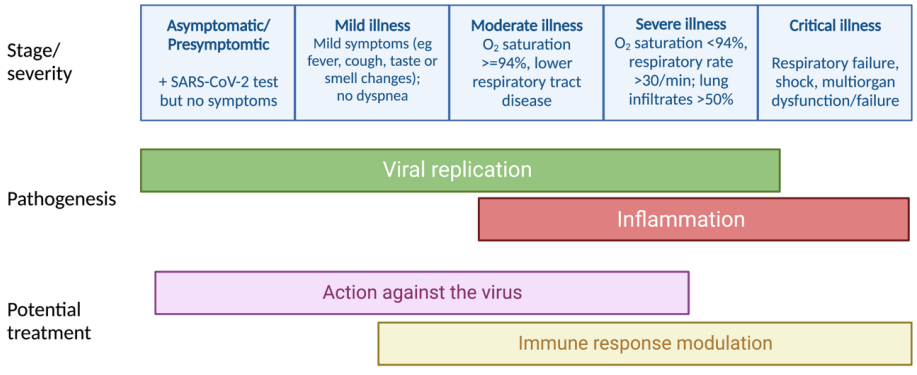



**Figure 7.** Therapeutic approaches to SARS-CoV-2 infection according to the different stages and severity of the disease [69]. Created with BioRender.com.



USC UNIVERSIDADE DE SANTIAGO DE COMPOSTELA

Multiple therapies have obtained emergency-use authorization (EUA) and, in some cases, approval from regulatory agencies as the FDA and the EMA. Fight **against viral structures or viral cycle** is especially important at the onset of infection. These treatments could be small molecules targeting the viral life cycle or antibodies against SARS-CoV-2, such as those found in convalescent plasma or monoclonal antibodies [69]. At the onset of the pandemic, there were no licensed antiviral agents for the treatment of this disease, so many therapies were used in clinical practice and were tested in clinical trials based on their *in vitro* activity. Nevertheless, many initially widely used drugs such as hydroxychloroquine, lopinavir or ritonavir, and ivermectin proved ineffective when studied in randomized clinical trials with adequate potency [70–72]. Better results have been obtained for remdesivir [73–75], nirmatrelvir-ritonavir [76] and molnupiravir [77].

**Anti-inflammatory drugs** may be more effective later in an infection, especially when the disease is caused by an over-amplified immune response and excessive inflammation [69]. Higher levels of acute phase reactants (e.g. ferritin) [78], proinflammatory cytokines (e.g. IL-6) [79] and markers of coagulation and fibrinolysis (e.g. D-dimer) have been associated with increased risk of death in COVID-19 patients [79,80]. The efficacy of **dexamethasone** was demonstrated by the Randomized Evaluation of COVID-19 Therapy (RECOVERY) group through the largest randomized clinical trial to date of glucocorticoids in patients with COVID-19 [81], where the results were positive in terms of mortality and corroborated by the WHO Rapid Evidence Appraisal for COVID-19 (REACT) Working Group [82]. **Tocilizumab** is a humanized monoclonal antibody against the IL-6 receptor, approved by the EMA for the treatment of SARS-CoV-2 infection. Early observational data suggest a survival benefit in hospitalized patients with COVID-19 receiving tocilizumab, especially when administered early in the disease course [83,84]. Subsequently, two large pragmatic randomized clinical trials showed a mortality benefit [85,86].

Antibodies play a key role in the adaptive immune response and are essential for protecting the host from pathogens. Passive administration of pathogen-specific polyclonal antibodies or monoclonal antibodies has been used to neutralize virus by targeting them and prevent its entry into host cells, thereby eliminating infection-associated disease [87]. Pathogen-specific neutralizing antibodies can be transduced from **patients who have recovered from viral infection** (i.e., convalescent plasma) or synthesized as **recombinant neutralizing mAbs** by established molecular engineering techniques. These neutralizing monoclonal antibodies are designed to target the SARS-CoV-2 receptor-binding spike protein, which mediates viral entry into host cells by binding to angiotensin-converting enzyme 2 (ACE2). Five **monoclonal antibody drugs** are currently approved by the EMA: sotrovimab, tixagevimab plus cilgavimab, regdanvimab, and casirivimab plus imdevimab [88].



USC UNIVERSIDADE DE SANTIAGO DE COMPOSTELA

In addition to these therapies, the use of **antithrombotic treatment** has also been shown to play an important role in this disease, as hospitalized patients with COVID-19 experience relatively high rates of morbid and potentially fatal haemostatic and thrombotic complications, particularly venous thromboembolism [89,90]. In addition, it is important to note that COVID-19-induced respiratory failure requires special consideration of the method of oxygen administration, the timing of intubation, and the use of prone position or adjuvant therapies for refractory hypoxemia [91].

As previously commented, **drug repositioning** is an efficient and rapid method to identify new uses of existing drugs with proven safety. Furthermore, this is a cost-effective way to treat disease outbreaks and several drugs have been successfully repurposed for SARS-CoV-2 treatment [92–101]. Proof of this is that numerous repurposed therapeutic molecules mentioned before have received emergency use authorization from the EMA, FDA and other regulatory agencies from various countries [91,102].

Using this strategy in conjunction with CF, **hospital pharmacy** could play an important role in the fight against COVID-19. Reformulation of previously approved drugs by adapting them to a new dosage or route of administration could **provide potential new treatment strategies** to reduce the transmission and prevent its progression to more severe stages. To date, some studies were intended for administration in the upper respiratory tract of previously approved drugs, as in the case of chlorhexidine [103], povidone-iodine [104], chloroquine [105], budesonide [106], and interferon beta-1a [107], among others.

### *Inhaled ethanol treatment*

The use of **antimicrobials** or **disinfectants** may have a place in the treatment of SARS-CoV-2, although the type of compound and route of administration must be chosen with great care, as the ultimate goal is to provide effective treatment without harming the patient. The biochemical characterization of SARS-CoV and MERS-CoV suggests that SARS-CoV-2 may be susceptible to disinfectants that have demonstrated activity against enveloped viruses. In this case, 0.1% sodium hypochlorite, 62-71° ethanol, and 0.5% hydrogen peroxide showed virucidal activity after one minute of contact with the virus [108,109].

It should be noted that **ethanol** used as a disinfectant should only be administered by topical dermal route due to the toxicity it can cause when administered by other routes. However, it is worth noting that ethanol is also used as an excipient/vehicle for drugs, both by the systemic route (e.g. Kaletra® solution contains 42% v/v ethanol) and by the inhalation route (inhaled salbutamol) [110–112]. On the other



USC UNIVERSIDADE DE SANTIAGO DE COMPOSTELA

hand, the use of ethanol by routes of administration other than those authorized is widely used in therapeutics as a compounded formulation, being used in catheter seals to prevent bacterial growth [113], in peripheral or central nervous blockade in terminal patients as neurolytic [114], in sclerotherapy of esophageal varices [115], in hemorrhage control in hepatocarcinoma surgery [116], debridement of corneal epithelium [117] or as an intravenous antidote in the treatment of antifreeze poisoning [118] (Fig. 8). Moreover, the use of ethanol by inhalation has also been used as a compounded formulation, and its use has been reported since 1956 for acute edema [119,120].

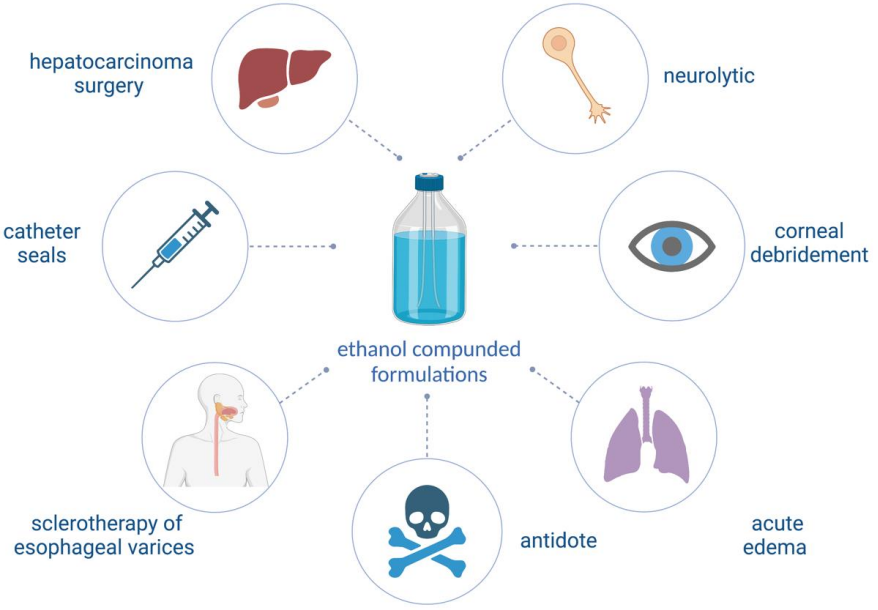



**Figure 8**. Uses of the ethanol compounded formulation. Created with BioRender.com.

Ethanol exerts its action at the level of the **viral envelope**, a lipid bilayer taken from the host cells in the assembly or budding stage of the viral life cycle, causing viral lysis with the consequent release and degradation of its contents [121]. In patients with mild disease, active virus was isolated in the throat and lungs only up to day 8 after the onset of symptoms, reaching peak viral load before day [122,123]. Thus, the administration of virucidal agents at the site of initial replication could reduce viremia in early stages of the infection and consequently, drastically reduce disease progression and improve prognosis.



USC UNIVERSIDADE DE SANTIAGO DE COMPOSTELA

## CONCLUDING REMARKS

Hospital pharmacy could play a very active and relevant role in offering therapeutic alternatives to patients who find themselves in a therapeutic gap. In this way, the development of compounded formulations from the galenic sections could provide therapeutic solutions for patients with rare diseases such as ocular cystinosis, as well as offering an alternative treatment for a respiratory infection that has never been seen before as COVID-19 (Fig. 9). This Doctoral thesis is focused on research and develop compounded formulations from the Hospital pharmacy departments to fill these therapeutic gaps. In both cases, prior to their use in humans, an adequate galenic characterization of the formulations is necessary to establish an adequate period of validity, as well as to study their pharmacokinetics through bioavailability studies that will allow to know their behavior once administered.

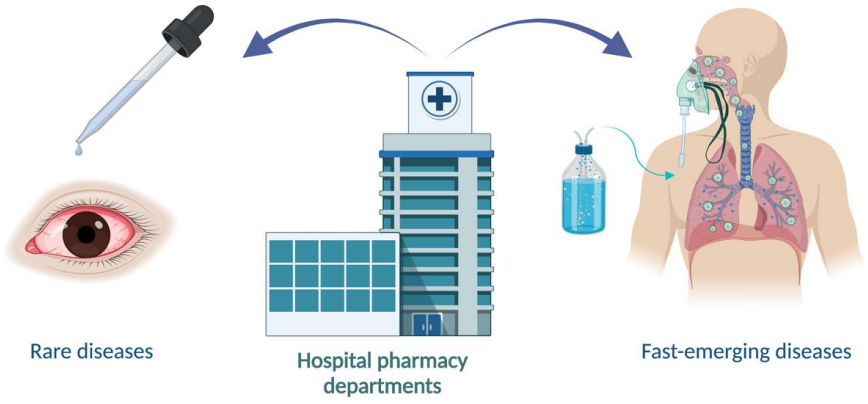



**Figure 9.** Development of compounded formulations from hospital pharmacy departments for the treatment of rare diseases as ocular cystinosis and fast-emerging pathologies as SARS-CoV-2 infection. Created with BioRender.com.



USC UNIVERSIDADE DE SANTIAGO DE COMPOSTELA

**REFERENCES**


1. Pérez-Encinas, M.; Lozano-Blázquez, A.; García-Pellicer, J.; Torre-Lloveras, I.; Poveda-Andrés, J.L.; Calleja-Hernández, M.Á. Encuesta Nacional de La SEFH-2019: Cartera de Servicios, Actividad Asistencial, Docencia e Investigación En Los Servicios de Farmacia Hospitalaria En España. *Farm. Hosp.* **2021**, 45, 32–40.

2. González Barcia, M.; Otero Espinar, F.J.; Mondelo García, C.; Fernández-Ferreiro, A. Elaboración de Medicamentos Personalizada En Los Servicios de Farmacia Hospitalaria:¿ Quo Vadis? *Revista de la OFIL* **2022**, 32, 87–88.

3. Ministerio de Sanidad y Consumo Real Decreto 175/2001, de 23 de Febrero, Por El Que Se Aprueban Las Normas de Correcta Elaboración y Control de Calidad de Fórmulas Magistrales y Preparados Oficinales; **2001**; Vol. BOE-A-2001-5185, pp. 9746–9755;.

4. Enfermedades Raras En Cifras | FEDER Available online: https://www.enfermedades-raras.org/enfermedades-raras/conoce-mas-sobre-er/enfermedades-raras-en-cifras (accessed on 5 January 2023).

5. Singulares Available online: https://www.enfermedades-singulares.com/public/ (accessed on 6 January 2023).

6. BOE.Es - DOUE-L-2000-80074 Reglamento (CE) No 141/2000 Del Parlamento Europeo y Del Consejo, de 16 de Diciembre de 1999, Sobre Medicamentos Huérfanos. Available online: https://www.boe.es/buscar/doc.php?id=DOUE-L-2000-80074 (accessed on 3 January 2023).

7. Cortés M., F. Las enfermedades raras. *Rev. Med. Clin. Condes.* **2015**, 26, 425–431.

8. Fernández-Ferreiro, A.; Luaces-Rodríguez, A.; Díaz-Tomé, V.; Gil-Martínez, M.; Ares, M.T.R.; Peralba, R.T.; Blanco-Méndez, J.; González-Barcia, M.; Otero-Espinar, F.J.; Lamas, M.J. Cysteamine ophthalmic hydrogel for the treatment of ocular cystinosis. *Farm. Hosp.* **2017**, 41, 678-687–687.

9. Li, H.; Zheng, S.; Liu, F.; Liu, W.; Zhao, R. Fighting against COVID-19: Innovative Strategies for Clinical Pharmacists. *Res. Social. Adm. Pharm.* **2021**, 17, 1813–1818.

10. Ministerio de Ciencia e Innovación. Gobierno de España. Investigaciones. Proyectos de Ciencia e Innovación Frente a La COVID-19 En España Available online: https://www.ciencia.gob.es/gl/Ministerio/Coronavirus/Investigaciones.html (accessed on 5 January 2023).




USC UNIVERSIDADE DE SANTIAGO DE COMPOSTELA

11. Castro-Balado, A.; Varela-Rey, I.; Bandín-Vilar, E.J.; Busto-Iglesias, M.; García-Quintanilla, L.; Mondelo-García, C.; Fernández-Ferreiro, A. Clinical Research in Hospital Pharmacy during the Fight against COVID-19. *Farm. Hosp.* **2020**, 44, 66–70.

12. Pushpakom, S.; Iorio, F.; Eyers, P.A.; Escott, K.J.; Hopper, S.; Wells, A.; Doig, A.; Guilliams, T.; Latimer, J.; McNamee, C.; et al. Drug Repurposing: Progress, Challenges and Recommendations. *Nat. Rev. Drug. Discov.* **2019**, 18, 41–58.

13. Breckenridge, A.; Jacob, R. Overcoming the Legal and Regulatory Barriers to Drug Repurposing. *Nat. Rev. Drug. Discov.* **2019**, 18, 1–2.

14. Guía de Buenas Prácticas de Preparación de Medicamentos En Servicios de Farmacia Hospitalaria. Ministerio de Sanidad Servicios Sociales e Igualdad. 2014. Available online: https://www.sefh.es/sefhpdfs/GuiaBPP_JUNIO_2014_VF.pdf (accessed on 5 January 2023)

15. Reda, A.; Van Schepdael, A.; Adams, E.; Paul, P.; Devolder, D.; Elmonem, M.A.; Veys, K.; Casteels, I.; van den Heuvel, L.; Levtchenko, E. Effect of Storage Conditions on Stability of Ophthalmological Compounded Cysteamine Eye Drops. *JIMD Rep.* **2017**, 42, 47–51.

16. Castro-Balado, A.; Mondelo-García, C.; González-Barcia, M.; Zarra-Ferro, I.; Otero-Espinar, F.J.; Ruibal-Morell, Á.; Aguiar-Fernández, P.; Fernández-Ferreiro, A. Ocular Biodistribution Studies Using Molecular Imaging. *Pharmaceutics* **2019**, 11, 237.

17. Sociedad Española de Radiofarmacia. ¿Qué es la Radiofarmacia? Available online: https://radiofarmacia.org/sobre-la-serfa/ (accessed on 28 December 2022).

18. García-Otero, X.; Mondelo-García, C.; González, F.; Perez-Fernandez, R.; Avila, L.; Antúnez-López, J.R.; González-Barcia, M.; Adan, A.; Aguiar, P.; Otero-Espinar, F.J.; et al. Anti-Inflammatory Effect of Tacrolimus/Hydroxypropyl-β-Cyclodextrin Eye Drops in an Endotoxin-Induced Uveitis Model. *Pharmaceutics* **2021**, 13, 1737.

19. Díaz-Tomé, V.; García-Otero, X.; Varela-Fernández, R.; Martín-Pastor, M.; Conde-Penedo, A.; Aguiar, P.; González-Barcia, M.; Fernández-Ferreiro, A.; Otero-Espinar, F.J. In Situ Forming and Mucoadhesive Ophthalmic Voriconazole/HPβCD Hydrogels for the Treatment of Fungal Keratitis. *Int. J. Pharm.* **2021**, 597, 120318.



USC UNIVERSIDADE DE SANTIAGO DE COMPOSTELA

20. Luaces-Rodríguez, A.; Del Amo, E.M.; Mondelo-García, C.; Gómez-Lado, N.; Gonzalez, F.; Ruibal, Á.; González-Barcia, M.; Zarra-Ferro, I.; Otero-Espinar, F.J.; Fernández-Ferreiro, A.; et al. PET Study of Ocular and Blood Pharmacokinetics of Intravitreal Bevacizumab and Aflibercept in Rats. *Eur. J. Pharm. Biopharm.* **2020**, 154, 330–337.

21. García-Otero, X.; Mondelo-García, C.; Bandín-Vilar, E.; Gómez-Lado, N.; Silva-Rodríguez, J.; Rey-Bretal, D.; Victoria Otero-Espinar, M.; Adan, A.; González-Barcia, M.; Aguiar, P.; et al. PET Study of Intravitreal Adalimumab Pharmacokinetics in a Uveitis Rat Model. *Int. J. Pharm.* **2022**, 627, 122261.

22. 22. Seoane-Viaño, I.; Gómez-Lado, N.; Lázare-Iglesias, H.; García-Otero, X.; Antúnez-López, J.R.; Ruibal, Á.; Varela-Correa, J.J.; Aguiar, P.; Basit, A.W.; Otero-Espinar, F.J.; et al. 3D Printed Tacrolimus Rectal Formulations Ameliorate Colitis in an Experimental Animal Model of Inflammatory Bowel Disease. *Biomedicines* **2020**, 8, 563.

23. Campaña-Seoane, M.; Pérez-Gago, A.; Vázquez, G.; Conde, N.; González, P.; Martinez, A.; Martínez, X.; García Varela, L.; Herranz, M.; Aguiar, P.; et al. Vaginal Residence and Pharmacokinetic Preclinical Study of Topical Vaginal Mucoadhesive W/S Emulsions Containing Ciprofloxacin. *Int. J. Pharm.* **2019**, 554, 276–283.

24. Tisdale, J.E. Research Conducted by Hospital Pharmacists: Integral Component of Daily Practice or Unrealistic Expectation? *Can. J. Hosp. Pharm.* **2018**, 71, 95–96.

25. SEFH | Revista de Farmacia Hospitalaria - Publicaciones Available online: https://www.sefh.es/revista-farmacia-hospitalaria.php?id=217&anio=2022 (accessed on 3 January 2023).

26. 26. Liang, H.; Labbé, A.; Baudouin, C.; Plisson, C.; Giordano, V. Long-Term Follow-up of Cystinosis Patients Treated with 0.55% Cysteamine Hydrochloride. *Br. J. Ophthalmol.* **2021**;105(5):608-613.

27. Orphanet: Cystinosis. Available online: https://www.orpha.net/consor/cgi-bin/Disease_Search.php?lng=ES&data_id=11&Disease_Disease_Search_diseaseGroup=cistinosis&Disease_Disease_Search_diseaseType=Pat&Enfermedad(es)/grupo%20de%20enfermedades=Cistinosis&title=Cistinosis&search=Disease_Search_Simple (accessed on 20 December 2022).

28. Cherqui, S.; Kalatzis, V.; Trugnan, G.; Antignac, C. The Targeting of Cystinosin to the Lysosomal Membrane Requires a Tyrosine-Based Signal and a Novel Sorting Motif. *J. Biol. Chem.* **2001**, 276, 13314–13321.



USC UNIVERSIDADE DE SANTIAGO DE COMPOSTELA

29. Bäumner, S.; Weber, L.T. Nephropathic Cystinosis: Symptoms, Treatment, and Perspectives of a Systemic Disease. *Front. Pediatr.* **2018**, 6, 58.

30. Syres, K.; Harrison, F.; Tadlock, M.; Jester, J.V.; Simpson, J.; Roy, S.; Salomon, D.R.; Cherqui, S. Successful Treatment of the Murine Model of Cystinosis Using Bone Marrow Cell Transplantation. *Blood* **2009**, 114, 2542–2552.

31. Nesterova, G.; Gahl, W.A. Cystinosis: The Evolution of a Treatable Disease. *Pediatr. Nephroly.* **2013**, 28, 51–59.

32. McKenzie, B.; Kay, G.; Matthews, K.H.; Knott, R.; Cairns, D. Preformulation of Cysteamine Gels for Treatment of the Ophthalmic Complications in Cystinosis. *Int. J. Pharm*. **2016**, 515, 575–582.

33. Andrzejewska, Z.; Nevo, N.; Thomas, L.; Chhuon, C.; Bailleux, A.; Chauvet, V.; Courtoy, P.J.; Chol, M.; Guerrera, I.C.; Antignac, C. Cystinosin Is a Component of the Vacuolar H+-ATPase-Ragulator-Rag Complex Controlling Mammalian Target of Rapamycin Complex 1 Signaling. *J. Am. Soc. Nephrol.* **2016**, 27, 1678–1688.

34. Pisoni, R.L.; Thoene, J.G.; Christensen, H.N. Detection and Characterization of Carrier-Mediated Cationic Amino Acid Transport in Lysosomes of Normal and Cystinotic Human Fibroblasts. Role in Therapeutic Cystine Removal? *J. Biol. Chem.* **1985**, 260, 4791–4798.

35. Gahl, W.A.; Kuehl, E.M.; Iwata, F.; Lindblad, A.; Kaiser-Kupfer, M.I. Corneal Crystals in Nephropathic Cystinosis: Natural History and Treatment with Cysteamine Eyedrops. *Mol. Gen. Metab*. **2000**, 71, 100–120.

36. Schneider, J.A. Approval of Cysteamine for Patients with Cystinosis. *Pediatr. Nephrol.* **1995**, 9, 254.

37. European Medicines Agency, 1997. Cystagon®. Prescribing Information. Available online: https://www.ema.europa.eu/en/medicines/human/EPAR/cystagon (accessed on 20 August 2022).

38. Food and Drug Administration, 2012. Cystaran®. Prescribing Information. Available online: https://www.accessdata.fda.gov/drugsatfda_docs/label/2012/200740s000lbl.pdf (accessed on 20 August 2022).

39. European Medicines Agency, 2016. Cystadrops®. Prescribing Information. Available online: https://www.ema.europa.eu/en/documents/product-



USC UNIVERSIDADE DE SANTIAGO DE COMPOSTELA

information/cystadrops-epar-product-information_es.pdf (accessed on 20 August 2022).

40. Food and Drug Administration, 2020. Cystadrops®. Prescribing Information. Available online: https://www.accessdata.fda.gov/drugsatfda_docs/label/2020/211302s000lbl.pdf (accessed on 20 August 2022).

41. Castro-Balado, A.; González-López, J.; Blanco-Mendez, J. Requerimientos Básicos Para La Elaboración de Colirios. In Formulación Magistral Oftálmica Antiinfecciosa; SEFH. Sociedad Española de Farmacia Hospitalaria, 2019; 63–70 ISBN 978-84-09-10764-3.

42. Castro-Balado, A.; Mondelo-García, C.; Zarra-Ferro, I.; Fernández-Ferreiro, A. New Ophthalmic Drug Delivery Systems. *Farm. Hosp.* **2020**, 44, 149–157.

43. Martín-Sabroso, C.; Alonso-González, M.; Fernández-Carballido, A.; Aparicio-Blanco, J.; Córdoba-Díaz, D.; Navarro-García, F.; Córdoba-Díaz, M.; Torres-Suárez, A.I. Limitations and Challenges in the Stability of Cysteamine Eye Drop Compounded Formulations. *Pharmaceuticals* **2022**, 15, 2.

44. Jimenez, J.; Washington, M.A.; Resnick, J.L.; Nischal, K.K.; Fedorchak, M.V. A Sustained Release Cysteamine Microsphere/Thermoresponsive Gel Eyedrop for Corneal Cystinosis Improves Drug Stability. *Drug Deliv. Transl. Res*. **2021**, 11, 2224–2238.

45. Atallah, C.; Charcosset, C.; Greige-Gerges, H. Challenges for Cysteamine Stabilization, Quantification, and Biological Effects Improvement. *J. Pharm. Anal.* **2020**, 10(6):499-516.

46. Purkiss, R. Stability of Cysteamine Hydrochloride in Solution. *J. Clin. Pharm. Ther*. **1977**, 2, 199–203.

47. Brodrick, A.; Broughton, H.M.; Oakley, R.M. The Stability of an Oral Liquid Formulation of Cysteamine. *J. Clin. Hosp. Pharm.* **1981**, 6, 67–70.

48. Dixon, P.; Powell, K.; Chauhan, A. Novel Approaches for Improving Stability of Cysteamine Formulations. *Int. J. Pharm.* **2018**, 549, 466–475.

49. Ross, M.; Mofford, J.; Tian, J.J.; Muirhead, B.; Hicks, E.A.; Sheardown, L.; Sheardown, H. Thermo-Responsive and Mucoadhesive Gels for the Treatment of Cystinosis. *Biomater. Adv.* **2023**, 144, 213235.



USC UNIVERSIDADE DE SANTIAGO DE COMPOSTELA

50. Buchan, B.; Kay, G.; Heneghan, A.; Matthews, K.H.; Cairns, D. Gel Formulations for Treatment of the Ophthalmic Complications in Cystinosis. *Int. J. Pharm.* **2010**, 392, 192–197.

51. Xia, L.-W.; Xie, R.; Ju, X.-J.; Wang, W.; Chen, Q.; Chu, L.-Y. Nano-Structured Smart Hydrogels with Rapid Response and High Elasticity. *Nat. Commun.* **2013**, 4, 2226.

52. Jimenez, J.; Resnick, J.L.; Chaudhry, A.B.; Gertsman, I.; Nischal, K.K.; DiLeo, M.V. Ocular Biodistribution of Cysteamine Delivered by a Sustained Release Microsphere/Thermoresponsive Gel Eyedrop. *Int. J. Pharm.* **2022**, 624, 121992.

53. Garcia-Millan, E.; Koprivnik, S.; Otero-Espinar, F.J. Drug Loading Optimization and Extended Drug Delivery of Corticoids from PHEMA Based Soft Contact Lenses Hydrogels via Chemical and Microstructural Modifications. *Int. J. Pharm.* **2015**, 487, 260–269.

54. Hsu, K.H.; Fentzke, R.C.; Chauhan, A. Feasibility of Corneal Drug Delivery of Cysteamine Using Vitamin E Modified Silicone Hydrogel Contact Lenses. *Eur. J. Pharm. Biopharm.* **2013**, 85, 531–540.

55. Dixon, P.; Fentzke, R.C.; Bhattacharya, A.; Konar, A.; Hazra, S.; Chauhan, A. In Vitro Drug Release and in Vivo Safety of Vitamin E and Cysteamine Loaded Contact Lenses. *Int. J. Pharm.* **2018**, 544, 380–391.

56. Liu, Z.; Kompella, U.B.; Chauhan, A. Gold Nanoparticle Synthesis in Contact Lenses for Drug-Less Ocular Cystinosis Treatment. *Eur. J. Pharm. Biopharm.* **2021**, 165, 271–278.

57. Marcano, D.C.; Shin, C.S.; Lee, B.; Isenhart, L.C.; Liu, X.; Li, F.; Jester, J.V.; Pflugfelder, S.C.; Simpson, J.; Acharya, G. Synergistic Cysteamine Delivery Nanowafer as an Efficacious Treatment Modality for Corneal Cystinosis. *Mol. Pharmaceutics* **2016**, 13, 3468–3477.

58. WHO Coronavirus (COVID-19) Dashboard Available online: https://covid19.who.int. (accessed on 20 August 2022)

59. Brian, D.A.; Baric, R.S. Coronavirus Genome Structure and Replication. In Coronavirus Replication and Reverse Genetics. *Curr. Top. Microbiol. Immunol*. **2005**; pp. 1–30 ISBN 978-3-540-26765-2.

60. Yang, H.; Rao, Z. Structural Biology of SARS-CoV-2 and Implications for Therapeutic Development. *Nat. Rev. Microbiol.* **2021**, 19, 685–700.



USC UNIVERSIDADE DE SANTIAGO DE COMPOSTELA

61. Harrison, A.G.; Lin, T.; Wang, P. Mechanisms of SARS-CoV-2 Transmission and Pathogenesis. *Trends. Immunol.* **2020**, 41, 1100–1115.

62. Wang, M.-Y.; Zhao, R.; Gao, L.-J.; Gao, X.-F.; Wang, D.-P.; Cao, J.-M. SARS-CoV-2: Structure, Biology, and Structure-Based Therapeutics Development. *Front. Cell. Infect. Microbiol.* **2020**, 10.

63. Lamers, M.M.; Haagmans, B.L. SARS-CoV-2 Pathogenesis. *Nat. Rev. Microbiol.* **2022**, 20, 270–284.

64. Forchette, L.; Sebastian, W.; Liu, T. A Comprehensive Review of COVID-19 Virology, Vaccines, Variants, and Therapeutics. *Curr. Med. Sci.* **2021**, 41, 1037–1051.

65. Baker, M.G.; Kvalsvig, A.; Verrall, A.J. New Zealand's COVID-19 Elimination Strategy. *Med. J. Aust.* **2020**;213(5):198-200.e1.

66. Majumder, J.; Minko, T. Recent Developments on Therapeutic and Diagnostic Approaches for COVID-19. *AAPS J.* **2021**, 23, 14.

67. Martín Sánchez, F.J.; Martínez-Sellés, M.; Molero García, J.M.; Moreno Guillén, S.; Rodríguez-Artalejo, F.J.; Ruiz-Galiana, J.; Cantón, R.; De Lucas Ramos, P.; García-Botella, A.; García-Lledó, A.; et al. Insights for COVID-19 in 2023. *Rev. Esp. Quimioter.* **2022**, martin13dec2022.

68. Zheng, C.; Shao, W.; Chen, X.; Zhang, B.; Wang, G.; Zhang, W. Real-World Effectiveness of COVID-19 Vaccines: A Literature Review and Meta-Analysis. *Int. J. Infect. Dis.* **2022**, 114, 252–260.

69. Gandhi, R.T. The Multidimensional Challenge of Treating Coronavirus Disease 2019 (COVID-19): Remdesivir Is a Foot in the Door. *Clin. Inf. Dis.* **2021**, 73, e4175–e4178.

70. Axfors, C.; Schmitt, A.M.; Janiaud, P.; van't Hooft, J.; Abd-Elsalam, S.; Abdo, E.F.; Abella, B.S.; Akram, J.; Amaravadi, R.K.; Angus, D.C.; et al. Mortality Outcomes with Hydroxychloroquine and Chloroquine in COVID-19 from an International Collaborative Meta-Analysis of Randomized Trials. *Nat. Commun.* **2021**, 12, 2349.

71. Arabi, Y.M.; Gordon, A.C.; Derde, L.P.G.; Nichol, A.D.; Murthy, S.; Beidh, F.A.; Annane, D.; Swaidan, L.A.; Beane, A.; Beasley, R.; et al. Lopinavir-Ritonavir and Hydroxychloroquine for Critically Ill Patients with COVID-19: REMAP-CAP Randomized Controlled Trial. *Intensive Care. Med.* **2021**, 47, 867–886.



USC UNIVERSIDADE DE SANTIAGO DE COMPOSTELA

72. Reis, G.; Silva, E.A.S.M.; Silva, D.C.M.; Thabane, L.; Milagres, A.C.; Ferreira, T.S.; dos Santos, C.V.Q.; Campos, V.H.S.; Nogueira, A.M.R.; de Almeida, A.P.F.G.; et al. Effect of Early Treatment with Ivermectin among Patients with Covid-19. *N. Engl. J. Med.* **2022**, 386, 1721–1731.

73. Gottlieb, R.L.; Vaca, C.E.; Paredes, R.; Mera, J.; Webb, B.J.; Perez, G.; Oguchi, G.; Ryan, P.; Nielsen, B.U.; Brown, M.; et al. Early Remdesivir to Prevent Progression to Severe Covid-19 in Outpatients. *N. Engl. J. Med.* **2022**, 386, 305–315.

74. Beigel, J.H.; Tomashek, K.M.; Dodd, L.E.; Mehta, A.K.; Zingman, B.S.; Kalil, A.C.; Hohmann, E.; Chu, H.Y.; Luetkemeyer, A.; Kline, S.; et al. Remdesivir for the Treatment of Covid-19 — Final Report. *N. Engl. J. Med.* **2020**, 383, 1813–1826.

75. WHO Solidaruty Trial Consortium. Remdesivir and Three Other Drugs for Hospitalised Patients with COVID-19: Final Results of the WHO Solidarity Randomised Trial and Updated Meta-Analyses. *Lancet* **2022**, 399, 1941–1953.

76. Hammond, J.; Leister-Tebbe, H.; Gardner, A.; Abreu, P.; Bao, W.; Wisemandle, W.; Baniecki, M.; Hendrick, V.M.; Damle, B.; Simón-Campos, A.; et al. Oral Nirmatrelvir for High-Risk, Nonhospitalized Adults with Covid-19. *N. Engl. J. Med.* **2022**, 386, 1397–1408.

77. Jayk Bernal, A.; Gomes da Silva, M.M.; Musungaie, D.B.; Kovalchuk, E.; Gonzalez, A.; Delos Reyes, V.; Martín-Quirós, A.; Caraco, Y.; Williams-Diaz, A.; Brown, M.L.; et al. Molnupiravir for Oral Treatment of Covid-19 in Nonhospitalized Patients. *N. Engl. J. Med.* **2022**, 386, 509–520.

78. Gupta, S.; Hayek, S.S.; Wang, W.; Chan, L.; Mathews, K.S.; Melamed, M.L.; Brenner, S.K.; Leonberg-Yoo, A.; Schenck, E.J.; Radbel, J.; et al. Factors Associated With Death in Critically Ill Patients With Coronavirus Disease 2019 in the US. *JAMA Intern. Med.* **2020**, 180, 1436–1447.

79. Del Valle, D.M.; Kim-Schulze, S.; Huang, H.-H.; Beckmann, N.D.; Nirenberg, S.; Wang, B.; Lavin, Y.; Swartz, T.H.; Madduri, D.; Stock, A.; et al. An Inflammatory Cytokine Signature Predicts COVID-19 Severity and Survival. *Nat. Med.* **2020**, 26, 1636–1643.

80. Short, S.A.P.; Gupta, S.; Brenner, S.K.; Hayek, S.S.; Srivastava, A.; Shaefi, S.; Singh, H.; Wu, B.; Bagchi, A.; Al-Samkari, H.; et al. D-Dimer and Death in Critically Ill Patients With Coronavirus Disease 2019. *Crit. Care. Med.* **2021**, 49, e500.



USC UNIVERSIDADE DE SANTIAGO DE COMPOSTELA

81. Group, T.R.C. Dexamethasone in Hospitalized Patients with Covid-19 — Preliminary Report. *N. Eng. J. Med.* **2020**.

82. The WHO Rapid Evidence Appraisal for COVID-19 Therapies (REACT) Working Group Association Between Administration of Systemic Corticosteroids and Mortality Among Critically Ill Patients With COVID-19: A Meta-Analysis. *JAMA* **2020**, 324, 1330–1341.

83. Gupta, S.; Wang, W.; Hayek, S.S.; Chan, L.; Mathews, K.S.; Melamed, M.L.; Brenner, S.K.; Leonberg-Yoo, A.; Schenck, E.J.; Radbel, J.; et al. Association Between Early Treatment With Tocilizumab and Mortality Among Critically Ill Patients With COVID-19. *JAMA Int. Med.* **2021**, 181, 41–51.

84. Guaraldi, G.; Meschiari, M.; Cozzi-Lepri, A.; Milic, J.; Tonelli, R.; Menozzi, M.; Franceschini, E.; Cuomo, G.; Orlando, G.; Borghi, V.; et al. Tocilizumab in Patients with Severe COVID-19: A Retrospective Cohort Study. *Lancet Rheumatol.* **2020**, 2, e474–e484.

85. Interleukin-6 Receptor Antagonists in Critically Ill Patients with Covid-19. *N. Engl. J. Med.* **2021**, 384, 1491–1502.

86. Abani, O.; Abbas, A.; Abbas, F.; Abbas, M.; Abbasi, S.; Abbass, H.; Abbott, A.; Abdallah, N.; Abdelaziz, A.; Abdelfattah, M.; et al. Tocilizumab in Patients Admitted to Hospital with COVID-19 (RECOVERY): A Randomised, Controlled, Open-Label, Platform Trial. *Lancet* **2021**, 397, 1637–1645.

87. Pantaleo, G.; Correia, B.; Fenwick, C.; Joo, V.S.; Perez, L. Antibodies to Combat Viral Infections: Development Strategies and Progress. *Nat. Rev. Drug Discov.* **2022**, 21, 676–696.

88. European Medicines Agency (EMA) COVID-19 Treatments Available online: https://www.ema.europa.eu/en/human-regulatory/overview/public-health-threats/coronavirus-disease-covid-19/treatments-vaccines/covid-19-treatments (accessed on 7 January 2023).

89. Al-Samkari, H.; Gupta, S.; Leaf, R.K.; Wang, W.; Rosovsky, R.P.; Brenner, S.K.; Hayek, S.S.; Berlin, H.; Kapoor, R.; Shaefi, S.; et al. Thrombosis, Bleeding, and the Observational Effect of Early Therapeutic Anticoagulation on Survival in Critically Ill Patients With COVID-19. *Ann. Intern. Med.* **2021**, 174, 622–632.

90. Al-Samkari, H.; Karp Leaf, R.S.; Dzik, W.H.; Carlson, J.C.T.; Fogerty, A.E.; Waheed, A.; Goodarzi, K.; Bendapudi, P.K.; Bornikova, L.; Gupta, S.; et al.



USC UNIVERSIDADE DE SANTIAGO DE COMPOSTELA

COVID-19 and Coagulation: Bleeding and Thrombotic Manifestations of SARS-CoV-2 Infection. *Blood* **2020**, 136, 489–500.

91. Murakami, N.; Hayden, R.; Hills, T.; Al-Samkari, H.; Casey, J.; Del Sorbo, L.; Lawler, P.R.; Sise, M.E.; Leaf, D.E. Therapeutic Advances in COVID-19. *Nat. Rev. Nephrol.* **2023**, 19, 38–52.

92. Dotolo, S.; Marabotti, A.; Facchiano, A.; Tagliaferri, R. A Review on Drug Repurposing Applicable to COVID-19. *Brief. Bioinform.* **2021**, 22, 726–741.

93. Yousefi H., Mashouri L., Okpechi SC., Alahari N., Alahari SK. Repurposing Existing Drugs for the Treatment of COVID-19/SARS-CoV-2 Infection: A Review Describing Drug Mechanisms of Action. *Biochem. Pharmacol.* **2021**, 183.

94. Aherfi, S.; Pradines, B.; Devaux, C.; Honore, S.; Colson, P.; Scola, B.L.; Raoult, D. Drug Repurposing against SARS-CoV-1, SARS-CoV-2 and MERS-CoV. *Future Microbio*l. **2021**, 16, 1341–1370.

95. Jeon, S.; Ko, M.; Lee, J.; Choi, I.; Byun, S.Y.; Park, S.; Shum, D.; Kim, S. Identification of Antiviral Drug Candidates against SARS-CoV-2 from FDA-Approved Drugs. *Antimicrob. Agents. Chemother.* **2020**, 64, e00819-20.

96. Yang, L.; Pei, R.-J.; Li, H.; Ma, X.-N.; Zhou, Y.; Zhu, F.-H.; He, P.-L.; Tang, W.; Zhang, Y.-C.; Xiong, J.; et al. Identification of SARS-CoV-2 Entry Inhibitors among Already Approved Drugs. *Acta Pharmacol. Sin.* **2021**, 42, 1347–1353.

97. Tsang, H.F.; Chan, L.W.C.; Cho, W.C.S.; Yu, A.C.S.; Yim, A.K.Y.; Chan, A.K.C.; Ng, L.P.W.; Wong, Y.K.E.; Pei, X.M.; Li, M.J.W.; et al. An Update on COVID-19 Pandemic: The Epidemiology, Pathogenesis, Prevention and Treatment Strategies. *Expert Rev. Anti. Infect. Ther.* **2021**, 19, 877–888.

98. Mouffak, S.; Shubbar, Q.; Saleh, E.; El-Awady, R. Recent Advances in Management of COVID-19: A Review. *Biomed. Pharmacother.* **2021**, 143, 112107.

99. Mølhave, M.; Agergaard, J.; Wejse, C. Clinical Management of COVID-19 Patients - An Update. *Semin. Nucl. Med.* **2022**, 52, 4–10.

100. Stasi, C.; Fallani, S.; Voller, F.; Silvestri, C. Treatment for COVID-19: An Overview. *Eur. J. Pharmacol.* **2020**, 889, 173644.

101. Thorlund, K.; Dron, L.; Park, J.; Hsu, G.; Forrest, J.I.; Mills, E.J. A Real-Time Dashboard of Clinical Trials for COVID-19. *Lancet Digit. Health* **2020**, 2, e286–e287.



USC UNIVERSIDADE DE SANTIAGO DE COMPOSTELA

102. Chakraborty, C.; Sharma, A.R.; Bhattacharya, M.; Agoramoorthy, G.; Lee, S.-S. The Drug Repurposing for COVID-19 Clinical Trials Provide Very Effective Therapeutic Combinations: Lessons Learned From Major Clinical Studies. *Front. Pharmacol.* **2021**; 12:704205.

103. Costa, D.D.; Brites, C.; Vaz, S.N.; de Santana, D.S.; Dos Santos, J.N.; Cury, P.R. Chlorhexidine Mouthwash Reduces the Salivary Viral Load of SARS-CoV-2: A Randomized Clinical Trial. *Oral Dis.* **2021**.

104. Zarabanda, D.; Vukkadala, N.; Phillips, K.M.; Qian, Z.J.; Mfuh, K.O.; Hatter, M.J.; Lee, I.T.; Rao, V.K.; Hwang, P.H.; Domb, G.; et al. The Effect of Povidone-Iodine Nasal Spray on Nasopharyngeal SARS-CoV-2 Viral Load: A Randomized Control Trial. *Laryngoscope* **2021**.

105. Thakar, A.; Panda, S.; Sakthivel, P.; Brijwal, M.; Dhakad, S.; Choudekar, A.; Kanodia, A.; Bhatnagar, S.; Mohan, A.; Maulik, S.K.; et al. Chloroquine Nasal Drops in Asymptomatic & Mild COVID-19: An Exploratory Randomized Clinical Trial. *Indian. J. Med. Res.* **2021**, 153, 151–158.

106. Ramakrishnan S, Nicolau DV Jr, Langford B, et al. Inhaled Budesonide in the Treatment of Early COVID-19 (STOIC): A Phase 2, Open-Label, Randomised Controlled Trial. *Lancet Respir. Med.* **2021**, 9 (7):763-772.

107. Monk, P.D.; Marsden, R.J.; Tear, V.J.; Brookes, J.; Batten, T.N.; Mankowski, M.; Gabbay, F.J.; Davies, D.E.; Holgate, S.T.; Ho, L.-P.; et al. Safety and Efficacy of Inhaled Nebulised Interferon Beta-1a (SNG001) for Treatment of SARS-CoV-2 Infection: A Randomised, Double-Blind, Placebo-Controlled, Phase 2 Trial. *Lancet Respir. Med.* **2021**, 9, 196–206.

108. Kampf, G. Efficacy of Ethanol against Viruses in Hand Disinfection. *J. Hosp. Infect.* 2018, **98**, 331–338.

109. Kampf, G.; Todt, D.; Pfaender, S.; Steinmann, E. Persistence of Coronaviruses on Inanimate Surfaces and Their Inactivation with Biocidal Agents. *J. Hosp. Infect.* **2020**, 104, 246–251.

110. Sweetman, S.C. Martindale: Guía Completa de Consulta Farmacoterapéutica; Pharma Editores, 2006; ISBN 978-84-95993-10-6.

111. Rowe, R.C.; Sheskey, P.; Quinn, M. Handbook of Pharmaceutical excipients; Libros Digitales - Pharmaceutical Press, 2009; ISBN 978-1-58212-135-2.

112. U.S. Pharmacopeia & National Formulary; United States Pharmacopeial Convention, Incorporated, 2006; ISBN 978-1-889788-47-0.



USC UNIVERSIDADE DE SANTIAGO DE COMPOSTELA

113. Opilla, M.T.; Kirby, D.F.; Edmond, M.B. Use of Ethanol Lock Therapy to Reduce the Incidence of Catheter-Related Bloodstream Infections in Home Parenteral Nutrition Patients. *.J Parente.r Enteral. Nutr.* **2007**, 31, 302–305.

114. Lipton, S. Pain Relief in Active Patients with Cancer: The Early Use of Nerve Blocks Improves the Quality of Life. *BMJ* **1989**, 298, 37–38.

115. Sarin, S.K.; Sachdeva, G.K.; Nanda, R.; Vij, J.C.; Anand, B.S. Endoscopic Sclerotherapy Using Absolute Alcohol. *Gut* **1985**, 26, 120–124.

116. Chung, S.C.; Lee, T.W.; Kwok, S.P.; Li, A.K. Injection of Alcohol to Control Bleeding from Ruptured Hepatomas. *BMJ* **1990**, 301, 421.

117. Yuksel, E.; Novruzlu, S.; Ozmen, M.C.; Bilgihan, K. A Study Comparing Standard and Transepithelial Collagen Cross-Linking Riboflavin Solutions: Epithelial Findings and Pain Scores. *J. Ocul. Pharmacol. Ther.* **2015**, 31, 296–302.

118. A Sepúlveda, R.; Selamé, E.; Roessler, E.; Tagle, R.; Valdivieso, A. Intoxicación Por Etilenglicol, Fisiopatología y Enfrentamiento Clínico. *Rev. Med. Chil.* **2019**, 147, 1572–1578.

119. Luisada, A.A.; Goldmann, M.A.; Weyl, R. Alcohol Vapor by Inhalation in the Treatment of Acute Pulmonary Edema. *Circulation* **1952**, 5, 363–369.

120. Zhang P; Yang Z; Zhao Y; Liu Y; Zhang L; Shao G Inhalation of Alcohol Vapor Driven by Oxygen Is a Useful Therapeutic Method for Postoperative Alcohol Withdrawal Syndrome in a Patient with Esophageal Cancer: A Case Report. - Abstract - Europe PMC Available online: https://europepmc.org/article/med/21511735 (accessed on 17 June 2020).

121. Nomura, T.; Nazmul, T.; Yoshimoto, R.; Higashiura, A.; Oda, K.; Sakaguchi, T. Ethanol Susceptibility of SARS-CoV-2 and Other Enveloped Viruses. *Biocontrol. Sci.* **2021**;26(3):177-180.

122. Baden, L.R.; Rubin, E.J. Covid-19 - The Search for Effective Therapy. *N. Engl. J. Med*. **2020**, 382, 1851–1852.

123. Wölfel, R.; Corman, V.M.; Guggemos, W.; Seilmaier, M.; Zange, S.; Müller, M.A.; Niemeyer, D.; Jones, T.C.; Vollmar, P.; Rothe, C.; et al. Virological Assessment of Hospitalized Patients with COVID-2019. *Nature* **2020**, 1–5.



USC UNIVERSIDADE DE SANTIAGO DE COMPOSTELA

USC
UNIVERSIDADE
DE SANTIAGO
DE COMPOSTELA

# CHAPTER 1

## OCULAR BIODISTRIBUTION STUDIES USING MOLECULAR IMAGING

USC
UNIVERSIDADE DE SANTIAGO DE COMPOSTELA

USC
UNIVERSIDADE
DE SANTIAGO
DE COMPOSTELA

# CHAPTER 1

## OCULAR BIODISTRIBUTION STUDIES USING MOLECULAR IMAGING


**ABSTRACT**

Classical methodologies used in ocular pharmacokinetics studies have difficulties to obtain information about topical and intraocular distribution and clearance of drugs and formulations. This is associated with multiple factors related to ophthalmic physiology, as well as the complexity and invasiveness intrinsic to the sampling. Molecular imaging is a new diagnostic discipline for in vivo imaging, which is emerging and spreading rapidly. Recent developments in molecular imaging techniques, such as positron emission tomography (PET), single-photon emission computed tomography (SPECT) and magnetic resonance imaging (MRI), allow obtaining reliable pharmacokinetic data, which can be translated into improving the permanence of the ophthalmic drugs in its action site, leading to dosage optimisation. They can be used to study either topical or intraocular administration. With these techniques it is possible to obtain real-time visualisation, localisation, characterisation and quantification of the compounds after their administration, all in a reliable, safe and non-invasive way. None of these novel techniques presents simultaneously high sensitivity and specificity, but it is possible to study biological procedures with the information provided when the techniques are combined. With the results obtained, it is possible to assume that molecular imaging techniques are postulated as a resource with great potential for the research and development of new drugs and ophthalmic delivery systems.



**Keywords:** ocular biodistribution; ocular permanence; molecular imaging; PET; SPECT; MRI





USC UNIVERSIDADE DE SANTIAGO DE COMPOSTELA

## 1. INTRODUCTION

The access of drugs to the ocular structures through the route of systemic administration is greatly hampered by the anatomical barriers that separate the eyeball from the general circulation. This makes it necessary to systemically administer high doses of drugs in order to reach therapeutic concentrations in the internal structures of the eye and the vitreous humour, which can cause toxicity and adverse effects [1]. Accordingly, topical application is considered the most suitable route of administration for the patient. This is due to the fact that the ocular surface is an easily accessible area, especially regarding pathologies affecting the anterior segment [2,3]. However, conventional ophthalmic dosage forms present a low ocular bioavailability due to the multiple barriers of the eye, such as the cornea, the conjunctiva, the retinal pigment epithelium and the dynamic barriers (tear replacement and blood and lymphatic drainage mechanisms). To improve topical administration in the anterior segment, several devices and systems for sustained drug release have been studied, such as polymers, colloidal systems, emulsions, cyclodextrins, collagen and contact lenses [4-8]. Studying and identifying new ophthalmic administration systems helps to improve the application and permanence of drugs, offering dosage regimens that increase the adherence of patients [9].

Moreover, the intraocular administration of drugs is more complex and is reserved for the treatment of intraocular pathologies in which concentrations of drugs are not reached, either topically or systemically. In this case, the intravitreal, periocular, subretinal and suprachoroidal routes of administration are the most commonly used [10]. The diversity of factors affecting biodistribution, the invasiveness and the risks associated with the technique and sampling (vitreous haemorrhage, retinal detachment and endophthalmitis) limit clinical pharmacokinetic research, making it difficult to study appropriate dosages. Furthermore, preclinical ocular pharmacokinetic studies usually involve sacrificing the animals at different times after administration and analysing different sections of the eye, with the risk of redistributing the compound due to the dissection methods [11]. This is inconvenient and costly and requires a large number of animals in each study.

To successfully develop new methods and techniques of ophthalmic drug delivery, it is important to have reliable ocular pharmacokinetic data. The complex and unique eye anatomy, as well as the invasiveness of the sampling, lead to the lack of complete knowledge of the ocular mechanisms for drug clearance, and therefore, for its pharmacokinetics [12,13]. In recent years, molecular imaging techniques have become a turning point for the development and characterisation of new drugs and formulations due to the fact that they are non-invasive and allow determining the distribution of the studied compound in real time.



USC UNIVERSIDADE DE SANTIAGO DE COMPOSTELA

## 2. MOLECULAR IMAGING MODALITIES IN OPHTHALMIC DRUG DELIVERY STUDIES

Molecular imaging techniques allow for the visualisation, characterisation and quantification of the biological procedures at the cellular and subcellular level [14,15], and their advantage over conventional study methods is that it is possible to take measurements from the same animal at different times without causing harm and with enough spatial and temporal resolution, so as to study different biological procedures in real time. Furthermore, it is possible to conduct a repetitive, uniform and relatively automatic study of the same living subject using identical or alternating biological images at different times. Thus, we can take advantage of the statistical power of longitudinal studies and reduce costs [14,16,17]. Moreover, it complies with the 3Rs principle of animal research proposed by Russel and Burch in 1959: replacement, reduction and refinement [18]. The current molecular imaging modalities include optic imaging-based techniques, positron emission tomography (PET), single-photon emission computed tomography (SPECT) and some magnetic resonance imaging (MRI) sequences [19]. Among this wide variety of tests, there is no perfect modality presenting at the same time high sensitivity, specificity, and time and spatial resolution; however, it is possible to study biological procedures when combining the information provided by each of them. The combination of two or more modalities allows for obtaining images of the same biological procedure in the same animal [20]. The most frequent combinations are those of high sensitivity with anatomic/morphologic techniques. Thus, the combinations commonly used are PET and SPECT, with great sensitivity, along with morphologic techniques like computed tomography (CT) scan and MRI [16].

## 3. POSITRON EMISSION TOMOGRAPHY

Positron emission tomography (PET) is a relatively new imaging modality mainly used to study brain metabolism, heart function and tumour detection [21]. The PET scanner detects photons emitted by a radiopharmaceutical (molecule of interest which has been previously labelled with a radioisotope), in a way that three-dimensional images are obtained from the concentration of the molecule throughout the body by means of data reconstruction [22,23]. Different radioisotopes can be used to create radiopharmaceuticals. The most commonly used are typically isotopes with short half-lives, such as $^{11}C$, $^{13}N$, $^{15}O$, $^{18}F$, $^{68}Ga$, $^{82}Rb$, or with longer half-lives, such as $^{124}I$ o $^{89}Zr$. The $^{18}F$ isotope is most often used in clinical practice, since its half-life is long enough to be able to produce commercial radiopharmaceuticals outside the place of study that can then be sent there [24].



USC UNIVERSIDADE DE SANTIAGO DE COMPOSTELA

This modality has not been widely used in the field of clinical ophthalmology to date [25], although its use is promising for the diagnosis of primary ocular tumours and for neurophysiologic studies [26,27,28,29,30]. In recent years, it has emerged in the research field as an essential tool for the study of the pharmacokinetics of different ophthalmic formulations, since it provides images of the drug's biodistribution and/or its effect on the eye. Below, its application to the study of intraocular and topical ocular routes of administration will be discussed.

The ophthalmic topical route of administration implies that the drug must overcome some physicochemical, metabolic and biological barriers in order to reach the desired action area. Physicochemical barriers include drug properties such as lipophilia, solubility, molecular size and shape and drug loss from the ocular surface due to nasolacrimal drainage. Metabolic barriers include the activity of cytochrome P450 enzymes in ocular tissues, and the biological barriers are the corneal epithelium, the systemic absorption of the conjunctival sac, the blood-vitreous barrier and the blood-retinal barrier [31].

The PET image provides a quantifiable signal on the pharmacokinetic profile of the topically administered radiopharmaceutical so that it is possible to obtain a signal in the eye after the instillation during the initial times, with a subsequent signal detection in the nasolacrimal duct and in the nasal cavity, given by that part of the formulations eliminated from the lacrimal sac towards the nasal cavity, as we can see in Figure 1 [32]. To do this, two conditions must be taken into account: the drug structure must not be significantly modified when being labelled with the radioisotope, and its effect on the organ function and its metabolism can be assessed through molecular image biomarkers that accumulate in the target organ [16].

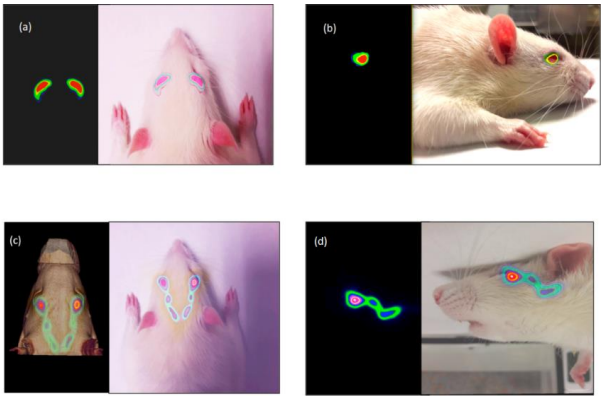



**Figure 1.** Fusion PET-CT-Real images of the rat's head. Tacrolimus eye drops remain on the ocular surface after instillation (a,b) subsequently observed as it is eliminated by the nasolacrimal ducts (c,d). Axial (a) and sagittal (b) PET image and fusion PET-real images (10 min). Axial (c) fusion PET-CT image and Sagittal (d) fusion PET-real images (90 min post-administration). Reproduced with permission from [32], published by Elsevier, 2018.



USC UNIVERSIDADE DE SANTIAGO DE COMPOSTELA

Through the PET technique, the behaviour of different types of polymers [33,34,35,36], such as chitosan labelled with $^{124}I$ or its combined derivative with N-acetylcysteine (NAC-chitosan) was studied [34]. Another topical ophthalmic hydrogel formulation composed by gellan and kappa-carrageenan gum (0.82% weight/volume) labelled with $^{18}F$ radiotracers was also assessed [33] (Figure 2 and Figure 3). In the aforementioned study, it was shown that it is possible to establish differences between the permanence on the ocular surface for different types of ophthalmic formulations by using different polymers as drug delivery vehicles; the technique proposed could be a safe method for this kind of future studies in humans. Some tacrolimus topical formulations for atopic keratoconjunctivitis [32], econazole-$\alpha$-cyclodextrin formulated in hydrogel for the treatment of fungal keratitis [37], and cysteamine dispersed in different types of hydrogel for the treatment of cystinosis [38] have also been studied. Furthermore, the PET technique allows for the quantitative analysis of the formulations' pharmacokinetic profile and the calculation of pharmacokinetic parameters, such as half-life and ophthalmic residence time [38].

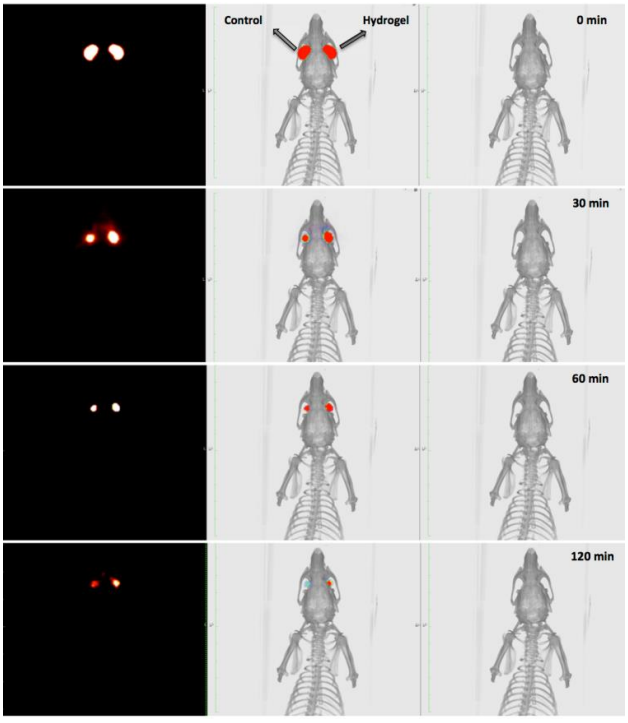



**Figure 2.** PET (left), CT (right), and PET/CT fused image. The biopermanence evaluation of the hydrogel labeled with $^{18}F$-fluorodeoxyglucose (FDG) (right eye) in rats compared to a saline solution containing $^{18}F$-FDG as control formulation (left eye). Reproduced from [33], which is licensed under a Creative Commons Attribution-NonCommercial-NoDerivatives 4.0 International License.



USC UNIVERSIDADE DE SANTIAGO DE COMPOSTELA

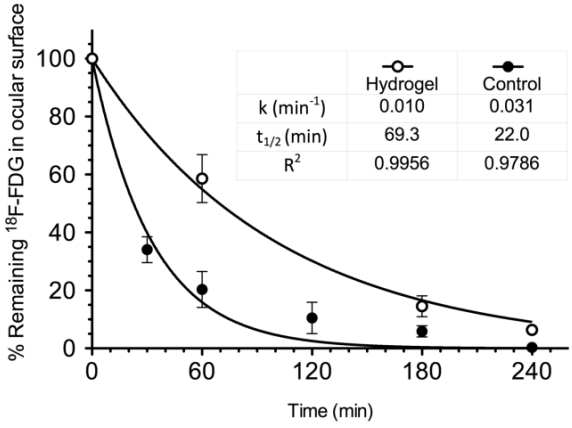



**Figure 3.** Kinetic profile of topical hydrogel labeled with $^{18}$F-FDG (blank circles) compared to a saline solution containing $^{18}$F-FDG as control solution (solid circles). Reproduced from [33], which is licensed under a Creative Commons Attribution-Non-Commercial-No Derivatives 4.0 International License.

With this technology, it is also possible to know the biodistribution of compounds at an intraocular level after their intravitreal administration and their pharmacokinetics (Figure 4 and Figure 5) [39]. It is important to bear in mind that in order to reach a sustained therapeutic concentration of drug in the vitreous, the administration frequency must be based on the drug's half-life. Its elimination in the vitreous humour can be affected by diverse factors, such as molecular weight, its physicochemical properties, its protein or melanin binding, its metabolism, the surgical procedure, the injected volume or ocular inflammation, as well as the membrane transport mechanisms [40].

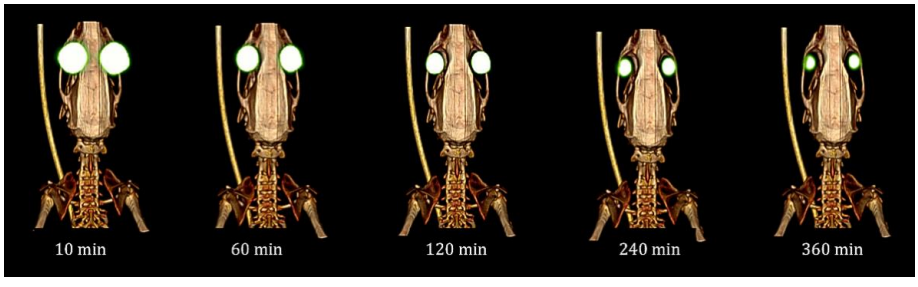



**Figure 4.** Fused image PET/CT showing the signal evolution of intravitreal injections in the rat eyes throughout time. Reproduced from [39], which is licensed under a Creative Commons Attribution-NonCommercial-NoDerivatives 4.0 International License.



USC UNIVERSIDADE DE SANTIAGO DE COMPOSTELA

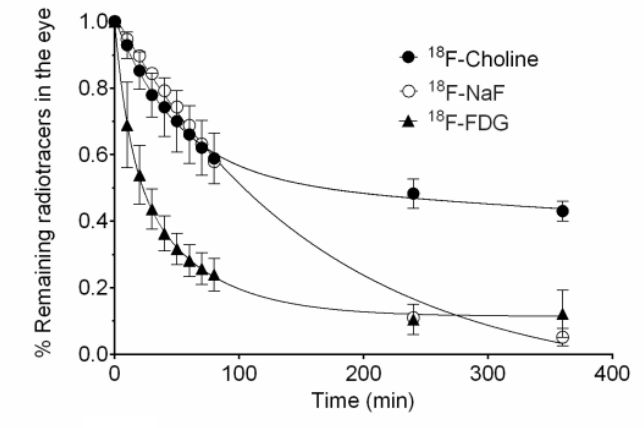



**Figure 5.** Intravitreal pharmacokinetic profile of $^{18}$F-FDG, $^{18}$FNaF, and $^{18}$F-Choline after intravitreal injection. Reproduced from [39], which is licensed under a Creative Commons Attribution-NonCommercial-NoDerivatives 4.0 International License.

When in vitro pharmacokinetic studies are carried out, there are a series of factors that are not usually kept in mind, such as the absence of convection in the vitreous [41-44], the protein and melanin binding or the drug's metabolism and its active transport [10,45]. Through classic in vivo pharmacokinetic studies of intravitreal injections, these aspects could be solved, but as it has been previously mentioned, they are limited due to the invasiveness of the technique [46,47]. Some models that allow the in vitro simulation of intravitreal pharmacokinetics have been proposed, and they keep in mind anatomy and ocular physiological aspects [45-50]. PET studies with anti-vascular endothelial growth factor (VEGF) drugs, such as bevacizumab and ranibizumab have also been conducted, and they allowed for the determination of the pharmacokinetic properties of these agents inside the vitreous cavity [29].

## 4. SPECT

SPECT (Single photon emission computed tomography) is a molecular imaging technique that provides a three-dimensional spatial distribution of the administered radiopharmaceuticals. The use of a planar technique known as scintigraphy is common (Figure 6) [51]. This technique follows the same rationale as the SPECT technique, but provides a projected image instead of three-dimensional images [52,53].



USC UNIVERSIDADE DE SANTIAGO DE COMPOSTELA

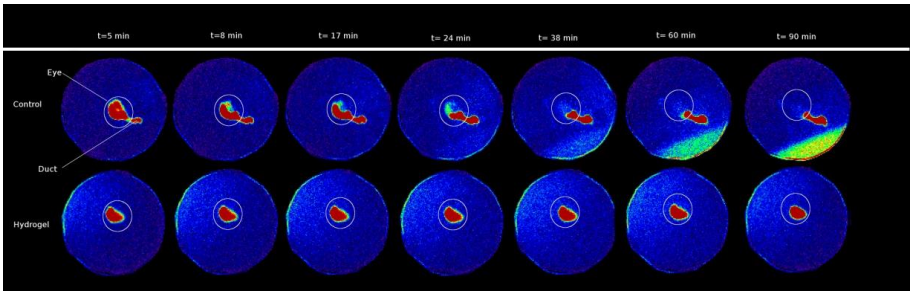



**Figure 6.** Scintigraphy image of a novel ion-sensitive hydrogel based on gellan gum and kappa-carrageenan. In the upper images (control eye), the signal decreases in the corneal surface, moving towards the nasolacrimal duct, while in the bottom images, signal obtained in the eye with hydrogel remains unchanged. Reproduced with permission from [51], published by Elsevier, 2017.

The radioisotopes used in SPECT images include technetium ($^{99m}$Tc), indium ($^{111}$In), iodine ($^{131}$I, $^{123}$I) and gallium ($^{67}$Ga) [10,52]. In the same way as the PET technique, the SPECT image provides useful information at a clinical and preclinical level by simultaneously combining molecular imaging and anatomical information obtained through CT images. This allows for a precise localisation and quantification of the radiolabelled imaging probe, thereby making it possible to observe the pharmacokinetic profile signal on the animal's anatomy [32,54]. Its applicability in both animal and human studies turns it into a translational research technique [55]. Like the PET technique, the labelling with a radionuclide must preserve the drug structure, and its effect on the organ's function and metabolism must be assessable through molecular image biomarkers [16].

Gamma scintigraphy was first assessed by Rossomondo et al. in 1972 [56] and was later used with modifications in preclinical studies [57] and in humans [58,59,60,61,62] to assess the lacrimal drainage and the lacrimal gland inflammation [63]. Subsequently, it has been used with the aim of understanding the ocular surface biodistribution of different formulations used as drug delivery vehicles in mice and humans, as it is the case for artificial lacrimal products that contain hydroxypropyl methylcellulose (HPMC), a combination of PVA and gellan gum for antiglaucoma drug release [64,65], PVA [66,67,68] or sodium hyaluronate [69]. Furthermore, with this technique the biodistribution and permanence on the ocular surface of ophthalmic ointments [70], liposomal formulations [71,72], nanoparticles [72] and microemulsions w/o [73] have also been studied. SPECT has been chosen for multiple ocular biopermanence studies of gels and gelation systems, such as carbomer [74] and chitosan-HPMC [76,76] based gels, thermosensitive poloxamer gels (Pluronic® F-127 and Pluronic® F-68 in combination) [77], in situ ion-sensitive and thermosensitive gelation systems based on a mixture of poloxamer (Pluronic®



USC UNIVERSIDADE DE SANTIAGO DE COMPOSTELA

F-127 and Pluronic® F-68) and chitosan for ofloxacin release [78]. Also, an in situ gelation system activated with ions and based on alginate and HMPC [79], another one activated by ions and pH-based in gellan gum and chitosan [80] and a ion-sensitive gel consisting of gellan gum and kappa-carrageenan [81] were studied. The SPECT/CT technique has made it possible to study the ocular biodistribution of 3-$^{123}$I-iodochloroquine, injected intravenously in rats [82], allowing the non-invasive quantification of drugs in the eye throughout the time and the melanin influence on the ocular distribution and elimination.

SPECT images of the intravitreal kinetics of heat shock protein 70 (HSP-70) protein in the retinal pigment epithelium of ex vivo bovine eyes have been obtained, as well as measurements of its cytoprotective effects against oxidative stress, which has appeared as a possible strategy against the degeneration of the retinal pigment epithelium [83].

Both PET and SPECT techniques present an elevated quantification sensitivity, although the values reached through PET (about nM) are higher than those obtained through SPECT. Both techniques provide three-dimensional images that enable the interpretation and quantification of the results in relation to other types of techniques, and even more so when they are combined with CT images, which provide high-resolution anatomical information.

Moreover, as previously mentioned, the labelling of the molecules to be studied can change the properties of some compounds, resulting in alterations in biodistribution. This especially occurs in the case of small molecules. On the contrary, the pharmacokinetics of proteins, large molecules and drug delivery systems are less sensitive to this kind of modifications [10]. In the case of ocular studies, the blood-retinal barrier is an important consideration, since changes in the molecular size and lipophilia can alter its permeability and cause changes in the vitreous clearance. The typical strategies include the use of peptide binding elements in the labelling of proteins [84], the encapsulation of hydrophilic or lipophilic compounds in liposomes or nanoparticles [85,86], radiometal radiotracers with DOTA complexes (1,4,7,10-tetraazaciclododecane-1,4,7,10-tetraacetic acid) [84]. The studied molecules are considered relatively stable since they can carry out the ligand synthesis in situ and present relatively long physical half-lives (that last from hours to days) [87,88]. It is important to bear in mind that, as previously stated, the labelling of the studied molecules must not significantly affect their structure, which could be translated into changes in its biodistribution and pharmacokinetics.

Another advantage is that the radioactive signal is not affected by changes in the environment, so it provides an excellent depth and a dynamic linear range of the measurements [10]. Regarding PET, the most common and important biological



USC UNIVERSIDADE DE SANTIAGO DE COMPOSTELA

elements (carbon, oxygen, nitrogen and fluorine) have positron-emitting isotopes, which facilitate the labelling of a wide variety of compounds through covalent bonds, leading to great versatility in the development of PET biomarkers in comparison with the $^{99m}$Tc (attached via bulky chelating linker groups) or $^{123}$I (which forms a biologically unstable bond with carbon) used in the SPECT technique. The molecular structure and chemical properties of the final molecule will be, in many occasions, almost identical to the initial one when it is possible to directly substitute the stable isotope for the radioisotope [16].

The main advantage of SPECT over PET is the possibility to use and detect a variety of radioactive agents based on radioisotopes with different energies, which allows for simultaneously visualising two or more molecular routes. Additionally, SPECT radionuclides have more specific activity in comparison with PET tracers and they are more long-lasting, which makes their application more economical [89]. The use of radiotracers in much lower dosages than the pharmacological ones (in the nano- or microgram range) allows for the safe acquisition of images without the interference of the radiotracer in the studied biological processes. Thus, they present similar pharmacokinetic characteristics but in the range of absence of therapeutic effects, while pharmacological dosages are in the milligram or gram range and are associated with pharmacodynamical effects. In this way, the lowest possible masses of injection compounds to be studied are obtained, guaranteeing the pharmacodynamical inertia of the image-creation process [16].

The injected dose of radiotracers in pharmacokinetics assays depends on the half-life of the radioisotopes, sensitivity of technique and the design of the study (timing, duration, etc.). Thus, in ocular studies with PET and SPECT different activities have been used from 10 MBq ($^{124}$I, half-life = 4.17 days) [35,90] to 1 MBq ($^{99m}$Tc half-life = 6 h) [34]. Obviously, this issue is especially relevant for the clinical implementation of these procedures due to the fact that a detailed assessment of the radiation protection of the patient must be performed previously. Eye lenses have very high radiosensitivity when compared with other organs and tissues and radiation doses around 2 Gy leads to the development of cataracts. A calculation of the dose delivered to the eye lens in a clinical study using the dose of radiotracers employed in preclinical studies provided values of radiation doses in the range of 10–20 mGy, which are significantly below the dose limits [33]. Molecular imaging has been widely used in clinical ophthalmology but the specific application for ocular pharmacokinetic studies is not still considered as reference for the design of pharmacokinetic clinical trials.

Another limitation of PET and SPECT images is their low spatial resolution (0.5–2 mm), which only allows visualizing the eye without details of tissues such as the retina. This becomes a problem for the delineation of the vitreous area, which



USC UNIVERSIDADE DE SANTIAGO DE COMPOSTELA

implies that the measurements cannot be exclusively restricted to the area of the vitreous [39]. For this reason, it is necessary to combine the computed tomography scan and the MRI for the anatomic localisation of tissues.

## 5. FLUORESCENCE

The optic fluorescence-based image has been used in ophthalmology since the 1980s. The original in vivo fluorometers, were developed as clinical instruments which aimed at determining the lacrimal flow rate, the aqueous renovation, the blood-retinal barriers (in diabetes) and the early formation of cataracts. The fluorometer allows the detection of fluorophore emission signals (e.g., fluorescein) after excitation through the transparent ocular tissues (e.g., cornea, aqueous humour, different depths of the visual axis through time). Fluorophotometry is limited to the evaluation of the movement of fluorescent compounds in the aqueous and vitreous humour. This technique has been used in vivo to control fluorescence levels, mainly in humans and rabbits [91].

Nowadays, there are various fluorophores available (such as Alexa Fluor dyes) that are compatible with in vivo fluorophotometers wavelengths. They have improved the brightness, the stability in the presence of light excitation and allow for more robust fluorescence spectrums in changing environments [92]. These features provide a dynamic range with longer linearity (fluorescence emission versus drug concentration) that allowed for the intravitreal pharmacokinetic control of ranibizumab in a 20 times concentration range [93].

This technique has been used for the development of an in situ gelation system Gelrite/alginate-based activated by ions for the ophthalmic administration of matrine, in which the time of permanence on the ocular surface was measured in human volunteers [94]. Some studies correlated the rheology and precorneal retention time in humans, proving that formulations based on gellan gum remained on the ocular surface for 1–3 h (depending on the polymer concentration), while poloxamer and carbomer formulations remained for less than 1 h [95-97].

As previously mentioned, the ranibizumab intravitreal kinetics have been recently studied using in vivo fluorophotometry (AlexaFluor tracer 488) and ELISA, being obtained pharmacokinetic parameters similar with both approaches. This study proved that it is crucial to use a minimum number of fluorophores for labelling, and select those with brightness, photosensitivity and sensitivity at minimal pH levels. It is possible to measure the effects of drugs and delivery systems on the blood ocular barrier by following the entrance of intravenous FITC-dextran to the eye.



USC UNIVERSIDADE DE SANTIAGO DE COMPOSTELA

This method was demonstrated to be used to study transscleral drug delivery [98-100].

The main advantage of this technique lies in its capacity to provide optical images with useful information about the pharmacokinetics of macromolecules and drug delivery systems in the eye [10,93]. One of the potential uses of this technique is the monitoring retention of drug delivery systems on both the ocular surface and vitreous. Currently, there are new in vivo fluorometers available that are more robust than the classic ocular in vivo fluorometer. This would allow potentially expanding the use of this methodology [10].

On the other hand, one of the main disadvantages of in vivo fluorophotometry is quantification accuracy, since the fluorescence signal depends on geometrical factors and fluorescence probe properties. The fluorescence emission depends on the medium (e.g., pH), the concentration (not linear relationship between signal-fluorophore concentration) and light exposure (photo-quenching) [101].

Moreover, only a few drugs present intrinsic fluorescence spectrums that would allow for obtaining non-invasive fluorometric images. Drugs that do not have intrinsic fluorescence should be labeled. The stability is usually one of the critical points for the correct development of the trial [10].

## 6. MAGNETIC RESONANCE IMAGING

Magnetic resonance imaging (MRI) is another imaging technique used for the study of ocular structures [102,103], pathologies [104,105] and ophthalmic drug delivery [11,106]. It is a non-invasive technique, like the previous ones, that provides transversal images from the inside of living organisms [107]. It allows for real-time determination of the distribution pattern of the compound of interest in the eye, without disturbing the tissue or the redistribution of said compound [11].

This method is based on nuclear magnetic resonance signals emitted by magnetically labelled nuclei (for example, Gd) [102]. The MRI depends on the magnetic properties of the tissues and its interactions with strong external magnetic fields [16]. It is a very versatile technique that provides morphological images with excellent contrast and spatial resolution (<50 mm for preclinical devices and 300 mm in experimental clinical devices of ultra-high field) [108]. Thus, it is possible to obtain information about tissue composition, perfusion, oxygenation, tissue elasticity, metabolism, and to detect molecular probes in just one acquisition session without radiation exposure [109].



USC UNIVERSIDADE DE SANTIAGO DE COMPOSTELA

MRI has been used in preclinical studies to determine permanence on the ocular surface of ion-sensitive hydrogels based on gellan gum and kappa carrageenan to be employed as vehicles for ophthalmic drug delivery [110] (Figure 7). Through this study, Ferreiro et al. assessed the time of in vivo corneal contact and the hydrogel residence place after its administration, showing the absence of liquid solution 30 minutes after delivery, whereas in the case of the gellan gum formulation, it was still present three hours after delivery. The main improvement of this method is the absence of a contrast agent. In fact, the large quantity of water retained in the gel increases the intensity of the signal and, therefore, MRI seems to be a good and relevant method for assessing the precorneal retention time of the in situ gelation delivery systems.

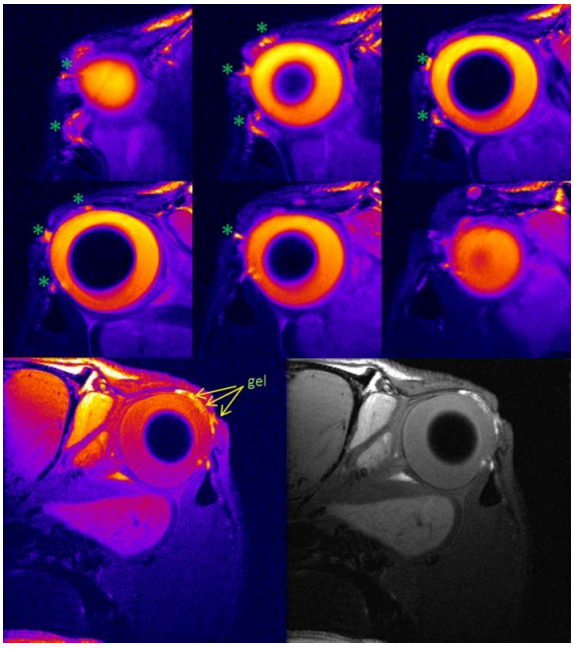



**Figure 7.** MRI of the rat eye rat 2 h after instillation of ion-sensitive hydrogel indicate the hyperintense signals caused by hydrogel. Reproduced with permission from [110], published by Elsevier, 2015.

In addition to the studies on animals, Bert et al. [111] studied solute diffusion through the anterior route in the human eye by using dynamic magnetic resonance with contrast. The pilocarpine effects on the blood-aqueous barrier after its topical application have been assessed in humans [112].

Diverse studies have demonstrated the usefulness of the MRI for characterising penetration routes, ocular barriers and dynamic procedures [113,114], transscleral



USC UNIVERSIDADE DE SANTIAGO DE COMPOSTELA

penetration routes, mechanisms that allow for an improved drug delivery flow, the location of periocular and intraocular devices (or implants) and its release kinetics in periocular, intrascleral, suprachoroidal and intravitreal administration, as well as the study of the ocular iontophoresis [106,115-125]. With the appropriate MRI contrast agents, it is possible to study the blood-aqueous barrier and the clearance in the anterior chamber, being this an important surmise that contrast agent clearance and water clearance in the aqueous humour are the same. The difference between them may lead to errors in the kinetic assessment of the aqueous humour [11].

MRI can be used in the posterior segment of the eye in order to examine the blood-retinal barrier and the vitreous fluidity in a non-invasive way [126-129]. The dysfunction in this barrier can be studied through MRI by using a contrast agent such as $GdDTPA^{2-}$, intravenously administrated into the retinal blood vessels and by controlling its dysfunction in the vitreous humour, which allows for quantifying the barrier's permeability after inducing lesion in the retina [104,129,130]. Similar studies have determined the effects of the endotoxininduced endophthalmitis and the experimental diabetic retinopathy in the blood-retinal barrier function [131,132], as well as ischemic-induced injuries [133] and their hyperpermeability after the sustained elevation of the vascular endothelial growth factor (VEGF) in the vitreous cavity [134]. For this reason, the MRI is a technique with potential for the study of ocular drug delivery systems for the treatment of posterior ocular diseases related to the blood-retinal barrier function.

In the intraocular drug delivery field, the pharmacokinetics of Gadolinium-DTPA after polymeric intraocular implants administration in rabbits have been studied with the MRI technique [115,123]. Furthermore, the biodistribution of magnetic micro- and nanoparticles subsequent to intraocular delivery has also been studied [135]. Nowadays, the dynamic contrast images modality (DCE-MRI) is the most commonly used for preclinical and early clinical assessment of anti-angiogenesis inhibitors like bevacizumab, sorafenib or sutinib [136].

One advantage of the MRI over other molecular imaging techniques is its excellent spatial resolution, but its usefulness in ocular pharmacokinetic studies is limited, as the quantification and sensitivity linear range (approximately 0.1 mM) is rather limited in comparison to radioimaging techniques [10]. MRI has a sensitivity from three to six orders of magnitude lower than the PET technique [137]. Thus, nowadays MRI images are not an attractive option for ocular pharmacokinetics studies. Nevertheless, in association with SPECT and PET, it can be a useful technique in order to improve radiolabelled molecules' localisation thanks to the anatomical information provided therein.



USC UNIVERSIDADE DE SANTIAGO DE COMPOSTELA

The majority of the contrast agents used in MRI are hydrophilic filler compounds that can establish specific interactions with the eye, potentially interfering with ocular clearance and pharmacokinetics in permanence time characterisation studies of hydrogels on the ocular surface [138].

One of the advantages that MRI offers over the PET and SPECT radiolabelling techniques is that $\gamma$ radiations emit relatively low energy levels in comparison to $\alpha$ and $\beta$ radiations, at the same time as the $^{99}$mTc exhibits a relatively short half-life (6 h). This is translated into a low risk for health associated with studies with this technique, both for trial subjects and for researchers [139]. Studies on mice have proven the absence of toxicity at the tissue level in epithelium and cornea with the use of Gd-DTPA as a contrast agent [125]. In addition to this, the magnetic resonance imaging projection is not affected by medium opacities such as cataracts [89].

## 7. OTHER IMAGING TECHNIQUES

### *7.1. Ultrasonography*

Ultrasound imaging uses acoustic transducers that send and receive ultrasound frequency energy to generate reflexion or direct transmission three-dimensional images [140]. Ultrasonography is the most used clinical imaging modality due to its low cost, availability and safety, and it is ideal for obtaining in vivo images in both animals and human patients. The image contrast depends on the image generation algorithm and its use of the backscatter, the sound reduction and the sound speed [141,142]. In ophthalmology, ultrasound probes of 10, 20, 40 and 50 MHz are used. However, the resolution is still the limiting factor. Recent advancements in imaging technology with high-resolution ultrasound devices and the development of specific microbubble contrast agents are promising for the future of molecular imaging [141,143].

In ophthalmology, this technique has been used in diagnostic procedures [144], in order to boost drug administration on the ocular surface (such as tobramycin and dexamethasone) [145,146], protein-loaded nanoparticles [147] and intravitreal administration [148], and to obtain information about juxtascleral administration [122].

### *7.2. Optical Coherence Tomography and Computed Tomography*

The recent introduction of new imaging techniques has improved many aspects of the ophthalmic procedures, both therapeutically and diagnostically. This is the case



USC UNIVERSIDADE DE SANTIAGO DE COMPOSTELA

for retina diagnostic techniques: optic coherence tomography (OCT) and OCT with angiography (OCTA) [149]. OCT generates images, interferometrically measuring the amplitude and the delay of the reflected or backscattered light, while OCTA also allows for the visualisation of the macular capillaries and the optical nerve head [150,151]. This technique has been used in comparative studies for artificial tears [152,153]. Its use is based on the measurement of the corneal thickness before and after topical formulation administration at different times. From the data obtained, it was observed that the hyaluronic acid increases the thickness of the lacrimal layer for 30 min in healthy subjects, showing good reproducibility.

CT is an imaging technique that does not require radioactive labelling or contrast, but whose functioning is based on the emission of a large series of two-dimensional X-ray images taken around a single rotation axis [141,154]. This technique has also been used in ocular studies, but as a tool for the anatomic support in the interpretation of images obtained through gammagraphy or PET [155]. Combined with these techniques, it provides an image of the subject's anatomy at the same time that the image of the radiologically labelled compound provides a quantifiable signal on the pharmacokinetic profile, as we can see in Figure 8 [32].

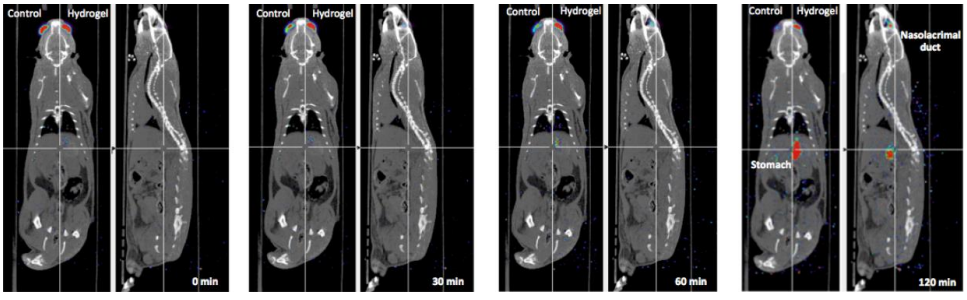



**Figure 8.** Fused whole-body PET/CT images (coronal and sagittal views). Reproduced from [33], which is licensed under a Creative Commons Attribution-NonCommercial-NoDerivatives 4.0 International License.

Table 1 summarizes imaging agents used in each technique and their administration, topical or intraocular and the spatial resolution achieved with each technique.



USC UNIVERSIDADE DE SANTIAGO DE COMPOSTELA

**Table 1.** Administration routes used in each molecular imaging technique, their imaging agents and spatial resolution.

| Technique | Administration | Imaging agents | Spatial resolution | Reference |
|---|---|---|---|---|
| **PET** | topical | $^{18}F$, $^{124}I$ | 1–2 mm | [31–38] |
| | intraocular | $^{18}F$, $^{124}I$ | | [29, 39] |
| **SPECT** | topical | $^{99m}Tc$,$^{131}I$, $^{123}I$, $^{111}In$, $^{67}Ga$ | 0.5–2 mm | [61–80] |
| | intraocular | $^{123}I$ | | [82] |
| **Fluorescence** | topical | Fluorescein, AlexaFluor 488 | 1–10 mm | [94–97] |
| | intraocular | Fluorescein, AlexaFluor 488 | | [98–100] |
| **Magnetic resonance imaging** | topical | Gadolinium | 25–100 μm | [109,110] |
| | intraocular | Gadolinium | | [114,122,134] |
| **Ultrasonography** | topical | Microbubbles | 30–100 μm | [144–147] |
| **Optical coherence tomography** | topical | None | 10–20 μm | [151,152] |

## 8. CONCLUSIONS

Molecular imaging techniques make it possible to obtain reliable pharmacokinetic data with the objective of improving the application and permanence of the ophthalmic drugs in its action site, leading to dosage optimisation. The disadvantages of the classical methodologies were the difficulty in obtaining information about topical and intraocular distribution and clearance, associated with multiple factors related to ophthalmic physiology, as well as complexity and invasiveness intrinsic to the sampling techniques. Contrary to these studies, the molecular imaging techniques allow for the real-time visualisation, localisation, characterisation and quantification of the compounds after their administration, all in a reliable, safe and non-invasive way. None of these techniques presents simultaneously high sensitivity and specificity, but it is possible to study biological procedures with the information provided when the techniques are combined. Therefore, molecular imaging techniques are postulated as a resource with great potential for the research and development of new drugs and ophthalmic delivery systems

## 9. REFERENCES

1. Ghate, D.; Edelhauser, H.F. Ocular drug delivery. *Expert Opin. Drug Deliv*. **2006**, 3, 275–287.



USC UNIVERSIDADE DE SANTIAGO DE COMPOSTELA

2. Carvalho, I.M.; Marques, C.S.; Oliveira, R.S.; Coelho, P.B.; Costa, P.C.; Ferreira, D.C. Sustained drug release by contact lenses for glaucoma treatment-a review. *J. Control. Release* **2015**, 202, 76–82.

3. Patel, A.; Cholkar, K.; Agrahari, V.; Mitra, A.K. Ocular drug delivery systems: An overview. *World J. Pharmacol*. **2013**, 2, 47–64.

4. Davies, N.M. Biopharmaceutical considerations in topical ocular drug delivery. *Clin. Exp. Pharmacol. Physiol*. **2000**, 27, 558–562.

5. Mainardes, R.M.; Urban, M.C.; Cinto, P.O.; Khalil, N.M.; Chaud, M.V.; Evangelista, R.C.; Daflon Gremiao, M.P. Colloidal carriers for ophthalmic drug delivery. *Curr. Drug Targets* **2005**, 6, 363–371.

6. Mietz, H.; Diestelhorst, M.; Rump, A.F.E.; Theisohn, M.; Klaus, W.; Krieglstein, G.K. Ocular concentrations of mitomycin C using different delivery devices. *Ophthalmologica* **1998**, 212, 37–42.

7. Taravella, M.J.; Balentine, J.; Young, D.A.; Stepp, P. Collagen shield delivery of ofloxacinto the human eye. *J. Cataract Refract. Surg.* **1999**, 25, 562–565.

8. Le Bourlais, C.; Acar, L.; Zia, H.; Sado, P.A.; Needham, T.; Leverge, R. Ophthalmic drug delivery systems—Recent advances. *Prog. Retinal Eye Res.* **1998**, 17, 33–58.

9. Yavuz, B.; Kompella, U.B. Ocular drug delivery. In *Pharmacologic Therapy of Ocular Disease*; Springer: Cham, Switzerland, ***2016***; pp. 57–93.

10. Del Amo, E.M.; Rimpelä, A.-K.; Heikkinen, E.; Kari, O.K.; Ramsay, E.; Lajunen, T.; Schmitt, M.; Pelkonen, L.; Bhattacharya, M.; Richardson, D. Pharmacokinetic aspects of retinal drug delivery. *Prog. Retinal Eye Res*. **2017**, 57, 134–185.

11. Li, S.; Kevin, J.; Lizak, M.; Jeong, E.-K. MRI in ocular drug delivery. *NMR Biomed.* **2008**, 21, 941–956.

12. Zimmerman, T.J. *Textbook of Ocular Pharmacology*; Lippincott Williams & Wilkins: Philadelphia, PA, USA, 1997.

13. Worakul, N.; Robinson, J.R. Ocular pharmacokinetics/pharmacodynamics. *Eur. J. Pharm. Biopharm*. **1997**, 44, 71–83.

14. Willmann, J.K.; Van Bruggen, N.; Dinkelborg, L.M.; Gambhir, S.S. Molecular imaging in drug development. Nat. Rev. Drug Discovery 2008, 7, 591.

15. Rudin, M.; Weissleder, R. Molecular imaging in drug discovery and development. *Nat. Rev. Drug Discovery* **2003**, 2, 123.

16. Cunha, L.; Szigeti, K.; Mathé, D.; Metello, L.F. The role of molecular imaging in modern drug development. *Drug Discovery Today* **2014**, 19, 936–948.



USC UNIVERSIDADE DE SANTIAGO DE COMPOSTELA

17. Capozzi, M.E.; Gordon, A.Y.; Penn, J.S.; Jayagopal, A. Molecular imaging of retinal disease. *J. Ocul. Pharmacol. Ther*. **2013**, 29, 275–286.

18. Russell, W.M.S.; Burch, R.L.; Hume, C.W. *The Principles of Humane Experimental Technique*; Methuen: London, UK, 1959; Volume 238.

19. James, M.L.; Gambhir, S.S. A molecular imaging primer: modalities, imaging agents, and applications. *Physiol. Rev*. **2012**, 92, 897–965.

20. Kagadis, G.C.; Loudos, G.; Katsanos, K.; Langer, S.G.; Nikiforidis, G.C. In vivo small animal imaging: current status and future prospects. *Med. Phys*. **2010**, 37, 6421–6442.

21. Bengel, F.M.; Higuchi, T.; Javadi, M.S.; Lautamäki, R. Cardiac positron emission tomography. *J. Am. Coll. Cardiol*. **2009**, 54, 1–15.

22. Lameka, K.; Farwell, M.D.; Ichise, M. Positron emission tomography. In *Handbook of Clinical Neurology*; Elsevier: Amsterdam, The Netherlands, 2016; Volume 135, pp. 209–227.

23. Chen, Z.-Y.; Wang, Y.-X.; Lin, Y.; Zhang, J.-S.; Yang, F.; Zhou, Q.-L.; Liao, Y.-Y. Advance of Molecular Imaging Technology and Targeted Imaging Agent in Imaging and Therapy. *BioMed Res*. Int. **2014**, 2014, 819324.

24. Okamura, N.; Harada, R.; Furukawa, K.; Furumoto, S.; Tago, T.; Yanai, K.; Arai, H.; Kudo, Y. Advances in the development of tau PET radiotracers and their clinical applications. *Ageing Res. Rev*. **2016**, 30, 107–113.

25. Pulagam, K.R.; Gómez-Vallejo, V.; Llop, J.; Rejc, L. Radiochemistry; a useful tool in the ophthalmic drug discovery. *Curr. Med. Chem*. **2019**. 501-22.

26. Sek, K.; Wilson, D.; Paton, K.; Benard, F. The role of 18F-FDG PET/CT in assessment of uveal melanoma and likelihood of primary tumour visualisation based on AJCC tumour size. *J. Nucl. Med*. **2016**, 57, 409.

27. García-Rojas, L.; Adame-Ocampo, G.; Alexánderson, E.; Tovilla-Canales, J.L. 18-fluorodeoxyglucose uptake by positron emission tomography in extraocular muscles of patients with and without Graves' ophthalmology. J. *Ophthalmol*, **2013**, 529187.

28. García-Rojas, L.; Adame-Ocampo, G.; Mendoza-Vázquez, G.; Alexánderson, E.; Tovilla-Canales, J.L. Orbital positron emission tomography/computed tomography (PET/CT) imaging findings in graves ophthalmopathy. *BMC Res. Notes* **2013**, 6, 353.

29. Christoforidis, J.B.; Carlton, M.M.; Knopp, M.V.; Hinkle, G.H. PET/CT imaging of I-124–radiolabeled bevacizumab and ranibizumab after intravitreal injection in a rabbit model. *Investigat. Ophthalmol. Visual Sci*. **2011**, 52, 5899–5903.



USC UNIVERSIDADE DE SANTIAGO DE COMPOSTELA

30. Wang, W.-F.; Ishiwata, K.; Kiyosawa, M.; Kawamura, K.; Oda, K.; Matsuno, K.; Kobayashi, T.; Mochizuki, M. Investigation of the use of positron emission tomography for neuroreceptor imaging in rabbit eyes. *Ophthalmic Res*. **2004**, 36, 255–263.

31. Yellepeddi, V.K.; Palakurthi, S. Recent advances in topical ocular drug delivery. *J. Ocul. Pharmacol. Ther*. **2016**, 32, 67–82.

32. Luaces-Rodríguez, A.; Touriño-Peralba, R.; Alonso-Rodríguez, I.; García-Otero, X.; González-Barcia, M.; Rodríguez-Ares, M.T.; Martínez-Pérez, L.; Aguiar, P.; Gómez-Lado, N.; Silva-Rodríguez, J. Preclinical characterization and clinical evaluation of tacrolimus eye drops. *Eur. J. Pharm. Sci.* **2018**, 120, 152–161.

33. Fernández-Ferreiro, A.; Silva-Rodríguez, J.; Otero-Espinar, F.J.; González-Barcia, M.; Lamas, M.J.; Ruibal, A.; Luaces-Rodriguez, A.; Vieites-Prado, A.; Sobrino, T.; Herranz, M.; et al. Positron Emission Tomography for the Development and Characterization of Corneal Permanence of Ophthalmic Pharmaceutical Formulations. *Invest. Ophthalmol. Visual Sci*. **2017**, 58, 772–780.

34. Dangl, D.; Hornof, M.; Hoffer, M.; Kuntner, C.; Wanek, T.; Kvaternik, H. In vivo Evaluation of Ocular Residence Time of 124I-labelled Thiolated Chitosan in Rabbits Using MicroPET Technology. *Invest. Ophthalmol. Visual Sci*. **2009**, 50, 3689.

35. Kuntner, C.; Wanek, T.; Hoffer, M.; Dangl, D.; Hornof, M.; Kvaternik, H.; Langer, O. Radiosynthesis and Assessment of Ocular Pharmacokinetics of 124 I-Labeled Chitosan in Rabbits Using Small-Animal PET. *Mol. Imaging Biol*. **2011**, 13, 222–226.

36. Schmetterer, L.; Höller, S.; Hornof, M. Chitosan in the treatment of dry eye. *Acta Ophthalmol*. **2010**, 88.

37. Díaz-Tomé, V.; Luaces-Rodríguez, A.; Silva-Rodríguez, J.; Blanco-Dorado, S.; García-Quintanilla, L.; Llovo-Taboada, J.; Blanco-Méndez, J.; García-Otero, X.; Varela-Fernández, R.; Herranz, M.; et al. Ophthalmic Econazole Hydrogels for the Treatment of Fungal Keratitis. *J. Pharm. Sci*. **2018**, 107, 1342–1351.

38. Luaces-Rodríguez, A.; Díaz-Tomé, V.; González-Barcia, M.; Silva-Rodríguez, J.; Herranz, M.; Gil-Martínez, M.; Rodríguez-Ares, M.T.; García-Mazás, C.; Blanco-Mendez, J.; Lamas, M.J. Cysteamine polysaccharide hydrogels: study of extended ocular delivery and biopermanence time by PET imaging. *Int. J. Pharm*. **2017**, 528, 714–722.

39. Fernández-Ferreiro, A.; Luaces-Rodríguez, A.; Aguiar, P.; Pardo-Montero, J.; González-Barcia, M.; García-Varela, L.; Herranz, M.; Silva-Rodríguez, J.; Gil-



USC UNIVERSIDADE DE SANTIAGO DE COMPOSTELA

Martínez, M.; Bermúdez, M.A.; et al. Preclinical PET Study of Intravitreal Injections. *Invest. Ophthalmol. Visual Sci*. **2017**, 58, 2843–2851.

40. Radhika, M.; Mithal, K.; Bawdekar, A.; Dave, V.; Jindal, A.; Relhan, N.; Albini, T.; Pathengay, A.; Flynn, H.W. Pharmacokinetics of intravitreal antibiotics in endophthalmitis. *J. Ophthalmic Inflamm. Infect*. **2014** 10;4:22.
41. Xu, J.; Heys, J.J.; Barocas, V.H.; Randolph, T.W. Permeability and diffusion in vitreous humor: implications for drug delivery. *Pharm. Res*. **2000**, 17, 664–669.
42. Gisladottir, S.; Loftsson, T.; Stefansson, E. Diffusion characteristics of vitreous humour and saline solution follow the Stokes Einstein equation. *Graefe's Arch. Clin. Exp. Ophthalmol.* **2009**, 247, 1677–1684.
43. Ohtori, A.; TOJo, K. In vivo/in vitro correlation of intravitreal delivery of drugs with the help of computer simulation. *Biol. Pharm. Bull*. **1994**, 17, 283–290.
44. Tojo, K.; Nakagawa, K.; Morita, Y.; Ohtori, A. A pharmacokinetic model of intravitreal delivery of ganciclovir. *Eur. J. Pharm. Biopharm*. **1999**, 47, 99–104.
45. Park, J.; Bungay, P.M.; Lutz, R.J.; Augsburger, J.J.; Millard, R.W.; Roy, A.S.; Banerjee, R.K. Evaluation of coupled convective–diffusive transport of drugs administered by intravitreal injection and controlled release implant. *J. Control. Release* **2005**, 105, 279–295.
46. Avery, R.L.; Castellarin, A.A.; Steinle, N.C.; Dhoot, D.S.; Pieramici, D.J.; See, R.; Couvillion, S.; Ma'an, A.N.; Rabena, M.D.; Le, K. Systemic pharmacokinetics following intravitreal injections of ranibizumab, bevacizumab or aflibercept in patients with neovascular AMD. *Br. J. Ophthalmol.* **2014**, 98, 1636–1641.
47. Bhagat, R.; Zhang, J.; Farooq, S.; Li, X.-Y. Comparison of the release profile and pharmacokinetics of intact and fragmented dexamethasone intravitreal implants in rabbit eyes. *J. Ocul. Pharmacol. Ther*. **2014**, 30, 854–858.
48. Balachandran, R.K.; Barocas, V.H. Computer modeling of drug delivery to the posterior eye: effect of active transport and loss to choroidal blood flow. *Pharm. Res*. **2008**, 25, 2685–2696.
49. Awwad, S.; Lockwood, A.; Brocchini, S.; Khaw, P.T. The PK-Eye: a novel in vitro ocular flow model for use in preclinical drug development. *J. Pharm. Sci.* **2015**, 104, 3330–3342.
50. Krishnamoorthy, M.K.; Park, J.; Augsburger, J.J.; Banerjee, R.K. Effect of retinal permeability, diffusivity, and aqueous humor hydrodynamics on pharmacokinetics of drugs in the eye. *J. Ocul. Pharmacol. Ther*. **2008**, 24, 255–267.
51. Fernández-Ferreiro, A.; Silva-Rodríguez, J.; Otero-Espinar, F.J.; González-Barcia, M.; Lamas, M.J.; Ruibal, A.; Luaces-Rodríguez, A.; Vieites-Prado, A.;



USC UNIVERSIDADE DE SANTIAGO DE COMPOSTELA

Lema, I.; Herranz, M.; et al. In vivo eye surface residence determination by high-resolution scintigraphy of a novel ion-sensitive hydrogel based on gellan gum and kappa-carrageenan. *Eur. J. Pharm. Biopharm*. **2017**, 114, 317–323.

52. Madsen, M.T. Recent advances in SPECT imaging. *J. Nucl. Med*. **2007**, 48, 661-73.
53. Wernick, M.N.; Aarsvold, J.N. *Emission Tomography: The Fundamentals of PET and SPECT*; Elsevier: Amsterdam, The Netherlands, 2004.
54. O'Connor, M.K.; Kemp, B.J. Single-Photon Emission Computed Tomography/Computed Tomography: Basic Instrumentation and Innovations. *Semin. Nucl. Med*. **2006**, 36, 258–266.
55. Gomes, C.M.; Abrunhosa, A.J.; Ramos, P.; Pauwels, E.K.J. Molecular imaging with SPECT as a tool for drug development. *Adv. Drug Deliv. Rev*. **2011**, 63, 547–554.
56. Rossomondo, R.M.; Carlton, W.H.; Trueblood, J.H.; Thomas, R.P. A new method of evaluating lacrimal drainage. *Arch. Ophthalmol*. **1972**, 88, 523–525.
57. Chrai, S.S.; Patton, T.F.; Mehta, A.; Robinson, J.R. Lacrimal and instilled fluid dynamics in rabbit eyes. *J. Pharm. Sci*. **1973**, 62, 1112–1121.
58. Wearne, M.J.; Pitts, J.; Frank, J.; Rose, G.E. Comparison of dacryocystography and lacrimal scintigraphy in the diagnosis of functional nasolacrimal duct obstruction. *Br. J. Ophthalmol*. **1999**, 83, 1032–1035.
59. Gencoglu, E.A.; Dursun, D.; Akova, Y.A.; Cengiz, F.; Yalcin, H.; Koyuncu, A. Tear clearance measurement in patients with dry eye syndrome using quantitative lacrimal scintigraphy. *Ann. Nucl. Med*. **2005**, 19, 581-7.
60. Detorakis, E.T.; Zissimopoulos, A.; Ioannakis, K.; Kozobolis, V.P. Lacrimal Outflow Mechanisms and the Role of Scintigraphy: Current Trends. *World J. Nucl. Med.* **2014**, 13, 16–21.
61. Kotina, E.D.; Tomashevskiĭ, I.O.; Luchshev, A.I.; At'kova, E.L.; Iartsev, V.D. Use of a new Indis computer program to analyze the results of lacrimal scintigraphy. *Vestn. Rentgenol. Radiol*. **2015**, 23–27.
62. Kim, D.J.; Baek, S.; Chang, M. Usefulness of the dacryoscintigraphy in patients with nasolacrimal duct obstruction prior to endoscopic dacryocystorhinostomy. *Graefe's Arch. Clin. Exp. Ophthalmol*. **2019**, 1535-1540
63. Jiang, C.; Li, X.; Zhao, M.; Dend, H.; Huang, J.; Liu, D.; Xu, X. Efficacy of 99mTc-DTPA orbital SPECT/CT on the evaluation of lacrimal gland inflammation in patients with thyroid associated ophthalmopathy. *J. Cent. South Univ. Med. Sci.* **2019**, 44, 322–328.



USC UNIVERSIDADE DE SANTIAGO DE COMPOSTELA

64. Greaves, J.L.; Wilson, C.G.; Birmingham, A.T.; Richardson, M.C.; Bentley, P.H. Scintigraphic studies on the corneal residence of a New Ophthalmic Delivery System (NODS): rate of clearance of a soluble marker in relation to duration of pharmacological action of pilocarpine. *Br. J. Clin. Pharmacol*. **1992**, 33, 603–609.

65. Meseguer, G.; Buri, P.; Plazonnet, B.; Rozier, A.; Gurny, R. Gamma scintigraphic comparison of eyedrops containing pilocarpine in healthy volunteers. *J. Ocul. Pharmacol. Ther*. **1996**, 12, 481–488.

66. Trueblood, J.H.; Rossomondo, R.M.; Carlton, W.H.; Wilson, L.A. Corneal contact times of ophthalmic vehicles. *Arch. Ophthalmol*. **1975**, 93, 127-30.

67. Zaki, I.; Fitzgerald, P.; Hardy, J.G.; Wilson, C.G. A comparison of the effect of viscosity on the precorneal residence of solutions in rabbit and man. *J. Pharm. Pharmacol*. **1986**, 38, 463–466.

68. Hardberger, R.; Hanna, C.; Boyd, C.M. Effects of drug vehicles on ocular contact time. *Arch. Ophthalmol*. **1975**, 93, 42–45.

69. Snibson, G.R.; Greaves, J.L.; Soper, N.D.; Tiffany, J.M.; Wilson, C.G.; Bron, A.J. Ocular surface residence times of artificial tear solutions. *Cornea* **1992**, 11, 288–293.

70. Greaves, J.L.; Wilson, C.G.; Birmingham, A.T. Assessment of the precorneal residence of an ophthalmic ointment in healthy subjects. *Br. J. Clin. Pharmacol.* **1993**, 35, 188-92.

71. Nagarsenker, M.S.; Londhe, V.Y.; Nadkarni, G.D. Preparation and evaluation of liposomal formulations of tropicamide for ocular delivery. *Int. J. Pharm*. **1999**, 190, 63–71.

72. Fitzgerald, P.; Hadgraft, J.; Kreuter, J.; Wilson, C.G. A γ-scintigraphic evaluation of microparticulate ophthalmic delivery systems: liposomes and nanoparticles. *Int. J. Pharm*. **1987**, 40, 81–84.

73. Alany, R.G.; Rades, T.; Nicoll, J.; Tucker, I.G.; Davies, N.M. W/O microemulsions for ocular delivery: Evaluation of ocular irritation and precorneal retention. *J. Control. Release* **2006**, 111, 145–152.

74. Wilson, C.G.; Zhu, Y.P.; Frier, M.; Rao, L.S.; Gilchrist, P.; Perkins, A.C. Ocular contact time of a carbomer gel (GelTears) in humans. *Br. J. Ophthalmol*. **1998**, 82, 1131–1134.

75. Gupta, H.; Aqil, M.; Khar, R.K.; Ali, A.; Bhatnagar, A.; Mittal, G.; Jain, S. Development and characterization of 99mTc-timolol maleate for evaluating efficacy of in situ ocular drug delivery system. *AAPS PharmSciTech* **2009**, 10, 540–546.



USC UNIVERSIDADE DE SANTIAGO DE COMPOSTELA

76. Felt, O.; Furrer, P.; Mayer, J.M.; Plazonnet, B.; Buri, P.; Gurny, R. Topical use of chitosan in ophthalmology: tolerance assessment and evaluation of precorneal retention. *Int. J. Pharm*. **1999**, 180, 185–193.

77. Wei, G.; Xu, H.; Ding, P.T.; Li, S.M.; Zheng, J.M. Thermosetting gels with modulated gelation temperature for ophthalmic use: the rheological and gamma scintigraphic studies. *J. Control. Release* **2002**, 83, 65–74.

78. Kashikar, V.S.; Gonjari, I.D. In situ gelling systems of ofloxacin: Comparative performance of in vivo precorneal drainage and pharmacokinetic study. *Asian J. Pharm*. *2014*, 7.

79. Liu, Z.; Li, J.; Nie, S.; Liu, H.; Ding, P.; Pan, W. Study of an alginate/HPMC-based in situ gelling ophthalmic delivery system for gatifloxacin. *Int. J. Pharm.* **2006**, 315, 12–17.

80. Gupta, H.; Velpandian, T.; Jain, S. Ion- and pH-activated novel in situ gel system for sustained ocular drug delivery. *J. Drug Target*. **2010**, 18, 499–505.

81. Greaves, J.L.; Wilson, C.G.; Rozier, A.; Grove, J.; Plazonnet, B. Scintigraphic assessment of an ophthalmic gelling vehicle in man and rabbit. *Cur. Eye Res*. **1990**, 9, 415–420.

82. Rimpelä, A.-K.; Schmitt, M.; Latonen, S.; Hagström, M.; Antopolsky, M.; Manzanares, J.A.; Kidron, H.; Urtti, A. Drug distribution to retinal pigment epithelium: studies on melanin binding, cellular kinetics, and single photon emission computed tomography/computed tomography imaging. *Mol. Pharm.* **2016**, 13, 2977–2986.

83. Subrizi, A.; Toropainen, E.; Ramsay, E.; Airaksinen, A.J.; Kaarniranta, K.; Urtti, A. Oxidative stress protection by exogenous delivery of rhHsp70 chaperone to the retinal pigment epithelium (RPE), a possible therapeutic strategy against RPE degeneration. *Pharm. Res*. **2015**, 32, 211–221.

84. Liu, S. Bifunctional coupling agents for radiolabeling of biomolecules and target-specific delivery of metallic radionuclides. *Adv. Drug Deliv. Rev*. **2008**, 60, 1347–1370.

85. Lehtinen, J.; Raki, M.; Bergström, K.A.; Uutela, P.; Lehtinen, K.; Hiltunen, A.; Pikkarainen, J.; Liang, H.; Pitkänen, S.; Määttä, A.-M. Pre-targeting and direct immunotargeting of liposomal drug carriers to ovarian carcinoma. *PloS ONE* **2012**, 7, e41410.

86. Psimadas, D.; Georgoulias, P.; Valotassiou, V.; Loudos, G. Molecular nanomedicine towards cancer: 111In-labeled nanoparticles. *J. Pharm. Sci*. **2012**, 101, 2271–2280.



USC UNIVERSIDADE DE SANTIAGO DE COMPOSTELA

87. Meikle, S.R.; Kench, P.; Kassiou, M.; Banati, R.B. Small animal SPECT and its place in the matrix of molecular imaging technologies. *Phys. Med. Biol*. **2005**, 50, R45.

88. Fass, L. Imaging and cancer: A review. *Mol. Oncol*. **2008**, 2, 115–152.

89. Ramos de Carvalho, J.E.; Verbraak, F.D.; Aalders, M.C.; van Noorden, C.J.; Schlingemann, R.O. Recent advances in ophthalmic molecular imaging. Sur. *Ophthalmol*. **2014**, 59, 393–413.

90. Ainsbury, E.A.; Bouffler, S.D.; Dörr, W.; Graw, J.; Muirhead, C.R.; Edwards, A.A.; Cooper, J. Radiation cataractogenesis: a review of recent studies. *Radiat. Res*. **2009**, 172, 1–9.

91. Knudsen, L.L. Ocular fluorophotometry in human subjects and in swine–with particular reference to long-term pharmacokinetics. *Acta Ophthalmol*. **2002**, 80, 1–24.

92. Wysocki, L.M.; Lavis, L.D. Advances in the chemistry of small molecule fluorescent probes. *Curr. Opin. Chem. Biol*. **2011**, 15, 752–759.

93. Dickmann, L.J.; Yip, V.; Li, C.; Abundes, J.J.; Maia, M.; Young, C.; Stainton, S.; Hass, P.E.; Joseph, S.B.; Prabhu, S.; et al. Evaluation of Fluorophotometry to Assess the Vitreal Pharmacokinetics of Protein Therapeutics. *Invest. Ophthalmol. Visual Sci.* **2015**, 56, 6991–6999.

94. Liu, Y.; Liu, J.; Zhang, X.; Zhang, R.; Huang, Y.; Wu, C. In Situ Gelling Gelrite/Alginate Formulations as Vehicles for Ophthalmic Drug Delivery. *AAPS PharmSciTech* **2010**, 11, 610–620.

95. Edsman, K.; Carlfors, J.; Petersson, R. Rheological evaluation of poloxamer as an in situ gel for ophthalmic use. *Eur. J. Pharm. Sci*. **1998**, 6, 105–112.

96. Carlfors, J.; Edsman, K.; Petersson, R.; Jörnving, K. Rheological evaluation of Gelrite® in situ gels for ophthalmic use. *Eur. J. Pharm. Sci*. **1998**, 6, 113–119.

97. Edsman, K.; Carlfors, J.; Harju, K. Rheological evaluation and ocular contact time of some carbomer gels for ophthalmic use. *Int. J. Pharm*. **1996**, 137, 233–241.

98. Berezovsky, D.E.; Patel, S.R.; McCarey, B.E.; Edelhauser, H.F. In Vivo Ocular Fluorophotometry: Delivery of Fluoresceinated Dextrans via Transscleral Diffusion in Rabbits. *Invest. Ophthalmol. Visual Sci*. **2011**, 52, 7038–7045.

99. Ghate, D.; Brooks, W.; McCarey, B.E.; Edelhauser, H.F. Pharmacokinetics of Intraocular Drug Delivery by Periocular Injections Using Ocular Fluorophotometry. *Invest. Ophthalmol. Visual Sci*. **2007**, 48, 2230–2237.

USC UNIVERSIDADE DE SANTIAGO DE COMPOSTELA

100. Lee, S.J.; Kim, E.S.; Geroski, D.H.; McCarey, B.E.; Edelhauser, H.F. Pharmacokinetics of Intraocular Drug Delivery of Oregon Green 488–Labeled Triamcinolone by Subtenon Injection Using Ocular Fluorophotometry in Rabbit Eyes. *Invest. Ophthalmol. Visual Sci*. **2008**, 49, 4506–4514.

101. Song, L.; Hennink, E.J.; Young, I.T.; Tanke, H.J. Photobleaching kinetics of fluorescein in quantitative fluorescence microscopy. *Biophys. J.* **1995**, 68, 2588.

102. Fanea, L.; Fagan, A.J. Magnetic resonance imaging techniques in ophthalmology. Mol. Vision 2012, 18, 2538.

103. Gomori, J.M.; Grossman, R.I.; Shields, J.A.; Augsburger, J.J.; Joseph, P.M.; DeSimeone, D. Ocular MR imaging and spectroscopy: an ex vivo study. *Radiology* **1986**, 160, 201–205.

104. Berkowitz, B.A.; Sato, Y.; Wilson, C.A.; De Juan, E. Blood-retinal barrier breakdown investigated by real-time magnetic resonance imaging after gadolinium-diethylenetriaminepentaacetic acid injection. *Invest. Ophthalmol. Visual Sci*. **1991**, 32, 2854–2860.

105. Kolodny, N.H.; Goode, S.T.; Ryan, W.; Freddo, T.F. Evaluation of therapeutic effectiveness using MR imaging in a rabbit model of anterior uveitis. *Exp. Eye Res*. **2002**, 74, 483–491.

106. Li, S.K.; Jeong, E.-K.; Hastings, M.S. Magnetic resonance imaging study of current and ion delivery into the eye during transscleral and transcorneal iontophoresis. *Invest. Ophthalmol. Visual Sci*. **2004**, 45, 1224–1231.

107. Richardson, J.C.; Bowtell, R.W.; Mäder, K.; Melia, C.D. Pharmaceutical applications of magnetic resonance imaging (MRI). *Adv. Drug Deliv. Rev*. **2005**, 57, 1191–1209.

108. Shah, N.J.; Oros-Peusquens, A.-M.; Arrubla, J.; Zhang, K.; Warbrick, T.; Mauler, J.; Vahedipour, K.; Romanzetti, S.; Felder, J.; Celik, A. Advances in multimodal neuroimaging: hybrid MR–PET and MR–PET–EEG at 3 T and 9.4 T. *J. Mag. Reson*. **2013**, 229, 101–115.

109. Koba, W.; Kim, K.; Lipton, M.L.; Jelicks, L.; Das, B.; Herbst, L.; Fine, E. Imaging Devices for Use in Small Animals. *Semin. Nucl. Med*. **2011**, 41, 151–165.

110. Fernández-Ferreiro, A.; González Barcia, M.; Gil-Martínez, M.; Vieites-Prado, A.; Lema, I.; Argibay, B.; Blanco Méndez, J.; Lamas, M.J.; Otero-Espinar, F.J. In vitro and in vivo ocular safety and eye surface permanence determination by direct and Magnetic Resonance Imaging of ion-sensitive hydrogels based on gellan gum and kappa-carrageenan. *Eur. J. Pharm. Biopharm*. **2015**, 94, 342–351.

111. Bert, R.J.; Caruthers, S.D.; Jara, H.; Krejza, J.; Melhem, E.R.; Kolodny, N.H.; Patz, S.; Freddo, T.F. Demonstration of an anterior diffusional pathway for



USC UNIVERSIDADE DE SANTIAGO DE COMPOSTELA

solutes in the normal human eye with high spatial resolution contrast-enhanced dynamic MR imaging. *Invest. Ophthalmol. Visual Sci*. **2006**, 47, 5153–5162.

112. Freddo, T.F.; Patz, S.; Arshanskiy, Y. Pilocarpine's effects on the blood-aqueous barrier of the human eye as assessed by high-resolution, contrast magnetic resonance imaging. *Exp. Eye Res.* **2006**, 82, 458–464.
113. Cheng, H.-M.; Kwong, K.K.; Xiong, J.; Chang, C. GdDTPA-enhanced magnetic resonance imaging of the aqueous flow in the rabbit eye. *Mag. Reson. Med.* **1991**, 17, 237–243.
114. Cheng, H.-M.; Kwong, K.K.; Xiong, J.; Woods, B.T. Visualization of water movement in the living rabbit eye. Graefe's Arch. *Clin. Exp. Ophthalmol*. **1992**, 230, 62–65.
115. Kim, H.; Robinson, M.R.; Lizak, M.J.; Tansey, G.; Lutz, R.J.; Yuan, P.; Wang, N.S.; Csaky, K.G. Controlled drug release from an ocular implant: an evaluation using dynamic three-dimensional magnetic resonance imaging. Invest. *Ophthalmol. Visual Sci*. **2004**, 45, 2722–2731.
116. Kim, S.H.; Csaky, K.G.; Wang, N.S.; Lutz, R.J. Drug elimination kinetics following subconjunctival injection using dynamic contrast-enhanced magnetic resonance imaging. *Pharm. Res.* **2008**, 25, 512–520.
117. Li, S.K.; Molokhia, S.A.; Jeong, E.-K. Assessment of subconjunctival delivery with model ionic permeants and magnetic resonance imaging. *Pharm. Res*. **2004**, 21, 2175–2184.
118. Molokhia, S.A.; Jeong, E.-K.; Higuchi, W.I.; Li, S.K. Examination of penetration routes and distribution of ionic permeants during and after transscleral iontophoresis with magnetic resonance imaging. *Int. J. Pharm*. **2007**, 335, 46–53.
119. Molokhia, S.A.; Jeong, E.-K.; Higuchi, W.I.; Li, S.K. Examination of barriers and barrier alteration in transscleral iontophoresis. *J. Pharm Sci*. **2008**, 97, 831–844.
120. Molokhia, S.A.; Jeong, E.-K.; Higuchi, W.I.; Li, S.K. Transscleral iontophoretic and intravitreal delivery of a macromolecule: study of ocular distribution in vivo and postmortem with MRI. *Exp. Eye Res*. **2009**, 88, 418–425.
121. Shi, X.; Liu, X.; Wu, X.; Lu, Z.-R.; Li, S.K.; Jeong, E.-K. Ocular pharmacokinetic study using T 1 mapping and Gd-chelate-labeled polymers. *Pharm. Res.* **2011**, 28, 3180–3188.
122. Jockovich, M.-E.; Murray, T.G.; Clifford, P.D.; Moshfeghi, A.A. Posterior juxtascleral injection of anecortave acetate: magnetic resonance and echographic imaging and localization in rabbit eyes. *Retina* **2007**, 27, 247–252.



USC UNIVERSIDADE DE SANTIAGO DE COMPOSTELA

123. Kim, H.; Lizak, M.J.; Tansey, G.; Csaky, K.G.; Robinson, M.R.; Yuan, P.; Wang, N.S.; Lutz, R.J. Study of ocular transport of drugs released from an intravitreal implant using magnetic resonance imaging. *Ann. Biomed. Eng*. **2005**, 33, 150–164.

124. Kolodny, N.H.; Freddo, T.F.; Lawrence, B.A.; Suarez, C.; Bartels, S.P. Contrast-enhanced magnetic resonance imaging confirmation of an anterior protein pathway in normal rabbit eyes. *Invest. Ophthalmol. Visual Sci*. **1996**, 37, 1602–1607.

125. Li, S.K.; Hao, J.; Liu, H.; Lee, J. MRI Study of Subconjunctival and Intravitreal Injections. *J. Pharm. Sci*. **2012**, 101, 2353–2363.

126. Berkowitz, B.A.; Wilson, C.A.; Tofts, P.S.; Peshock, R.M. Effect of vitreous fluidity on the measurement of blood-retinal barrier permeability using contrast-enhanced MRI. *Mag. Reson. Med*. **1994**, 31, 61–66.

127. Plehwe, W.E.; McRobbie, D.W.; Lerski, R.A.; Kohner, E.M. Quantitative magnetic resonance imaging in assessment of the blood-retinal barrier. *Invest. Ophthalmol. Visual Sci*. **1988**, 29, 663–670.

128. Berkowitz, B.A.; Tofts, P.S.; Sen, H.A.; Ando, N.; De Juan, E. Accurate and precise measurement of blood-retinal barrier breakdown using dynamic Gd-DTPA MRI. *Invest. Ophthalmol. Visual Sci*. **1992**, 33, 3500–3506.

129. Sen, H.A.; Berkowitz, B.A.; Ando, N.; de Juan, E. In vivo imaging of breakdown of the inner and outer blood-retinal barriers. *Invest. Ophthalmol. Visual Sci*. **1992**, 33, 3507–3512.

130. Sato, Y.; Berkowitz, B.A.; Wilson, C.A.; de Juan, E. Blood-retinal barrier breakdown caused by diode vs argon laser endophotocoagulation. *Arch. Ophthalmol*. **1992**, 110, 277–281.

131. Metrikin, D.C.; Wilson, C.A.; Berkowitz, B.A.; Lam, M.K.; Wood, G.K.; Peshock, R.M. Measurement of blood-retinal barrier breakdown in endotoxin-induced endophthalmitis. *Invest. Ophthalmol. Visual Sci*. **1995**, 36, 1361–1370.

132. Berkowitz, B.A.; Roberts, R.; Luan, H.; Peysakhov, J.; Mao, X.; Thomas, K.A. Dynamic contrast-enhanced MRI measurements of passive permeability through blood retinal barrier in diabetic rats. *Invest. Ophthalmol. Visual Sci*. **2004**, 45, 2391–2398.

133. Wilson, C.A.; Berkowitz, B.A.; Funatsu, H.; Metrikin, D.C.; Harrison, D.W.; Lam, M.K.; Sonkin, P.L. Blood-retinal barrier breakdown following experimental retinal ischemia and reperfusion. *Exp. Eye Res*. **1995**, 61, 547–557.



USC UNIVERSIDADE DE SANTIAGO DE COMPOSTELA

134. Alikacem, N.; Yoshizawa, T.; Nelson, K.D.; Wilson, C.A. Quantitative MR Imaging Study of Intravitreal Sustained Release of VEGF in Rabbits. *Invest. Ophthalmol. Visual Sci.* **2000**, 41, 1561–1569.

135. Raju, H.B.; Hu, Y.; Padgett, K.R.; Rodriguez, J.E.; Goldberg, J.L. Investigation of nanoparticles using magnetic resonance imaging after intravitreal injection. *Clin. Exp. Ophthalmol*. **2012**, 40, 100–107.

136. O'Connor, J.P.; Jackson, A.; Parker, G.J.; Jayson, G.C. DCE-MRI biomarkers in the clinical evaluation of antiangiogenic and vascular disrupting agents. *Br. J. Cancer* **2007**, 96, 189.

137. Waerzeggers, Y.; Monfared, P.; Ullrich, R.; Viel, T.; Jacobs, A.H. Multimodality imaging: overview of imaging techniques (CT, MRI, PET, optical imaging) and impact of multimodality imaging on drug development. In *Trends on the Role of PET in Drug Development*; World Scientific: Singapore, **2012**; pp. 319–382.

138. Fernández-Ferreiro, A. Manejo, seguridad y optimización de las formulaciones tópicas oftálmicas en Servicios de Farmacia Hospitalaria. PhD Thesis, Universidade de Santiago de Compostela, Santiago de Compostela, Spain, 2015.

139. Destruel, P.-L.; Zeng, N.; Maury, M.; Mignet, N.; Boudy, V. In vitro and in vivo evaluation of in situ gelling systems for sustained topical ophthalmic delivery: state of the art and beyond. *Drug Discovery Today* **2017**, 22, 638–651.

140. Eter, N. Molecular imaging in the eye. *Br. J. Ophthalmol*. **2010**, 94, 1420–1426.

141. Cai, W.; Chen, X. Nanoplatforms for targeted molecular imaging in living subjects. *Small* **2007**, 3, 1840–1854.

142. López-Barneo, J.; Pardal, R.; Ortega-Sáenz, P. Cellular mechanism of oxygen sensing. *Ann. Rev. Physiol*. **2001**, 63, 259–287.

143. Mankoff, D.A. Molecular imaging as a tool for translating breast cancer science. *Breast Cancer Res*. **2008**, 10, S3.

144. Kendall, C.J.; Prager, T.C.; Cheng, H.; Gombos, D.; Tang, R.A.; Schiffman, J.S. Diagnostic Ophthalmic Ultrasound for Radiologists. *Neuroimaging Clin. N. Am*. **2015**, 25, 327–365.

145. Nabili, M.; Patel, H.; Mahesh, S.P.; Liu, J.; Geist, C.; Zderic, V. Ultrasound-Enhanced Delivery of Antibiotics and Anti-Inflammatory Drugs into the Eye. *Ultrasound Med. Biol*. **2013**, 39, 638–646.

146. Nabili, M.; Mahesh, S.; Geist, C.; Zderic, V. 2088977 Ultrasound-Enhanced Delivery of Anti-Inflammatory Ophthalmic Drugs. *Ultrasound Med. Biol*. **2015**, 41, S63.



USC UNIVERSIDADE DE SANTIAGO DE COMPOSTELA

147. Huang, D.; Wang, L.; Dong, Y.; Pan, X.; Li, G.; Wu, C. A novel technology using transscleral ultrasound to deliver protein loaded nanoparticles. *Eur. J. Pharm. Biopharm.* **2014**, 88, 104–115.

148. Huang, D.; Chen, Y.-S.; Thakur, S.S.; Rupenthal, I.D. Ultrasound-mediated nanoparticle delivery across ex vivo bovine retina after intravitreal injection. *Eur. J. Pharm. Biopharm*. **2017**, 119, 125–136.

149. Virgili, G.; Menchini, F.; Casazza, G.; Hogg, R.; Das, R.R.; Wang, X.; Michelessi, M. Optical coherence tomography (OCT) for detection of macular oedema in patients with diabetic retinopathy. *Cochrane Database Syst. Rev*. **2015**, 1, CD008081.

150. Veverka, K.K.; Abouchehade, J.E.; Iezzi Jr, R.; Pulido, J.S. Noninvasive grading of radiation retinopathy: the use of optical coherence tomography angiography. *Retina* **2015**, 35, 2400–2410.

151. Spaide, R.F.; Fujimoto, J.G.; Waheed, N.K.; Sadda, S.R.; Staurenghi, G. Optical coherence tomography angiography. *Prog. Retinal Eye Res.* **2018**, 64, 1–55.

152. Wang, J.; Aquavella, J.; Palakuru, J.; Chung, S. Repeated measurements of dynamic tear distribution on the ocular surface after instillation of artificial tears. *Invest. Ophthalmol. Visual Sci*. **2006**, 47, 3325–3329.

153. Kaya, S.; Schmidl, D.; Schmetterer, L.; Witkowska, K.J.; Unterhuber, A.; Aranha dos Santos, V.; Baar, C.; Garhöfer, G.; Werkmeister, R.M. Effect of hyaluronic acid on tear film thickness as assessed with ultra-high resolution optical coherence tomography. *Acta Ophthalmol.* **2015**, 93, 439–443.

154. Brenner, D.J.; Hall, E.J. Computed Tomography — An Increasing Source of Radiation Exposure. *N. Engl. J. Med*. **2007**, 357, 2277–2284.

155. At'kova, E.L.; Tomashevskiĭ, I.O.; Luchshev, A.I.; Iartsev, V.D. Single-photon emission computed tomography in combination with X-ray computed tomography in the study of lacrimal passages. First results. *Vest. Rentgenol. Radiol.* **2014**, 26–30.



USC UNIVERSIDADE DE SANTIAGO DE COMPOSTELA

# CHAPTER 2

## RECENT RESEARCH IN OCULAR CYSTINOSIS: DRUG DELIVERY SYSTEMS, CYSTEAMINE DETECTION METHODS AND FUTURE PERSPECTIVES

USC
UNIVERSIDADE DE SANTIAGO DE COMPOSTELA

USC
UNIVERSIDADE
DE SANTIAGO
DE COMPOSTELA

# CHAPTER 2

## RECENT RESEARCH IN OCULAR CYSTINOSIS: DRUG DELIVERY SYSTEMS, CYSTEAMINE DETECTION METHODS AND FUTURE PERSPECTIVES


**ABSTRACT**

Cystinosis is a rare genetic disorder characterized by the accumulation of cystine crystals in different tissues and organs. Although renal damage prevails during initial stages, the deposition of cystine crystals in the cornea causes severe ocular manifestations. At present, cysteamine is the only topical effective treatment for ocular cystinosis. The lack of investment by the pharmaceutical industry, together with the limited stability of cysteamine, make it available only as two marketed presentations (Cystaran® and Cystadrops®) and as compounding formulations prepared in pharmacy departments. Even so, new drug delivery systems (DDSs) need to be developed, allowing more comfortable dosage schedules that favor patient adherence. In the last decades, different research groups have focused on the development of hydrogels, nanowafers and contact lenses, allowing a sustained cysteamine release. In parallel, different determination methods and strategies to increase the stability of the formulations have also been developed. This comprehensive review aims to compile all the challenges and advances related to new cysteamine DDSs, analytical determination methods, and possible future therapeutic alternatives for treating cystinosis.



**Keywords:** cystinosis; ophthalmic administration; cysteamine; drug delivery systems; analytical chemistry methods





USC UNIVERSIDADE DE SANTIAGO DE COMPOSTELA

## 1. INTRODUCTION

Cystinosis is a rare autosomal recessive disease that affects about 1 in 100,000–200,000 people among the general population [1], characterized by high levels of cystine within the lysosomes in cells of certain types of tissues. The accumulation of this substance is caused by mutations in the CTNS gene which codes for cystinosin, the carrier that transports cystine out of the lysosome [2,3]. The presence of cystine crystals in different tissues leads to the progressive impairment and dysfunction of multiple organs, such as kidneys, pancreas, brain, thyroid and eyes [4]. The disease, if it remains untreated, results in death from renal failure by the second decade of life [5].

Although renal damage prevails in premature forms of the disease, all forms of cystinosis affect ocular structures: cornea, conjunctiva, iris, ciliary body, choroid, retina and optic nerve. The most frequently described ocular manifestation is the deposition of cystine crystals in the cornea, but the exact mechanisms of crystal formation are not yet fully understood. Stromal crystals have a needle shape and are oriented parallel to the corneal stromal lamellae [6], which suggests that the structure of collagen in the stroma plays a very important role in the evolution of cystine crystals [7]. This deposition is one of the most troublesome complications affecting the quality of life of patients with cystinosis, especially as the prognosis improves and life expectancy increases, causing photophobia, visual impairment and, finally, blindness [8,9]. In addition, this accumulation with time can cause corneal scars, keratitis and cataracts [10].

Corneal crystals are visible on ophthalmological examination as of 16 months of age in most patients [11]. Recent exploration techniques with in vivo confocal microscopy and optical coherence tomography (OCT), anterior segment optical coherence tomography (AS-OCT) and in vivo confocal microscopy (IVCM) of the anterior segment, are useful methods to evaluate crystals and detect their morphological characteristics and corneal alterations [12,13].

Early diagnosis and treatment of the ocular manifestations of childhood nephropathic cystinosis are essential. Therefore, early initiation and adherence to topical therapy have a significant impact on disease progression [8]. Nowadays, although new prodrug strategies based on N-acyl or glutaric acid derivatives of cystamine have been researched [14,15], the aminothiol cysteamine remains the only available treatment of cystinosis [16]. It lowers intracellular levels of cystine by forming a cysteamine–cysteine mixed disulfide, which can egress the lysosome using the undamaged excretion pathway for lysine [17] (Figure 1). The authorization of oral cysteamine (Cystagon®) by the Food and Drug Administration (FDA) in 1994, and by the European Medicine Agency (EMA) in



USC UNIVERSIDADE DE SANTIAGO DE COMPOSTELA

1997, has totally changed the management and prognosis of the patients with cystinosis [11,18,19]. However, it does not prevent corneal crystal accumulation because it cannot reach the cornea due to its lack of vascularization [20]. Consequently, it is necessary to instill cysteamine on the ocular surface in order to eliminate the cystine crystals at this location [11].

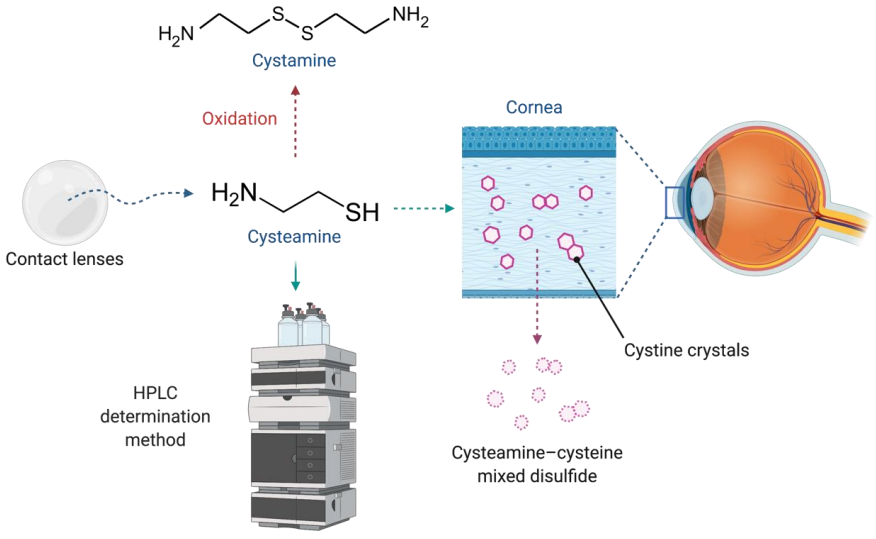



**Figure 1.** Cysteamine released from a drug delivery system to the ocular surface, where it forms the complex cysteamine-cysteine, facilitating the removal of cystine crystals from the cornea. Cysteamine is easily oxidized to cystamine, and can be detected from several determination methods, such as high-performance liquid chromatography (HPLC). Created with BioRender.com.

In 2012 Cystaran® (0.44% cysteamine ophthalmic solution) was approved by the FDA as an orphan drug indicated for the treatment of corneal cystine crystal deposits. The posology indicated in the prescribing information is one drop in each eye, every waking hour [21]. This posology, with its very frequent administrations, complicates patient's adherence to the treatment. In order to improve this aspect, in 2017 Cystadrops® (0.55% cysteamine ophthalmic solution) was approved by the EMA and by the FDA in 2020 [22]. It contains sodium carmellose which provides a high viscosity to the formulation, achieving a longer residence time on the ocular surface and allowing a dosage of just four times per day [23]. Therapeutic options marketed for ophthalmic treatment are scarce. Although ethical issues sometimes should outweigh economical and feasibility issues, the pharmaceutical industry does not allocate sufficient resources for the study of rare diseases and the development of orphan drugs. Because the commercialized cysteamine



USC UNIVERSIDADE DE SANTIAGO DE COMPOSTELA

presentations are not available in most countries, hospital pharmacy departments are responsible for preparing homemade eyedrops as a therapeutic alternative [24]. The problem is that on many occasions, these formulations lack exhaustive stability controls under different storage conditions, cysteamine being a very easily oxidizable molecule [25].

Concerning topical treatments for ocular cystinosis, the patients' therapeutic compliance is a major factor. In this regard, a new topical treatment, which only needs administrations every several hours or even days, would improve it [5]. The problem of the necessary frequent administration of topical cysteamine stems from the fact that eye drops are rapidly cleared from the ocular surface due to reflex tearing, constant blinking and nasolacrimal drainage resulting in a short contact time on the eye [26]. In addition, this organ has the tendency to maintain its residence volume at approximately 10 μL and, consequently, the bioavailability of a topically applied drug is typically <5% [27].

In this context, the development of new drug delivery systems (DDSs) which can overcome the high ocular clearance of conventional cysteamine eye drops is a major issue in ophthalmology research [28]. The increase of patient compliance with systems that delay the delivery of cysteamine and, consequently, minimize its frequency of administration is a key factor for improving the treatment of the pathology [20]. The aim of this comprehensive review is to make an overview of the new challenges in ocular cystinosis topical treatment, including cysteamine determination methods, developed DDSs and possible future therapeutic alternatives.

## 2. DRUG DELIVERY SYSTEMS (DDSs)

Ocular drug delivery has always been a challenge due to the limitations of conventional eye drops. The high tear turnover rate (1 μL/mL), loss of drug due to rapid blinking, reflex tear production, the tear-film barrier and high nasolacrimal drainage are factors that limit the absorption of topically applied ophthalmic formulations. To increase the drug bioavailability, a higher residence time on the ocular surface needs to be achieved. During the last decades, research has been done on the development of DDSs offering longer retention and a sustained release of the drug molecule to pass through these barriers [29]. The variability of DDSs intended for ophthalmic administration has experienced a large increase in the last decade. However, the difficulties associated with the stability of cysteamine, combined with the fact that cystinosis is a rare disease, means the development of DDSs intended to treat this disease has been more limited than in other ophthalmic diseases (Figure 2).



USC UNIVERSIDADE DE SANTIAGO DE COMPOSTELA

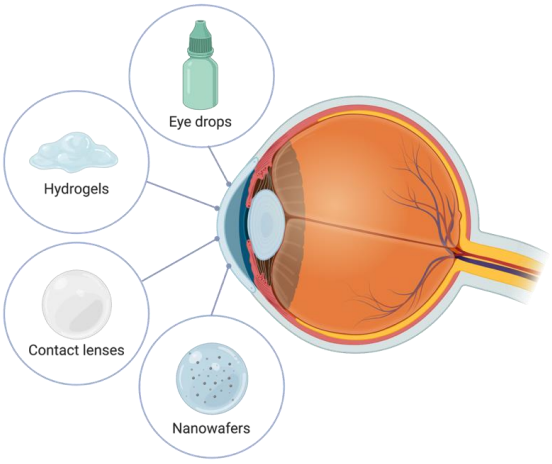



**Figure 2.** Drug delivery systems developed for cysteamine ophthalmic administration. Created with BioRender.com.

### *2.1. Hydrogels*

Hydrogels are networks of polymer chains extensively swollen with water, which they retain within their structure. Their porosity and high-water content make hydrogels suitable for encapsulation of water-soluble drugs, since they are processed at room temperature and organic solvents are rarely needed [30,31].

Hydrogels can be designed from natural or synthetic polymers. Natural polymers present the advantage of minimal toxicity due to their high biocompatibility. However, their main drawback is their considerably shorter drug release compared to synthetic hydrogels, which limits their use as long-term sustained DDS [31,32].

By formulating cysteamine as a bioadhesive ophthalmic gel with controlled drug release, the administration frequency could be reduced and, consequently, increase therapeutic compliance. Particularly, hydrogels which are transparent and bioadhesive are highly desirable for topical ophthalmic application [10]. Concerning the treatment of ocular cystinosis, several types of polymers have been used for the development of topical hydrogels.

#### 2.1.1. Synthetic Hydrogels

Synthetic hydrogels based on poly(acrylic acid) (PAA), commercially available as Carbopol®, can be obtained crosslinked with allylsucrose or allylpentaerythrol (carbomer) for pharmaceutical application. PAA is highly coiled and tightly packed but once dispersed in water the polymer swells to form a colloidal dispersion that



USC UNIVERSIDADE DE SANTIAGO DE COMPOSTELA

behaves as an anionic electrolyte. In addition, the nonNewtonian pseudoplastic rheology of PAA hydrogels enhances the process of blinking because it causes an important reduction in apparent viscosity as a function of the high external shear-stresses applied by the eyelid [5]. Considering these properties, Buchan et al. designed a hydrogel composed of carbomer 934 for the topical administration of cysteamine on the ocular surface. The formed hydrogel was bioadhesive, transparent and offered significantly less resistance to blinking than Newtonian liquids of equivalent consistency, resulting in longer contact times on the surface of the eye. Furthermore, dissolution studies showed a first-order release of the active drug from the sample matrix with no destruction of the gel properties due to the addition of cysteamine. Accordingly, the authors affirm that this kind of hydrogels based on pseudoplastic fluids form weak networks with desirable properties to increase the residence time of cysteamine on the ocular surface [5].

For their part, McKenzie et al. carried out rheology, bioadhesion, dissolution and stability studies with several synthetic polymers in order to test their suitability for ophthalmic delivery. In this sense, they agree with Buchan et al. regarding the fact that carbomer 934 is suitable for ophthalmic delivery of cysteamine. However, their studies showed problems related to gel opacity [10].

Although both previous formulations have been characterized, they lack in vivo studies which are indispensable to show the permanence of the gels on the ocular surface, especially considering that the aim of the studies was to extend the retention time of the cysteamine.

### 2.1.2. Natural Hydrogels

Regarding ophthalmic delivery of cysteamine using natural hydrogels, Bozda et al. synthetized viscous solutions of cysteamine hydrochloride by using hydroxypropylmethyl-cellulose (HPMC) and evaluated in vitro characteristics and stability. All the viscous solutions tested showed nonNewtonian flow behavior. Concerning in vitro release tests, they revealed that more than 80% of cysteamine hydrochloride was released from the HPMC solutions in 8 h. In addition, the formulations produced no irritation when they were tested on rabbit eyes [33].

On the other hand, McKenzie et al. showed that sodium hyaluronate and hydroxyethyl cellulose were both suitable for ophthalmic delivery of cysteamine. Among the obtained results, it is necessary to highlight the fact that sodium hyaluronate displayed optimum performance in the preformulation tests, being pseudoplastic and bioadhesive, as well as releasing cysteamine over 40 min [10].



USC UNIVERSIDADE DE SANTIAGO DE COMPOSTELA

In these sense, Luaces-Rodríguez et al. [9,24] selected two different polysaccharide hydrogels to formulate cysteamine: an ion sensitive hydrogel with the polymers gellan gum and kappa-carrageenan, and another composed of hyaluronic acid [10,34]. In this regard, the authors performed in vitro (characterization of the hydrogels, drug release and cell toxicity) and ex vivo (transcorneal permeation and Hen´s Egg Chorioallantoic membrane (HET-CAM)) assays. On the one hand, in vitro release studies determined that both hydrogels can control the release of cysteamine over time, showing zero-order kinetics for 4 h. At the same time, they affirmed that these hydrogels could act as corneal absorption promoters, as they allow a higher permeation of cysteamine through bovine cornea compared to a solution. On the other hand, ex vivo assays showed no irritation on the ocular surface. Finally, the authors also accomplished in vivo studies based on direct measures of biopermanence time by positron emission tomography (PET), demonstrating that both formulations presented a high retention time on the ocular surface of rats [9]. Hydrogels previously described, as well as their main characteristics, are listed in Table 1.

**Table 1.** Hydrogels developed as cysteamine delivery systems.

| Polymer name | Polymer type | % released cysteamine | Time | Reference |
|---|---|---|---|---|
| Carbomer 934 | Synthetic | 80 | 210 min[1] | [5] |
| Hyaluronic acid | Natural | 60.7 | 24 h | [9] |
| 88% Deacylated gellan gum and 12% kappa carrageenan | Natural | 36.3 | 24 h | [9] |
| Carbomer 934 | Synthetic | 80 | 20 min | [10] |
| Hydroxyethyl cellulose | Natural | 80 | 14 min | [10] |
| Hyaluronic acid | Natural | 80 | 14 min | [10] |
| Hydroxypropylmethyl-cellulose | Natural | 81,2 | 8 h | [33] |

[1] Cystamine–phenylalanine conjugate.

In spite of the fact that important advances have been made regarding the development of new hydrogels, further studies should be carried out. Specifically, regarding the development of smart hydrogels which can be very advantageous because they dramatically change their volume and other properties in response to environmental stimuli such as temperature or pH [35]. In addition, the synthesis of hydrogels based on nanoparticles could be a very promising strategy, which has provided interesting results in other pathologies [36].



USC UNIVERSIDADE DE SANTIAGO DE COMPOSTELA

### *2.2. Nanowafers*

Nanowafers are tiny transparent circular discs that can be applied on the ocular surface with a fingertip [37]. Marcano et al. synthetised cysteamine-nanowafers via a hydrogel template strategy. In this study, they fabricated poly(vinyl alcohol) (PVA) nanowafers loaded with cysteamine. They contained arrays of drug-loaded nanoreservoirs from which the drug was released in a tightly controlled way for an extended period of time. At the end of this period, the nanowafer dissolved and faded away. Cysteamine-nanowafers are highly transparent; in fact, the refractive index of a cysteamine-nanowafer is very close to that of a soft contact lens. Hence, nanowafer application on the cornea does not affect the normal vision. These authors found that cysteamine was stable in the nanowafer and in a therapeutically effective form for up four months when stored at room temperature [26].

In addition, they carried out in vivo studies to determine the efficacy of the cysteamine-nanowafer in comparison to topical cysteamine eye drop formulation (0.44%). Two groups of CTNS−/− mice (three per group) were treated with the cysteamine-nanowafer (10 μg of cysteamine, once a day) and cysteamine eye drops (5 μL, 22 μg) twice a day for 30 days. These studies revealed that compared to the baseline corneal cystine crystal volume, cysteamine eye drops reduced the crystal volume by 55%, while cysteamine-nanowafer reduced the crystal volume by 90%, confirming that the cysteamine nanowafer treatment was significantly more efficacious. The authors stated that this higher efficacy was due to the longer residence time of the drug molecules on the eye achieved with the nanowafer, which enabled their diffusion into the ocular surface epithelium [26].

The development of this nanowafer means a very innovative and interesting alternative to properly control cysteamine release on the ocular surface. In this sense, other studies are needed to explore the possibilities that nanosystems, which have demonstrated successful results for other pathologies, could offer for ocular cystinosis treatment [36,38].

### *2.3. Contact Lenses*

#### 2.3.1. Contact Lenses as Drug Delivery Systems

Contact lenses (CLs) are medical devices widely used by over 125 million individuals in the world to correct vision problems [39] and were proposed as ocular DDSs since the first prototypes were synthesized nearly 50 years ago. CLs are polymeric structures formed after a polymerization process of different monomers in the presence of a crosslinking agent. This system absorbs a large amount of water (30–80%) to form hydrogels having an aqueous phase permeable to oxygen. Depending on the nature and proportion of the different monomers that



USC UNIVERSIDADE DE SANTIAGO DE COMPOSTELA

make up the polymeric structure of the CLs, conventional hydrogels or silicone hydrogels can be obtained. Modern materials currently used are an evolution of the well-known lens materials based on poly-2-hydroxyethylmetacrilate (p-HEMA) and silicone hydrogels [40,41].

Over the last two decades, the use of CLs as DDSs has been studied for the treatment of numerous ophthalmic pathologies [42]. Once a CL is placed over the eye, a thin layer of fluid is formed between the lens and the cornea, which takes about 30 min to dilute. When a drug is included in this layer, the time of contact between the drug and the cornea would be increased and, therefore, bioavailability would increase to approximately 50% when compared to the administration of ocular drops (between 1–5%). Further, conjunctival absorption would diminish and, consequently, a smaller amount of drug would enter the systemic circulation, avoiding the appearance of adverse effects [39]. This increase in bioavailability would allow reduction of the dosage, enabling high therapeutic compliance for patients, and correct vision problems at the same time. The main limitation they present as DDSs is that polymers that make up the lenses and drugs have low affinity, leading to insufficient drug loading and too rapid delivery [43]. The main objective of many investigations in recent years has been to achieve a controlled and sustained drug release from the CL to the tear film located between the CL and the cornea so that corneal absorption can take place from there.

### 2.3.2. Modified Contact Lenses

The simplest method for incorporating drugs into CLs is by immersing them in concentrated solutions of the active ingredient although, as previously mentioned, this technique tends to lead to insufficient charges and excessively rapid releases. To achieve controlled sustained release, a series of modifications have been studied, such as the incorporation of polymeric nanoparticles, microemulsions, micelles, liposomes, diffusion barriers (e.g., vitamin E) and sophisticated loading techniques such as molecular imprinting, ion ligand polymeric systems, drug-loaded films or supercritical fluid technology. With all that, it is important to note that the final modified lenses must maintain the conditions of oxygen permeability, transparency, comfort, water content, mechanical properties, ionic permeability, relatively neutral pH, tonicity and stability, preferably at room temperature [40,43,44].

Cysteamine is a hydrophilic small molecule (77.15 g/mol) and easily oxidizable, that shows little affinity for unmodified commercial CLs, giving rise to short releases and risking toxicity effects. Vitamin E can be incorporated into commercial silicone hydrogel CLs as a diffusion barrier, a strategy initially proposed by Peng et al. [45-49], achieving a higher bioavailability than eye drops. Vitamin E is a biocompatible hydrophobic molecule that exhibits low solubility in water, and which creates a



USC UNIVERSIDADE DE SANTIAGO DE COMPOSTELA

tortuous pathway prolonging the drug diffusion time through the CL. Hydrophilic drugs like cysteamine must overcome the said obstacle to reach the ocular surface, increasing diffusion time. A vitamin E barrier is included through immersion of CLs in a solution of vitamin E in ethanol. The composition of the solution may differ according to the desired amount to be administered. Subsequently, the CL has to be placed in water to remove any remaining of ethanol, while the vitamin gets trapped within the CL. The antioxidant properties of vitamin E provide a certain degree of protection for a molecule as sensitive to oxidation as cysteamine. In addition, Vitamin E incorporation can block UV radiation, an additional benefit to cystinosis patients. On the other hand, even though the transparency of the CL is not affected, it can affect its size, oxygen diffusion and ionic permeability, which depend on the thickness of the barrier [39,50].

Hsu et al. studied the use vitamin-E-modified silicone-hydrogel CLs to extend the delivery of cysteamine. ACUVUE OASYS® (Senofilcon A) with 19.14% vitamin and 1-DAY ACUVUE® TruEye™ (Narafilcon B) with 10.22% vitamin E prolonged release durations about 3 h and 25 min, respectively. The mass of cysteamine released from the CLs decreased when vitamin E was incorporated. ACUVUE® OASYS® delivered about 583.4 μg of drug, but with the incorporation of 19.14% vitamin E this decreased to 408.8 μg. In the same way, the 1-DAY ACUVUE® TruEye™ released 654.9 μg, but the mass released was reduced to 600.1 and 527.7 μg for 10.22% and 22.24% vitamin E loadings, respectively. Authors predicted that either a single 19.14% vitamin E loaded ACUVUE® OASYS® or two 10.22% vitamin E loaded 1-DAY ACUVUE® TruEye™ per day were the safest options to deliver therapeutic doses of cysteamine to cornea. Results were based on an in vivo mathematical model used as an initial predictor of dose-related toxicity in animal studies. In this work it was also concluded that it was not clear whether a two hour release duration may be enough, since the current therapy uses 8–10 eye drops administered throughout the day [50].

Years later, Dixon et al. showed that vitamin E incorporation into CLs increases the duration of cysteamine release in silicone-hydrogels ACUVUE® OASYS® (Senofilcon A) and ACUVUE® TruEye™ (Narafilcon A), the effect being more pronounced in TruEye™, possibly due to the low solubility of vitamin E in the lens matrix and higher aspect ratio of the barriers. The change observed in the composition of ACUVUE® TruEye™ in regard to Hsu's work, was due to the fact that since 2010, the brand gradually replaced Narafilcon B to Narafilcon A [51]. They also explored the effect of vitamin E incorporation in p-HEMA hydrogel CLs, ACUVUE® Moist® (Etafilcon A). Release durations were significantly increased in ACUVUE® TruEye™ to 0.90, 2.0, and 4.0 h for vitamin E loadings of 10%, 20%, and 30%, respectively. For ACUVUE®OASYS® lenses, release durations increased to 0.89, 2.15, and 4.25 h for 10, 20 and 30% loadings, respectively. Vitamin E incorporation did not significantly increase the release duration for hydrogel



USC UNIVERSIDADE DE SANTIAGO DE COMPOSTELA

ACUVUE® Moist® lenses, suggesting that vitamin E did not form barriers in hydrogel lenses. This data, along with the high aspect ratio in silicone hydrogels suggests that barriers could be forming at the interface of the silicone and hydrogel phases. Both cysteamine mass loaded and partition coefficients decreased for increasing vitamin E loadings, as seen in Table 2. CLs would need to be worn for about 4–5 h each day, less time than the typical duration of daily-wear. Finally, they also showed that daily use of cysteamine-loaded CLs did not cause any adverse response in the eyes of rabbits over a seven-day use [52].

Recently, the same research group developed CLs with carbon black to obtain tinted lenses to mitigate photophobia reducing transmittance. The presence of cystine crystals in the cornea causes photophobia, or extreme light sensitivity, in patients with cystinosis [53] which, after years of squinting, can cause intractable blepharospasm [54,55]. This incorporation can be used in cysteamine-vitamin E-loaded lenses, maintaining controlled release and keeping the lens parameters when carbon black concentrations of 0.3% are used [56]. Despite the advances made in the development of CLs as cysteamine delivery systems, more studies are needed to allow for their optimization. For this, it is important to select those CLs that have a more suitable composition for correct loading and release, and to develop methods that allow better control of release without affecting any of the CL's parameters and preserving the stability of the cysteamine. Composition, total amount of cysteamine released and release time of the previously described CLs are summarized in Table 2.

**Table 2.** Contact lenses developed as cysteamine delivery systems.

| Commercial name | Material | Diffusion barrier | Total cysteamine release amount (μg) | Release duration | Reference |
|---|---|---|---|---|---|
| **1-DAY ACUVUE® TruEye™** | Narafilcon B (silicone hydrogel) | 10.22% VE[1] | 600.1 ± 27.2 | 25 min | [50] |
| **1-DAY ACUVUE® TruEye™** | Narafilcon B (silicone hydrogel) | 22.24% VE | 527.7 ± 21.7 | 90 min | [50] |
| **ACUVUE® OASYS®** | Senofilcon A (silicone hydrogel) | 19.14% VE | 408.8 ± 33.9 | 3 h | [50] |
| **1-DAY ACUVUE® TruEye™** | Narafilcon A (silicone hydrogel) | 10% VE | 651 ± 31.2 | 0.90 h | [52] |
| **1-DAY ACUVUE® TruEye™** | Narafilcon A (silicone hydrogel) | 20% VE | 603.1 ± 21.2 | 2 h | [52] |
| **1-DAY ACUVUE® TruEye™** | Narafilcon A (silicone hydrogel) | 30% VE | 538.9 ± 17.3 | 4 h | [52] |
| **ACUVUE® OASYS®** | Senofilcon A (silicone hydrogel) | 10% VE | 464.0 ± 8.6 | 0.89 h | [52] |
| **ACUVUE® OASYS®** | Senofilcon A (silicone hydrogel) | 20% VE | 408.1 ± 36.7 | 2.15 | [52] |
| **ACUVUE® OASYS®** | Senofilcon A (silicone hydrogel) | 30% VE | 345.0 ± 33.2 | 4.25 h | [52] |
| **Noncommercial** | - | 0.3% CB[2] | 148 ± 10 | 10 min | [56] |
| **Noncommercial** | - | 0.3% CB + 20% VE | 123 ± 7 | 40 min | [56] |

[1] VE: vitamin E; [2] CB: carbon black.



USC UNIVERSIDADE DE SANTIAGO DE COMPOSTELA

CLs are presented as DDSs easy to administer and comfortable to the patient with dosing schedules that lead to better adherence than those obtained under frequent instillation of ophthalmic drops. Despite this, CLs are not available on the market due to issues like drug stability during processing/manufacturing, achievement of zero-order release kinetics, avoidance of drug release during the post-manufacturing monomer extraction step, protein adherence, drug release during storage and cost-benefits. However, they have potential applicability in the field of ophthalmic compounding, as drugs and excipients can be easily loaded onto them under sterile conditions as part of a relatively simple low-cost formulation process [43].

## 3. STABILITY AND ANALYTICAL DETERMINATION METHODS

### *3.1. Cysteamine Structure and Stability Properties*

Cysteamine (also known as β-mercaptoethylamine, 2-aminoethanethiol, 2-mercaptoethylamine, thioethanolamine and mercaptamine) is an aminothiol compound ($HS\text{-}CH_2\text{-}CH_2\text{-}NH_2$) whose endogenous production occurs during the degradation of coenzyme A, when pantetheine is formed during the co-enzyme A metabolism cycle [57,58]. The efficacy of cysteamine in cystinosis treatment may be limited by its unpleasant organoleptic properties, strong hygroscopicity and chemical instability. The latter is especially important to take into account for the development of new ophthalmic formulations, being important to have a good determination method that allows its qualitative and quantitative detection, as well as distinguishing between its main oxidation metabolite cystamine.

Cysteamine exposure to air once the eye drop bottle is opened results in a short shelf life [25]. This degradation is due to a thiol functional group which immediately reacts with oxygen to produce a disulphide called cystamine, which is not effective at treating the cystine crystals located in the cornea [2,59]. This oxidation process takes place easily and rapidly in air and solution as a zero-order reaction, which indicates that the concentration of cysteamine decreases linearly with time [60]. The removal of oxygen from a solution of cysteamine by packing under nitrogen, and the addition of ascorbic acid, increase its stability. However, this technique showed lower efficacy in comparison with chelating agents such as disodium edetate [61,62]. In addition, it is also important to take into account the nature of the container, being preferable to use those materials that prevent the passage of oxygen inside. Other strategies to increase its stability have been used, such as the reduction of the pH (between 4.1 and 4.5) and freezing [63].

Dixon et al. evaluated two approaches for preventing the oxidation of cysteamine to increase the time of use after opening the bottle to one month. Firstly, they studied the use of antioxidants such as catalase enzyme and vitamins C and E,



USC UNIVERSIDADE DE SANTIAGO DE COMPOSTELA

showing that catalase is the most effective additive, decreasing the oxidation rate by 58%. Secondly, the incorporation of diffusion barriers to prevent oxygen from reaching the cysteamine solution were investigated. This was accomplished by two methods: formulation of a hydrophobic layer which floats on the surface of the aqueous solution, and integration of OMAC® oxygen resistant material into the eye drop bottle. Both delayed the onset of cysteamine degradation and decreased the rate of degradation [63].

In this sense, another important barrier for the development of cysteamine topical formulations is the fact that its physicochemical properties combined with its low molecular weight (77.15 g/mol) make its quantification a difficult issue, which is still trying to be solved nowadays [64].

### *3.2. Cysteamine Analytical Determination Methods*

Diverse analytical methods have been proposed in the literature to detect and quantify cysteamine in nonbiological and biological samples (plasma and urine) such as high-performance liquid chromatography (HPLC) with fluorescence and ultraviolet (UV) detection, high-voltage electrophoresis, ion-exchange column chromatography, enzymatic assay and gas chromatography with flame ionization and photometric detection. The choice of the most adequate method for each situation is difficult because it must be based on several parameters such as the type of sample [60]. Cysteamine structure does not present a chromophore in its structure, so that conventional analytical methods with UV absorbance or fluorescence detection are not useful if the molecule remains unchanged. For its detection and quantification with these techniques, a derivatization process is necessary. In the last four decades, numerous derivatization agents were applied and optimized [65-81]. Most of the methods described below have not been specifically used for the determination of cysteamine from DDSs, but rather most of them have been purposed for the determination of cysteamine in biological samples and in cosmetic products.

#### 3.2.1. High-Performance Liquid Chromatography (HPLC)

Cysteamine detection by HPLC is performed using fluorescence, UV, and electrochemical detections. As mentioned before, when fluorescence and UV detectors are used, derivatization is usually needed [65-81], while for electrochemical methods this is not required. Derivatization agents, conditions and elution times are summarized in Table 3. Among methods depicted in this table, it is worth highlighting the one recently published by Kim et al. It is a simple and effective analytical method for the quantitation of cysteamine using reversed-phase HPLC for simultaneous determination of cysteamine and cystamine, in which the previous derivatization process is not necessary [64].



USC UNIVERSIDADE DE SANTIAGO DE COMPOSTELA

**Table 3.** HPLC detection methods for cysteamine.

| Derivatization Agent | Stationary Phase | Mobile Phase | Flow Rate (mL/min) | Detector [1] | T (°C) | Elution Time (min) | Limit of Detection | Ref. |
|---|---|---|---|---|---|---|---|---|
| 2-chloro-1-methylquinolinium tetrafluoroborate | C18 (5 µm; 4.6 mm × 150 mm) | Gradient elution or isocratic elution (trichloro acetic acid and acetonitrile) | 1 | UV | 25 | 9 | 0.1 µM | [76] |
| Monobromo-bimane | C18 (5 µm; 4.6 mm × 150 mm) | Gradient elution (methanol, acetic acid and water) | 1.5 | FL | RT | 12.5 | nmol | [68] |
| Monobromo-bimane | C18 (3 µm; 4.6 mm × 150 mm) | Acetonitrile | 1.5 | FL | RT | 4.3 | 50 nM | [69] |
| Monobromo-bimane | C18 (5 µm; 2.1 mm × 100 mm) | Water: methanol (65:35) | 0.3 | FL | - | 11 | 2 nM | [70] |
| Ammonium 7-fluorobenzo-2-oxa-1,3-diazole-4-sulphonate | C18 (8–10 µm; 3.9 mm × 300 mm) | Gradient elution (methanol and sodium acetate) | 1 | FL | RT | 10 | 0.07 pmol | [71] |
| Ammonium 7-fluorobenzo-2-oxa-1,3-diazole-4-sulphonate | C18 (5 µm; 2.0 mm × 250 mm) | Phosphate buffer: $CH_3CN$ (96:4) | 0.3 | FL | 30 | 5 | 0.47 µM | [72] |
| N-(1-pyrenyl) maleimide | C18 (5 µm; 4.6 mm × 250 mm) | Acetonitrile: water (70:30) | 1 | FL | RT | 10 | 0.01 nM | [77] |
| 7-chloro-N-[2-(dimethylamino)ethyl]-2,1,3-benzoxadiazole-4-sulfonamide | C18 (2 nm, 4.6 mm × 150 mm) | Gradient elution (water, acetonitrile and trifluoroacetic acid) | 0.6 | FL | 50 | 6.4 | 154 fmol | [79] |
| 4-fluoro-7-sulfamoyl benzofurazan | C18 (3 µm; 3.9 mm × 150 mm) | 2.5% methanol and ammonium acetate | 1 | FL | - | - | - | [80] |
| 6-aminoquinolyl-N-hydroxysuccinimidyl carbamate | C18 (5 µm; 2.1 mm × 150 mm) | Gradient elution (sodium acetate and trimethyl- amine, acetonitrile and water) | 0.3 | FL | RT | 29 | 0.77 pmol | [81] |
| - | C18 (5 µm; 4.6 mm × 250 mm) | NaHpSO in phosphoric acid:acetonitrile (85:15) | 1 | UV | 25 | 6.9 | 0.032 µg | [64] |
| 5,5′-dithiobis-(2-nitrobenzoic) acid | C18 (5 µm, 4.6 mm × 250 mm) | Gradient elution (formic acid and acetonitrile) | 1.0 | UV | RT | 26 | 3.3 mg | [82] |

[1] FL: HPLC coupled with fluorescence detection; UV: HPLC coupled with UV detection; RT: Room temperature

### 3.2.2. Ion-Exchange Column Chromatography

The detection of cysteamine by ion-exchange column chromatography using an amino acid analyzer was accomplished in 1978 by Hsiung et al. Unfortunately, cysteamine was detected after 268 min, which is a long time that may lead to the oxidation of the product during the analysis [83]. Years later, Ida et al. used o-phthalaldehyde in the presence of 2-mercaptoethanol and sodium hypochlorite as a derivatization agent. This method was found to be suitable for evaluating the cysteamine and cystamine content in various organs and tissues [74].

### 3.2.3. Enzymatic Essay

This assay consists of the inhibition of d-amino acid oxidase enzyme activity by the product of the reaction occurring between cysteamine and bromopyruvate. Thus, the enzyme activity is proportional to the amount of cysteamine [84]. In 1987, Duffel et al. described a new method based on the oxidation of cysteamine to hypotaurine by the action of cysteamine dioxygenase. Consequently, the quantification of oxygen uptake was proportional to cysteamine concentration [85].

### 3.2.4. Gas Chromatography

The most used derivative agents for quantification of cysteamine by flame ionization are pivaldehyde (2,2-dimethylpropanal) and (trimethylsilyl) trifluoracetamide [65,66]. On the other hand, regarding flame photometric detection, isobutylchloroformate was used as the derivatization agent in a sensitive and selective method developed by Kataoka et al. [73,75]. Derivation agents, carrier gas, columns and temperature conditions of gas chromatography methods are described in Table 4.

**Table 4.** Gas chromatography detection of cysteamine.

| Derivatization agent | Carrier gas | Column used | Temperature (°C) | Limit of detection | Ref. |
|---|---|---|---|---|---|
| **Pivaldehyde[1]** | Helium (35 mL/min) | 5% SE-30 5′x 1/8″ | From 80° to 250 °C at 10°/min | 8 pmole | [65] |
| **(Trimethylsilyl) trifluoro acetamide[1]** | Helium (80 mL/min) | 2% SE-30 6 ft. ¼ | From 75° to 230 °C at 8°/min | Sub nanomole | [66] |
| **Isobutyl Chloroformate[2]** | Nitrogen (8 mL/min) | DB-210 15 m x 0.53 mm | From 170° to 250 °C at 5°/min | 2 pmole | [73] |
| **Isobutyl Chloroformate[2]** | Nitrogen (10 mL/min) | DB-210 15 m x 0.53 mm | From 170° to 250 °C at 5°/min | 2 pmole | [75] |

[1] Flame ionization; [2] Flame photometric detection



USC UNIVERSIDADE DE SANTIAGO DE COMPOSTELA

### 3.2.5. Electrochemical Detection

As previously commented, cysteamine is easily oxidized to cystamine, a process that can be electrochemically detected. These types of reactions consist of the gain or loss of electrons followed by subsequent rearrangements. Diverse electrodes have been used. Kelly et al. [86] described the first electrochemical detection of cysteamine when cysteamine was first analyzed by HPLC with an electrochemical detector with a platinum electrode or a single gold/mercury electrode [87,88]. Later, modified electrodes have been used due to high overpotential and low electrical signals associated with the use of unmodified electrodes. Raoof et al. fabricated a functionalized single-wall carbon nanotube modified glassy carbon electrode [89]. In later years, several research groups worked on the development of new modified electrodes: carbon paste electrode [90-95], multiwall carbon nanotubes paste electrode [96-99] and screen-printed electrode [100]. The modified electrodes mentioned above are summarized in Table 5.

Electrochemical methods showed a linear relationship between the catalytic oxidation peak and cysteamine concentration, being applicable in certain concentration ranges and different samples [60].



USC UNIVERSIDADE DE SANTIAGO DE COMPOSTELA

**Table 5.** Electrochemical detection methods.

| Electrode | Mediator | Concentrations Range (μM) | Limit of Detection (μM) | References |
|---|---|---|---|---|
| Single-wall carbon nanotube modified glassy carbon electrode | 1,2-*N*-aphthoquinone-4-sulfonic acid sodium | 5.0–270 | 3.0 | [89] |
| Carbon paste electrode | *N*,*N*-dimethylaniline/ferrocyanide | 80–1140 | 79.7 | [90] |
| Carbon paste electrode | (9, 10-dihydro-9, 10-ethanoanthracene-11, 12-dicarboximido)-4-Ethylbenzene-1, 2-diol and nickel-oxidecarbon nanotube | 0.01–250 | 0.007 | [91] |
| Carbon paste electrode | Ferrocene carboxaldehyde and nickel-oxide nanoparticle | 0.09–300 | 0.06 | [92] |
| Carbon paste electrode | Acetylferrocene and Nickel-oxide-carbon nanotube | 0.1–600 | 0.07 | [93] |
| Carbon paste electrode | *N*-(4-hydroxyphenyl)-3,5-Dinitrobenzamide and magnesium oxide nanoparticles | 0.03–600 | 0.009 | [94] |
| Carbon paste electrode | NiO dope Pt nanostructure hybrid (NiO–Pt–H) | 0.003–200 | 0,0005 | [95] |
| Multiwall carbon nanotubes paste electrode | Isoproterenol | 0.3–450.0 | 0.09 | [96] |
| Multiwall carbon nanotubes paste Electrode | Ferrocene | 0.7–200 | 0.3 | [97] |
| Multiwall carbon nanotubes paste electrode | 3,4-Dihydroxycinnamic acid | 0.25–400 | 0.09 | [98] |
| Multiwall carbon nanotubes paste electrode | Promazine hydrochloride | Two dynamic ranges of 2.0–346.5 μM and 346.5–1912.5 μM | 0.8 | [99] |
| Screen printed electrode | $La_2O_3/Co_3O_4$ | 1.0–700.0 | 0.3 | [100] |

## 4. CURRENT SITUATION AND FUTURE PERSPECTIVES

At present, and as previously mentioned, only two presentations are available on the market for the treatment of ocular cystinosis despite new developments in the field of cysteamine DDSs. The first commercialized one was Cystaran®, which consists of an aqueous solution of 0.44% cysteamine, and the second, Cystadrops®, whose composition is sodium carmellose, which provides greater viscosity and biopermanence on the ocular surface. Due to this addition, Cystadrops® presents a more comfortable dosage schedule (administrated every 4 h) than Cystaran® (administered every hour while awake) [21-23]. Along with these presentations, in the last few years topical compounding formulations prepared by hospital pharmacy services have also been used for the treatment of ocular cystinosis [24,44]. Many of these compounding formulations lacked clinical trials to evaluate their efficacy in clinical practice.

Nowadays, at clinicaltrials.gov there is only one ongoing clinical trial recruiting for the evaluation of a new therapy for the treatment of cystinosis. This study is a phase 1/2 clinical trial (NCT03897361) that will assess the safety and efficacy of enriched gene-corrected hematopoietic stem cells isolated from patients affected with cystinosis. The subjects receive marrow cytoreduction with busulfan prior to infusion of the genetic investigational product CTNS-RD-04 [101].

According to a quality assessment of investigational studies in the therapeutic use of cysteamine in cystinosis, only a few references provide an adequate quality level in order to stablish an acceptable strength of recommendation [102]. At present there is only one randomized clinical trial that could report on the efficacy and safety of cysteamine eye drops in preventing eye complications associated with cystinosis [20]. However, this trial does not have a sufficient quality level to issue a recommendation about cysteamine use in this indication. All other studies [103-106], although classified as randomized studies, cannot be considered as such, as they do not employ a real randomization per patient. These studies employ a per eye randomization so that the same patient receives the intervention treatment in one eye, and the control in the other. This, while a common practice in ophthalmology clinical trials, is not recommended [107], as it does not imply a real randomization as to the effect that this element of clinical research study design can have on bias reduction.

The only randomized clinical trial available [20] compared a viscous commercial presentation with an hydrochloride cysteamine concentration of 0.55% with a hospital pharmacy formulation of 0.10%. It used as its primary end point the difference from the baseline density assessment of cysteamine crystals measured through IVCM. Photophobia was included as a secondary end point. In the results



USC UNIVERSIDADE DE SANTIAGO DE COMPOSTELA

analysis, taking into account the number of eyes rather than the number of patients, there was a loss of assessment of 33% of the eyes in the intervention group and 47% of the eye evaluations of the control group. In this analysis, the preparation in the form of 0.55% viscous gel found a 40.4% reduction in density, compared to 0.7% in the control group. The selected primary variable was a subjective variable, which would have been required to improve the internal validity of the analysis as a blind study. Instead, the design of the study was open, which increased uncertainty about the results obtained. In addition, the loss of patients could have resulted in the invalidity of the results, while the selection as a comparator of a concentration formulation more than five times lower could have justified the differences.

A recent systematic review and meta-analysis concluded that the viscous formulation of cysteamine 0.55% was better than standard formulation of cysteamine 0.1% in terms of efficacy. The lack of efficacy of the standard formulation might have been due to use of low dose (0.1% in the standard formulation group compared to 0.55% in the viscous formulation group). However, relative stability and requirement of less frequent application of the viscous solution gave an added advantage. Although, occurrences of local adverse events were more in the viscous formulation group, they were manageable. More trials with equivalent doses between the standard and viscous formulation to evaluate the comparative safety and efficacy are needed [16,107]. However, despite the low quality evidence, prospective observational studies suggest that cysteamine continues to be considered as a useful therapeutic strategy to delay ocular signs and symptoms associated with this systemic pathology [1].

At present, in order to overcome the main drawbacks linked to the use of conventional eye dosage forms, new DDSs are being developed for the treatment of ocular cystinosis. In spite of the fact that significant advances have been made in the area, there are still some unexplored alternatives which must be studied because of their promising in vivo results in other diseases, such as liposomes and nanoparticles developed for the treatment of glaucoma or age-related macular degeneration [36,38,108].

Nowadays, other pathways have been recently explored to improve the treatment of ocular cystinosis. Andrzejewska et al. hypothesized that cystinosin could have other roles in addition to transporting cystine out of the lysosome. In this sense, they found that the mammalian target of the rapamycin complex 1 (mTORC1) pathway, which serves as a core regulator of cellular metabolism, proliferation, survival and autophagy, was downregulated in proximal tubular cell lines derived from Ctns2/2 mice. Decrease of lysosomal cystine levels due to the administration of cysteamine did not rescue mTORC1 activation in these cells, suggesting that the downregulation of mTORC1 was due to the absence of cystinosin rather than to the



USC UNIVERSIDADE DE SANTIAGO DE COMPOSTELA

accumulation of cystine. In conclusion, their results showed a dual role for cystinosin as a cystine transporter and as a component of the mTORC1 pathway, and highlighted the need to develop new treatments not only dependent on lysosomal cystine depletion [109].

Another approach to the improvement of ocular cystinosis treatment was carried out by Thoene et al. The therapeutic use of transmembrane proteins, such as cystinosin, is limited because of irreversible denaturation when they are not in their native lipid membrane. In this regard, these authors showed that microvesicles containing functional cystinosin were spontaneously produced by infecting *Spodoptera frugiperda* cells (Sf9) with baculovirus containing human wild-type CTNS. Furthermore, they demonstrated that the addition of such microvesicles containing cystinosin green fluorescent protein (GFP) to ex vivo rabbit ocular globes yielded punctate perinuclear green fluorescence in the corneal keratocytes. These results support potential therapeutic use of these cystinosin containing microvesicles in treating ocular cystinosis with the advantage of administering twice per month instead of daily topical administration. However, further preclinical and clinical trials should be done in order to confirm the obtained results [110].

Finally, in 2020 Hollywood et al. generated the first human induced pluripotent stem cell (iPSC) and kidney organoid models of cystinosis. They used several techniques to examine hallmarks of cystinosis, including cystine accumulation, lysosome size, the autophagy pathway and apoptosis in the cystinosis models. Compared with controls, these cystinosis models exhibited elevated cystine levels, increased apoptosis and defective basal autophagy. On the one hand, cysteamine treatment ameliorated this phenotype except for abnormalities in apoptosis and basal autophagy. On the other hand, they found that treatment with everolimus, an inhibitor of the mTOR pathway, reduced the number of large lysosomes, decreased apoptosis and activated autophagy, but it did not rescue the defect in cystine loading. Accordingly, dual treatment of cystinotic iPSCs or kidney organoids with cysteamine and everolimus corrected all of the observed phenotypic abnormalities. Consequently, the authors suggested that combination therapy with cysteamine and everolimus may be the future of cystinosis treatment, improving upon current therapeutic treatments [111].

## 5. CONCLUSIONS

Cystinosis is a rare metabolic disease for which, even today, there is no definitive cure. To prevent its progression, cysteamine is systemically administered allowing the formation of the cysteamine-cysteine complex, which prevents the accumulation of cystine crystals in the body's tissues. To achieve effective concentrations in the



USC UNIVERSIDADE DE SANTIAGO DE COMPOSTELA

cornea, its topical administration is required. Two presentations are marketed as ophthalmic drops (Cystaran® and Cystadrops®), which present complicated dosage schedules that make treatment compliance difficult. For all these reasons, it is important to develop new DDSs that would allow increasing the corneal residence time, ocular bioavailability and comfort for the patient. This development remains challenging, since cysteamine is a very sensitive compound to oxidation, and whose analytical determination is complex.

In the last decades, different research groups have focused on the development of hydrogels, nanowafers and contact lenses, which allow a sustained release of cysteamine for longer periods of time compared to eye drops. However, new DDSs, which have offered promising possibilities in other diseases such as liposomes and nanoparticles, must be explored. For the characterization of ophthalmic formulations, it is important to have a good analytical determination method, although most of the proposed ones have not been developed for this objective. Even so, more studies are still needed to achieve optimal cysteamine release that favors comfortable dosage schedules without compromising drug stability, and thus offer a definitive ophthalmic treatment that prevents the advance of the ocular cystinosis, as well as exploring new therapeutic alternatives that allow the disease to be addressed by other pathways.

## 6. REFERENCES

1. Liang, H.; Labbé, A.; Baudouin, C.; Plisson, C.; Giordano, V. Long-term follow-up of cystinosis patients treated with 0.55% cysteamine hydrochloride. *Br. J. Ophthalmol*. **2021**;105(5):608-613.
2. Shams, F.; Livingstone, I.; Oladiwura, D.; Ramaesh, K. Treatment of corneal cystine crystal accumulation in patients with cystinosis. *Clin. Ophthalmol. Auckl. NZ* **2014**, 8, 2077–2084.
3. Biswas, S.; Gaviria, M.; Malheiro, L.; Marques, J.P.; Giordano, V.; Liang, H. Latest Clinical Approaches in the Ocular Management of Cystinosis: A Review of Current Practice and Opinion from the Ophthalmology Cystinosis Forum. *Ophthalmol. Ther*. **2018**, 7, 307–322.
4. Syres, K.; Harrison, F.; Tadlock, M.; Jester, J.V.; Simpson, J.; Roy, S.; Salomon, D.R.; Cherqui, S. Successful treatment of the murine model of cystinosis using bone marrow cell transplantation. *Blood* **2009**, 114, 2542–2552.
5. Buchan, B.; Kay, G.; Heneghan, A.; Matthews, K.H.; Cairns, D. Gel formulations for treatment of the ophthalmic complications in cystinosis. *Int. J. Pharm*. **2010**, 392, 192–197.



USC UNIVERSIDADE DE SANTIAGO DE COMPOSTELA

6. Alsuhaibani, A.H.; Khan, A.O.; Wagoner, M.D. Confocal microscopy of the cornea in nephropathic cystinosis. *Br. J. Ophthalmol*. **2005**, 89, 1530–1531.

7. Dixon, P.; Christopher, K.; Chauhan, A. Potential role of stromal collagen in cystine crystallization in cystinosis patients. *Int. J. Pharm*. **2018**, 551, 232–240.

8. Nesterova, G.; Gahl, W.A. Cystinosis: The evolution of a treatable disease. Pediatr. *Nephrol. Berl. Ger*. **2013**, 28, 51–59.

9. Luaces-Rodríguez, A.; Díaz-Tomé, V.; González-Barcia, M.; Silva-Rodríguez, J.; Herranz, M.; Gil-Martínez, M.; Rodríguez-Ares, M.T.; García-Mazás, C.; Blanco-Mendez, J.; Lamas, M.J.; et al. Cysteamine polysaccharide hydrogels: Study of extended ocular delivery and biopermanence time by PET imaging. *Int. J. Pharm*. **2017**, 528, 714–722.

10. McKenzie, B.; Kay, G.; Matthews, K.H.; Knott, R.; Cairns, D. Preformulation of cysteamine gels for treatment of the ophthalmic complications in cystinosis. *Int. J. Pharm*. **2016**, 515, 575–582.

11. Gahl, W.A.; Kuehl, E.M.; Iwata, F.; Lindblad, A.; Kaiser-Kupfer, M.I. Corneal Crystals in Nephropathic Cystinosis: Natural History and Treatment with Cysteamine Eyedrops. *Mol. Genet. Metab.* **2000**, 71, 100–120.

12. Csorba, A.; Maka, E.; Maneschg, O.A.; Szabó, A.; Szentmáry, N.; Csidey, M.; Resch, M.; Imre, L.; Knézy, K.; Nagy, Z.Z. Examination of corneal deposits in nephropathic cystinosis using in vivo confocal microscopy and anterior segment optical coherence tomography: An age-dependent cross sectional study. *BMC Ophthalmol*. **2020**, 20, 73.

13. Kowalczyk, M.; Toro, M.D.; Rejdak, R.; Załuska, W.; Gagliano, C.; Sikora, P. Ophthalmic Evaluation of Diagnosed Cases of Eye Cystinosis: A Tertiary Care Center's Experience. *Diagnostics* **2020**, 10, 911.

14. McCaughan, B.; Kay, G.; Knott, R.M.; Cairns, D. A potential new prodrug for the treatment of cystinosis: Design, synthesis and in-vitro evaluation. *Bioorg. Med. Chem. Lett.* **2008**, 18, 1716–1719.

15. Omran, Z.; Moloney, K.A.; Benylles, A.; Kay, G.; Knott, R.M.; Cairns, D. Synthesis and in vitro evaluation of novel pro-drugs for the treatment of nephropathic cystinosis. *Bioorg. Med. Chem*. **2011**, 19, 3492–3496.

16. Kaur, S.; Sarma, P.; Kaur, H.; Prajapat, M.; Shekhar, N.; Bhattacharyya, J.; Kaur, H.; Kumar, S.; Medhi, B.; Ram, J.; et al. Efficacy and safety of topical cysteamine in corneal cystinosis: A systematic review and meta- analysis. *Am. J. Ophthalmol*. **2020**, 223:275-285

17. Pisoni, R.L.; Thoene, J.G.; Christensen, H.N. Detection and characterization of carrier-mediated cationic amino acid transport in lysosomes of normal and



USC UNIVERSIDADE DE SANTIAGO DE COMPOSTELA

cystinotic human fibroblasts. Role in therapeutic cystine removal? *J. Biol. Chem.* **1985**, 260, 4791–4798.

18. European Medicines Agency. Cystagon®. Prescribing Information. 1997. Available online: https://www.ema.europa.eu/en/medicines/human/EPAR/cystagon (accessed on 7 November 2020).
19. Schneider, J.A. Approval of cysteamine for patients with cystinosis. Pediatr. Nephrol. *Berl. Ger*. **1995**, 9, 254.
20. Liang, H.; Labbé, A.; Le Mouhaër, J.; Plisson, C.; Baudouin, C. A New Viscous Cysteamine Eye Drops Treatment for Ophthalmic Cystinosis: An Open-Label Randomized Comparative Phase III Pivotal Study. *Investig. Opthalmol. Vis. Sci*. **2017**, 58, 2275-2283.
21. Food and Drug Administration. Cystaran®. Prescribing Information. 2012. Available online: https://www.accessdata.fda.gov/drugsatfda_docs/label/2012/200740s000lbl.pdf (accessed on 7 November 2020).
22. Food and Drug Administration. Cystadrops®. Prescribing Information. 2020. Available online: https://www.accessdata.fda.gov/drugsatfda_docs/label/2020/211302s000lbl.pdf (accessed on 7 November 2020).
23. European Medicines Agency. Cystadrops®. Prescribing Information. 2016. Available online: https://www.ema.europa.eu/en/documents/product-information/cystadrops-epar-product-information_es.pdf (accessed on 7 November 2020).
24. Fernández-Ferreiro, A.; Luaces-Rodríguez, A.; Díaz-Tomé, V.; Gil-Martínez, M.; Ares, M.T.R.; Peralba, R.T.; Blanco-Méndez, J.; González-Barcia, M.; Otero-Espinar, F.J.; Lamas, M.J. Cysteamine ophthalmic hydrogel for the treatment of ocular cystinosis. *Farm. Hosp*. **2017**, 41, 678–687.
25. Reda, A.; Van Schepdael, A.; Adams, E.; Paul, P.; Devolder, D.; Elmonem, M.A.; Veys, K.; Casteels, I.; van den Heuvel, L.; Levtchenko, E. Effect of Storage Conditions on Stability of Ophthalmological Compounded Cysteamine Eye Drops. *JIMD Rep*. **2017**, 42, 47–51.
26. Marcano, D.C.; Shin, C.S.; Lee, B.; Isenhart, L.C.; Liu, X.; Li, F.; Jester, J.V.; Pflugfelder, S.C.; Simpson, J.; Acharya, G. Synergistic Cysteamine Delivery Nanowafer as an Efficacious Treatment Modality for Corneal Cystinosis. *Mol. Pharm.* **2016**, 13, 3468–3477.
27. Mannermaa, E.; Vellonen, K.-S.; Urtti, A. Drug transport in corneal epithelium and blood-retina barrier: Emerging role of transporters in ocular pharmacokinetics. *Adv. Drug Deliv. Rev.* **2006**, 58, 1136–1163.



USC UNIVERSIDADE DE SANTIAGO DE COMPOSTELA

28. Almeida, H.; Amaral, M.H.; Lobão, P.; Lobo, J.M.S. In situ gelling systems: A strategy to improve the bioavailability of ophthalmic pharmaceutical formulations. *Drug Discov. Today* **2014**, 19, 400–412.

29. Gote, V.; Sikder, S.; Sicotte, J.; Pal, D. Ocular Drug Delivery: Present Innovations and Future Challenges. *J. Pharmacol. Exp. Ther*. **2019**, 370, 602–624.

30. Ahmed, E.M. Hydrogel: Preparation, characterization, and applications: A review. *J. Adv. Res.* **2015**, 6, 105–121.

31. Luaces-Rodríguez, A.; Mondelo-García, C.; Zarra-Ferro, I.; González-Barcia, M.; Aguiar, P.; Fernández-Ferreiro, A.; Otero-Espinar, F.J. Intravitreal anti-VEGF drug delivery systems for age-related macular degeneration. *Int. J. Pharm.* **2020**, 573, 118767.

32. Hu, C.-C.; Chaw, J.-R.; Chen, C.-F.; Liu, H.-W. Controlled release bevacizumab in thermoresponsive hydrogel found to inhibit angiogenesis. *Biomed. Mater. Eng.* **2014**, 24, 1941–1950.

33. Bozdag, S.; Gumus, K.; Gumus, O.; Unlu, N. Formulation and in vitro evaluation of cysteamine hydrochloride viscous solutions for the treatment of corneal cystinosis. *Eur. J. Pharm. Biopharm*. **2008**, 70, 260–269.

34. Fernández-Ferreiro, A.; González Barcia, M.; Gil-Martínez, M.; Vieites-Prado, A.; Lema, I.; Argibay, B.; Blanco Méndez, J.; Lamas, M.J.; Otero-Espinar, F.J. In vitro and in vivo ocular safety and eye surface permanence determination by direct and Magnetic Resonance Imaging of ion-sensitive hydrogels based on gellan gum and kappa-carrageenan. *Eur. J. Pharm. Biopharm. Off. J. Arbeitsgemeinschaft Pharm. Verfahrenstechnik EV* **2015**, 94, 342–351.

35. Xia, L.-W.; Xie, R.; Ju, X.-J.; Wang, W.; Chen, Q.; Chu, L.-Y. Nano-structured smart hydrogels with rapid response and high elasticity. *Nat. Commun*. **2013**, 4, 2226.

36. Bhatt, P.; Narvekar, P.; Lalani, R.; Chougule, M.B.; Pathak, Y.; Sutariya, V. An in vitro Assessment of Thermo-Reversible Gel Formulation Containing Sunitinib Nanoparticles for Neovascular Age-Related Macular Degeneration. *AAPS PharmSciTech* **2019**, 20, 281.

37. Yuan, X.; Marcano, D.C.; Shin, C.S.; Hua, X.; Isenhart, L.C.; Pflugfelder, S.C.; Acharya, G. Ocular Drug Delivery Nanowafer with Enhanced Therapeutic Efficacy. *ACS Nano* **2015**, 9, 1749–1758.

38. Shokry, M.; Hathout, R.M.; Mansour, S. Exploring gelatin nanoparticles as novel nanocarriers for Timolol Maleate: Augmented in-vivo efficacy and safe histological profile. *Int. J. Pharm*. **2018**, 545, 229–239.



USC UNIVERSIDADE DE SANTIAGO DE COMPOSTELA

39. Holgado, M.A.; Anguiano-Domínguez, A.; Martín-Banderas, L. Contact lenses as drug-delivery systems: A promising therapeutic tool. *Arch. Soc. Espanola Oftalmol.* **2020**, 95, 24–33.

40. García-Millán, E.; Castro-Balado, A.; Fernández-Ferreiro, A.; Otero-Espinar, F.J. Contact Lenses as Drug Delivery Systems. In *Recent Progress in Eye Research*; Eye and Vision Research Developments; Nova Science Publishers, Inc.: New York, NY, USA, 2017; pp. 91–154. ISBN 978-1-5361-2761-4.

41. Musgrave, C.S.A.; Fang, F. Contact Lens Materials: A Materials Science Perspective. *Materials* **2019**, 12, 261.

42. Novack, G.D.; Barnett, M. Ocular Drug Delivery Systems Using Contact Lenses. *J. Ocul. Pharmacol. Ther*. **2020**, 36, 595–601.

43. Castro-Balado, A.; Mondelo-García, C.; Zarra-Ferro, I.; Fernández-Ferreiro, A. New ophthalmic drug delivery systems. *Farm. Hosp*. **2020**, 44, 149–157.

44. Fernández-Ferreiro, A.; Castro-Balado, A.; García Quintanilla, L.; Lamas, M.; Otero-Espinar, F.; Mendez, J.; Gómez-Ulla, F.; Gil-Martínez, M.; Tomé, V.; Luaces-Rodríguez, A.; et al. *Formulación Magistral Oftálmica Antiinfecciosa*; SEFH. Sociedad Española de Farmacia Hospitalaria: Madrid, Spain, 2019; ISBN 978-84-09-10764-3.

45. Peng, C.-C.; Kim, J.; Chauhan, A. Extended delivery of hydrophilic drugs from silicone-hydrogel contact lenses containing Vitamin E diffusion barriers. *Biomaterials* **2010**, 31, 4032–4047.

46. Peng, C.-C.; Chauhan, A. Extended cyclosporine delivery by silicone—Hydrogel contact lenses. *J. Control. Release* **2011**, 154, 267–274.

47. Peng, C.-C.; Burke, M.T.; Chauhan, A. Transport of Topical Anesthetics in Vitamin E Loaded Silicone Hydrogel Contact Lenses. *Langmuir* **2012**, 28, 1478–1487.

48. Peng, C.-C.; Ben-Shlomo, A.; Mackay, E.O.; Plummer, C.E.; Chauhan, A. Drug Delivery by Contact Lens in Spontaneously Glaucomatous Dogs. *Curr. Eye Res.* **2012**, 37, 204–211.

49. Peng, C.-C.; Burke, M.T.; Carbia, B.E.; Plummer, C.; Chauhan, A. Extended drug delivery by contact lenses for glaucoma therapy. *J. Control. Release* **2012**, 162, 152–158.

50. Hsu, K.-H.; Fentzke, R.C.; Chauhan, A. Feasibility of corneal drug delivery of cysteamine using vitamin E modified silicone hydrogel contact lenses. *Eur. J. Pharm. Biopharm.* **2013**, 85, 531–540.

51. New 1-Day ACUVUE® TruEye® Brand Contact Lenses (narafilcon A) Now Available in U.S. Johnson & Johnson. Available online:



USC UNIVERSIDADE DE SANTIAGO DE COMPOSTELA

https://www.jnj.com/media-center/press-releases/new-1-day-acuvue-trueye-brand-contact-lenses-narafilcon-a-now-available-in-us (accessed on 10 November 2020).

52. Dixon, P.; Fentzke, R.C.; Bhattacharya, A.; Konar, A.; Hazra, S.; Chauhan, A. In vitro drug release and in vivo safety of vitamin E and cysteamine loaded contact lenses. *Int. J. Pharm*. **2018**, 544, 380–391.

53. Dureau, P.; Broyer, M.; Dufier, J.-L. Evolution of ocular manifestations in nephropathic cystinosis: A long-term study of a population treated with cysteamine. *J. Pediatr. Ophthalmol. Strabismus* **2003**, 40, 142–146.

54. Mancini, G.M.; Havelaar, A.C.; Verheijen, F.W. Lysosomal transport disorders. *J. Inherit. Metab. Dis*. **2000**, 23, 278–292.

55. Gahl, W.A. Cystinosis coming of age. Adv. Pediatr. 1986, 33, 95–126.

56. Dixon, P.; Chauhan, A. Carbon Black Tinted Contact Lenses for Reduction of Photophobia in Cystinosis Patients. *Curr. Eye Res*. **2019**, 44, 497–504.

57. Besouw, M.; Masereeuw, R.; van den Heuvel, L.; Levtchenko, E. Cysteamine: An old drug with new potential. *Drug Discov. Today* **2013**, 18, 785–792.

58. PubChem Cysteamine. Available online: https://pubchem.ncbi.nlm.nih.gov/compound/6058 (accessed on 20 October 2020).

59. Labbé, A.; Baudouin, C.; Deschênes, G.; Loirat, C.; Charbit, M.; Guest, G.; Niaudet, P. A new gel formulation of topical cysteamine for the treatment of corneal cystine crystals in cystinosis: The Cystadrops OCT-1 study. *Mol. Genet. Metab.* **2014**, 111, 314–320.

60. Atallah, C.; Charcosset, C.; Greige-Gerges, H. Challenges for cysteamine stabilization, quantification, and biological effects improvement. *J. Pharm. Anal*. **2020**; 10(6): 499-516

61. Purkiss, R. Stability of Cysteamine Hydrochloride in Solution. *J. Clin. Pharm. Ther.* **1977**, 2, 199–203.

62. Brodrick, A.; Broughton, H.M.; Oakley, R.M. The stability of an oral liquid formulation of cysteamine. *J. Clin. Hosp. Pharm*. **1981**, 6, 67–70.

63. Dixon, P.; Powell, K.; Chauhan, A. Novel approaches for improving stability of cysteamine formulations. *Int. J. Pharm*. **2018**, 549, 466–475.

64. Kim, Y.; Na, D.H. Simultaneous Determination of Cysteamine and Cystamine in Cosmetics by Ion-Pairing Reversed-Phase High-Performance Liquid Chromatography. *Toxicol. Res*. **2019**, 35, 161–165.



USC UNIVERSIDADE DE SANTIAGO DE COMPOSTELA

65. Jellum, E.; Bacon, V.A.; Patton, W.; Pereira, W.; Halpern, B. Quantitative determination of biologically important thiols and disulfides by gas-liquid chromatography. *Anal. Biochem*. **1969**, 31, 339–347.

66. Lofberg, R.T. Gas Chromatographic Analysis of Aminothiol Radioprotective Compounds. *Anal. Lett*. **1971**, 4, 77–86.

67. Fahey, R.C.; Newton, G.L.; Dorian, R.; Kosower, E.M. Analysis of biological thiols: Quantitative determination of thiols at the picomole level based upon derivatization with monobromobimanes and separation by cation-exchange chromatography. *Anal. Biochem*. **1981**, 111, 357–365.

68. Newton, G.L.; Dorian, R.; Fahey, R.C. Analysis of biological thiols: Derivatization with monobromobimane and separation by reverse-phase high-performance liquid chromatography. *Anal. Biochem*. **1981**, 114, 383–387.

69. Pastore, A.; Massoud, R.; Motti, C.; Lo Russo, A.; Fucci, G.; Cortese, C.; Federici, G. Fully automated assay for total homocysteine, cysteine, cysteinylglycine, glutathione, cysteamine, and 2-mercaptopropionylglycine in plasma and urine. *Clin. Chem*. **1998**, 44, 825–832.

70. Stachowicz, M.; Lehmann, B.; Tibi, A.; Prognon, P.; Daurat, V.; Pradeau, D. Determination of total cysteamine in human serum by a high-performance liquid chromatography with fluorescence detection. *J. Pharm. Biomed. Anal*. **1998**, 17, 767–773.

71. Toyo'oka, T.; Imai, K. High-performance liquid chromatography and fluorometric detection of biologically important thiols, derivatized with ammonium 7-fluorobenzo-2-oxa-1,3-diazole-4-sulphonate (SBD-F). *J. Chromatogr*. **1983**, 282, 495–500.

72. Ichinose, S.; Nakamura, M.; Maeda, M.; Ikeda, R.; Wada, M.; Nakazato, M.; Ohba, Y.; Takamura, N.; Maeda, T.; Aoyagi, K.; et al. A validated HPLC-fluorescence method with a semi-micro column for routine determination of homocysteine, cysteine and cysteamine, and the relation between the thiol derivatives in normal human plasma. *Biomed. Chromatogr*. **2009**, 23, 935–939.

73. Kataoka, H.; Tanaka, H.; Makita, M. Determination of total cysteamine in urine and plasma samples by gas chromatography with flame photometric detection. *J. Chromatogr. B Biomed. Appl*. **1994**, 657, 9–13.

74. , Y.; Ohkuma, S.; Kuriyama, K. Determination of cystamine by high-performance liquid chromatography. *Anal. Biochem*. **1984**, 136, 352–356.

75. Kataoka, H.; Imamura, Y.; Tanaka, H.; Makita, M. Determination of cysteamine and cystamine by gas chromatography with flame photometric detection. *J. Pharm. Biomed. Anal.* **1993**, 11, 963–969.



USC UNIVERSIDADE DE SANTIAGO DE COMPOSTELA

76. Kuśmierek, K.; Głowacki, R.; Bald, E. Determination of total cysteamine in human plasma in the form of its 2-S-quinolinium derivative by high performance liquid chromatography. *Anal. Bioanal. Chem*. **2005**, 382, 231–233.

77. Ogony, J.; Mare, S.; Wu, W.; Ercal, N. High performance liquid chromatography analysis of 2-mercaptoethylamine (cysteamine) in biological samples by derivatization with N-(1-pyrenyl) maleimide (NPM) using fluorescence detection. *J. Chromatogr. B Anal. Technol. Biomed. Life. Sci*. **2006**, 843, 57–62.

78. Masuda, M.; Toriumi, C.; Santa, T.; Imai, K. Fluorogenic derivatization reagents suitable for isolation and identification of cysteine-containing proteins utilizing high-performance liquid chromatography-tandem mass spectrometry. *Anal. Chem*. **2004**, 76, 728–735.

79. Asamoto, H.; Ichibangase, T.; Saimaru, H.; Uchikura, K.; Imai, K. Existence of low-molecular-weight thiols in Caenorhabditis elegans demonstrated by HPLC-fluorescene detection utilizing 7-chloro-N-[2-(dimethylamino)ethyl]-2,1,3-benzoxadiazole-4-sulfonamide. *Biomed. Chromatogr*. **2007**, 21, 999–1004.

80. Bousquet, M.; Gibrat, C.; Ouellet, M.; Rouillard, C.; Calon, F.; Cicchetti, F. Cystamine metabolism and brain transport properties: Clinical implications for neurodegenerative diseases. *J. Neurochem*. **2010**, 114, 1651–1658.

81. Soriano, B.D.; Tam, L.-T.T.; Lu, H.S.; Valladares, V.G. A fluorescent-based HPLC assay for quantification of cysteine and cysteamine adducts in Escherichia coli-derived proteins. *J. Chromatogr. B* **2012**, 880, 27–33.

82. Huynh, P.T.N.; Nguyen, P.H.; Nguyen, M.A. Determination of cysteamine in animal feeds by high performance liquid chromatography with diode-array detection (HPLC-DAD). *Sci. Technol. Dev. J.* **2018**, 21, 37–43.

83. Hsiung, M.; Yeo, Y.Y.; Itiaba, K.; Crawhall, J.C. Cysteamine, penicillamine, glutathione, and their derivatives analyzed by automated ion exchange column chromatography. *Biochem. Med*. **1978**, 19, 305–317.

84. Ricci, G.; Nardini, M.; Chiaraluce, R.; Duprè, S.; Cavallini, D. Detection and determination of cysteamine at the nanomole level. *J. Appl. Biochem*. **1983**, 5, 320–329.

85. Duffel, M.W.; Logan, D.J.; Ziegler, D.M. Cysteamine and cystamine. *Methods Enzymol.* **1987**, 143, 149–154.

86. Kelly, M.J.; Perrett, D.; Rudge, S.R. The determination of cysteamine in physiological fluids by HPLC with electrochemical detection. *Biomed. Chromatogr*. **1987**, 2, 216–220.



USC UNIVERSIDADE DE SANTIAGO DE COMPOSTELA

87. Smolin, L.A.; Schneider, J.A. Measurement of total plasma cysteamine using high-performance liquid chromatography with electrochemical detection. *Anal. Biochem*. **1988**, 168, 374–379.

88. Garcia, R.A.G.; Hirschberger, L.L.; Stipanuk, M.H. Measurement of cyst(e)amine in physiological samples by high performance liquid chromatography. *Anal. Biochem*. **1988**, 170, 432–440.

89. Raoof, J.B.; Ojani, R.; Chekin, F. Fabrication of functionalized carbon nanotube modified glassy carbon electrode and its application for selective oxidation and voltammetric determination of cysteamine. *J. Electroanal. Chem*. **2009**, 633, 187–192.

90. Ojani, R.; Raoof, J.-B.; Zarei, E. Electrocatalytic Oxidation and Determination of Cysteamine by Poly-N,N-dimethylaniline/Ferrocyanide Film Modified Carbon Paste Electrode. *Electroanalysis* **2009**, 21, 1189–1193.

91. Karimi-Maleh, H.; Biparva, P.; Hatami, M. A novel modified carbon paste electrode based on NiO/CNTs nanocomposite and (9, 10-dihydro-9, 10-ethanoanthracene-11, 12-dicarboximido)-4-ethylbenzene-1, 2-diol as a mediator for simultaneous determination of cysteamine, nicotinamide adenine dinucleotide and folic acid. *Biosens. Bioelectron*. **2013**, 48, 270–275.

92. Karimi-Maleh, H.; Salimi-Amiri, M.; Karimi, F.; Khalilzadeh, M.A.; Baghayeri, M. A Voltammetric Sensor Based on NiO Nanoparticle-Modified Carbon-Paste Electrode for Determination of Cysteamine in the Presence of High Concentration of Tryptophan. Available online: https://www.hindawi.com/journals/jchem/2013/946230/ (accessed on 30 October 2020).

93. Salmanpour, S.; Abbasghorbani, M.; Karimi, F.; Bavandpour, R.; Wen, Y. Electrocatalytic Determination of Cysteamine Uses a Nanostructure Based Electrochemical Sensor in Pharmaceutical Samples. *Curr. Anal. Chem*. **2017**, 13, 40–45.

94. Arabali, V.; Karimi-Maleh, H. Electrochemical determination of cysteamine in the presence of guanine and adenine using a carbon paste electrode modified with N-(4-hydroxyphenyl)-3,5-dinitrobenzamide and magnesium oxide nanoparticles. *Anal. Methods* **2016**, 8, 5604–5610.

95. Karimi-Maleh, H.; Karimi, F.; Orooji, Y.; Mansouri, G.; Razmjou, A.; Aygun, A.; Sen, F. A new nickel-based co-crystal complex electrocatalyst amplified by NiO dope Pt nanostructure hybrid; a highly sensitive approach for determination of cysteamine in the presence of serotonin. *Sci. Rep.* **2020**, 10, 11699.

96. Keyvanfard, M.; Ahmadi, M.; Karimi, F.; Alizad, K. Voltammetric determination of cysteamine at multiwalled carbon nanotubes paste electrode



USC UNIVERSIDADE DE SANTIAGO DE COMPOSTELA

in the presence of isoproterenol as a mediator. *Chin. Chem. Lett.* **2014**, 25, 1244–1246.

97. Taherkhani, A.; Karimi-Maleh, H.; Ensafi, A.A.; Beitollahi, H.; Hosseini, A.; Khalilzadeh, M.A.; Bagheri, H. Simultaneous determination of cysteamine and folic acid in pharmaceutical and biological samples using modified multiwall carbon nanotube paste electrode. *Chin. Chem. Lett*. **2012**, 23, 237–240.
98. Keyvanfard, M.; Sami, S.; Karimi-Maleh, H.; Alizad, K. Electrocatalytic determination of cysteamine using multiwall carbon nanotube paste electrode in the presence of 3,4-dihydroxycinnamic acid as a homogeneous mediator. *J. Braz. Chem. Soc*. **2013**, 24, 32–39.
99. Rezaei, B.; Khosropour, H.; Ensafi, A.A. Sensitive voltammetric determination of cysteamine using promazine hydrochloride as a mediator and modified multi-wall carbon nanotubes carbon paste electrodes. *Ionics* **2014**, 20, 1335–1342.
100. Mohammadi, S.Z.; Tajik, S.; Beitollahi, H.; Barani, Z. Sensitive Cysteamine Determination Using Disposable Electrochemical Sensor Based on Modified Screen Printed Electrode. *Biquarterly Iran. J. Anal. Chem*. **2019**, 6, 57–64.
101. Stem Cell Gene Therapy for Cystinosis—Full Text View—ClinicalTrials.gov. Available online: https://clinicaltrials.gov/ct2/show/NCT03897361 (accessed on 24 November 2020).
102. Makuloluwa, A.K.; Shams, F. Cysteamine hydrochloride eye drop solution for the treatment of corneal cystine crystal deposits in patients with cystinosis: An evidence-based review. *Clin. Ophthalmol*. **2018**, 12, 227–236.
103. Kaiser-Kupfer, M.I.; Gazzo, M.A.; Datiles, M.B.; Caruso, R.C.; Kuehl, E.M.; Gahl, W.A. A randomized placebo-controlled trial of cysteamine eye drops in nephropathic cystinosis. *Arch. Ophthalmol. Chic. Ill 1960* **1990**, 108, 689–693.
104. Iwata, F.; Kuehl, E.M.; Reed, G.F.; McCain, L.M.; Gahl, W.A.; Kaiser-Kupfer, M.I. A Randomized Clinical Trial of Topical Cysteamine Disulfide (Cystamine) versus Free Thiol (Cysteamine) in the Treatment of Corneal Cystine Crystals in Cystinosis. *Mol. Genet. Metab*. **1998**, 64, 237–242.
105. Bradbury, J.A.; Danjoux, J.P.; Voller, J.; Spencer, M.; Brocklebank, T. A randomised placebo-controlled trial of topical cysteamine therapy in patients with nephropathic cystinosis. *Eye Lond. Engl*. **1991**, 5, 755–760.
106. Tsilou, E.T. A multicentre randomised double masked clinical trial of a new formulation of topical cysteamine for the treatment of corneal cystine crystals in cystinosis. *Br. J. Ophthalmol*. **2003**, 87, 28–31.



USC UNIVERSIDADE DE SANTIAGO DE COMPOSTELA

107. Varner, P. Ophthalmic pharmaceutical clinical trials: Design considerations. *Clin. Investig.* **2015**, 5, 457–475.

108. Hathout, R.M. Particulate Systems in the Enhancement of the Antiglaucomatous Drug Pharmacodynamics: A Meta-Analysis Study. *ACS Omega* **2019**, 4, 21909–21913.

109. Andrzejewska, Z.; Nevo, N.; Thomas, L.; Chhuon, C.; Bailleux, A.; Chauvet, V.; Courtoy, P.J.; Chol, M.; Guerrera, I.C.; Antignac, C. Cystinosin is a Component of the Vacuolar H+-ATPase-Ragulator-Rag Complex Controlling Mammalian Target of Rapamycin Complex 1 Signaling. *J. Am. Soc. Nephrol. JASN* **2016**, 27, 1678–1688.

110. Thoene, J.G.; DelMonte, M.A.; Mullet, J. Microvesicle delivery of a lysosomal transport protein to ex vivo rabbit cornea. *Mol. Genet. Metab. Rep*. **2020**, 23, 100587.

111. Hollywood, J.A.; Przepiorski, A.; D'Souza, R.F.; Sreebhavan, S.; Wolvetang, E.J.; Harrison, P.T.; Davidson, A.J.; Holm, T.M. Use of human induced pluripotent stem cells and kidney organoids to develop a cysteamine/mtor inhibition combination therapy for cystinosis. *J. Am. Soc. Nephrol*. **2020**, 31, 962–982.



USC UNIVERSIDADE DE SANTIAGO DE COMPOSTELA

USC
UNIVERSIDADE
DE SANTIAGO
DE COMPOSTELA

# CHAPTER 3

## CYSTEAMINE EYE DROPS IN HYALURONIC ACID PACKAGED IN INNOVATIVE SINGLE-DOSE SYSTEMS: STABILITY AND OCULAR BIOPERMANENCE

USC
UNIVERSIDADE DE SANTIAGO DE COMPOSTELA

USC
UNIVERSIDADE
DE SANTIAGO
DE COMPOSTELA

# CHAPTER 3

## CYSTEAMINE EYE DROPS IN HYALURONIC ACID PACKAGED IN INNOVATIVE SINGLE-DOSE SYSTEMS: STABILITY AND OCULAR BIOPERMANENCE


### ABSTRACT

Cystinosis is a rare genetic disorder characterized by the accumulation of cystine crystals in different tissues and organs causing, among other symptoms, severe ocular manifestations. Cysteamine eye drops are prepared in hospital pharmacy departments to facilitate access to treatment, for which vehicles that provide adequate biopermanence, as well as adaptable containers that maintain its stability, are required. Difficulties related to cysteamine preparation, as well as its tendency to oxidize to cystamine, show the importance of conducting rigorous galenic characterization studies. This work aims to develop and characterize an ophthalmic compounded formulation of cysteamine prepared with hyaluronic acid and packaged in innovative single-dose systems. For this task, the effect of different storage temperatures and the presence/absence of nitrogen on the physicochemical stability of the formulation and its packaging was studied in a scaled manner, until reaching the optimal storage conditions. The results showed that 0.55% cysteamine, prepared with hyaluronic acid and packaged in single-dose containers, is stable for 30 days when stored at −20 °C. In addition, opening vials every 4 h at room temperature after 30 days of freezing maintains the stability of the cysteamine formulation for up to 16 h. Moreover, ocular biopermanence studies were conducted using molecular imaging, concluding that the biopermanence offered by the vehicle is not affected by the freezing process, where a half-life of 31.11 min for a hyaluronic acid formulation stored for 30 days at −20 °C was obtained, compared with 14.63 min for 0.9% sodium chloride eye drops.



**Keywords:** cystinosis; ophthalmic administration; cysteamine; compounded formulation; PET





USC UNIVERSIDADE DE SANTIAGO DE COMPOSTELA

## 1. INTRODUCTION

Cystinosis is considered a rare autosomal recessive lysosomal disease that affects approximately 100,000–200,000 people in the general population [1,2]. It is characterized by the lysosomal accumulation of cystine crystals, the disulfide of the amino acid cysteine, with low solubility in water. Mutations in the CTNS gene, which encodes cystinosin, the carrier that transports cystine from the lysosome, are responsible for this cumulative process [3]. The presence of cystine crystals in different tissues leads to the progressive damage and dysfunction of multiple organs, such as the pancreas, brain, thyroid, kidneys, and eyes [4]. The most frequently described ocular manifestation is the deposition of cystine crystals in the cornea, but it also affects other eye structures, causing visual impairment and eventually, blindness [5-7].

Currently, the aminothiol cysteamine remains the only available treatment of cystinosis [8], although other pathways have been recently explored to expand therapeutic options [9-12]. Cysteamine lowers intracellular levels of cystine by forming a cysteamine–cysteine mixed disulfide, which resembles lysine and leaves the lysosome using a "lysine transport system" [8,13]. The authorization of oral cysteamine (Cystagon®) in 2012 by the Food and Drug Administration (FDA), followed by the delayed-release formulation years later (Procysbi®), has completely changed the management and prognosis of cystinosis [14-16]. However, systemic cysteamine has a low ocular bioavailability due to the lack of corneal vascularization, so it must be administered by the ophthalmic route. Cystaran® 0.44% eye drops received FDA approval in 2012 as an orphan drug, requiring administration of one drop per eye every waking hour [17], which complicates patient compliance. To improve this aspect, Cystadrops® 0.55% was subsequently approved by the European Medicines Agency (EMA) and the FDA in 2017 and 2021, respectively [18,19]. This formulation contains sodium carboxymethylcellulose that provides high viscosity, thus achieving a longer residence time on the ocular surface and allowing its administration four times a day [19].

Commercial cysteamine preparations are not available in most countries, as access is sometimes delayed due to mandatory procedures and authorizations. In this scenario, hospital pharmacy departments (HPD) are responsible for preparing cysteamine ophthalmic compounded formulations as a therapeutic alternative [20]. These formulations need to be properly developed with appropriate galenic characterization studies prior to their translation into clinical practice [21]. Cysteamine is an easily oxidizable molecule whose exposure to the air reduces its shelf life, since the thiol functional group immediately reacts with oxygen to form a disulfide called cystamine, which is ineffective in the treatment of cystinosis [21-23]. This process occurs quickly in air and solution [24], making it difficult to develop



USC UNIVERSIDADE DE SANTIAGO DE COMPOSTELA

adequate determination methods that allow the simultaneous detection of cysteamine and cystamine [25]. Strategies such as packaging under a nitrogen atmosphere, adding antioxidants, reducing the pH, and lowering the temperature in storage, effectively increase its stability [26,27,28].

Classical compounded formulations of cysteamine eye drops are produced in HPD with 0.9% sodium chloride (NaCl), but these require frequent instillations while the patient is awake due to its low ocular biopermanence. To optimize the formulation and avoid these difficult dosage schedules, our group developed and characterized a bioadhesive cysteamine hydrogel with high ocular permanence, using hyaluronic acid 0.4% as a vehicle [6,20,29]. However, after four years of producing this formulation in our center, we have detected in the internal quality controls that important parameters, such as the molecular weight of the sodium hyaluronate used (supplied by the same distributor authorized by the Spanish Agency of Medicines and Medical Devices), exhibited important variations of up to 40% in the different batches produced. In addition, other substances, including proteins, nucleic acids, metals, and chlorate content, have been detected [30,31]. According to previous publications, this could significantly interfere with compounding and stability studies using different batches, as they would no longer be reproducible [32-35]. To overcome this problem, we have decided to use commercialized eye drops that contain 0.4% hyaluronic acid (Aquoral®). This choice offers the advantages of a constant source, a dependable purification technique, and a certified molecular weight in the hyaluronate used.

When transferring compounded formulations to clinical practice, it is important to take into account the comfort of the patient and the pharmacy staff in charge of the preparation. Therefore, packaging in single-dose systems would allow the use of one disposable container per day, while the rest of the dispensed batch could be kept at low-temperature conditions that favor the stability of the active ingredient, in this case, cysteamine. The use of one single-dose container per day would facilitate its handling and transportation by patients, also reducing the number of visits to the hospital for dispensing treatment. When using these single-dose containers, it is necessary to devise a system that allows easy and fast filling, but without entailing a workload in the formulation production circuit. At the same time, it is important to consider whether storage at low temperatures can negatively affect the physical properties of the compounded formulation, or the properties of the container.

The objective of this work is to develop and characterize an ophthalmic compounded formulation of 0.55% cysteamine, packaged in single-dose containers, for its elaboration from HPD. The stability study of the formulation and its final container was carried out in a scaled manner under different storage conditions



USC UNIVERSIDADE DE SANTIAGO DE COMPOSTELA

(with/without nitrogen saturation, refrigerated or frozen) for 30 days to achieve the most optimal form of conservation. Their chemical (cysteamine and cystamine content, pH), physical (osmolality and viscosity), and microbiological stability, as well as packaging elasticity after storage at low temperatures, were evaluated. An in-use stability study was also conducted at room temperature to simulate conditions for opening the eye drops prior to administration. Finally, a preclinical ocular biopermanence study was carried out by PET/CT imaging.

## 2. MATERIALS AND METHODS

### *2.1. Materials*

Cysteamine hydrochloride (cysteamine purity 97%) was obtained from Apollo Scientific (Stockport, UK) and 1-Heptanesulphone acid sodium salt was obtained from Sigma Aldrich (St. Louis, MO, USA). Cystamine dihydrochloride (Cystamine purity 97%) was obtained from Thermo Fisher Scientific (Geel, Belgium). Aquoral® eye drops (0.4% w/v % hyaluronic acid (HA), sodium chloride, sodium citrate, citric acid monohydrate, water for injectable preparations) were purchased from Esteve (Barcelona, Spain). Acetonitrile UHPLC-MS grade and acetic acid were purchased from VWR Chemicals (Radnor, PA, USA). Balanced Salt Solution (BSS®) was purchased from Alcon (Geneva, Switzerland). Ultrapure water from MilliQ, Merck Millipore (Madrid, Spain) was used. As a packaging material, COL Eye Drops System® made with polyvinyl chloride (PVC) and di-n-octyl phthalate/di(2-ethylhexyl) phthalate (DOP/DEHP), free from Biomed Device (Modena, Italy), were used as single-dose containers.

### *2.2. Elaboration and Packaging of Cysteamine Hydrochloride Sterile Solutions*

Initially, 275 mg of cysteamine were dissolved in 10 mL of BSS via magnetic stirring. To achieve a cysteamine concentration of 0.55%, sufficient Aquoral® (AQ) was used as a diluent. Finally, sterilizing filtration was performed with a 0.22 μm membrane filter (Stericup® Merck Millipore ExpressTM PLUS) under vacuum. The compounded formulation was produced in triplicate.

Single-dose systems were filled under aseptic conditions in a horizontal laminar flow cabinet by generating an initial vacuum using the coupled syringe, connections, and filters, according to the manufacturer's instructions [36,37]. Successive aspirations and expulsions of the air contained inside the system were carried out until the complete collapse of the single-dose containers was achieved. Through the lateral connection, 30 mL of each of the formulations were aspirated



USC UNIVERSIDADE DE SANTIAGO DE COMPOSTELA

with the syringe incorporated in the system. The previously generated vacuum enables a homogeneous filling of the single-dose units (approximately 1.3–1.5 mL per vial) once the corresponding stopcocks are opened. In the case of single-dose vials saturated with nitrogen, an epidural needle was immersed in the 30 mL formulation contained in the syringe after the plunger was withdrawn. Nitrogen sparging was performed through the needle connected to a 0.22 µm filter for a total of 5 min per system, plugging the syringe opening with the plunger as much as possible. The filling of the vials was carried out as mentioned above.

Finally, each single-dose container was individually sealed with a heat-sealing gun provided by the manufacturer, and its correct closure was individually checked.

### *2.3. Cysteamine and Cystamine Quantification*

The quantification of cysteamine and cystamine in the compounded formulations was analyzed by ultra-high-performance liquid chromatography (UHPLC) using a modified version of the method proposed by Kim et al. [38]. The analysis was performed with a UHPLC coupled with photodiode array detection (PDA), using an ACQUITY UPLC H-Class System (Waters®) with ACQUITY PDA detector (Waters®).

We employed an ACQUITY® BEH C18 column (2.1 × 50 mm, 1.7 µm, Waters®) at a temperature of 45 °C. The mobile phase was a mixture of aqueous 4 mM sodium 1-heptane sulfonate:acetonitrile in gradient mode, as shown in Table 1. The wavelengths used for the detection of cysteamine and cystamine were 215 nm and 244 nm, respectively. Data were collected and processed with Empower 3 Software (2002−2019 Waters®) Application Manager.

**Table 1.** Gradient UHPLC quantification method for cysteamine and cystamine. The mobile phase A was an aqueous solution of 4 mM sodium 1-heptane sulfonate, and the mobile phase B was acetonitrile.

| Time | Mobile phase A (%) | Mobile phase B (%) |
|---|---|---|
| 0 | 95.0 | 5.0 |
| 0.50 | 95.0 | 5.0 |
| 2.50 | 70.0 | 30.0 |
| 3.20 | 95.0 | 5.0 |
| 6.0 | 95.0 | 5.0 |

All test samples were diluted 1:50 with 0.1% acetic acid and analyzed by UHPLC, setting the injection volume to 5 µL.



USC UNIVERSIDADE DE SANTIAGO DE COMPOSTELA

### *2.4. Storage Stability Study*

Single-dose vials, with and without nitrogen saturation, were stored, protected from light, in a refrigerator (2–8 °C) or freezer (−20 °C). Initially, the storage stability study was carried out for a period of 30 days. Storage stability tests were performed in triplicate and conducted on days 0, 3, 7, 15, 21, and 30. All samples were kept at room temperature for at least 30 min prior to analysis to avoid measurement errors due to temperature variations.

Based on the most stable storage conditions, an in-use stability study was carried out once the vials were opened.

#### 2.4.1. Determination of pH and Osmolarity

The pH of the formulations was determined with a BasiC20® pH meter, while the osmolarity was measured with a cryoscopic freezing point osmometer (OsmoSpecial1®) in 150 µL aliquots. Each determination was carried out in triplicate on days 0, 3, 7, 15, 21, and 30.

#### 2.4.2. Viscosity Tests

The viscosity of cysteamine compounded formulations was determined on days 0, 15, and 30 in triplicate, with a rotational viscometer (Anton Paar ViscoQC 300® with PTD 80 Peltier Temperature). For this, 2 mL of each formulation were introduced into the equipment, and the measurement was carried out at 25 °C and 100 revolutions per minute (rpm). A one-way ANOVA was carried out to determine if there were significant differences.

In addition, a viscosity speed-scan test was also performed at different rpm in order to analyze the rheological behavior of cysteamine eye drops in hyaluronic acid.

#### 2.4.3. Microbiological Stability

Each formulation was analyzed on days 0 and 30 to determine microbiological stability. Aliquots of 1.5 mL were added to plates containing blood agar, Sabouraud agar, and fluid thioglycolate medium. Subsequently, plates were cultured at 37 °C for 48 h, 15 days, and 10 days, respectively. At the end of each incubation period, the plates were inspected for any signs of microbiological growth.

#### 2.4.4. Statistical Analysis

The Pharmaceutical Codex was used to establish the expiry date of the compounded formulations, which was set at a reduction ≥10% of cysteamine with respect to the



USC UNIVERSIDADE DE SANTIAGO DE COMPOSTELA

initial concentration [39]. Changes in pH and osmolality were considered unacceptable if their values exceeded the acceptance criteria for ophthalmic applications [40,41]. Microbiological stability was considered acceptable when no microbial growth occurred in the cultured samples.

The results of the different assays were compared by multivariate analysis of variance using Graph Pad Prism® v.9.0.1 software.

#### 2.4.5. Elasticity of Single-Dose Containers

The effect of refrigerated and frozen storage on the mechanical strength of single-dose containers was studied in triplicate, measuring its elastic properties using a precision universal testing machine, Shimadzu Autograph AGS-X Series, with a load cell of 1 kN using Trapezium X material testing operation software (Shimadzu corporation, Kyoto, Japan). Measurements were made at time 0 and after 30 days of storage in the refrigerator or freezer. After emptying the content, the head of the single dose was cut and positioned with the help of adjustable clamps in the press at each of its ends. The tensile test speed was 0.2 cm/s, and force-displacement curves were recorded during the experiment to determine elastic modulus (Young's modulus). A one-way ANOVA was carried out to determine whether there were significant differences.

### *2.5. In-Use Stability Study*

Once the storage stability data was known, the in-use assay was carried out using vials previously stored under the best conditions. These vials were opened at room temperature, protected from light, every 4 h for 24 h, removing two drops per opening, except for during 8 h of sleep. The concentration of cysteamine and cystamine was measured at each of the openings.

### *2.6. In Vivo Evaluation of the Residence Time on the Ocular Surface*

In vivo studies were carried after storage stability data were available, using vials previously stored under optimal conditions. The aim of this assay was to determine whether the freezing/thawing process significantly affects the ocular biopermanence properties of the formulation. An initial measurement was made on the day of preparation, followed by a measurement at day 30 of vials stored in the freezer. In addition, NaCl 0.9%, without bioadhesive properties, was used as a control formulation.

These studies were performed on four male Sprague Dawley rats (8 eyes), with an average weight of 250 g, supplied by the University of Santiago de Compostela



USC UNIVERSIDADE DE SANTIAGO DE COMPOSTELA

(Santiago, Spain). The animals were kept in individual cages, with free access to food and water, in a room under controlled temperature (22 ± 1 °C) and humidity (60 ± 5%) and with day-night cycles regulated by artificial light (12/12 h). The animals were treated according to the guidelines for laboratory animals (National Research Council (US) Committee for the Update of the Guide for the Care and Use of Laboratory Animals, 2011; The Association for Research in Vision and Ophthalmology, 2014). Experiments were approved by the Animal Experimentation Ethics Committee of the Health Research Institute of Santiago de Compostela.

To quantitatively evaluate ocular permanence, radiolabeling of the formulation was performed following the method described in previous works of our group [6,42]. Positron emission tomography (PET) images were acquired using the ALBIRA PET/CT preclinical imaging system (Bruker Biospin, Woodbridge, CT, USA). Prior to image acquisition, the animals were anesthetized in a gas chamber with an administration of 3% isoflurane in oxygen, an anesthetic method that continued during acquisition through an inhalation mask. Throughout the procedure, the respiratory rate was monitored, and after each examination, the animals were awakened.

Once asleep, 7.5 μL of each formulation previously labeled with $^{18}$F-fluorodeoxyglucose ($^{18}$F-FDG) (formulation:FDG ratio 10:1) was instilled with an automatic micropipette into the conjunctival fornix. The range of radioactivity administered in each eye was between 0.15–0.25 MBq. Immediately after instillation, a 10 min individual PET was acquired, and at 30, 60, 90, and 120 min. Once the images were reconstructed using 6 iterations, they were analyzed with Amide's Medical Image Data Analysis Tool [43], manually drawing regions of interest (ROI) with a spherical shape of 15 × 15 × 15 mm delimiting the signal area in each eye. Finally, the percentage of activity (%) at a certain time was corrected for radioactive decay with the help of a one compartment model using GraphPad Prism® 8 v.8.2.1 software. A non-compartmental analysis was also performed by calculating the remaining percentage of the formulations versus time.

## 3. RESULTS

### *3.1. Cysteamine and Cystamine Quantification*

The UHPLC-PDA determination method employed is highly specific and allows for the simultaneous detection of both cysteamine and cystamine, in only 6 min. A narrow, symmetrical, and well-defined chromatographic peak of cysteamine was obtained with an elution time of 1.12 min, while for cystamine, it was obtained at



USC UNIVERSIDADE DE SANTIAGO DE COMPOSTELA

minute 2.46 (Figure 1). The analytical method was validated for linearity, accuracy, precision, and detection and quantification limits for cysteamine and cystamine. A linear calibration curve was obtained over a cysteamine and cystamine concentration range of 0.5–10 mg/mL ($R^2$ = 0.999). The limit of detection (LOD) and limit of quantitation (LOQ) were 0.25 mg/L and 0.5 mg/L, respectively, for both compounds. Compliance with the analytical validation standards of the European Medicines Agency (EMA) was also ascertained [44].

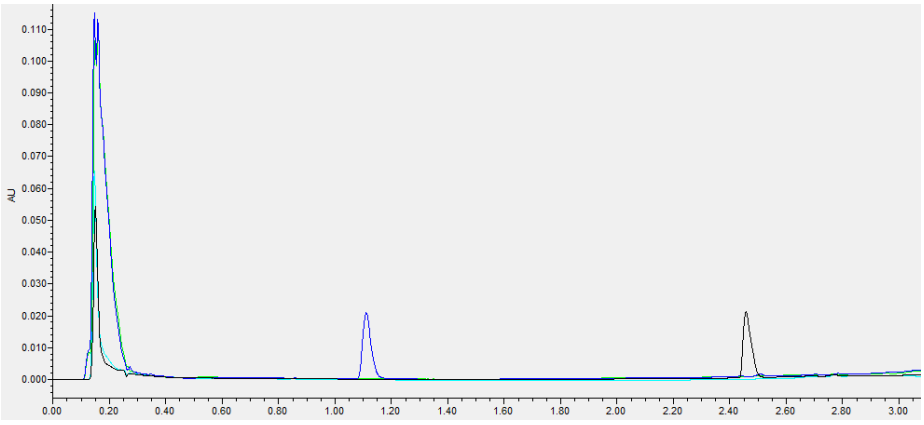



**Figure 1.** UHPLC chromatogram overlays showing the elution profiles of cysteamine at 215 nm (dark blue) and its oxidation product cystamine at 244 nm (black) in the studied matrix, Aquoral® (green at 215 nm, light blue at 244 nm). Data were collected and processed with Empower® 3 Software Application Manager.

### *3.2. Storage Stability Study*

The variation in the cysteamine concentration of the compounded formulations made with AQ and packaged in single-dose containers over time under the different experimental conditions is shown in Figure 2. Cysteamine concentrations fell below 90% after day 7 when kept refrigerated, without noting any relevant differences in terms of saturation with nitrogen (n.s., two-way ANOVA followed by Tukey´s multiple comparison test). On the other hand, stability increased considerably when single-dose containers were stored in the freezer, having a physicochemical stability of up to 30 days prior to opening. As observed for storage in the refrigerator, saturation with nitrogen did not affect the concentration of cysteamine. In parallel to the decrease in cysteamine concentration, there was an increase in cystamine concentration throughout the study, as shown in Figure S2 of the Supplementary Material.



USC UNIVERSIDADE DE SANTIAGO DE COMPOSTELA

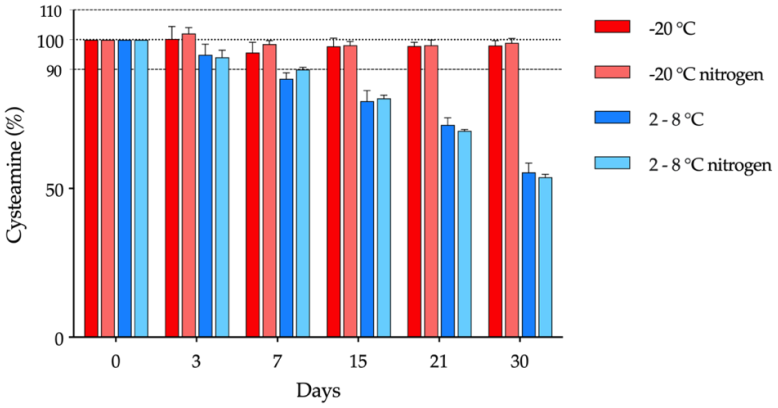



**Figure 2.** Cysteamine content with respect to the initial concentration throughout the study for each of the temperature settings (refrigeration/freezing) and in the presence/absence of nitrogen.

Cysteamine showed zero-order degradation kinetics, since the rate of reaction was independent of drug concentration. The degradation rate constants (K) of formulations preserved at 2–8 °C, in which significant degradation occurred, were calculated using the Arrhenius Equation (1):

$$K = A \cdot e^{-Ea/R \cdot T} \qquad (1)$$

where K is the degradation rate constant; A is the frequency factor assumed independent of temperature, which represents the frequency of collisions between reactant molecules at a standard concentration; Ea is the activation energy (J/mol); R is the gas constant (8.314 J/mol·K); and T is the temperature expressed in Kelvin. Results are shown in Table 2.

**Table 2.** Degradation rate constants (K) from storage stability studies. SDk: standard deviation of K; $r^2$: goodness-of-fit measure for linear regression models.

| Storage conditions | K (%/day) | SDk (%/day) | $r^2$ |
|---|---|---|---|
| 2-8 °C | 1.414 | 0.05502 | 0.9270 |
| 2-8 °C nitrogen | 1.496 | 0.02904 | 0.9808 |

### 3.2.1. pH and Osmolality

Variations in the pH of the cysteamine compounded formulations under the two preservation conditions over time are depicted in Figure 3a. With the use of the AQ



USC UNIVERSIDADE DE SANTIAGO DE COMPOSTELA

as a vehicle, the pH remained stable (6.5–6.8) throughout the stability study under freezing or refrigeration. Likewise, nitrogen saturation did not cause variations with respect to the vials that contained oxygen. These constant pH values are probably due to some buffering effect exerted by the excipients (sodium citrate and citric acid monohydrate) present in the AQ eye drops [45].

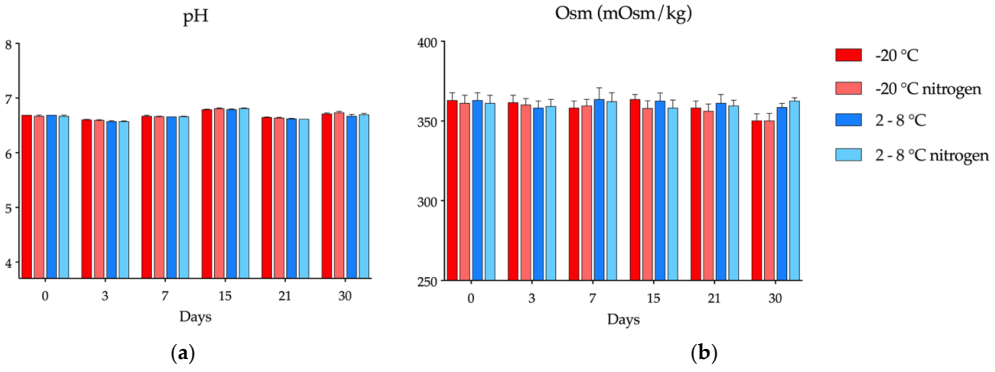



**Figure 3.** Variation in pH and osmolality (mOsm/kg) of the 5.5 mg/mL cysteamine formulation in Aquoral® on days 0, 3, 7, 15, 21 and 30: (**a**) pH; (**b**) osmolality.

Osmolality values (around 350 mOsm/Kg) of the formulations under the four experimental conditions remained between ±5% of the initial values over the study period (Figure 3b), being the dispersion of the values greater at day 30.

### 3.2.2. Viscosity tests

The initial viscosity of the formulations, measured at 25 °C and 100 rpm, was found to be around 30 mPa·s, as seen in Figure 4. On day 15 of the study, single-dose vials stored in the freezer showed a statistically significant drop in viscosity ($p$ = 0.0098) with respect to that measured at day 0. On day 30, no statistically significant changes were observed with respect to the previous measurement on day 15, although the differences with respect to day 0 were maintained ($p$ = 0.0057). On the other hand, for samples preserved in the refrigerator, viscosity hardly varied between days 0, 15, and 30. It was also observed that saturation with nitrogen did not introduce variations in the viscosity of the formulation when comparing vials kept at the same temperature.



USC UNIVERSIDADE DE SANTIAGO DE COMPOSTELA

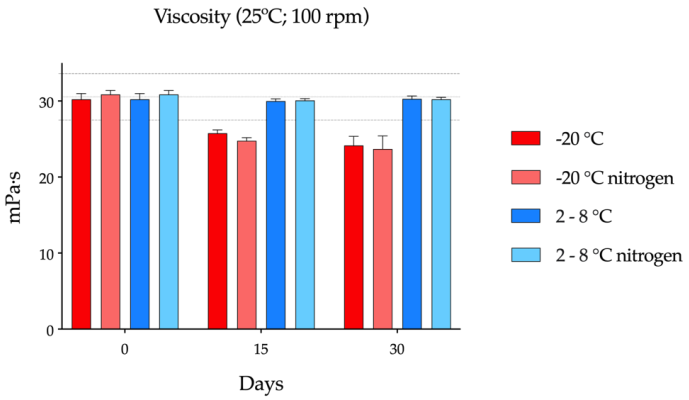



**Figure 4.** Viscosity variation measured at 25 °C and 100 revolutions per minute throughout the study period of the cysteamine formulations in Aquoral® stored in a freezer (-20 °C)/refrigerator (2–8 °C) and with/without nitrogen saturation.

The pseudoplastic behavior of HA has been observed regarding the present results, since the viscosity values decrease as the shear force increases. The viscosity values with respect to different rpm in all the formulations are represented in Figures S3–S5.

3.2.3. Microbiological Stability

No microbial growth was observed in any of the compounded formulations during the storage period, which indicates that adequate storage of the samples was maintained under all study conditions.

3.2.4. Elasticity of Single-Dose Containers

Young's modulus (E) is the ratio between the tensile stress (force per unit area) and the deformation of the solid material in the linear elastic region of the force-displacement curve. It is calculated using the following Equation (2):

$$E = \frac{\sigma}{\varepsilon} \quad (2)$$

where E is the Young's modulus, σ is the force per unit area, and ε is the proportional deformation. Young's modulus values were obtained in this study by Trapezium X software directly from the slope of the tensile stress-deformation curve in the initial linear elastic region of the trace, considering the dimension of the probe used in the experiment. The results showed no statistically significant differences between the two storage temperatures of the containers over time (Figure 5). In addition, the change in volume of the content with freezing did not cause modifications in its elastic properties.



USC UNIVERSIDADE DE SANTIAGO DE COMPOSTELA

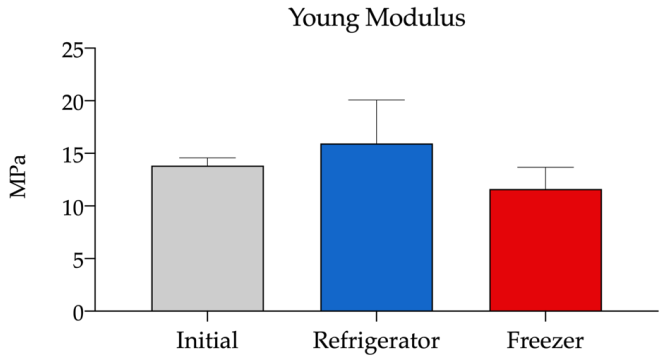



**Figure 5.** Young's modulus of the COL Eye Drops® vials used for the stability study at the initial time and after 30 days stored in the refrigerator (2–8 °C) and freezer (−20 °C).

Considering these results, freezing without nitrogen is postulated as the best and most practical storage condition. With vials stored under these conditions for 30 days, the in-use stability study was evaluated, with the aim of determining their chemical stability after being opened, simulating their real-life use.

### *3.3. In-Use Stability Study*

As in the storage assay, while the concentration of cysteamine decreased, cystamine concentration increased throughout the study. At the time of opening, a slight decrease in the cysteamine concentration was already observed, as well as a slight increase in the cystamine concentration, which is consistent with the degradation detected after 30 days of storage at −20 °C (Figure 2). After opening each single-dose container 5 times every 4 h at room temperature (16 h after removal from the freezer and initial opening), the concentration of cysteamine remained above 90% with respect to the initial concentration on day on which the formulation was prepared. These results indicate that single-dose vials stored for up to 30 days in the freezer can be used throughout a day, excluding the 8 h of sleep, once thawed and opened.

### *3.4. In Vivo Evaluation of the Residence Time on the Ocular Surface*

The residence time on the ocular surface of the pharmaceutical compounding was calculated immediately after its preparation and after being stored in the freezer for 30 days using small-animal PET imaging in rats. Figure 6 shows the permanence of these formulations from the eye compared to NaCl 0.9% (control). A strong signal immediately after instillation was observed and, after 120 min of contact, a considerable percentage of hydrogel remained on the ocular surface. This behavior is observed in a similar way, with no statistically significant differences, throughout the different PET images, for day 0 after formulation and day 30 after formulation, when stored at −20 °C.



USC UNIVERSIDADE DE SANTIAGO DE COMPOSTELA

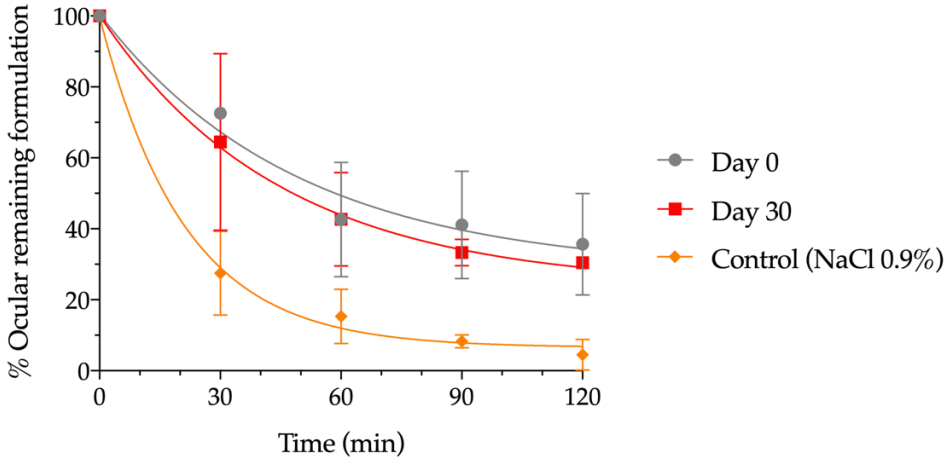



**Figure 6.** Percentage of formulation remaining on the ocular surface with respect to time zero determined by PET at day 0 and day 30 after storage in the freezer, as compared with NaCl 0.9%.

Data were fitted to a mono exponential equation dependent on time, as shown in Figure 6, and the pharmacokinetic parameters obtained by fitting to the one-compartmental model. A half-life of 33.86 min for day 0 after formulation and 31.11 min for day 30 after formulation, when stored at −20 °C, was obtained, demonstrating no influence of freezing on this parameter and showing an ocular residence time more than two-fold higher than for NaCl 0.9%, whose half-life was 14.63 min.

Figure 7 shows an axial view of the PET registration images of animal heads immediately after administration and 30, 60, 90, and 120 min after instillation, showing the distribution of the labelled formulation. Initially, the formulation is located on the surface of the eye. After 2 h, the concentration in the eye was still significant, indicating a long retention time on the ocular surface. An additional radiotracer signal was detected in the nasolacrimal duct and nasal cavity, as part of the formulation entered the nasal cavity from the lacrimal sac.



USC UNIVERSIDADE DE SANTIAGO DE COMPOSTELA

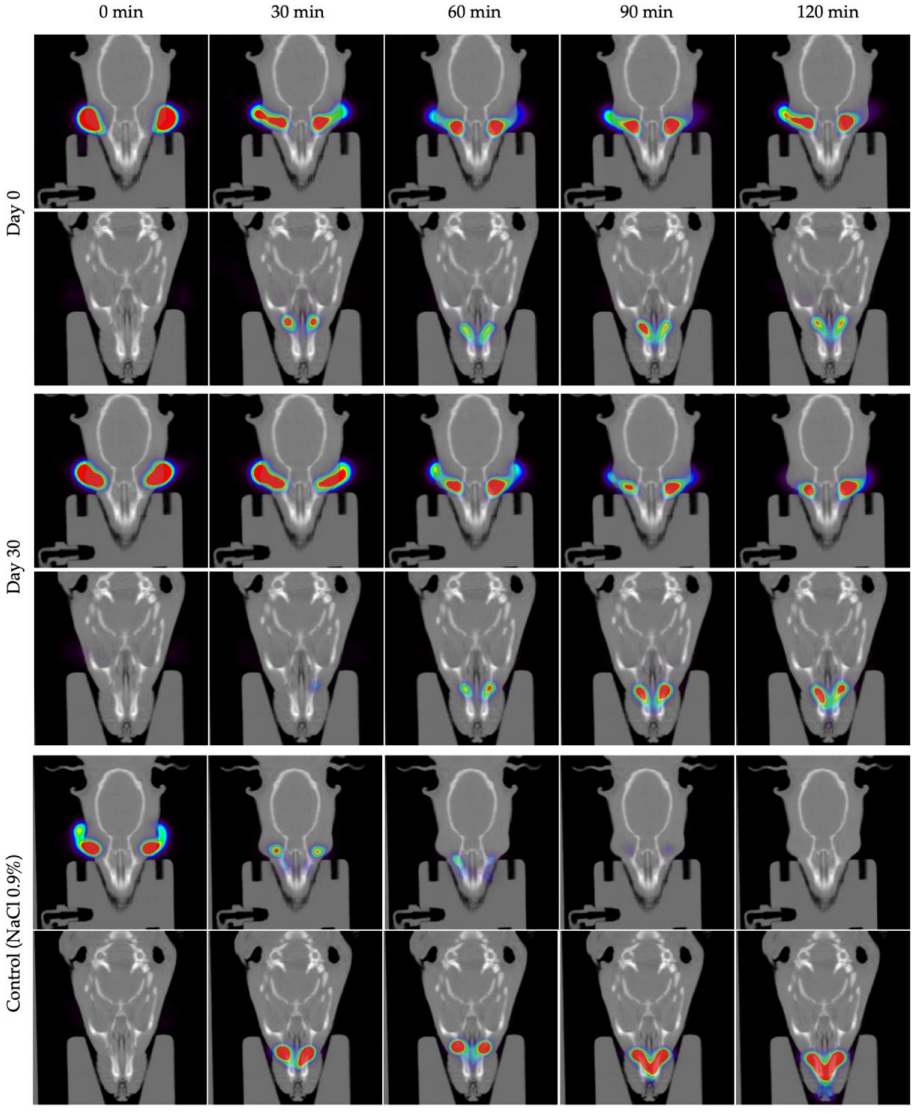



**Figure 7.** Positron emission tomography (PET) images (maximum intensity projections, coronal views) obtained at different time points after ocular administration of eye drops labelled with $^{18}$F-fluorodeoxyglucose ($^{18}$F-FDG).



USC UNIVERSIDADE DE SANTIAGO DE COMPOSTELA

## 4. DISCUSSION

Currently, only two commercial ophthalmic presentations of cysteamine (Cystaran® and Cystadrops®) are authorized for the treatment of cystinosis, but they are not commercialized in all countries [25]. Thus, pharmaceutical compounding from HPD can constitute a therapeutic alternative, avoiding the difficulty of access to treatment by some patients [46].

Undoubtedly, the physicochemical instability of cysteamine has been one of the greatest challenges when developing ophthalmic formulations with an acceptable period of validity that allows for adequate therapeutic compliance and avoids numerous hospital visits to collect the medication. Cysteamine is very unstable in a solution, where it rapidly converts to cystamine, a non-toxic molecule, but without therapeutic effect. Several strategies have been shown to effectively reduce cysteamine oxidation, such oxygen removal, decreasing temperature, the addition of antioxidant compounds—such as ascorbic acid or disodium edetate (EDTA)—or solution acidification [24,25,47]. To date, several stability studies of cysteamine formulations have been published [6,20,21,25,48], but the lack of uniformity in their preparation (vehicles, excipients, packaging, storage conditions, etc.) and the different determination methods used have led to irreproducible results.

The aim of the present work is to find a simple method of elaboration and conservation of an ophthalmic compounded formulation of cysteamine for an adequate translation to clinical practice. This is intended to offer a practical solution to processing services and to facilitate dispensing of the drug to patients. Our results showed that the new vehicle and single-dose packaging system used in this work allowed the treatment to be dispensed for a long period of time, as long as the containers were stored under low-temperature conditions. With this innovative system, it is possible to use one vial per day with the possibility of closing it, while the rest of the batch can be kept at a low temperature. On the contrary, the use of multidose vials is associated with greater contact with oxygen after opening, since the air contained inside the container is renewed with each opening, favoring the oxidation of cysteamine. A compounded formulation of 0.55% cysteamine, produced with a commercial preparation of 0.4% HA, was stored under refrigeration (2–8 °C) or freezing (−20 °C). To prevent oxidation, saturation with nitrogen was also studied. Physicochemical, microbiological, and mechanical studies were carried out for a period of 30 days, discarding those storage conditions that were inadequate in achieving a long period of validity, until optimal conditions were achieved. Considering all these data, an in-use stability study was carried out.

For this study, a new determination method was developed based on the one previously proposed by Kim et al. [38], which allows for the detection of both



USC UNIVERSIDADE DE SANTIAGO DE COMPOSTELA

cysteamine and cystamine, in a short analysis period of just 6 min. Our results showed that the cysteamine compounded formulation was not stable beyond 7 days when stored at 2–8 °C in single dose vials, which is impractical for patients and HPDs daily work, but when preserved at −20 °C, a stability of at least 30 days was achieved. These findings are consistent with those previously published in the literature reporting that oxidation to cystamine is favored at high temperatures [21,47,49,50,51]. Reda et al. previously showed the effects of storage in the refrigerator and freezer for up to 52 weeks, where it was seen that conservation at −20 °C guaranteed a longer period of validity [21]. Although the results differ slightly from those of the present work, it is important to consider the differences in terms of the composition of the mixture, final packaging, and determination method.

In addition to temperature, the presence of oxygen has also been described as a relevant factor that plays an important role in the chemical stability of cysteamine [48]. Therefore, in order to prevent oxidation, the saturation of the formulation with nitrogen was also studied. However, in the present study, this strategy did not provide less degradation at any of the temperatures or times studied with respect to formulations without nitrogen, as can be seen in Figure 2. This result can possibly be explained due to the material that makes up the single-dose COL containers, PVC, with known oxygen permeability [52]. This permeability may allow for the passage of oxygen through the material, losing the beneficial effect that the initial saturation of the formulations with nitrogen may have had. For this reason, it is important to consider the functionality and composition of the containers in which cysteamine formulations are packaged. In this regard, Cystaran® is supplied in an opaque, white, low-density polyethylene (LDPE) bottle with a LDPE-controlled dropper tip and closed with a polypropylene screw cap. As LPDE is permeable to oxygen, Cystaran® must be stored frozen between −25 °C and −15 °C to remain stable for over one year [21]. After thawing the bottle, it must be stored at 2 °C to 25 °C and discarded after one week [17]. Regarding Cystadrops®, it can be stored for six months refrigerated prior to opening, with no need of being frozen. This is possible due to its packaging, which consist of a sealed amber vial with a bromobutyl stopper and an aluminium seal, which have a very low permeability to oxygen [28,49]. Before opening the bottle, the seal and stopper must be removed and replaced by a PVC dropper with a high-density polyethylene (HDPE) closure, which mandates that the bottle must be discarded after one week once opened (storage temperature <25 °C) [19]. Regarding the single-dose PVC system used in the present study, its oxygen permeability does not entail a problem for the stability of the formulation when it is frozen. For this reason, nitrogen saturation is ruled out to increase stability in the monodose vials. Furthermore, nitrogen is a resource that



USC UNIVERSIDADE DE SANTIAGO DE COMPOSTELA

is scarcely available in HPDs, adding significant complexity to the manufacturing process.

Regarding the vehicle used for the elaboration, HA was chosen because it has several advantages. On the one hand, it alleviates part of the irritative symptomatology previously described in other cysteamine formulations [53,54,55,56]. This is achieved due to its restorative properties that enhance corneal epithelium healing, improve the function of the ocular surface, increase the stability of the precorneal tear film, and protect/restore the morphology and distribution of the goblet cells responsible for the secretion of mucins [57,58,59,60]. On the other hand, HA reduces the ocular clearance of cysteamine by increasing its retention time on the ocular surface, favoring its ocular bioavailability, as has been demonstrated in previous works [6,7]. According to Sandri et al. [61], hyaluronic acid, especially that of low molecular weight (<202 kDa), exhibits penetration enhancement properties comparable to, or even better than, chitosan hydrochloride, depending on the compound. In this way, cysteamine permeates into the cornea and reaches the lysosomes of the corneal cells where cystine crystals accumulate [14]. Aquoral® has been selected in this study as a source of HA because it is classified as a medical device used for the treatment of dry eye, which allows for keeping both the origin and the molecular weight of HA constant, something that would be more difficult to achieve if HA was obtained as a raw material due to the high variability reported between different manufacturers and batches [32,57]. According to previous publications, these variations may seriously interfere with compounding and stability studies, as they would no longer be reproducible [32-35].

Pescina et al. showed that cysteamine oxidation decreases at an acidic pH of 4.2, being a pH-dependent reaction, while corneal penetration was found to be poor at pH 4.2, but enhanced at pH 7 [47]. With this reasoning, it might be hypothesized that better cysteamine stability results could be achieved by lowering the pH of ophthalmic preparations, but it is necessary to consider that ocular administration of solutions with a pH too far from the tear pH (7.4–7.7) could cause discomfort in the eye. Formulated with a pH of 4.1–4.5, Cystaran® used this strategy to reduce cystamine degradation [17,47,62]. This correlation between pH and cysteamine stability agrees with the European Assessment report regarding Cystadrops® (pH 4.6–5.4), which states that low buffered pH, along with high viscosity, are the contributing factors to ocular irritation and inflammation, but this has to be weighed against the benefits of the stability of the active substance [53]. Both presentations use benzalkonium chloride as a preservative and as a trans-corneal permeation enhancer, which can produce toxic effects [40]. The most reported ocular adverse events (incidence around 10% or greater) were eye pain, blurred vision, eye irritation, ocular hyperaemia, eye pruritus, increased lacrimation, eye deposit, and



USC UNIVERSIDADE DE SANTIAGO DE COMPOSTELA

instillation site discomfort [2,22,54,55], many of which are related to the pathology itself. In the case of commercial presentations, pH reduction below physiological values was chosen in order to improve the stability of cysteamine with the consequent problems that this entails. On the contrary, in the present work, a pH value to the physiological value has been chosen, with constant values around 6.7. These values are achieved because of the citric acid/citrate buffer system present in the Aquoral® commercial formulation [45], avoiding the excessive tearing associated with formulations with a lower pH [40]. The present proposal for distribution in single-dose containers allows us to maintain acceptable cysteamine stability at a physiological pH due to freezing effects, which also favors the corneal permeation of the active ingredient [47].

Regarding osmolality, it remained practically constant throughout the study in all formulations, with values around 350 mOsm/Kg, similar to those previously published [50]. Although these values are higher than the 289 ± 21 mOsm/L reported for tears, considerably higher values are found in the commercial formulations of other active ingredients used in the treatment of chronic ocular pathologies, such as Travatan® (travoprost) or Vividrin iso EDO® (chromoglicin acid), with 368.5 and 341 mOsm/L, respectively [41,63].

Although freezing provides chemical stability to cysteamine, preventing its rapid degradation, it is unknown if this process can affect the physical properties of the formulation itself or of the final packaging. To determine whether this process significantly affected the properties of HA, viscosity studies were carried out on the day of its preparation, as well as after 15 and 30 days of storage in the refrigerator/freezer. From these data, it was possible to see that the viscosity remained practically constant at 2–8 °C, while on days 15 and 30, a drop was observed in those stored at −20 °C. This may be explained due to changes in polymer conformation during the freeze/thaw processes [64]. The present cysteamine compounded formulation maintained the pseudoplastic behavior of HA previously described in the literature [65,66,67] during all storage times and conditions, by decreasing its viscosity with increasing shear force, as seen in Figures S3–S5.

The clinical implications that the drop in viscosity of the frozen formulations may have on ocular biopermanence is unknown, so we decided to carry out a study using an in vivo molecular imaging technique with the most promising formulation in terms of stability. For determination, 0.9% NaCl was used as a control, as it is one of the most widely used vehicles in the preparation of eye drops compounded formulations produced in HPD [40,68]. Our results showed that the decrease in the viscosity of the frozen formulations did not translate into relevant clinical changes, and their bioadhesive properties were maintained. This was demonstrated by the lack of relevant differences in ocular biopermanence between the formulations



USC UNIVERSIDADE DE SANTIAGO DE COMPOSTELA

made with AQ before and after thawing. These ocular biopermanence results are in line with those previously published [6]. Another relevant aspect that we wanted to assess with this work was whether the single-dose container could be altered by the freezing/thawing process. We observed that the elasticity of the single-dose vials remained constant after 30 days of storage, both in the refrigerator and in the freezer, despite the increase in the internal volume caused by the freezing of the content inside the containers.

After characterizing the formulation under different storage conditions for 30 days, its chemical stability in-use after opening was determined. Conditions were established to simulate its use in real life, opening the single-dose container 5 times a day and storing it at room temperature. We have confirmed that the vial can be used within the first 16 h of the day after 30 days of storage in the freezer. This allows for convenient transport, thanks to its portability, with no need for refrigeration, thus facilitating the administration of the drops throughout the day, therefore increasing the therapeutic adherence of the patients. These results cannot be compared with those previously published by Martín-Sabroso et al. due to methodological differences. The previous work used a different vehicle and final containers and performed the stability study using vials stored in the refrigerator and opened 4 times a day for 7 days, where degradation ranging from 30% to 60% was observed for all the formulations after 7 days of use [48].

Regarding the limitations of the present study, some aspects of the formulation and the vials used have not been characterized in depth. For instance, the behavior of HA after the freeze/thaw process requires further studies to better characterize the vehicle. A cryoprotective compound could be used as an excipient in future formulations to prevent the properties from being modified by freezing [69]. Moreover, measuring the oxygen permeability of the single-dose container would explain why bubbling with nitrogen provides scarcely any improvement in the chemical stability of cysteamine. Finally, it would also be interesting to know whether this parameter is affected by the freezing/thawing processes.

## 5. CONCLUSIONS

Hospital pharmacy departments play a relevant role in facilitating access to drugs when these are not readily available in all countries, such as orphan drugs. Cysteamine eye drops are used to treat ocular cystinosis, which is an easily oxidizable molecule that requires rigorous stability studies to establish an adequate period of validity. With the aim to find a simple method of preparation and conservation of an ophthalmic compounded formulation of 0.55% cysteamine in HA, packaging in single-dose containers and subsequent freezing for 30 days,



USC UNIVERSIDADE DE SANTIAGO DE COMPOSTELA

protected from light, are proposed. These conditions preserved the stability and biopermanence of the formulation and the integrity of the packaging material, which was scarcely affected by the low temperatures. Once thawed, vials can be used for 16 h, allowing for the administration of cysteamine every 4 h. These results favor a quick and easy transfer to clinical practice, eluding complex production processes such as nitrogen saturation, and avoiding numerous hospital visits to collect the compounded formulation, facilitating better therapeutic adherence of patients to treatment.

## 6. REFERENCES


1. Orphanet: Cystinosis. Available online: https://www.orpha.net/consor/cgi-bin/OC_Exp.php?lng=en&Expert=213 (accessed on 2 July 2022).
2. Liang, H.; Labbé, A.; Baudouin, C.; Plisson, C.; Giordano, V. Long-Term Follow-up of Cystinosis Patients Treated with 0.55% Cysteamine Hydrochloride. *Br. J. Ophthalmol.* **2020**, *105*, 608–613.
3. Cherqui, S.; Kalatzis, V.; Trugnan, G.; Antignac, C. The Targeting of Cystinosin to the Lysosomal Membrane Requires a Tyrosine-Based Signal and a Novel Sorting Motif*. *J. Biol. Chem.* **2001**, *276*, 13314–13321.
4. Syres, K.; Harrison, F.; Tadlock, M.; Jester, J.V.; Simpson, J.; Roy, S.; Salomon, D.R.; Cherqui, S. Successful Treatment of the Murine Model of Cystinosis Using Bone Marrow Cell Transplantation. *Blood* **2009**, *114*, 2542–2552.
5. Nesterova, G.; Gahl, W.A. Cystinosis: The Evolution of a Treatable Disease. *Pediatric Nephrol.* **2013**, *28*, 51–59.
6. Luaces-Rodríguez, A.; Díaz-Tomé, V.; González-Barcia, M.; Silva-Rodríguez, J.; Herranz, M.; Gil-Martínez, M.; Rodríguez-Ares, M.T.; García-Mazás, C.; Blanco-Mendez, J.; Lamas, M.J.; et al. Cysteamine Polysaccharide Hydrogels: Study of Extended Ocular Delivery and Biopermanence Time by PET Imaging. *Int. J. Pharm.* **2017**, *528*, 714–722.
7. McKenzie, B.; Kay, G.; Matthews, K.H.; Knott, R.; Cairns, D. Preformulation of Cysteamine Gels for Treatment of the Ophthalmic Complications in Cystinosis. *Int. J. Pharm.* **2016**, *515*, 575–582.
8. Kaur, S.; Sarma, P.; Kaur, H.; Prajapat, M.; Shekhar, N.; Bhattacharyya, J.; Kaur, H.; Kumar, S.; Medhi, B.; Ram, J.; et al. Efficacy and Safety of Topical Cysteamine in Corneal Cystinosis: A Systematic Review and Meta- Analysis. *Am. J. Ophthalmol.* **2020**, *223*, 275–285.




USC UNIVERSIDADE DE SANTIAGO DE COMPOSTELA

9. Andrzejewska, Z.; Nevo, N.; Thomas, L.; Chhuon, C.; Bailleux, A.; Chauvet, V.; Courtoy, P.J.; Chol, M.; Guerrera, I.C.; Antignac, C. Cystinosin Is a Component of the Vacuolar H+-ATPase-Ragulator-Rag Complex Controlling Mammalian Target of Rapamycin Complex 1 Signaling. *J. Am. Soc. Nephrol.* **2016**, *27*, 1678–1688.

10. Thoene, J.G.; DelMonte, M.A.; Mullet, J. Microvesicle Delivery of a Lysosomal Transport Protein to Ex Vivo Rabbit Cornea. *Mol. Genet. Metab. Rep.* **2020**, *23*, 100587.

11. Hollywood, J.A.; Przepiorski, A.; D'Souza, R.F.; Sreebhavan, S.; Wolvetang, E.J.; Harrison, P.T.; Davidson, A.J.; Holm, T.M. Use of Human Induced Pluripotent Stem Cells and Kidney Organoids to Develop a Cysteamine/Mtor Inhibition Combination Therapy for Cystinosis. *J. Am. Soc. Nephrol.* **2020**, *31*, 962–982.

12. Liu, Z.; Kompella, U.B.; Chauhan, A. Gold Nanoparticle Synthesis in Contact Lenses for Drug-Less Ocular Cystinosis Treatment. *Eur. J. Pharm. Biopharm.* **2021**, *165*, 271–278.

13. Pisoni, R.L.; Thoene, J.G.; Christensen, H.N. Detection and Characterization of Carrier-Mediated Cationic Amino Acid Transport in Lysosomes of Normal and Cystinotic Human Fibroblasts. Role in Therapeutic Cystine Removal? *J. Biol. Chem.* **1985**, *260*, 4791–4798.

14. Gahl, W.A.; Kuehl, E.M.; Iwata, F.; Lindblad, A.; Kaiser-Kupfer, M.I. Corneal Crystals in Nephropathic Cystinosis: Natural History and Treatment with Cysteamine Eyedrops. *Mol. Genet. Metab.* **2000**, *71*, 100–120.

15. European Medicines Agency. Cystagon® Prescribing Information. 1997. Available online: https://www.ema.europa.eu/en/medicines/human/EPAR/cystagon (accessed on 5 August 2022).

16. Schneider, J.A. Approval of Cysteamine for Patients with Cystinosis. *Pediatric Nephrol.* **1995**, *9*, 254.

17. Food and Drug Administration. Cystaran® Prescribing Information. 2012. Available online: https://www.accessdata.fda.gov/drugsatfda_docs/label/2012/200740s000lbl.pdf (accessed on 20 August 2022).

18. Food and Drug Administration. Cystadrops® Prescribing Information. 2020. Available online: https://www.accessdata.fda.gov/drugsatfda_docs/label/2020/211302s000lbl.pdf (accessed on 20 August 2022).

19. European Medicines Agency. Cystadrops® Prescribing Information. 2016. Available online: https://www.ema.europa.eu/en/documents/product-



USC UNIVERSIDADE DE SANTIAGO DE COMPOSTELA

information/cystadrops-epar-product-information_es.pdf (accessed on 20 August 2022).

20. Fernández-Ferreiro, A.; Luaces-Rodríguez, A.; Díaz-Tomé, V.; Gil-Martínez, M.; Ares, M.T.R.; Peralba, R.T.; Blanco-Méndez, J.; González-Barcia, M.; Otero-Espinar, F.J.; Lamas, M.J. Cysteamine ophthalmic hydrogel for the treatment of ocular cystinosis. *Farm. Hosp.* **2017**, *41*, 678–687.

21. Reda, A.; van Schepdael, A.; Adams, E.; Paul, P.; Devolder, D.; Elmonem, M.A.; Veys, K.; Casteels, I.; van den Heuvel, L.; Levtchenko, E. Effect of Storage Conditions on Stability of Ophthalmological Compounded Cysteamine Eye Drops. In *JIMD Reports*; Springer: Berlin/Heidelberg, Germany, 2017; Volume 42, pp. 47–51.

22. Labbé, A.; Baudouin, C.; Deschênes, G.; Loirat, C.; Charbit, M.; Guest, G.; Niaudet, P. A New Gel Formulation of Topical Cysteamine for the Treatment of Corneal Cystine Crystals in Cystinosis: The Cystadrops OCT-1 Study. *Mol. Genet. Metab.* **2014**, *111*, 314–320.

23. Jimenez, J.; Washington, M.A.; Resnick, J.L.; Nischal, K.K.; Fedorchak, M.V. A Sustained Release Cysteamine Microsphere/Thermoresponsive Gel Eyedrop for Corneal Cystinosis Improves Drug Stability. *Drug Deliv. Transl. Res.* **2021**, *11*, 2224–2238.

24. Atallah, C.; Charcosset, C.; Greige-Gerges, H. Challenges for Cysteamine Stabilization, Quantification, and Biological Effects Improvement. *J. Pharm. Anal.* **2020**, *10*, 499–516.

25. Castro-Balado, A.; Mondelo-García, C.; Varela-Rey, I.; Moreda-Vizcaíno, B.; Sierra-Sánchez, J.F.; Rodríguez-Ares, M.T.; Hermelo-Vidal, G.; Zarra-Ferro, I.; González-Barcia, M.; Yebra-Pimentel, E.; et al. Recent Research in Ocular Cystinosis: Drug Delivery Systems, Cysteamine Detection Methods and Future Perspectives. *Pharmaceutics* **2020**, *12*, 1177.

26. Purkiss, R. Stability of Cysteamine Hydrochloride in Solution. *J. Clin. Pharm. Ther.* **1977**, *2*, 199–203.

27. Brodrick, A.; Broughton, H.M.; Oakley, R.M. The Stability of an Oral Liquid Formulation of Cysteamine. *J. Clin. Hosp. Pharm.* **1981**, *6*, 67–70.

28. Dixon, P.; Powell, K.; Chauhan, A. Novel Approaches for Improving Stability of Cysteamine Formulations. *Int. J. Pharm.* **2018**, *549*, 466–475.

29. Carracedo, G.; Pastrana, C.; Serramito, M.; Rodriguez-Pomar, C. Evaluation of Tear Meniscus by Optical Coherence Tomography after Different Sodium Hyaluronate Eyedrops Instillation. *Acta Ophthalmol.* **2019**, *97*, e162–e169.

USC UNIVERSIDADE DE SANTIAGO DE COMPOSTELA

30. Acofarma Fórmulas Magistrales. Distribuidor de Productos para Farmacias Analysis Bulletin—Sodium Hyaluronate. Available online: https://productoquimico.acofarma.com (accessed on 5 August 2022).

31. Agencia Española de Medicamentos y Productos Sanitarios. Registro Unificado de Empresas de Sustancias Activas. Available online: https://labofar.aemps.es/labofar/registro/ruesa/consulta.do#nav-no (accessed on 5 August 2022).

32. Snetkov, P.; Zakharova, K.; Morozkina, S.; Olekhnovich, R.; Uspenskaya, M. Hyaluronic Acid: The Influence of Molecular Weight on Structural, Physical, Physico-Chemical, and Degradable Properties of Biopolymer. *Polymers* **2020**, *12*, 1800.

33. Olejnik, A.; Goscianska, J.; Zielinska, A.; Nowak, I. Stability determination of the formulations containing hyaluronic acid. *Int. J. Cosmet. Sci.* **2015**, *37*, 401–407.[

34. Falcone, S.J.; Palmeri, D.M.; Berg, R.A. Rheological and cohesive properties of hyaluronic acid. *J. Biomed. Mater. Res. Part A* **2006**, *76A*, 721–728.

35. Bothner, H.; Wik, O. Rheology of Hyaluronate. *Acta Oto-Laryngol.* **1987**, *104*, 25–30.

36. Biomed Device-Care in a Revolutionary Way. COL® Video-Kit for the Preparation of Aliquots of Eye Drops with Hemocomponents. Available online: https://www.youtube.com/watch?v=FCorvJXkUZw (accessed on 5 August 2022).

37. Biomed Device-Care in a Revolutionary Way. COL® Eye Drops System. Available online: http://col-eyedrops.com/index.php/it/eye-drops-system/col (accessed on 5 August 2022).

38. Kim, Y.; Na, D.H. Simultaneous Determination of Cysteamine and Cystamine in Cosmetics by Ion-Pairing Reversed-Phase High-Performance Liquid Chromatography. *Toxicol. Res.* **2019**, *35*, 161–165.

39. Lund, W. *The Pharmaceutical Codex: Principles and Practice of Pharmaceutics*; The Pharmaceutical Press: London, UK, 1994; ISBN 0-85369-290-4.

40. Fernández-Ferreiro, A.; Castro-Balado, A.; García Quintanilla, L.; Lamas, M.; Otero-Espinar, F.; Mendez, J.; Gómez-Ulla, F.; Gil-Martínez, M.; Tomé, V.; Luaces-Rodríguez, A.; et al. *Formulación Magistral Oftálmica Antiinfecciosa*; SEFH Sociedad Española de Farmacia Hospitalaria: Madrid, Spain, 2019; ISBN 978-84-09-10764-3.

41. Dutescu, R.M.; Panfil, C.; Schrage, N. Osmolarity of Prevalent Eye Drops, Side Effects, and Therapeutic Approaches. *Cornea* **2015**, *34*, 560–566.



USC UNIVERSIDADE DE SANTIAGO DE COMPOSTELA

42. Fernández-Ferreiro, A.; Silva-Rodríguez, J.; Otero-Espinar, F.J.; González-Barcia, M.; Lamas, M.J.; Ruibal, A.; Luaces-Rodriguez, A.; Vieites-Prado, A.; Sobrino, T.; Herranz, M.; et al. Positron Emission Tomography for the Development and Characterization of Corneal Permanence of Ophthalmic Pharmaceutical Formulations. *Investig. Ophthalmol. Vis. Sci.* **2017**, *58*, 772–780.

43. Loening, A.M.; Gambhir, S.S. AMIDE: A Free Software Tool for Multimodality Medical Image Analysis. *Mol. Imaging* **2003**, *2*, 131–137.

44. Committee for Medicinal Products for Human Use (CHMP). European Medicines Agency Guideline on Bioanalytical Method Validation. Available online: https://www.ema.europa.eu/en/documents/scientific-guideline/guideline-bioanalytical-method-validation_en.pdf (accessed on 22 September 2022).

45. Esteve Aquoral®. Available online: https://aquoral.es/aquoral-lagrimas-artificiales-alivio-rapido-y-duradero/aquoral/ (accessed on 5 August 2022).

46. Abbas, N.; Hasan, S.S.; Curley, L.; Babar, Z.-U.-D. Access to Medicines—A Systematic Review of the Literature. *Res. Soc. Adm. Pharm.* **2020**, *16*, 1166–1176.

47. Pescina, S.; Carra, F.; Padula, C.; Santi, P.; Nicoli, S. Effect of PH and Penetration Enhancers on Cysteamine Stability and Trans-Corneal Transport. *Eur. J. Pharm. Biopharm.* **2016**, *107*, 171–179.

48. Martín-Sabroso, C.; Alonso-González, M.; Fernández-Carballido, A.; Aparicio-Blanco, J.; Córdoba-Díaz, D.; Navarro-García, F.; Córdoba-Díaz, M.; Torres-Suárez, A.I. Limitations and Challenges in the Stability of Cysteamine Eye Drop Compounded Formulations. *Pharmaceuticals* **2022**, *15*, 2.

49. Makuloluwa, A.K.; Shams, F. Cysteamine Hydrochloride Eye Drop Solution for the Treatment of Corneal Cystine Crystal Deposits in Patients with Cystinosis: An Evidence-Based Review. *Clin. Ophthalmol.* **2018**, *12*, 227–236.

50. Bozdag, S.; Gumus, K.; Gumus, O.; Unlu, N. Formulation and in Vitro Evaluation of Cysteamine Hydrochloride Viscous Solutions for the Treatment of Corneal Cystinosis. *Eur. J. Pharm. Biopharm.* **2008**, *70*, 260–269.

51. U.S. Cysteamine Eye Drop Development. Available online: http://www.cystinosis.com/Documents/EyeDropPaper.html (accessed on 5 August 2022).

52. Bastarrachea, L.; Dhawan, S.; Sablani, S.S. Engineering Properties of Polymeric-Based Antimicrobial Films for Food Packaging: A Review. *Food Eng. Rev.* **2011**, *3*, 79–93.

53. European Medicines Agency. European Public Assessment Report (EPAR) for Cystadrops. Available online: https://www.ema.europa.eu/en/medicines/human/EPAR/cystadrops (accessed on 5 August 2022).



USC UNIVERSIDADE DE SANTIAGO DE COMPOSTELA

54. Food and Drug Administration. FDA Drug Approval Package: Cystadrops. Available online: https://www.accessdata.fda.gov/drugsatfda_docs/nda/2020/211302Orig1s000TOC.cfm (accessed on 5 August 2022).

55. Liang, H.; Labbé, A.; Le Mouhaër, J.; Plisson, C.; Baudouin, C. A New Viscous Cysteamine Eye Drops Treatment for Ophthalmic Cystinosis: An Open-Label Randomized Comparative Phase III Pivotal Study. *Investig. Ophthalmol. Vis. Sci.* **2017**, *58*, 2275-2283.

56. Yang, Y.-J.; Lee, W.-Y.; Kim, Y.-J.; Hong, Y.-P. A Meta-Analysis of the Efficacy of Hyaluronic Acid Eye Drops for the Treatment of Dry Eye Syndrome. *Int. J. Environ. Res. Public Health* **2021**, *18*, 2383.

57. Aragona, P.; Simmons, P.A.; Wang, H.; Wang, T. Physicochemical Properties of Hyaluronic Acid-Based Lubricant Eye Drops. *Transl. Vis. Sci. Technol.* **2019**, *8*, 2.

58. Posarelli, C.; Passani, A.; Del Re, M.; Fogli, S.; Toro, M.D.; Ferreras, A.; Figus, M. Cross-Linked Hyaluronic Acid as Tear Film Substitute. *J. Ocul. Pharmacol. Ther.* **2019**, *35*, 381–387.

59. Troiano, P.; Monaco, G. Effect of Hypotonic 0.4% Hyaluronic Acid Drops in Dry Eye Patients: A Cross-over Study. *Cornea* **2008**, *27*, 1126–1130.

60. Ang, B.C.H.; Sng, J.J.; Wang, P.X.H.; Htoon, H.M.; Tong, L.H.T. Sodium Hyaluronate in the Treatment of Dry Eye Syndrome: A Systematic Review and Meta-Analysis. *Sci. Rep.* **2017**, *7*, 9013.

61. Sandri, G.; Rossi, S.; Ferrari, F.; Bonferoni, M.C.; Zerrouk, N.; Caramella, C. Mucoadhesive and Penetration Enhancement Properties of Three Grades of Hyaluronic Acid Using Porcine Buccal and Vaginal Tissue, Caco-2 Cell Lines, and Rat Jejunum. *J. Pharm. Pharmacol.* **2004**, *56*, 1083–1090.

62. Datta, S.; Baudouin, C.; Brignole-Baudouin, F.; Denoyer, A.; Cortopassi, G.A. The Eye Drop Preservative Benzalkonium Chloride Potently Induces Mitochondrial Dysfunction and Preferentially Affects LHON Mutant Cells. *Investig. Ophthalmol. Vis. Sci.* **2017**, *58*, 2406–2412.

63. Özalp, O.; Atalay, E.; Alataş, İ.Ö.; Küskü Kiraz, Z.; Yıldırım, N. Assessment of Phosphate and Osmolarity Levels in Chronically Administered Eye Drops. *Turk. J. Ophthalmol.* **2019**, *49*, 123–129.

64. Casey-Power, S.; Ryan, R.; Behl, G.; McLoughlin, P.; Byrne, M.E.; Fitzhenry, L. Hyaluronic Acid: Its Versatile Use in Ocular Drug Delivery with a Specific Focus on Hyaluronic Acid-Based Polyelectrolyte Complexes. *Pharmaceutics* **2022**, *14*, 1479.



USC UNIVERSIDADE DE SANTIAGO DE COMPOSTELA

65. Johnson, R.S.; Niedermeier, W.; Bobo, P. The Pseudoplastic Behavior of Aqueous Solutions of Hyaluronic Acid. *Biorheology* **1971**, *7*, 177–187.

66. Ahumada, L.A.C.; González, M.X.R.; Sandoval, O.L.H.; Olmedo, J.J.S. Evaluation of Hyaluronic Acid Dilutions at Different Concentrations Using a Quartz Crystal Resonator (QCR) for the Potential Diagnosis of Arthritic Diseases. *Sensors* **2016**, *16*, 1959.

67. García-Abuín, A.; Gómez-Díaz, D.; Navaza, J.M.; Regueiro, L.; Vidal-Tato, I. Viscosimetric Behaviour of Hyaluronic Acid in Different Aqueous Solutions. *Carbohydr. Polym.* **2011**, *85*, 500–505.

68. Klang, M.G. Sterile Preparation Formulation. In *Compounding Sterile Preparations*, 4th ed.; American Society of Health-System Pharmacists (ASHP): Bethesda, MD, USA, 2018; pp. 51–66. ISBN 978-1-58528-484-9.

69. ScienceDirect Topics. Cryoprotective Agent—An Overview. Available online: https://www.sciencedirect.com/topics/pharmacology-toxicology-and-pharmaceutical-science/cryoprotective-agent (accessed on 24 August 2022).



USC UNIVERSIDADE DE SANTIAGO DE COMPOSTELA

USC
UNIVERSIDADE
DE SANTIAGO
DE COMPOSTELA

## 7. SUPPLEMENTARY MATERIAL

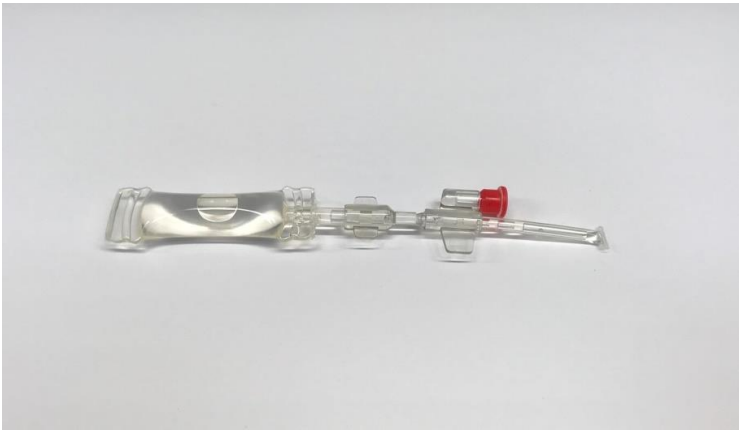


**Figure S1.** COL Eye Drops System® used in the stability study, provided from Biomed Device.

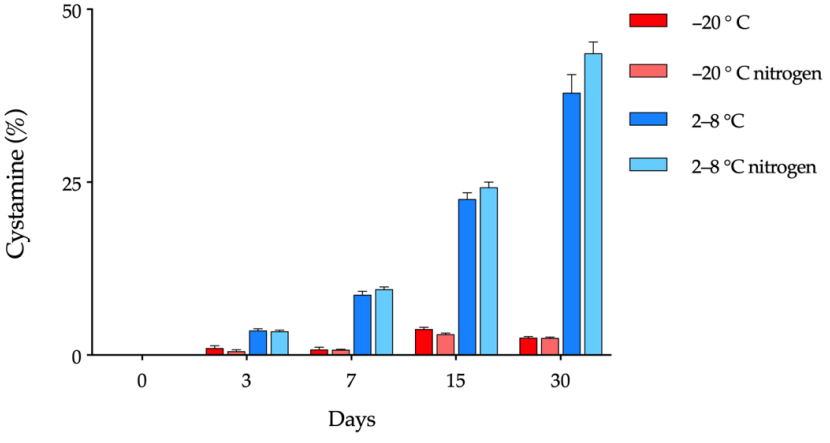



**Figure S2.** Cystamine content with respect to the initial concentration throughout the study for each of the temperature settings (refrigeration/freezing) and presence/absence of nitrogen.



USC UNIVERSIDADE DE SANTIAGO DE COMPOSTELA

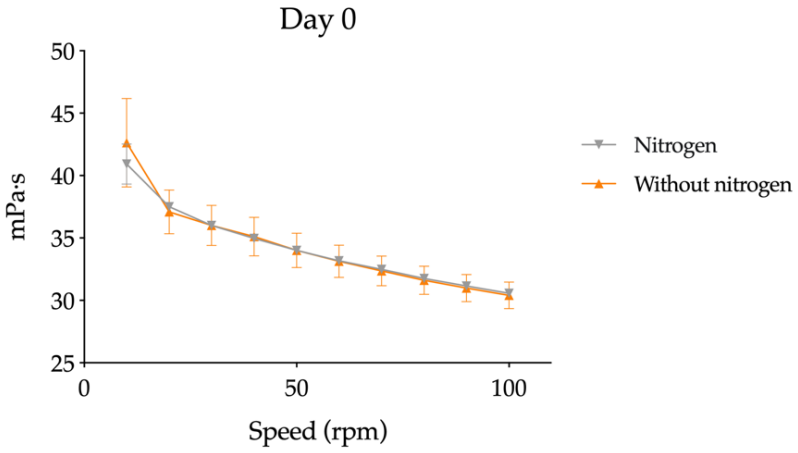



**Figure S3.** Speed-scan test at 25 °C of the cysteamine formulations with presence/absence of nitrogen at day 0, where the viscosity is measured at different revolutions per minute (rpm).

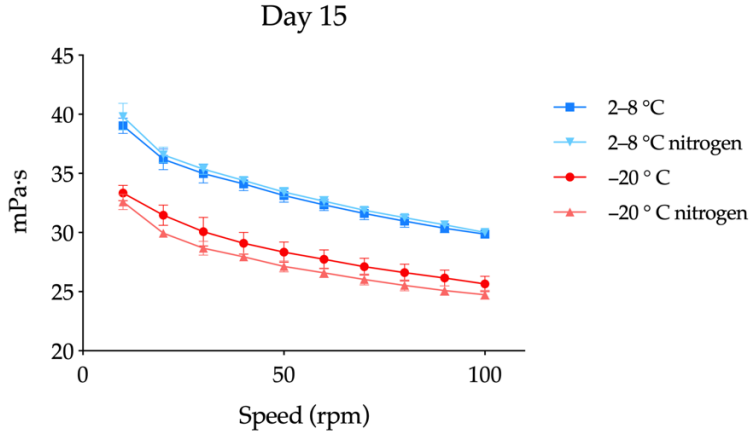



**Figure S4.** Speed-scan test at 25 °C of the cysteamine formulations stored at different temperature conditions and presence/absence of nitrogen at day 15, where the viscosity is measured at different rpm.



USC UNIVERSIDADE DE SANTIAGO DE COMPOSTELA

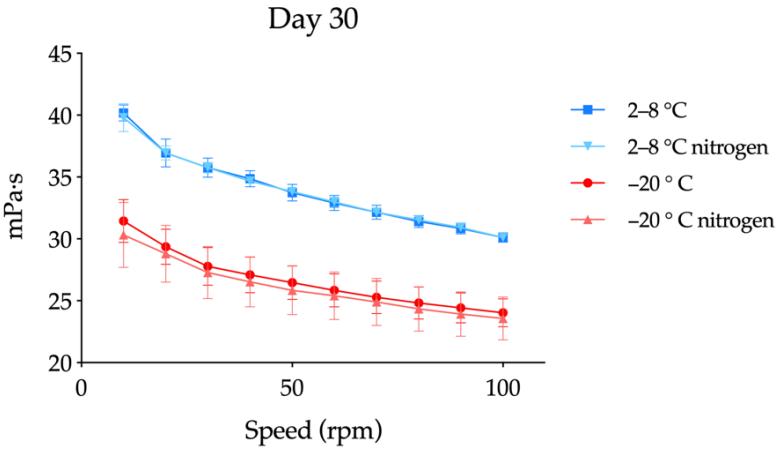



**Figure S5.** Speed-scan test at 25 °C of the cysteamine formulations stored at different temperature conditions and presence/absence of nitrogen at day 30, where the viscosity is measured at different rpm.



USC UNIVERSIDADE DE SANTIAGO DE COMPOSTELA

USC
UNIVERSIDADE
DE SANTIAGO
DE COMPOSTELA

# CHAPTER 4

## DEVELOPMENT AND CHARACTERIZATION OF INHALED ETHANOL AS A NOVEL PHARMACOLOGICAL STRATEGY CURRENTLY EVALUATED IN A PHASE II CLINICAL TRIAL FOR EARLY-STAGE SARS-COV-2 INFECTION

USC
UNIVERSIDADE DE SANTIAGO DE COMPOSTELA

USC
UNIVERSIDADE
DE SANTIAGO
DE COMPOSTELA

# CHAPTER 4

## DEVELOPMENT AND CHARACTERIZATION OF INHALED ETHANOL AS A NOVEL PHARMACOLOGICAL STRATEGY CURRENTLY EVALUATED IN A PHASE II CLINICAL TRIAL FOR EARLY-STAGE SARS-COV-2 INFECTION


### ABSTRACT

Inhaled administration of ethanol in the early stages of COVID-19 would favor its location on the initial replication sites, being able to reduce the progression of the disease and improving its prognosis. Before evaluating the efficacy and safety of this novel therapeutic strategy in humans, its characterization is required. The developed 65° ethanol formulation is stable at room temperature and protected from light for 15 days, maintaining its physicochemical and microbiological properties. Two oxygen flows have been tested for its administration (2 and 3 L/min) using an automated headspace gas chromatographic analysis technique (HS-GC-MS), with that of 2 L/min being the most appropriate one, ensuring the inhalation of an ethanol daily dose of 33.6 ± 3.6 mg/min and achieving more stable concentrations during the entire treatment (45 min). Under these conditions of administration, the formulation has proven to be safe, based on histological studies of the respiratory tracts and lungs of rats. On the other hand, these results are accompanied by the first preclinical molecular imaging study with radiolabeled ethanol administered by this route. The current ethanol formulation has received approval from the Spanish Agency of Medicines and Medical Devices for a phase II clinical trial for early-stage COVID-19 patients, which is currently in the recruitment phase (ALCOVID-19; EudraCT number: 2020-001760-29).



**Keywords:** COVID-19; SARS-CoV-2; inhaled ethanol; molecular imaging; PET





USC UNIVERSIDADE DE SANTIAGO DE COMPOSTELA

## 1. INTRODUCTION

Coronaviruses (CoVs) are single-stranded RNA viruses which can infect animals and humans, causing respiratory, gastrointestinal, hepatic and neurologic diseases [1]. In December 2019, several health authorities reported patients with pneumonia of an unknown cause, which were epidemiologically linked to a seafood market in Wuhan, China. The pathogen, a novel coronavirus (SARS-CoV-2), was identified by local hospitals and the infection was called coronavirus infectious disease 2019 (COVID-19) [2,3]. In March 2020, the World Health Organization (WHO) classified COVID-19 as a pandemic, and in January 2021, a year after its eruption, there have been more than 93 million confirmed cases and two million deaths [4].

Since the outbreak of the COVID-19 pandemic, it has been seen that compliance of control measures such as physical distancing, the use of masks, hand cleaning, tracing contacts, testing of exposed or symptomatic persons and isolation have restricted transmissions [5]. Even so, these actions have not been implemented uniformly, and they have not shown to be enough to prevent the spread of SARS-CoV-2.

Vaccines are needed to produce group immunity and reduce COVID-19 morbidity and mortality. In this sense, several vaccine platforms have been implicated in the rapid development of candidate vaccines [6,7,8], which allowed the starting of the vaccination process worldwide in December 2020.

According to the pathological characteristics of COVID-19, especially for patients with moderate to severe COVID-19, several treatment strategies have been developed, including, among others, antiviral agents, inflammation inhibitors/antirheumatic drugs and low molecular weight heparins [9,10]. Concerning new therapies, it is necessary to highlight the administration of convalescent plasma with high IgG titers against SARS-CoV-2, which have revealed promising results, although further studies are required [11]. In addition, regarding antivirals, plitidepsin has demonstrated potent preclinical efficacy against SARS-CoV-2 by targeting the host protein eEF1A, and it is being tested in a proof of concept study to evaluate its safety profile (NCT04382066) [12]. Another possible alternative is treatment with monoclonal antibodies, such as bamlanivimab, which is currently evaluated in an expanded access program (NCT04603651) [13], or the cocktail of monoclonal antibodies anti-spike SARS-CoV-2, which is being tested in ambulatory adult and pediatric patients (NCT04425629) [14].

Despite all the above, it has been seen that, in the early stages, antiviral drugs can prevent the progression of the disease, while dexamethasone [15], immunomodulators and antiviral drugs seem to improve the clinical outcome of



USC UNIVERSIDADE DE SANTIAGO DE COMPOSTELA

patients with severe COVID-19 [9]. However, treatment remains elusive in early stages, in which there are few strategies that can bring benefits; some strategies have failed, and others are under evaluation [11].

In pandemic situations like this, a significant number of patients find themselves in a therapeutic vacuum, without effective drugs to address their treatment. In this context, drug repositioning is a strategy to generate additional value from an approved drug, using it for a different therapeutic purpose than that for which it was originally intended [16]. The absence of evidence-based treatments for COVID-19 has led to the start of a large number of clinical trials in order to offer patients the most effective and safest therapeutic options. In this sense, the genetic characteristics of SARS-CoV and MERS-CoV suggest that SARS-CoV-2 may be susceptible to disinfectants such as ethanol, with a graduation between 62–71°, with proven activity against enveloped viruses [17,18].

In early stages of the disease, active viruses are located in the throat and lungs. This way, the administration of viricidal agents in the initial replication place could decrease viremia in the first stages of the disease, and consequently reduce its progression and improve the prognosis drastically [19]. In hospital pharmacy departments, it is common to elaborate ethanol formulations for their use in non-usual routes of administration. Ethanol was used in catheter seals to prevent bacterial growth [20], as a neurolytic in the peripheral or central nervous block in terminally ill patients [21], in esophageal varicose sclerotherapy [22], hemorrhage control in hepatocellular carcinoma surgeries [23], debridement of the corneal epithelium [24] or even as an intravenous antidote in the treatment of ethylene glycol or methanol poisoning [25].

COVID-19 causes a particularly severe illness in older adults. The percentage of hospitalized patients within this age group is high [11], and over 95% of total death cases occurred in people older than 60 years, with more than 50% of all deaths being people aged 80 years or older [3,26,27]. In this situation, with no alternatives among commercial medicines, it is necessary to develop new therapeutic approaches which can be an adequate option in elderly patients. In this sense, the local administration of ethanol could be effective against a viral envelope with no systemic adverse effects [28,29].

This study presents a novel pharmacological strategy against SARS-CoV-2 with inhaled ethanol and its galenic, toxicological and pharmacokinetic characterization. The current ethanol formulation has received approval from the Spanish Agency of Medicines and Medical Devices to test its efficacy-safety in a phase II clinical trial in elderly patients with COVID-19, which is currently in the recruitment phase (ALCOVID-19; EudraCT number: 2020-001760-29) [30].



USC UNIVERSIDADE DE SANTIAGO DE COMPOSTELA

## 2. MATERIALS AND METHODS

This work includes an initial galenic characterization phase, in which the physiochemical and microbiological stability of the formulation in humidifying flasks was determined, as well as the concentration of vaporized ethanol through two oxygen flows. Subsequently, a two-part preclinical phase was carried out. On the one hand, an in vivo study to ensure the safety of the ethanol administered by this route was performed in Sprague-Dawley rats. On the other hand, evaporated ethanol was radiolabeled, and its pharmacokinetics in rats were studied using molecular imaging techniques with positron emission tomography/computed tomography (PET/TC). Lastly, a preliminary clinical study was carried out in six healthy volunteers divided into two groups (1:1), who were subjected to the administration of 15 minutes of oxygen therapy at 2 L/min and 3 L/min flow through a Ventimask® (Flexicare, Mountain Ash, UK) face mask. These data are depicted in the Supplementary Materials, including Figures S1 and S2.

### *2.1. Preparation of the 65° Ethanol Solution and Stability Determination in Disposable Humidifying Bottles*

A volume of 250 mL of 65° ethanol solution was packaged in disposable humidifier bottles (INTL CE0482. Ref. 3230, generously donated by Oximesa Nippon Gases, Madrid, Spain). To prepare, the starting point was 163 mL of 99.5° ethanol with PhEur indication on its label (PanReac AppliChem®, Darmstadt, Germany), which was measured using a graduated cylinder, and completed with sterile water (Fresnius Kabi®, Barcelona, Spain) up to 250 mL. After homogenization, it was necessary to wait until it reached room temperature to measure ethanol graduation with a 60–70° Gay-Lussac alcoholmeter (Boeco®, Hamburg, Germany). Sterilizing vacuum filtration through a 0.22-micron filter was performed in a horizontal laminar flow cabinet.

In order to determine the stability of ethanol over 15 days in a disposable humidifying bottle, an initial ethanol graduation measurement was carried out, and then once weekly using the 60–70° Gay-Lussac alcoholmeter. During this period, the ethanol solution was kept in a fully sealed humidifier bottle at room temperature, and protected from light. Parallel to this, a microbiological study was carried out by extraction of three 3 mL samples: one sample before sterilizing filtration and another after this process on day 0; and the last one after 15 days of storage at room temperature and protected from light. These samples were cultivated in a thioglycollate broth (Merck®, Darmstadt, Germany), Columbia blood agar (Merck®, Darmstadt, Germany) and Sabouraud (Merck®, Darmstadt, Germany). All mediums were incubated aerobically at 37 °C; thioglycollate for 10



USC UNIVERSIDADE DE SANTIAGO DE COMPOSTELA

days; and blood and Sabouraud agar plates for 48 h. Sabouraud agar plates were subsequently incubated for 13 days in aerobiosis at room temperature.

### *2.2. Determination of Ethanol in the Administered Oxygen Flow*

A flow of oxygen was made to pass through a humidifier containing the 65° ethanol solution. The effect of two oxygen flows was compared: 2 and 3 L/min. These flows cause the evaporation of the ethanol in the humidifier. This determination of evaporated ethanol will allow choosing the optimal oxygen flow that causes the evaporation without generating aerosols, with this being best suited to its use later in the clinical trial.

The ethanol quantification has been carried out by an automated headspace gas chromatographic mass spectrometry analysis (HS-GC-MS) (Figure 1). It was performed using a Finnigan Trace GC Ultra chromatograph coupled with a Finnigan Trace DSQ mass detector, equipped with a Thermo Scientific Head Space (HS) TriPlus autosampler (Thermo Fisher Scientific, San José, CA, USA). Sampling was performed in 21.5 mL HS glass vials, which were previously sealed. The septum was perforated with two needles to allow a way in and a way out for the gas. Then, oxygen enriched in ethanol generated in the humidifier was flushed for 2 min in each vial to replace all of its internal air, and guarantee that the sample was representative. The samples were collected at several intervals of time, as follows: 0–2 min; 2–4 min; 6–8 min; 13–15 min; 28–30 min; and 43–45 min, in order to determine the concentration of ethanol at 2, 4, 8, 15, 30 and 45 min of administration, respectively. All experiments were performed in triplicate for the two flow rates tested (2 L/min and 3 L/min). The vials were maintained and refrigerated before HS-GC-MS analysis.

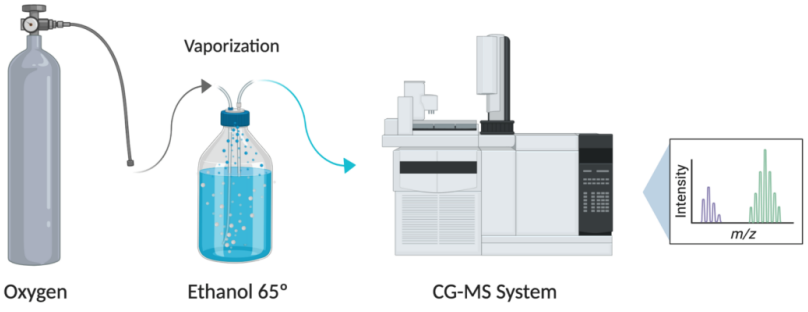



**Figure 1.** Diagram of the oxygen flow system and humidifier with 65° ethanol coupled to a gas chromatography mass spectrometry (GC-MS) system. Created with BioRender.com.



USC UNIVERSIDADE DE SANTIAGO DE COMPOSTELA

Samples were incubated at 45 °C for 4 min, before 0.2 mL of headspace gas was withdrawn by the autosampler, using a 2.5 mL syringe heated at 50 °C. The gas volume was injected into the inlet of the Trace GC set at 175 °C in a constant temperature split mode, at a split ratio of 50:1 and the split flow of 50 mL/min. The analytical column was a Rxi-624Sil MS, 30 m in length, with an internal diameter of 0.25 mm (1.4 μm film thickness) from Restek (Bellefonte, PA, USA). Helium was used as carrier gas at a flow rate of 1.0 mL/min in a constant flow mode. The oven temperature was initially set at 40 °C for 4 min, then increased at a rate of 50 °C/min until 120 °C, and held at 120 °C for 2.5 min. The total runtime of each analysis was 10 min. The temperatures of the GC transfer line and the ion source of the MS were set at 220 °C and 200 °C, respectively. The mass spectrometer was operated in an electron impact ionization (EI+) mode, and the chromatograms were acquired in full scan mode over the m/z range of 20–150, from 2 to 10 min, at a scan rate of 3.55 scans/s. The chromatographic peak of ethanol was identified by comparison with reference spectra from the NIST 2011/Wiley 9 Combined Mass Spectral Library, using NIST Mass Spectral Search Program (version 2.0), and confirmed by comparison of its retention time (3.4 min), with that obtained by analysis of authentic standard under the same conditions. The instrument control and data acquisition and processing were performed with Xcalibur 2.0.7 software (Thermo Fisher Scientific Inc., Waltham, MA, USA).

The calibration curve of ethanol was prepared in 21.5 mL HS glass vials, which were previously sealed with Teflon septum caps, by adding different volumes of 99.5% (0.5–2 μL) ethanol to reach the headspace (vapor phase) concentrations in the range of 20–100 mg/L. The equation and determination coefficient obtained from three replicates were $y = 82.285x + 9.8808$ and $R^2 = 0.9993$, respectively.

### *2.3. Preclinical Studies*

#### 2.3.1. Ethanol Exposure Toxicological Studies and Immunohistochemical Analysis

These studies were carried out on six female Sprague-Dawley rats (four receiving inhaled ethanol and two control rats). They were supplied by the animal facilities at the University of Santiago de Compostela, and the average weight was 250 ± 25 g. During the experiments, animals were kept in individual cages under a controlled temperature (22 ± 1 °C) and humidity (60 ± 5%) conditions, with day-night cycles regulated by artificial light (12/12 h) and fed *ad libitum*. All animal experiments complied with the ARRIVE guidelines [31] and were carried out in accordance with the EU Directive 2010/63/EU for animal experiments, being approved by the Galician Network Committee for Ethics Research. All experimental procedures



USC UNIVERSIDADE DE SANTIAGO DE COMPOSTELA

were approved by the ethical committee and the local authorities before conducting experimental work.

For the administration, 65° ethanol was placed in a disposable humidifier and vaporized by passing an oxygen flow of 2 L/min. The generated ethanol vapors went through a tube to an inhalation chamber of 20 × 20 × 25 cm (Bioseb, FL, USA) (Figure 2). For exposure to the ethanol vapours, each rat was placed in the chamber for 15 min every 8 h (three times a day) for five consecutive days. Following the exposure time, each rat was removed from the inhalation chamber and returned to its individual cage.

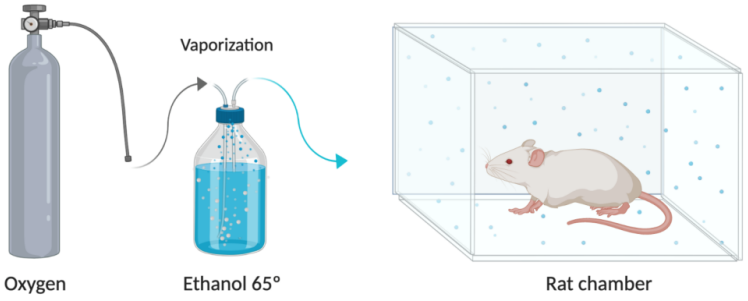



**Figure 2.** Oxygen flow system and humidifier with 65° ethanol coupled to the inhalation chamber, where the rats are exposed to ethanol vapor for inhalation. Created with BioRender.com.

The animals were sacrificed by an intracardiac injection of 5 mL of potassium chloride (1 mEq/mL; B. Braun Medical, S.A, Barcelona, Spain) at day +6 of the initiation assay. Upper respiratory tracts were removed and individually fixed in 10% formalin, dehydrated, paraffin embedded, sectioned in slices with 4 μm thickness, and stained with H&E (haematoxylin and eosin). The samples were blindly evaluated by a lung pathologist specialist using a microscope (Zeiss, Oberkochen, Germany). Sections were examined using light microscopy, and digital images were acquired using Leica® software (Leica Microsystems, Wetzlar, Alemania). Analyses were performed at a final magnification of ×1000. Five nonoverlapping fields of view per section from two to three sections (from different regions of the lung, esophagus and trachea) per animal were analyzed.

### 2.3.2. Preclinical Pharmacokinetics

The preclinical pharmacokinetic studies were carried out with positron emission tomography/computed tomography (PET/TC) methodology using radiolabeled ethanol. The use of molecular imaging, particularly PET/TC, provides a non-



USC UNIVERSIDADE DE SANTIAGO DE COMPOSTELA

invasive imaging technique that visualizes the distribution of different radiotracers over time in animal models [32]. In this study, 1-$^{11}$C-ethanol has been synthetized in order to know the distribution of ethanol administered into the respiratory tract in rats along time, in order to assess the tolerance and safety of the administration of vaporized ethanol three times a day for five days in Sprague-Dawley rats.

*Synthesis of 1-$^{11}$C-Ethanol*

The synthesis of 1-$^{11}$C-ethanol was carried out using a TRACERlab FXC Pro synthesis module (GE Healthcare, Chicago, IL, USA). [$^{11}$C]$CO_2$ was generated in an IBA Cyclone 18/9 cyclotron (IBA RadioPharma Solutions Headquarter, Louvain-la-Neuve, Belgium) by proton irradiation (target current = 22 μA, integrated current = 2 μAh) of a gas $N_2/O_2$ mixture (99/1, starting pressure = 20 bar) with high energy (18 MeV) protons. The radioactive gas was first trapped in a molecular sieve oven at room temperature and then released by heating at 180 °C under nitrogen flow (20 mL/min). The released [$^{11}$C]$CO_2$ was bubbled in a reaction vial containing $CH_3MgBr$ (1M solution in THF, 250 μL, Merck®, Darmstadt, Germany). After complete trapping, $LiAlH_4$ (1M solution in THF, 500 μL, Merck®, Darmstadt, Germany) was added, and the resulting mixture was stirred at 80 °C for 5 min. The solvent was then evaporated under helium flow (5 min, 60 °C; then 1 min, 80 °C). The reactor was cooled to 40 °C and aqueous HCl (4 M, 1 mL) was immediately added. The solution was stirred for 30 s, filtered using a 0.2 μm filter, and purified by high-performance liquid chromatography (HPLC) using a Mediterranea SEA18 (250 × 10 mm, 5 μm particle size) (Teknokroma Analítica, Barcelona, Spain) column as a stationary phase and ultrapure water as the mobile phase (flow rate = 5 mL/min). The purified product (retention time = 7.7 min; total collected volume of ca. 2 mL) was collected in a vial and diluted 1:1 with a physiologic saline solution. The amount of radioactivity of the final radiotracer was measured in a dose calibrator (PETDOSE HC, Comecer, Castel Bolognese RA, Italy). Radiochemical purity was determined by HPLC, using an Agilent 1200 Series HPLC system (Agilent Technologies, Santa Clara, CA, USA) with a multiple wavelength UV detector ($\lambda$ = 254 nm) and a radiometric detector (Raytest, Elysia-raytest GmbH, Straubenhardt, Germany). A Tracer Excel 120 C8 (250 × 4.6 mm, 5 μm particle size) (Teknokroma Analítica, Barcelona, Spain) was used as stationary phase and purified water as mobile phase (flow rate = 1 mL/min; retention time = 3.95 min).

*Lung PET Studies*

Three healthy female Sprague-Dawley rats ($n$ = 3) weighting 350 ± 10 g were used in this study. For PET studies, anesthesia was induced with 5% isoflurane and maintained by 1.5 to 2% of isoflurane in 100% $O_2$. The labelled compound (ca. 7



USC UNIVERSIDADE DE SANTIAGO DE COMPOSTELA

MBq, 100 μL) was administered through endotracheal insufflations using the PennCentury MicroSprayer® Aerosolizer (FMJ-250 High Pressure Syringe Model, Penn-Century, Inc., Wyndmoor, PA, USA) and a small animal laryngoscope (Penn-Century, Model LS-2) (Penn-Century. Inc. Wyndmoor, USA) for the correct visualization of the epiglottis. After administration, the animal was quickly moved into the PET camera, and the PET acquisition began. The time gap between administration of the dose and start of image acquisition was 1 min. During imaging, rats were kept normothermic using a heating blanket (Homeothermic Blanket Control Unit; Bruker, MA, USA). PET Imaging was performed using an eXploreVista-CT small animal PET-CT system (GE Healthcare, Chicago, IL, USA). Whole body dynamic images were acquired in four bed positions (20 frames: 4 × 5 s, 4 × 15 s, 4 × 30 s, 4 × 60 s, 4 × 120 s; total acquisition time = 61.33 min) in the 400–700 keV energetic window. After each PET acquisition, a CT scan (X-ray energy: 40 kV, intensity: 140 μA) was performed for a later attenuation correction in the image reconstruction, as well as for the unequivocal localization of the radioactivity. Random and scatter corrections were also applied to the reconstructed image. PET-CT images of the same animal were co-registered and analyzed using the PMOD image processing tool (PMOD Technologies Ltd., Zürich, Switzerland). Volumes of interest (VOIs) were placed on major organs (lungs, liver, kidneys, heart and brain), and time–activity curves (decay corrected) were obtained as cps/cm$^3$ in each organ. Curves were transformed into real activity (Bq/cm$^3$) curves by using a calibration factor, obtained from previous scans performed on a phantom (micro-deluxe, Data spectrum Corp., Durham, NC, USA) under the same experimental conditions (isotope, reconstruction algorithm and energetic window).

## 3. RESULTS

### *3.1. Stability of the 65° Ethanol Pharmaceutical Compounding and Flow Oxygen Effect*

The graduation of the humidifying bottle with the hydro-alcoholic solution under storage conditions (without use) remained stable for 15 days, with no microbiological growth observed at the end of said period.

The formulation maintains optimal concentrations (decreases less than 5% of the initial concentration) at the end of the three daily applications, with both flows tested (2 and 3 L/min). With the flow of 2 L/min, a solution graduation of 64.1° was maintained (98.2% of the original concentration of the hydro-alcoholic mixture), while at the flow of 3 L/min, the graduation obtained was 63.3° (97.8%). The ethanol content of the initial solution, in the humidifier bottle, decreased 4.63 g at 2 L/min



USC UNIVERSIDADE DE SANTIAGO DE COMPOSTELA

and 5.38 g at 3 L/min, after 45 min of administration. The difference between flow rates was 0.75 g of ethanol emitted per day, higher for a flow of 3 L/min, which represents 16% more than the total amount achieved with the flow of 2 L/min, as shown in Figure 3a.

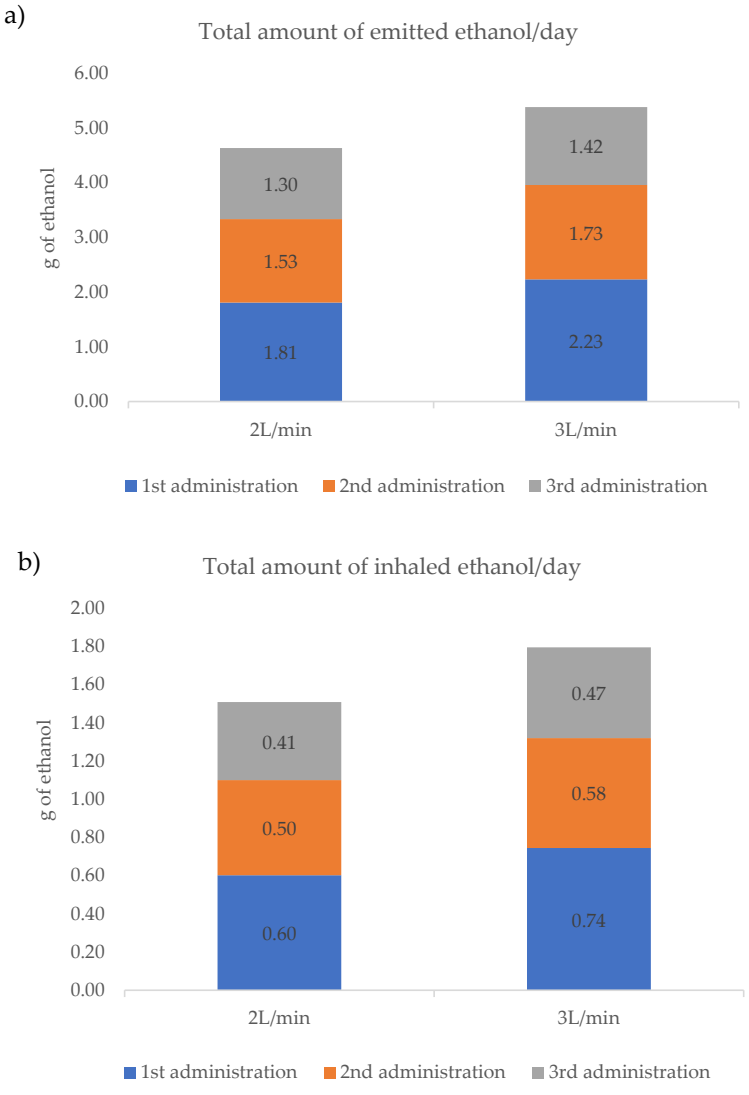



**Figure 3.** (**a**) The total amount of ethanol evaporated from the initial solution, according to GC-MS data determined by calculation of the areas under concentration-time curves (AUC), and (**b**) the estimated total amount of ethanol inhaled by human adults taking into account the recommended short-term exposure values for inhalation, in sedentary or passive activity (**b**), after the 45 min of treatment at 2 L/min and 3 L/min.



USC UNIVERSIDADE DE SANTIAGO DE COMPOSTELA

Considering the minute ventilation of 5 L/min for human adults recommended for short-term exposure [33], and the inhalation:exhalation (I:E) ratio of 1:2, the total amount of ethanol inhaled after the three daily administrations at 2 L/min and 3 L/min was 1.51 g and 1.79 g, respectively (Figure 3b). The difference in the total amount of the inhaled ethanol between flow rates was 0.28 g higher for the highest flow rate used.

Kinetic parameters of the ethanol vaporization in the oxygen stream, for both flow rates tested, are shown in Figure 4. Second-degree polynomial equations were developed from the experimental data, and areas under the concentration-time curves (AUC) were calculated to determine the amount of ethanol emitted during the treatments. At the flow rate of 2 L/min, the average concentrations of ethanol yielded (51.5 ± 4.5 mg/L of oxygen (8.7% CV)) were higher than that observed at 3 L/min (39.9 ± 5.7 mg/L of oxygen (14.4% CV)) during the 45 min of treatment. The concentration of ethanol decreased slightly during the time for both flow rates tested. In the first 15 min, the average concentrations of ethanol determined at a flow rate of 2 L/min and 3 L/min were 56.6 ± 1.9 (3.4% CV) and 46.6 ± 3.1 mg/L (6.6% CV), respectively. In the second period (15–30 min) of the experiment, the average concentrations were 51.0 ± 1.6 (3.2% CV) and 38.6 ± 2.0 mg/L (5.2% CV), and finally, in the last period of 15 min, the concentrations of ethanol were 46.5 ± 1.46 (2.9% CV) and 34.0 ± 1.0 mg/L (3.0% CV), for 2 L/min and 3 L/min, respectively.

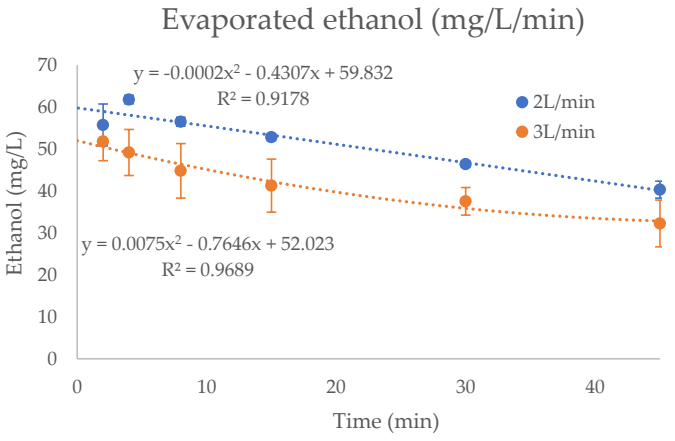



**Figure 4.** Ethanol concentration (mg/L) in the vapor phase of oxygen generated in the humidifier, during the 45 minutes of treatment, at 2 L/min and 3 L/min.

Following the previous consideration for the I:E ratio, the average concentrations of inhaled ethanol at flow rates of 2 L/min and 3 L/min were 6.70 ± 0.75 mg/L/min (11.2% CV) and 7.99 ± 1.12 mg/L/min (14.7% CV), respectively. The concentrations



USC UNIVERSIDADE DE SANTIAGO DE COMPOSTELA

were slightly higher for the highest flow rate, since the dilution with the assistant air was lower. Specifically, the inhaled concentrations (mg/L/min) at the different administrations were: 7.55 ± 0.27 (0–15min), 6.70 ± 0.27 (15–30 min) and 5.58 ± 0.26 (30–45 min) at the flow rate of 2 L/min; and 9.37 ± 0.62 (0–15 min), 7.76 ± 0.41 (15–30 min), 6.81 ± 0.19 (30–45 min) at the flow rate of 3 L/min.

Taking into account the total amount of ethanol emitted per minute of treatment (mg/min), the values were lower for the flow rate of 2 L/min (100.1 ± 11.5 mg/min (11.5% CV)) than the 3 L/min (average of 119.7 ± 17.1 mg/min (14.3% CV)), as shown in Figure 5. These differences were higher in the first minutes of ethanol enriched oxygen administration, with total amounts of ethanol of 112.7 ± 4.1 (3.7% CV) for 2 L/min flow rate and 139.7 ± 9.2 (6.6% CV) for 3 L/min, and decreased during the time of around 23% and 27%, respectively. For the second and third administrations at 2 L/min flow rate, the amounts of ethanol were 99.7 ± 4.2 (4.2% CV) and 87.4 ± 4.2 (4.2% CV), respectively, whereas at a flow rate of 3 L/min, the values observed were 115.8 ± 6.0 (5.2% CV) and 102.6 ± 3.0 (2.9% CV).

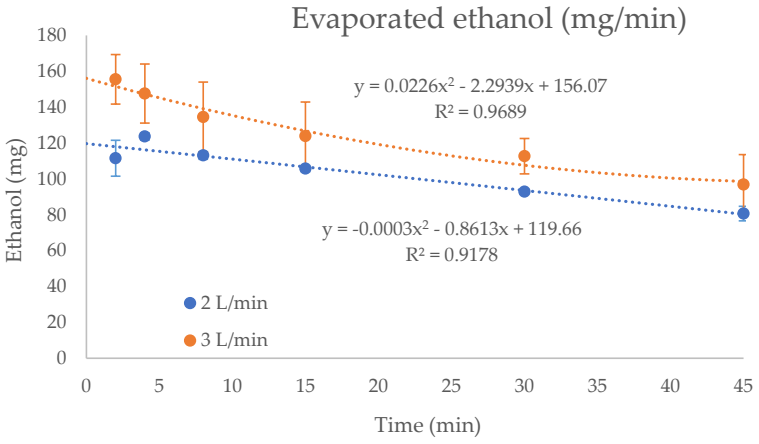



**Figure 5.** Amount of ethanol (mg) in the vapor phase of oxygen generated in the humidifier, during the 45 minutes of treatment, at the flow rates of 2 L/min and 3 L/min.

Therefore, based on previous considerations, the estimated final average amounts of inhaled ethanol (mg/min) were 33.6 ± 3.6 (10.7% CV) and 40.0 ± 5.7 (14.2% CV) at the flow rate of 2 L/min and 3 L/min, respectively. At the flow rate of 2 L/min, analysis of variance (ANOVA) showed no significant differences ($p > 0.05$) among the doses of inhaled ethanol during the three administrations: 37.60 ± 2.04 (0–15 min); 33.36 ± 1.34 (15–30 min); and 29.31 ± 1.32 (30–45 min). On the contrary, significant differences ($p < 0.001$) were observed at the flow rate of 3 L/min: 46.55 ± 1.02 (0–15 min); 38.57 ± 2.00 (15–30 min); and 34.04 ± 1.01 (30–45 min).



USC UNIVERSIDADE DE SANTIAGO DE COMPOSTELA

### *3.2. Preclinical Studies*

#### 3.2.1. Ethanol Exposure Toxicological Studies and Immunohistochemical Analysis

Tissue and air-space fractions (atelectasis), oedema and congestion were evaluated in the paraffin-embedded sections of lung tissue stained with hematoxylin and eosin. There were no typical patterns of pulmonary toxicities along the respiratory tract, as can be seen in Figure 6 (a. lung; b. and c. trachea and d. and e. esophagus).

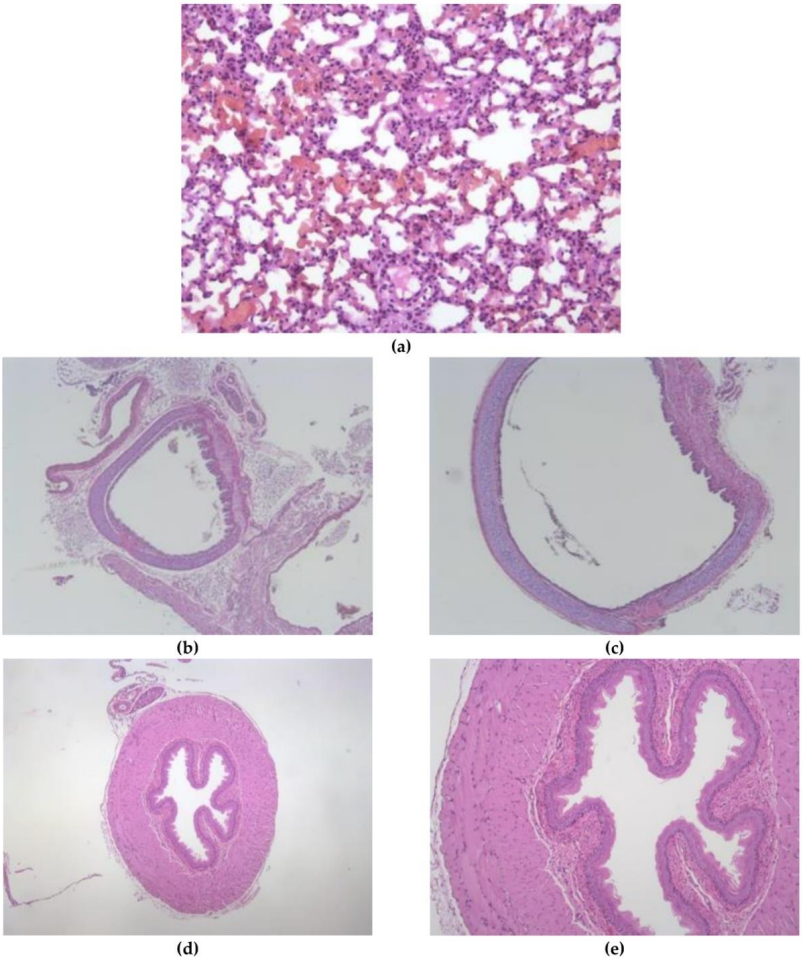



**Figure 6.** Upper respiratory tracts fixed in 10% formalin, dehydrated, paraffin embedded, sectioned in slices with 4 μm thickness and stained with H&E: (**a**) Lung (200×) with description of absence damage; (**b**,**c**) Trachea (10×, 40×) with description of absence damage; and (**d**,**e**) Esophagus (40×, 100×) with description of absence damage.



USC UNIVERSIDADE DE SANTIAGO DE COMPOSTELA

### 3.2.2. Pharmacokinetics

*Synthesis of 1-$^{11}$C-Ethanol*

The synthesis of 1-$^{11}$C-ethanol has been previously reported [34,35]. In these previous works, the final purification of the labeled compound was achieved by fractional distillation. In our hands, this synthetic approach resulted in the presence of radioactive impurities in the final solution. The undesired by-products were co-eluted with methanol (retention time = 3.5 min) and isopropanol (retention time = 4.7 min) under our analytical HPLC conditions (Figure 7a) and accounted for ca. 20% of total radioactivity. Taking into account that our aim was to obtain radiochemically pure 1-$^{11}$C-ethanol, and that the overall yield was not a critical aspect, we decided to assay a purification method based on HPLC. After a filtration step to remove any eventual precipitate due to incomplete dissolution of the solid residue after the addition of hydrochloric acid, a good separation of the different peaks could be achieved when water was used as the mobile phase.

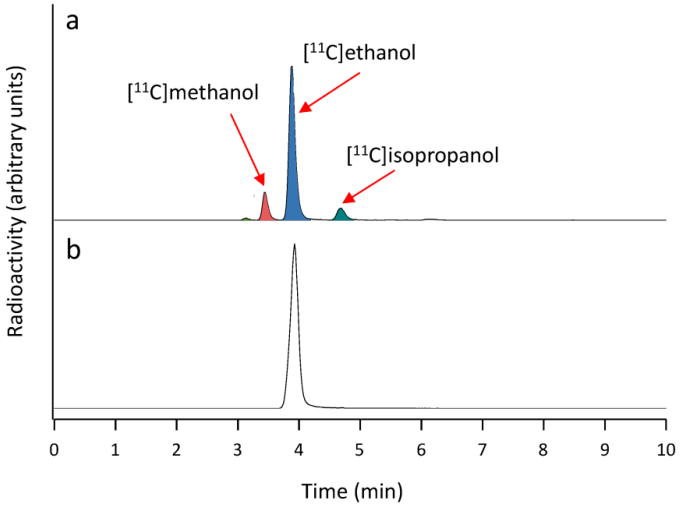



**Figure 7.** (**a**) Chromatograms (radioactivity detector) obtained after analysis of the reaction crude; (**b**) chromatograms (radioactivity detector) obtained in quality control analysis of the purified 1-$^{11}$C-ethanol.

Under these conditions, approximately 600 MBq of pure 1-$^{11}$C-ethanol (radiochemical purity > 99%; Figure 7 b) could be obtained in average production time of 30 min (decay corrected radiochemical yield of around 7%). This amount of radioactivity, which was ready for administration after simple dilution with physiologic saline solution, was sufficient to tackle subsequent in vivo studies in rodents (see below).



USC UNIVERSIDADE DE SANTIAGO DE COMPOSTELA

*Lung PET Studies*

PET studies were carried out to determine the biodistribution of 1-$^{11}$C-ethanol in rats after intratracheal insufflation. Administration was carried out using the Penn-Century MicroSprayer® Aerosolizer, which is reported to provide around a 20 μm droplet size [36]. According to our previous results, this is a very appropriate system for the quantitative administration of aerosols in the rat lung [36]. Due to the administration process, dynamic images could be started around one minute after administration, and hence initial distribution data (0.1 min after administration) was lost. Dynamic PET images (Figure 8) show a very fast lung clearance ($t_{1/2}$ = 1.43 min), with most of the radioactivity already cleared from the lungs at $t$ = 1 min.

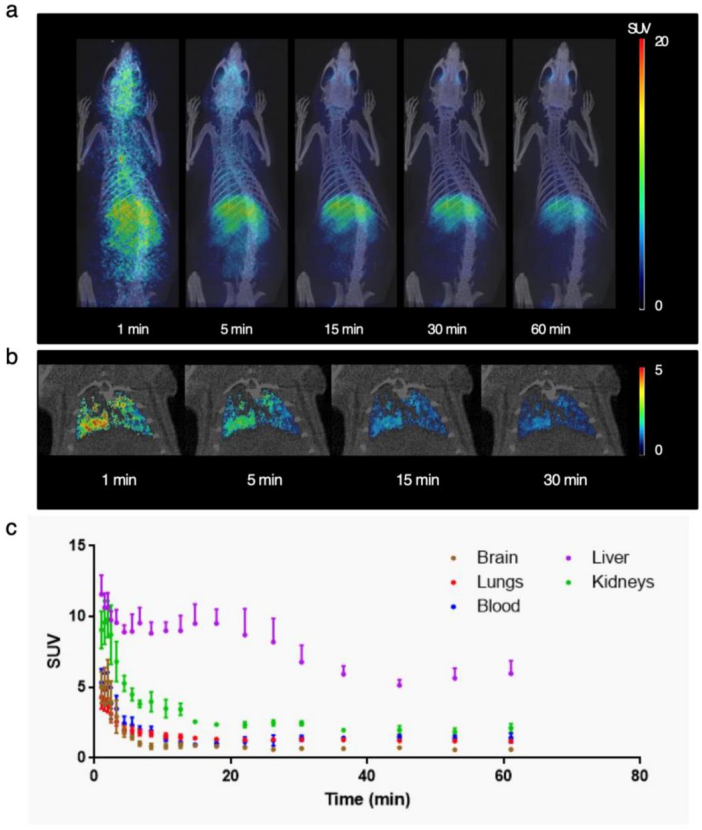



**Figure 8.** (**a**) Positron emission tomography (PET) images (maximum intensity projections, coronal views) obtained at different time points after intratracheal administration of 1-$^{11}$C-ethanol. Images have been coregistered with 3D-rendered computed tomography (CT) images for anatomical localization of the radioactive signal; (**b**) PET images (coronal projections) corresponding to the segmented lungs at different times points after administration; images have been coregistered with representative CT slices; (**c**) time activity curves obtained after quantification of volumes of interest drawn in different organs. Values are expressed as standard uptake values (SUV), mean ± standard error mean, $n$ = 3.



USC UNIVERSIDADE DE SANTIAGO DE COMPOSTELA

The presence of radioactivity delocalized over the whole animal at early time points suggest translocation to the blood, followed by progressive accumulation in the liver (Figure 8), suggesting metabolic oxidation to acetaldehyde by alcohol dehydrogenase and cytochrome P450, which are extensively present in this organ.

## 4. DISCUSSION

The emergency period of the COVID-19 outbreak has forced the scientific community to generate evidence against the clock [37]. Despite the recent development of vaccines to prevent the disease, new therapeutic alternatives to treat the established disease should be studied [38,39]. According to the pathological characteristics of COVID-19 and different clinical stages, especially for patients with moderate to severe disease, antiviral agents, inflammation inhibitors/antirheumatic drugs, low molecular weight heparins and convalescent plasma with high IgG titers against SARS-CoV-2 have been used and tested [9,10,11]. In the early stages of the disease, the treatment of COVID-19 remains elusive. There are few strategies that can bring benefits, some strategies have failed, and others are under evaluation [11,40,41,42,43].

Faced with therapeutic gaps such as these, clinicians are forced to resort to therapeutic alternatives such as drug repositioning and pharmaceutical compounding. The genetic characteristics of SARS-CoV and MERS-CoV suggest that SARS-CoV-2 may be susceptible to disinfectants with proven activity against enveloped viruses [17,18]. Ethanol exerts its action against a viral envelope; a lipid bilayer taken from the host cells in the assembly or budding stage of the viral cycle, causing viral lysis with the consequent release and degradation of its content [19]. Active viruses in throat and lungs were isolated in patients with a mild condition only up to day 8 after the onset of symptoms, reaching the peak of the viral load before day 5. This way, the administration of viricidal agents in the place of initial replication could decrease viremia in the first stages of the disease, and consequently reduce the progression of the disease and improve its prognosis [29,44]. For this reason, the administration of inhaled ethanol could be presented as a new therapeutic strategy to prevent the progression of COVID-19 infections [45]. Our hypothesis of treatment with inhaled ethanol focuses on its use in institutionalized elderly patients, since certain therapies used to date were contraindicated or discouraged in this age group, where COVID-19 has severe outcomes with a high mortality rate [46]. Prior to the start of a phase II clinical trial for early-stage COVID-19 older adult patients, already approved by the Spanish Agency of Medicines and Medical Devices (ALCOVID-19; EudraCT number 2020-001760-29), galenic, toxicological and pharmacokinetic characterization of the inhaled ethanol compounded formulation has been necessary.



USC UNIVERSIDADE DE SANTIAGO DE COMPOSTELA

After the vaporization of 65° ethanol for 45 minutes in three administrations, there is a decrease in the alcohol content of the hydro-alcoholic mixture contained in the disposable humidifiers compared to the initial values. Through bubbling oxygen at different flows through the 65° ethanol solution, evaporation of the mixture is favored. The vapor pressure of ethanol is much higher than the vapor pressure of water, since ethanol has a boiling point (78.4 °C) considerably lower than water (100 °C) [47]. For this reason, the gas produced after bubbling oxygen through the 65° ethanol solution will have a higher ethanol concentration than the starting mixture.

Considering the minute ventilation of 5 L/min for human adults recommended for short-term exposure [33], and the I:E ratio of 1:2, the average concentrations of inhaled ethanol in the three administrations of ethanol were 6.70 mg/L/min and 7.99 mg/L/min for the flow rates of 2 L/min and 3 L/min, respectively, which correspond to the total amounts of ethanol per minute of 33.52 mg/min and 39.88 mg/min. These amounts were lower than those observed by Bessonneau and Thomas [48] in a study related to the exposure after hand disinfection, where the total inhaled dose of ethanol ranged between 150.8 and 219.26 mg/min. The total amount of alcohol vaporized during the flushing of oxygen through the formulation increased with the flow rate of oxygen, as observed by other studies described in the literature [49]. The concentrations of ethanol per min (mg/L/min) emitted in the humidifier were lower at the flow rate of 3 L/min (see Figure 4), as the higher flow rate of oxygen could not reach the equilibrium with ethanol at the same time and carried less ethanol vapor per liter (mg/L). The administration during the time of treatment was more stable at the flow rate of 2 L/min than 3 L/min (see Figure 4).

The total amount of ethanol evaporated (mg/min) was slightly higher at the higher flow rate (3 L/min), as there was more oxygen available to carry ethanol (see Figure 5). This phenomenon is manifested in the results obtained in this study, where the concentrations of the mixture, after the three bubbling cycles, have been reduced to 98.2% and 97.8%, compared to the original concentration with 2 L/min and 3 L/min flows, respectively. The total amount of ethanol evaporated after three administrations in the 45 min of treatment was 4.64 g at the 2 L/min flow rate, and 5.38 g at the 3 L/min flow rate (see Figure 3a).

A study performed by Zhang [50] demonstrated that deposition of ethanol in several local sites of the respiratory tract using a human upper airway model depended on fluid flows and diffusion parameters. Lower flow rates allowed higher percentages of ethanol deposition in the respiratory tract than higher flows. Instead, at higher flow rates, the concentration gradient near to the wall increases alongside the mass transfer coefficient, and consequently the absorption of ethanol. This author concluded that if the objective is deposition of ethanol and not its absorption, the use of low flow rates should be recommended, due to the extended vapor



USC UNIVERSIDADE DE SANTIAGO DE COMPOSTELA

residence times at low flow rates. This is in line with our approach, in which we seek ethanol deposition with minimal systemic absorption, which could produce drug interactions or adverse reactions.

On the other hand, it is convenient to highlight the safety of the current pharmacological strategy proposed. Preclinical studies in rats and mice that inhaled ethanol provide the greatest evidence available to date for characterizing the risks of inhalation of ethanol [51,52]. The observed adverse effects were attributed to systemic and chronic exposure to ethanol, regardless of the route of administration [53]. Choi et al. analyzed the efficacy and safety of the administration of proteins carried in absolute ethanol in rats. No allergic or inflammatory responses were shown, nor was damage to the alveolar barrier, or cell lysis that could indicate acute toxic effects in the lungs or airways [54]. These results are in line with what was observed in the present study after the administration of ethanol in Sprague-Dawley rats (females, 250 g (BW), with minute ventilation of 130 mL/min) every 8 hours for five days, with an inhalation period of 15 min. Bavis et al. described that rats with the same characteristics as used in our assays have a minute ventilation 0.130 L/min [55]. Taking this into account, in our experiments at 2 L/min, the rats were exposed to a total estimated amount of ethanol of 301.3 mg/day, which corresponds to a dose of 1.2 g/kg/day. At the same flow, in our study, 151 g were estimated as inhaled by human in a day. Considering a human body weight of 60 kg, the dose administrated would correspond to 0.025 g/kg/day. Thus, in the preclinical study, the exposure limits were overestimated up to 40-fold higher than those applied in the human volunteers. No significant differences were observed through histological staining by a lung pathologist specialist between the rodents that received ethanol compared to those that received control. Lung, trachea and esophagus samples were described as absent of damage.

To our knowledge, no molecular imaging studies have been published to date to characterize the biodistribution of radiolabeled ethanol administered through the respiratory tract. In order to obtain a first orientation of the possible residence time of ethanol in the lung, a PET/CT study has been carried out in rats, therefore being the first research about pulmonary kinetics of ethanol administered by this route. The PET/CT images obtained after the administration of 1-$^{11}$C-ethanol show radioactivity at initial times at the level of respiratory tract and lungs, followed by a fast and delocalized distribution over the whole animal. These findings suggest a translocation of ethanol to the circulatory system, followed by progressive accumulation in its main organ of metabolism, the liver. These results are in line with that previously observed by Gifford et al., in which 1-$^{14}$C-ethanol was administered intravenously in order to determine sites of concentration of ethanol or its metabolites, which may contribute to its toxicological and pharmacokinetic properties [56].



USC UNIVERSIDADE DE SANTIAGO DE COMPOSTELA

At this point, a new line of future research opens so that specialized centers can test its virucidal potential. Nowadays, our group are testing the clinical efficacy and safety of this new pharmacological strategy in 170 early-stage COVID-19 institutionalized elderly patients. This clinical trial will allow us to know if the stablished ethanol concentration is effective, if the exposure time is adequate and also the toxicity profile of inhaled ethanol. This may be possible thanks to the recent approval of the phase II clinical trial authorized by the Spanish Agency of Medicines and Medical Devices (ALCOVID-19; EudraCT: 2020-001760-29).

## 5. CONCLUSIONS

This research work aims to show the development and results of the galenic, pharmacokinetic and toxicological characterization of inhaled ethanol as a potential therapy against SARS-CoV-2. The developed 65° ethanol compounded formulation remains stable at room temperature and protected from light for 15 days. The most convenient flow rate for ethanol administration is 2 L/min, ensuring the inhalation of an ethanol daily dose of 33.6 ± 3.6 mg/min, and achieving more stable concentrations during the entire treatment (45 min). Furthermore, it has also been found to show satisfactory pharmacokinetic and toxicological characteristics through PET/CT studies and histological analysis of respiratory tract and lung tissue in rats. Clinical safety and efficacy are currently being studied in a phase II clinical trial (ALCOVID-19; EudraCT number: 2020-001760-29) for early-stage COVID-19-institutionalized patients.

## 6. REFERENCES

1. Weiss, S.R.; Leibowitz, J.L. Coronavirus Pathogenesis. *Adv. Virus Res.* **2011**, *81*, 85–164.

2. Jin, Y.; Yang, H.; Ji, W.; Wu, W.; Chen, S.; Zhang, W.; Duan, G. Virology, Epidemiology, Pathogenesis, and Control of COVID-19. *Viruses* **2020**, *12*, 372.

3. Rothan, H.A.; Byrareddy, S.N. The Epidemiology and Pathogenesis of Coronavirus Disease (COVID-19) Outbreak. *J. Autoimmun.* **2020**, *109*, 102433.

4. WHO. Coronavirus Disease (COVID-19) Dashboard. Available online: https://covid19.who.int (accessed on 16 January 2021).

5. Baker, M.G.; Kvalsvig, A.; Verrall, A.J. New Zealand's COVID-19 Elimination Strategy. *Med. J. Aust.* **2020**, *213*, 198-200.



USC UNIVERSIDADE DE SANTIAGO DE COMPOSTELA

6. Baden, L.R.; Sahly, H.M.E.; Essink, B.; Kotloff, K.; Frey, S.; Novak, R.; Diemert, D.; Spector, S.A.; Rouphael, N.; Creech, C.B.; et al. Efficacy and Safety of the MRNA-1273 SARS-CoV-2 Vaccine. *N. Engl. J. Med.* **2020**, *384*, 403-416.

7. Polack, F.P.; Thomas, S.J.; Kitchin, N.; Absalon, J.; Gurtman, A.; Lockhart, S.; Perez, J.L.; Pérez Marc, G.; Moreira, E.D.; Zerbini, C.; et al. Safety and Efficacy of the BNT162b2 MRNA Covid-19 Vaccine. *N. Engl. J. Med.* **2020**, *383*, 2603–2615.

8. Knoll, M.D.; Wonodi, C. Oxford-AstraZeneca COVID-19 Vaccine Efficacy. *Lancet* **2021**, *397*, 72–74.

9. Stasi, C.; Fallani, S.; Voller, F.; Silvestri, C. Treatment for COVID-19: An Overview. *Eur. J. Pharmacol.* **2020**, *889*, 173644.

10. Li, Y.; Liu, S.; Zhang, S.; Ju, Q.; Zhang, S.; Yang, Y.; Wang, H. Current Treatment Approaches for COVID-19 and the Clinical Value of Transfusion-Related Technologies. *Transfus. Apher. Sci.* **2020**, *59*, 102839.

11. Libster, R.; Pérez Marc, G.; Wappner, D.; Coviello, S.; Bianchi, A.; Braem, V.; Esteban, I.; Caballero, M.T.; Wood, C.; Berrueta, M.; et al. Early High-Titer Plasma Therapy to Prevent Severe Covid-19 in Older Adults. *N. Engl. J. Med.* **2021**, 384, 610-618.

12. PharmaMar Multicenter. Randomized, Parallel and Proof of Concept Study to Evaluate the Safety Profile of Three Doses of Plitidepsin in Patients with COVID-19 Requiring Hospitalization. 2020. Available online: clinicaltrials.gov (accessed on 25 January 2021).

13. Eli Lilly and Company. Expanded Access Information for Physicians for Bamlanivimab (LY3819253) Emergency Investigational New Drug (EIND). 2021. Available online: clinicaltrials.gov (accessed on 25 February 2021).

14. Regeneron Pharmaceuticals. A Master Protocol Assessing the Safety, Tolerability, and Efficacy of Anti-Spike (S) SARS-CoV-2 Monoclonal Antibodies for the Treatment of Ambulatory Patients with COVID-19. 2021. Available online: clinicaltrials.gov (accessed on 25 February 2021).

15. Group, T.R.C. Dexamethasone in Hospitalized Patients with Covid-19—Preliminary Report. *N. Engl. J. Med.* **2020**, *384*, 693-704.

16. Andersen, P.I.; Ianevski, A.; Lysvand, H.; Vitkauskiene, A.; Oksenych, V.; Bjørås, M.; Telling, K.; Lutsar, I.; Dumpis, U.; Irie, Y.; et al. Discovery and



USC UNIVERSIDADE DE SANTIAGO DE COMPOSTELA

Development of Safe-in-Man Broad-Spectrum Antiviral Agents. *Int. J. Infect. Dis.* **2020**, *93*, 268–276.

17. Kampf, G.; Todt, D.; Pfaender, S.; Steinmann, E. Persistence of Coronaviruses on Inanimate Surfaces and Their Inactivation with Biocidal Agents. *J. Hosp. Infect.* **2020**, *104*, 246–251.

18. Laboratory Biosafety Guidance Related to Coronavirus Disease (COVID-19). Available online: https://www.who.int/publications-detail-redirect/laboratory-biosafety-guidance-related-to-coronavirus-disease-(covid-19) (accessed on 21 June 2020).

19. Kratzel, A.; Todt, D.; V'kovski, P.; Steiner, S.; Gultom, M.; Thao, T.T.N.; Ebert, N.; Holwerda, M.; Steinmann, J.; Niemeyer, D.; et al. Inactivation of Severe Acute Respiratory Syndrome Coronavirus 2 by WHO-Recommended Hand Rub Formulations and Alcohols. *Emerg. Infect. Dis.* **2020**, *26*, 1592–1595.

20. Opilla, M.T.; Kirby, D.F.; Edmond, M.B. Use of Ethanol Lock Therapy to Reduce the Incidence of Catheter-Related Bloodstream Infections in Home Parenteral Nutrition Patients. *JPEN J. Parenter. Enteral Nutr.* **2007**, *31*, 302–305.

21. Lipton, S. Pain Relief in Active Patients with Cancer: The Early Use of Nerve Blocks Improves the Quality of Life. *BMJ* **1989**, *298*, 37–38.

22. Sarin, S.K.; Sachdeva, G.K.; Nanda, R.; Vij, J.C.; Anand, B.S. Endoscopic Sclerotherapy Using Absolute Alcohol. *Gut* **1985**, *26*, 120–124.

23. Chung, S.C.; Lee, T.W.; Kwok, S.P.; Li, A.K. Injection of Alcohol to Control Bleeding from Ruptured Hepatomas. *BMJ* **1990**, *301*, 421.

24. Yuksel, E.; Novruzlu, S.; Ozmen, M.C.; Bilgihan, K. A Study Comparing Standard and Transepithelial Collagen Cross-Linking Riboflavin Solutions: Epithelial Findings and Pain Scores. *J. Ocul. Pharmacol. Ther.* **2015**, *31*, 296–302.

25. Sepúlveda, R.A.; Selamé, E.; Roessler, E.; Tagle, R.; Valdivieso, A. Intoxicación Por Etilenglicol, Fisiopatología y Enfrentamiento Clínico. *Rev. Med. Chil.* **2019**, *147*, 1572–1578.

26. Statement—Older People Are at Highest Risk from COVID-19, but All Must Act to Prevent Community Spread. Available online: http://www.euro.who.int/en/health-topics/health-emergencies/coronavirus-covid-19/statements/statement-older-people-are-at-highest-risk-from-covid-19,-but-all-must-act-to-prevent-community-spread (accessed on 8 June 2020).

USC UNIVERSIDADE DE SANTIAGO DE COMPOSTELA

27. Li, P.; Chen, L.; Liu, Z.; Pan, J.; Zhou, D.; Wang, H.; Gong, H.; Fu, Z.; Song, Q.; Min, Q.; et al. Clinical Features and Short-Term Outcomes of Elderly Patients with COVID-19. *Int. J. Infect. Dis.* **2020**, *97*, 245–250.

28. Kampf, G. Efficacy of Ethanol against Viruses in Hand Disinfection. *J. Hosp. Infect.* **2018**, *98*, 331–338.

29. Yan, R.; Zhang, Y.; Li, Y.; Xia, L.; Guo, Y.; Zhou, Q. Structural Basis for the Recognition of SARS-CoV-2 by Full-Length Human ACE2. *Science* **2020**, *367*, 1444–1448.

30. Ensayo Clínico Fase II Para Evaluar La Eficacia y Seguridad de Etanol Inhalado En El Tratamiento de La COVID-19 En Estadio Inicial. Available online: https://reec.aemps.es/reec/estudio/2020-001760-29 (accessed on 9 January 2021).

31. Kilkenny, C.; Browne, W.; Cuthill, I.C.; Emerson, M.; Altman, D.G. NC3Rs Reporting Guidelines Working Group Animal Research: Reporting in Vivo Experiments: The ARRIVE Guidelines. *Br. J. Pharmacol.* **2010**, *160*, 1577–1579.

32. Seoane-Viaño, I.; Gómez-Lado, N.; Lázare-Iglesias, H.; Barreiro-de Acosta, M.; Silva-Rodríguez, J.; Luzardo-Álvarez, A.; Herranz, M.; Otero-Espinar, F.; Antúnez-López, J.R.; Lamas, M.J.; et al. Longitudinal PET/CT Evaluation of TNBS-Induced Inflammatory Bowel Disease Rat Model. *Int. J. Pharm.* **2018**, *549*, 335–342.

33. U.S. EPA. *Exposure Factors Handbook 2011 Edition (Final Report)*; EPA/600/R-09/052F; U.S. Environmental Protection Agency: Washington, DC, USA, 2011.

34. Gulyás, B.; Vas, A.; Halldin, C.; Sóvágó, J.; Sandell, J.; Olsson, H.; Fredriksson, A.; Stone-Elander, S.; Farde, L. Cerebral Uptake of (Ethyl-11C) Vinpocetine and 1-(11C) Ethanol in Cynomolgous Monkeys: A Comparative Preclinical PET Study. *Nucl. Med. Biol.* **2002**, *29*, 753–759.

35. DeGrazia, J.A.; Rodden, A.F.; Teresi, J.D.; Busick, D.D.; Walz, D.R. Radioscintigraphic Studies of 11C Distribution in Cats given 1-11 C-Ethanol. *J. Nucl. Med.* **1975**, *16*, 73–76.

36. Cossío, U.; Gómez-Vallejo, V.; Flores, M.; Gañán-Calvo, B.; Jurado, G.; Llop, J. Preclinical Evaluation of Aerosol Administration Systems Using Positron Emission Tomography. *Eur. J. Pharm. Biopharm.* **2018**, *130*, 59–65.

37. Castro-Balado, A.; Varela-Rey, I.; Bandín-Vilar, E.J.; Busto-Iglesias, M.; García-Quintanilla, L.; Mondelo-García, C.; Fernández-Ferreiro, A. Clinical Research in



USC UNIVERSIDADE DE SANTIAGO DE COMPOSTELA

Hospital Pharmacy during the Fight against COVID-19. *Farm. Hosp.* **2020**, *44*, 66–70.

38. Dai, L.; Gao, G.F. Viral Targets for Vaccines against COVID-19. *Nat. Rev. Immunol.* **2020**, *21*, 73-82.

39. Fernández-Ferreiro, A.; González-Barcia, M. The Human Being, the Only Animal That Needs a Master to Live. *OFIL·ILAPHAR* **2020**, *30*, 179–182.

40. Cao, B.; Wang, Y.; Wen, D.; Liu, W.; Wang, J.; Fan, G.; Ruan, L.; Song, B.; Cai, Y.; Wei, M.; et al. A Trial of Lopinavir–Ritonavir in Adults Hospitalized with Severe Covid-19. *N. Engl. J. Med.* **2020**, *382*, 1787-1799.

41. RECOVERY Collaborative Group; Horby, P.; Mafham, M.; Linsell, L.; Bell, J.L.; Staplin, N.; Emberson, J.R.; Wiselka, M.; Ustianowski, A.; Elmahi, E.; et al. Effect of Hydroxychloroquine in Hospitalized Patients with Covid-19. *N. Engl. J. Med.* **2020**, *383*, 2030–2040.

42. Stone, J.H.; Frigault, M.J.; Serling-Boyd, N.J.; Fernandes, A.D.; Harvey, L.; Foulkes, A.S.; Horick, N.K.; Healy, B.C.; Shah, R.; Bensaci, A.M.; et al. Efficacy of Tocilizumab in Patients Hospitalized with Covid-19. *N. Engl. J. Med.* **2020**, *383*, 2333–2344.

43. Li, L.; Zhang, W.; Hu, Y.; Tong, X.; Zheng, S.; Yang, J.; Kong, Y.; Ren, L.; Wei, Q.; Mei, H.; et al. Effect of Convalescent Plasma Therapy on Time to Clinical Improvement in Patients with Severe and Life-Threatening COVID-19: A Randomized Clinical Trial. *JAMA* **2020**, *324*, 460–470.

44. Talavera, B.; García-Azorín, D.; Martínez-Pías, E.; Trigo, J.; Hernández-Pérez, I.; Valle-Peñacoba, G.; Simón-Campo, P.; de Lera, M.; Chavarría-Miranda, A.; López-Sanz, C.; et al. Anosmia Is Associated with Lower In-Hospital Mortality in COVID-19. *J. Neurol. Sci.* **2020**, *419*, 117163.

45. Shintake, T. Possibility of Disinfection of SARS-CoV-2 (COVID-19) in Human Respiratory Tract by Controlled Ethanol Vapor Inhalation. *arXiv* **2020**, arXiv:2003.12444.

46. Ly, T.D.A.; Zanini, D.; Laforge, V.; Arlotto, S.; Gentile, S.; Mendizabal, H.; Finaud, M.; Morel, D.; Quenette, O.; Malfuson-Clot-Faybesse, P.; et al. Pattern of SARS-CoV-2 Infection among Dependant Elderly Residents Living in Long-Term Care Facilities in Marseille, France, March–June 2020. *Int. J. Antimicrob. Agents* **2020**, *56*, 106219.

USC UNIVERSIDADE DE SANTIAGO DE COMPOSTELA

47. Durst, H.D.; Gokel, G.W. *Química Orgánica Experimental*; Editorial Reverté: Barcelona, Spain, 1985; ISBN 978-84-291-7155-6.

48. Bessonneau, V.; Thomas, O. Assessment of Exposure to Alcohol Vapor from Alcohol-Based Hand Rubs. *Int. J. Environ. Res. Public Health* **2012**, *9*, 868–879.

49. Luisada, A.A.; Goldmann, M.A.; Weyl, R. Alcohol Vapor by Inhalation in the Treatment of Acute Pulmonary Edema. *Circulation* **1952**, *5*, 363–369.

50. Zhang, Z.; Kleinstreuer, C.; Kim, C.S. Transport and Uptake of MTBE and Ethanol Vapors in a Human Upper Airway Model. *Inhal. Toxicol.* **2006**, *18*, 169–184.

51. Rogers, J.; Wiener, S.G.; Bloom, F.E. Long-Term Ethanol Administration Methods for Rats: Advantages of Inhalation over Intubation or Liquid Diets. *Behav. Neural Biol.* **1979**, *27*, 466–486.

52. MacLean, R.R.; Valentine, G.W.; Jatlow, P.I.; Sofuoglu, M. Inhalation of Alcohol Vapor: Measurement and Implications. *Alcohol. Clin. Exp. Res.* **2017**, *41*, 238–250.

53. Gilpin, N.W.; Richardson, H.N.; Cole, M.; Koob, G.F. Vapor Inhalation of Alcohol in Rats. *Curr. Protoc. Neurosci.* **2008**, *44*, 9-29.

54. Choi, W.S.; Murthy, G.G.K.; Edwards, D.A.; Langer, R.; Klibanov, A.M. Inhalation Delivery of Proteins from Ethanol Suspensions. *Proc. Natl. Acad. Sci. USA* **2001**, *98*, 11103–11107.

55. Bavis, R.W.; Johnson, R.A.; Ording, K.M.; Otis, J.P.; Mitchell, G.S. Respiratory Plasticity after Perinatal Hypercapnia in Rats. *Respir. Physiol. Neurobiol.* **2006**, *153*, 78–91.

56. Gifford, A.N.; Espaillat, M.P.; Gatley, S.J. Biodistribution of Radiolabeled Ethanol in Rodents. *Drug Metab. Dispos.* **2008**, *36*, 1853–1858.



USC UNIVERSIDADE DE SANTIAGO DE COMPOSTELA

## 7. SUPPLEMENTARY MATERIAL

### Supplementary Material S1. Preliminary Clinical Studies

**Methods**: A group of 6 healthy volunteers (five men and one woman), with an age of 39 ± 16 years (24-63) and a BMI of 22 ± 2 kg/m$^2$, were divided in two groups and subjected to the administration of 15 minutes of oxygen therapy (3 volunteers 2L/min flow and 3 volunteers 3L/min flow through a face mask Ventimask® (Flexicare, Mountain Ash, United Kingdom), using ethanol 65° solution as humectant. Ethanol was vaporized by passing oxygen through the disposable humidifier, which, instead of water, contains the ethanol solution (Figure S1). Safety has been assessed by observing volunteers during the whole process and recording oxygen saturation and heart rate during inhalation time. These measurements were performed using a PM-100 Medisana® (Medisana, Barcelona, Spain) pulse oximeter. Otherwise, systolic and diastolic blood pressure have been recorded at the beginning and end of inhalation. In order to evaluate the ethanol passage to systemic route, a plasma determination was performed at the end of inhalation (Siemens, Flex® ETOH reagent cartridge; Siemens Healthcare Diagnostics, Madrid, Spain). Finally, volunteers were kept under observation during 30 min and were asked about tolerance and subjective perception during and after the monitored period.

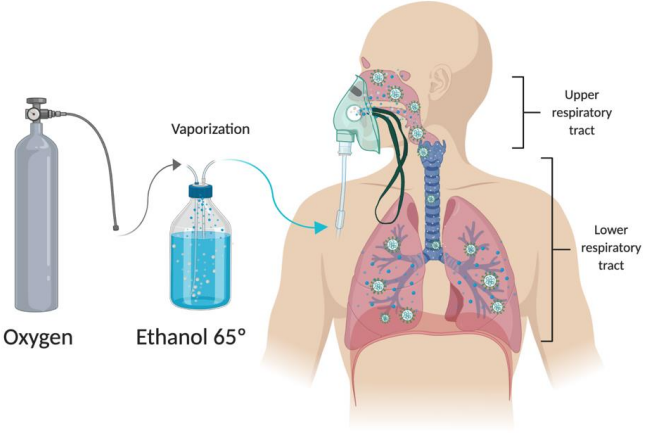



**Figure S1.** Therapeutic approach scheme to the use of inhaled ethanol. Created with BioRender.com.

**Results**: The inhalation of the hydro-alcohol mixture has been safe in both groups with no detected alterations of the physiological parameters. The heart rate was not altered during the inhalation period, with similar behaviors in both groups. On the other hand, the oxygen saturation rises slightly from the beginning of inhalation, something normal for being administering oxygen therapy. Neither systolic nor diastolic pressure undergo significant variations at the beginning and end after 15



USC UNIVERSIDADE DE SANTIAGO DE COMPOSTELA

minutes of inhalation, although a slight decrease is observed, more notable in the case of the group that receives ethanol at a flow of 3 L/min (Figure S2). Finally, no plasmatic concentrations of ethanol have been detected after the inhalation period. During inhalation-time subjects have not shown any psychomotor disturbance or any other effect. The subjective perception of the subjects has been positive in all cases without showing adverse reactions. The good results obtained on clinical safety must be interpreted with caution, since it involves a limited number of patients.

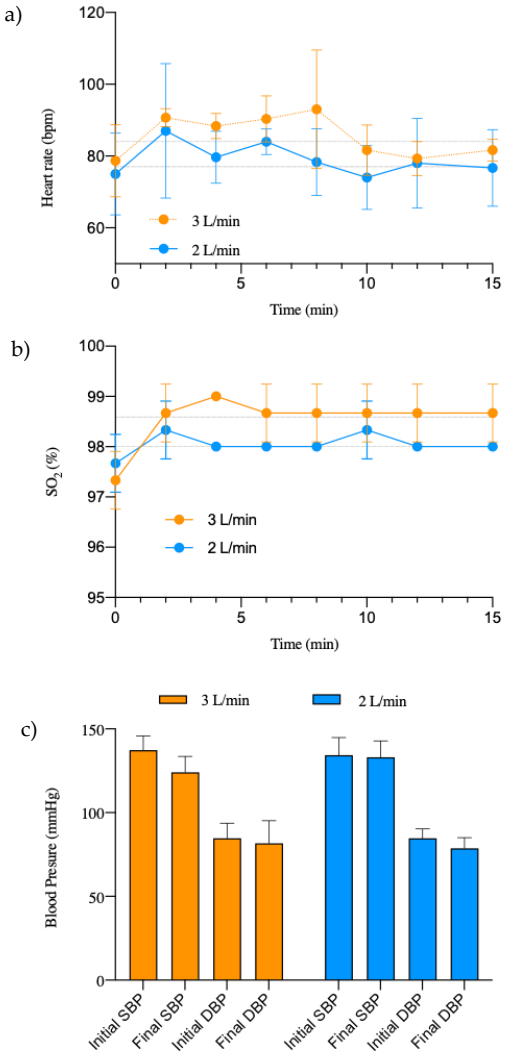



**Figure S2.** Physiological safety parameters monitored during inhalation. (**a**) Heart Rate (**b**) Oxygen Saturation (**c**) Systolic Blood Pressure (SBP) and Diastolic Blood Pressure (DBP) before and after inhalation.



USC UNIVERSIDADE DE SANTIAGO DE COMPOSTELA

# CHAPTER 5

## EFFICACY AND SAFETY OF INHALED ETHANOL IN EARLY-STAGE SARS-CoV-2 INFECTION IN OLDER ADULTS: A PHASE II RANDOMIZED CLINICAL TRIAL

USC
UNIVERSIDADE DE SANTIAGO DE COMPOSTELA

USC
UNIVERSIDADE
DE SANTIAGO
DE COMPOSTELA

# CHAPTER 5

## EFFICACY AND SAFETY OF INHALED ETHANOL IN EARLY-STAGE SARS-CoV-2 INFECTION IN OLDER ADULTS: A PHASE II RANDOMIZED CLINICAL TRIAL


### ABSTRACT

**Background**: Inhaled ethanol in the early stages of SARS-CoV-2 infection may reduce the viral load, decreasing progression and improving prognosis. The ALCOVID-19 trial was designed to study the efficacy and safety of inhaled ethanol in older adults at initial phases of infection.

**Methods**: Randomized, triple-blind, placebo-controlled phase II clinical trial. Experimental group (n = 38) inhaled 65° ethanol through an oxygen flow, while in the control group (n = 37), water for injection was used. General endpoint was to evaluate disease progression according to the modified World Health Organization (WHO) Clinical Progression Scale. Specific effectiveness endpoints were body temperature, oxygen saturation, viral load assessed by cycle threshold (Ct) on real-time polymerase chain reaction (RT-PCR), analytical biomarkers and use of antibiotics or corticosteroids. Specific safety outcomes were the absence of ethanol in plasma, electrographic, analytical, or respiratory alterations.

**Results**: In the intention-to-treat population, no differences were found regarding disease progression. Mean Ct values increased over time in both groups, being numerically higher in the ethanol group, reaching a value above 33 only in the ethanol group on day 14, a value above which patients are considered non-infective. No differences were found in the other specific effectiveness endpoints. Inhaled ethanol was proven to be safe as no plasma ethanol was detected, and there were no electrocardiographic, analytical, or respiratory alterations.

**Conclusions**: The efficacy of inhaled ethanol in terms of the progression of SARS-CoV-2 infection was not demonstrated in the present trial. However, it is positioned as a safe treatment for elderly patients with early-stage COVID-19.



**Keywords:** Inhaled ethanol; elderly; COVID-19; SARS-CoV-2; randomized controlled trial





USC UNIVERSIDADE DE SANTIAGO DE COMPOSTELA

## 1. INTRODUCTION

In the early stages of the COVID-19 pandemic outbreak, rapid spread and high mortality forced the scientific community to research against the clock [1]. Serious efforts were made worldwide to rapidly develop effective vaccines, which have been responsible for the change in the paradigm of the disease [2]. Prior to vaccination, the elderly population was especially susceptible to SARS-CoV-2 infection, in which severity and number of deaths have had a greater impact [3,4]. The percentage of hospitalizations in the first wave was high, and over 95% of total deaths occurred in people older than 60 years, with more than 50% of all deaths being people aged 80 years or older [5,6].

As a consequence of this dramatic situation, clinicians have been forced to resort to alternatives such as compounded formulations and drug repositioning. Numerous studies have been carried out in humans focused on previously approved drugs for the treatment of other pathologies [7,8], including antiviral agents, monoclonal antibodies and inflammation inhibitors/antirheumatic drugs, among others [9]. However, only a small number of drugs have been approved by drug agencies for the treatment of COVID-19.

There is a large amount of evidence demonstrating the antiviral effects of ethanol with a graduation between 62–71° [10,11], possibly due to solvent action on lipids and protein denaturation [12-16]. In early stages of the disease, viral replication occurs in the epithelial layer of the upper respiratory tract [17]. The use of inhaled ethanol could act as an antiseptic in the upper airways against SARS-CoV-2 at initial stages, reducing viral load more rapidly than in the natural course of infection with no systemic adverse effects [15]. Since inhaled ethanol is not commercialized, its preparation as a compounded formulation and galenic characterization was previously carried out by our group [18].

The current phase II clinical trial received the approval from the Spanish Agency of Medicines and Medical Devices to test the efficacy-safety of the 65° ethanol formulation in elderly patients with COVID-19 (ALCOVID-19; EudraCT number: 2020-001760-29) [19].

## 2. MATERIALS AND METHODS

### *2.1. Trial Design*

A randomized, triple-blind, placebo-controlled phase II clinical trial was conducted in a geriatric ward in Spain between 26 October 2020 and 19 March 2021 (when the



USC UNIVERSIDADE DE SANTIAGO DE COMPOSTELA

last patient completed follow-up). The trial was approved by the institutional review boards of the participating institutions and the autonomous region of Galicia (registration number: 2020/218), being supervised by an independent data and safety monitoring board.

### *2.2. Trial Patients*

Starting in September 2020, a geriatric institution was transformed into a low-complexity inpatient unit for mildly ill residents infected with SARS-CoV-2 from other nursing homes. Patients aged 65 years or older who tested positive by real-time polymerase chain reaction (RT-PCR) test for SARS-CoV-2 at the time of screening were identified, and their eligibility was assessed.

Patients had to be in the initial stage of the disease, with <7 days of symptoms, absence of dyspnea and pneumonia, oxygen saturation ($SpO_2$) in room air >93% or partial pressure of oxygen >70 mmHg and respiratory rate <25 per minute. Exclusion criteria included severe respiratory disease, chronic broncho-pneumopathy, or potential diseases that may interfere with inhaled experimental treatment. The complete list of inclusion and exclusion criteria is detailed in Table S1 of the Supplementary Material. All participants agreed to participate by signing the informed consent.

### *2.3. Randomization and Intervention*

The experimental treatment of 65° hydroalcoholic ethanol (ethanol 65% (v/v)) compounded formulation or water for injection (control) were elaborated at 20 °C and packaged in humidifiers in the hospital pharmacy department, under sterile conditions, as described in our previous work [18]. Preparations were assigned to the corresponding batch to maintain the blind and sent to the geriatric ward. Allocation of treatments was carried out randomly in a 1:1 ratio according to their order of inclusion on a master randomization list.

Patients in the experimental group received oxygen at 2 L/min moistened with the 65° ethanol compounded formulation contained in the humidifier (INTL CE0482. Ref. 3230, Oximesa Nippon Gases, Madrid, Spain) connected to a Ventimask® (Flexicare Medical Ltd. Mountain Ash, UK), every 8 h (inhalation time 15 min) for 5 days. In the placebo group, water for injection was used instead. In both groups, recommended treatment according to the protocol of COVID-19 clinical management established by the Spanish Ministry of Health at the beginning of the trial was administered concomitantly.



USC UNIVERSIDADE DE SANTIAGO DE COMPOSTELA

### *2.4 Data Collection*

Study visits were scheduled from the day 1, or baseline visit, when the subject received the study medication or placebo for the first time. The duration of participation was 28 days divided into 8 visits on days 1, 2, 3, 5, 10, 14, 21 and 28. Data were recorded into the web application Research Electronic Data Capture (REDCap) (Vanderbilt University, Nashville, TN, USA), as shown schematically in Figure 1. On day 1, data related to risk factors, symptoms and chronic treatments were collected. Disease progression was assessed according to the modified World Health Organization (WHO) Clinical Progression Scale (Table S2) on days 5, 14 and 28, as well as hospital admissions, and duration of hospitalization. $SpO_2$ was registered on days 1, 5, 10, 14, 21 and 28, while temperature and antipyretic treatment were registered once daily on each day of experimental treatment administration.

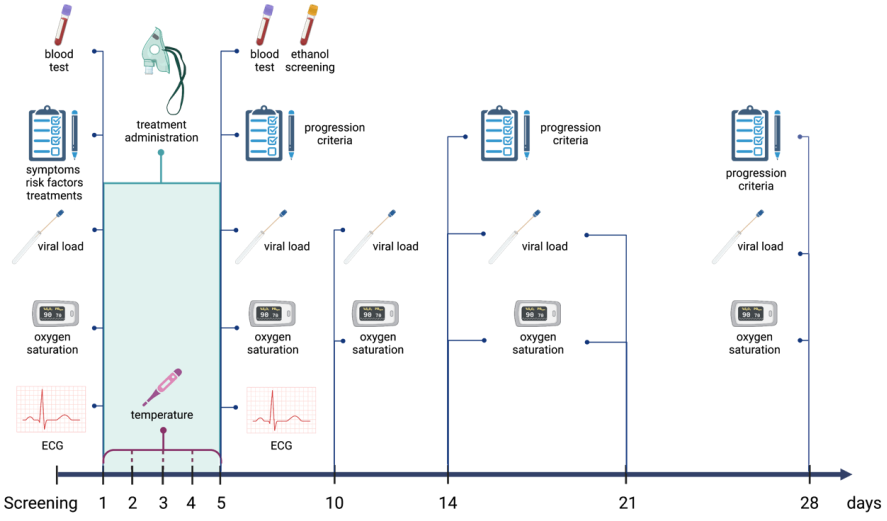



**Figure 1.** Trial design: study visits, collected variables and administration of the study medication. ECG: electrocardiogram. Created with BioRender.com.

Nasopharyngeal samples were taken with a swab and virus transport medium (UTM®, COPAN Diagnostics Inc., Murrieta, CA, USA) on days 1, 5, 10, 14, 21 and 28. RNA extraction (Hamilton STARlet, Reno, NV, USA) and RT-PCR (Allplex 2019 nCoV Assay, Seegene, Republic of Korea) detecting the genes E, RdRP and N were performed. The RT-PCR provides a cycle threshold (Ct) value for each of the genes, a semi-quantitative measure which represents how many PCR cycles are required to detect RNA [20], with higher values corresponding to low viral load and vice versa. The present technique has a specificity of 100% and a limit of detection of 100 RNA copies/PCR reactions [21]. A Ct value of 40 is undetectable and considered the



USC UNIVERSIDADE DE SANTIAGO DE COMPOSTELA

lower limit of detection. For the analysis, the arithmetic means of Ct values between the three genes in each patient were calculated. Ct values of the N gene were also analyzed separately, as this is the most conserved one [22]. A patient who achieves a Ct value above 33 after a previous positive test was considered non-infectious for SARS-CoV-2 [23,24], allowing the isolation to be lifted.

Blood tests were performed at the baseline visit and at the end-of-treatment visit (day 5), including basic biochemical parameters, complete blood count, coagulation study, and inflammation/infection biomarkers. These parameters were classified as indicators of treatment efficacy and/or safety, as shown in Table S3 [25,26]. It should be noted that some of the safety biomarkers have also been described as prognostic indicators of the disease [25,26]. Concomitant treatments were recorded during the study. For the analysis, corticosteroid doses were equated to equivalent doses of prednisone [27]. On the end-of-treatment visit, blood ethanol was determined. An electrocardiogram was performed on days 1 and 5. Occurrence of adverse effects was recorded during the entire study period.

### *2.5 Trial End Points*

#### 2.5.1. General Outcome

The general outcome was to evaluate the progression to stages of greater severity of COVID-19 according to the modified WHO Clinical Progression Scale (Table S2) [28].

#### 2.5.2. Specific Effectiveness Outcomes

One of the prespecified specific outcomes related to treatment efficacy was to evaluate the evolution of hypoxemia using the $SpO_2$ with pulse oximetry. Normalization of body temperature, defined as axillary temperature <37.5 °C without antipyretic treatment, was measured once daily during treatment administration days.

Evolution of viral load was estimated and evaluated indirectly through Ct of the SARS-CoV-2 genes, E, RdRP and N. Biomarkers associated with COVID-19 disease progression were studied to assess the efficacy of the experimental treatment at the baseline visit and at the end-of-treatment visit (day 5) (Table S3). Lastly, the need for antibiotics and corticosteroids were also considered during the entire study period.

#### 2.5.3. Specific Safety Outcomes

Blood ethanol determination was carried out on the last day of treatment to verify the absence of systemic absorption. To ensure cardiovascular safety, an



USC UNIVERSIDADE DE SANTIAGO DE COMPOSTELA

electrocardiogram was performed during baseline and end-of-treatment visit (day 5) and, to assess the systemic safety, liver and renal function were monitored at baseline and end of treatment (Table S3). Information regarding the appearance of any adverse effect was collected during the administration of the experimental treatment, as well as in the subsequent follow-up visits.

### *2.6. Early Trial Termination*

To contain SARS-CoV-2 infections among institutionalized elderly patients when the number of COVID-19 cases was high, a specific center was opened to house all the positives detected in nursing homes for elderly people and avoid hospital overcrowding. However, this center was closed when the number of cases decreased after vaccination, forcing the early termination of the clinical trial.

### *2.7. Statistical Analysis*

Hospitalization rate in COVID-19 patients over 60 years was about 70%. With this intervention, it was considered that it could decrease to 40%. A superiority limit of 10% was set, so that it would be necessary to include 71 patients/group to ensure a power of 80% to draw conclusions with a significance level of 5%. Considering expected losses of 10%, it would be necessary to include 78 patients/arm, 156 in total. Statistical analysis was performed with SAS® 9.4 (SAS Institute Inc., Cary, NC, USA). Normality was studied using the Shapiro–Wilk test. Quantitative variables with normal and non-normal distributions were compared using independent *t*-test and Mann–Whitney test, respectively; variables with normal and abnormal distributions for paired groups were compared using paired *t*-test and a Wilcoxon signed-rank test, respectively. Qualitative variables were compared using Chi-square or Fisher's exact test. Statistically significant values are considered those whose $p$-value is $<0.05$.

## 3. RESULTS

### *3.1. Trial Population*

From 26 October 2020 to 19 March 2021, a total of 76 patients met the eligibility criteria and provided informed consent. One patient became ineligible before enrollment. Therefore, 75 patients with SARS-CoV-2 infection underwent randomization and were included in the intention-to-treat analysis; 38 were assigned to receive inhaled 65° ethanol and 37 inhaled placebo (Figure 2).



USC UNIVERSIDADE DE SANTIAGO DE COMPOSTELA

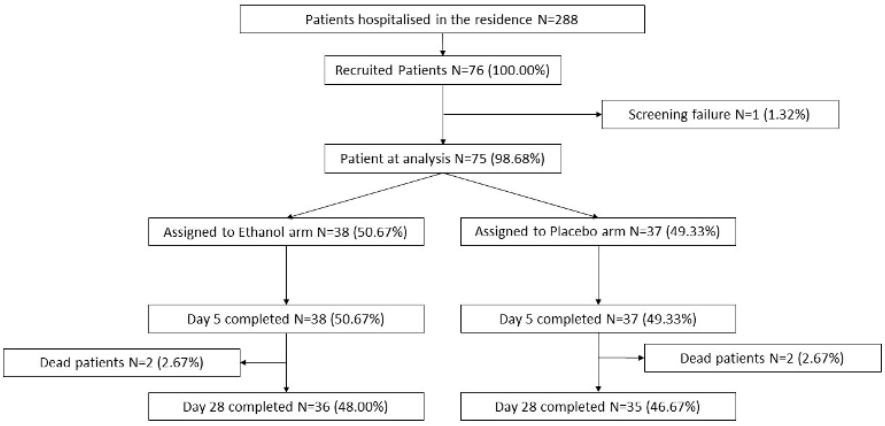



**Figure 2.** Trial flow chart showing patient enrollment, group allocation and deaths.

The median age was 83.0 years (IQR: 77.0–89.0), with 62 patients (82.7%) older than 75 years. A total of 51 patients (68.0%) were women. Baseline demographic characteristics and risk factors are summarized in Table 1. The most prevalent chronic pathology was hypertension (69.3%), followed by diabetes mellitus (26.3%) and cardiovascular disease (24.0%). Only half of the patients included presented symptoms (Table 1), with the most frequent being general discomfort (34.7%) and cough (36.0%).

**Table 1.** Demographic characteristics and risk factors of the intention-to-treat population.

| | **Ethanol (N = 38)** | **Placebo (N = 37)** | **Total (N = 75)** | ***p* Value** |
|---|---|---|---|---|
| Demographic Characteristics | | | | |
| Woman, N (%) | 23 (60.5) | 28 (75.7) | 51 (68.0) | 0.5759 |
| Age, mean (SD) | 82.5 (8.3) | 83.6 (8.2) | 83.0 (8.2) | 0.9834 |
| Advanced age [1], N (%) | 30 (78.9) | 32 (86.5) | 62 (82.7) | 0.5437 |
| Cancer, N (%) | 5 (13.2) | 1 (2.7) | 6 (8.0) | 0.1997 |
| Cardiovascular disease, N (%) | 11 (28.9) | 7 (18.9) | 18 (24.0) | 0.4189 |
| Hypertension, N (%) | 27 (71.1) | 25 (67.6) | 52 (69.3) | 0.8054 |
| Diabetes mellitus, N (%) | 13 (34.2) | 7 (18.9) | 20 (26.7) | 0.1921 |
| Obesity, N (%) | 7 (18.4) | 3 (8.1) | 10 (13.3) | 0.3091 |
| Symptoms | | | | |
| Patients with at least one symptom, N (%) | 20 (52.6) | 17 (45.9) | 37 (49.3) | 0.6466 |
| Fever, N (%) | 4 (10.5) | 3 (8.3) | 7 (9.5) | >0.9999 |
| General discomfort, N (%) | 14 (36.8) | 12 (32.4) | 26 (34.7) | 0.8093 |
| Dyspnea, N (%) | 4 (10.5) | 1 (2.7) | 5 (6.7) | 0.3580 |
| Cough, N (%) | 15 (39.5) | 12 (32.4) | 27 (36.0) | 0.6321 |
| Loss of smell, N (%) | 1 (2.6) | 0 (0.0) | 1 (1.3) | >0.9999 |
| Loss of taste, N (%) | 0 (0.0) | 0 (0.0) | 0 (0.0) | - |
| Diarrhea, N (%) | 1 (2.6) | 0 (0.0) | 1 (1.3) | >0.9999 |
| Abdominal pain, N (%) | 1 (2.6) | 0 (0.0) | 1 (1.3) | >0.9999 |
| Days with symptoms until admission, mean (SD) | 1.7 (1.5) | 1.6 (1.4) | 1.7 (1.5) | 0.8006 |

[1] Advanced age: ≥75 years old.



USC UNIVERSIDADE DE SANTIAGO DE COMPOSTELA

Chronic treatments at the baseline visit, classified by therapeutic groups according to the Anatomical Therapeutic Chemical Classification System (ATC), are shown in Table S4. The most frequent were antithrombotic agents (86.7%) and drugs against peptic ulcer and gastroesophageal reflux (92.0%). Differences between groups were found in antidepressants, prescribed to a greater extent in the placebo group ($p$ = 0.0133), and in drugs used in benign prostatic hypertrophy, with more prescriptions in the ethanol group ($p$ = 0.0253).

### *3.2. General Outcome*

The number of patients per group classified according to the modified WHO Clinical Progression Scale at days 1, 5 (end of treatment), 14, and 28 are shown in Table S5. Most patients were classified in severity stages ranging from ambulatory mild disease to hospitalized with moderate disease. Notably, no patient progressed to the more severe stages of hospitalization requiring high-flow oxygen therapy or mechanical/invasive ventilation techniques in either of the two groups.

Results are shown graphically in Figure 3, where the cumulative percentage of progressions with respect to the previous visit in both treatment groups is represented. Statistical analysis showed no differences in disease progression between groups (Table S6), indicating that progression to more severe stages of the disease occur in a similar way regardless of treatment received.

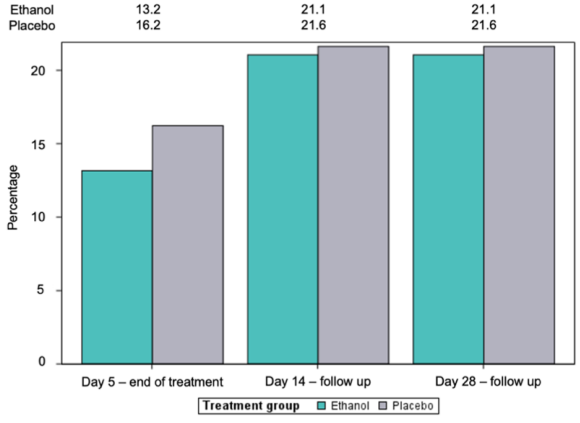



**Figure 3.** Cumulative relative frequency (%) of patients in both treatment groups who progress according to the modified WHO Clinical Progression Scale. Percentages were calculated based on the populations of each group (n = 38 in ethanol group and n = 37 in placebo group).

A total of 7 patients (19.4%) in the ethanol group and 6 (16.7%) in the placebo group required hospital admission. The median time from study inclusion to hospitalization was 6 days (IQR: 3.0–9.0) and 6.5 days (IQR: 4.0–7.0), respectively.



USC UNIVERSIDADE DE SANTIAGO DE COMPOSTELA

The average days of hospitalization were 10.5 (SD: 7.1) in the ethanol group and 8.5 (SD: 8.5) in the placebo group, although this difference was not significant. Two patients died in each group, in the ethanol group before day 14, while in the placebo group they died between days 14 and 28.

### *3.3. Specific Effectiveness Outcomes*

#### 3.3.1. Oxygen Saturation, Temperature, and Antipyretic Treatment Administration

The evolution of $SpO_2$ and the presence of hypoxia are shown in Tables S7 and S8, with median values ranging between 95–96% in both groups. Regarding body temperature, median values did not exceed 37 °C at any study visit (Table S9). The administration of antipyretic treatment is shown in Table S10. No statistically significant differences were found in any of these parameters.

#### 3.3.2. Evolution of Viral Load

Ct mean values of the three genes (N, E and RdRP) per patient was calculated and, subsequently, the mean for each of group at the baseline visit, and days 5, 10 and 14 was obtained (Figure 4). Mean Ct values for both groups were 23.1 at the baseline (SD ethanol: 5.0; SD placebo: 5.2), showing similar viral load. At subsequent visits, Ct values increased as viral load decreased, with ethanol group being nominally higher on days 5 and 14, and lower on day 10, compared to the placebo group, although differences were not statistically significant. The number of RT-PCR tests decreased considerably over the course of the study visits, as patients who had previously tested negative were not retested again. Due to this loss of data, no Ct values are reported for days 21 and 28.

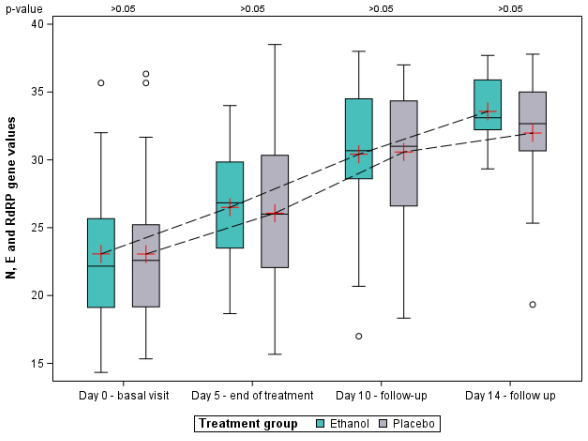



**Figure 4.** Cycle threshold (Ct) values of the three genes (N, E and RdRP) up to visit on day 14. Mean is represented by a red cross, median is represented by the horizontal line contained in the box, and the first and third quartiles by the lower and upper limits of the box, respectively. The mean Ct values at each visit are linked together by a dashed line for each of the groups.



USC UNIVERSIDADE DE SANTIAGO DE COMPOSTELA

Mean Ct values of the three genes on the day-14 visit were 33.6 (95% CI: 31.6–35.6) for the ethanol group and 32.0 (95% CI: 29.5–34.5) for the placebo group. The cut-off point of 33 Ct, which marks non-infectivity for SARS-CoV-2 after a previous positive test, was only exceeded by the ethanol group. Although these differences were not statistically significant, this would have an impact in terms of lifting isolation, facilitating the discharge of patients to their original nursing homes.

Similar behavior was observed with the N gene (Figure 5). In this case, no differences were found between groups at the baseline visit either, while the mean Ct values in the ethanol group were always numerically higher with respect to the placebo group for the study visits on days 5, 10 and 14. At day 14, the mean Ct value of the N gene in the ethanol group was 33 (95% CI: 30.8–35.2), while for the placebo group it was 31.5 (95% CI: 28.9–34.1). Despite this, statistical significance was also not reached for any of the study visits.

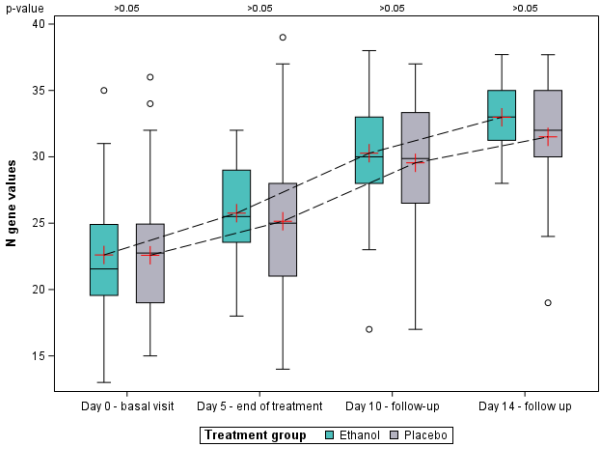



**Figure 5.** Cycle threshold (Ct) values oh the N gene up to visit on day 14. Mean is represented by a red cross, median is represented by the horizontal line contained in the box, and the first and third quartiles by the lower and upper limits of the box, respectively. The mean Ct values at each visit are linked together by a dashed line for each of the groups.

### 3.3.3. Biomarkers Associated with COVID-19 Disease Progression

In terms of efficacy biomarkers, differences were only found in procalcitonin at baseline visit with higher values in the ethanol group (0.0306), while differences were not significant at the end-of-treatment visit (Table S11). Considering percentage of change between visits (Table S12), creatinine kinase was significantly reduced by 36.08% in the ethanol group versus 11.65% in the placebo group ($p$ = 0.0020). Regarding C-reactive protein (CRP), it remained unchanged in the ethanol group, while it was increased in the placebo group by 50% ($p$ = 0.0379). This



USC UNIVERSIDADE DE SANTIAGO DE COMPOSTELA

difference was studied in greater depth, noting that in the ethanol group CRP was reduced in 48.6% of the patients, while in the placebo group it was reduced only in 28.6% of the participants, although the loss of data (n = 35 in both groups) hindered obtaining statistical significance.

3.3.4. Use of Corticosteroids and Antibiotics

Corticosteroids were prescribed in 19 patients in each group (ethanol 50.0%; placebo 51.4%). The median time in days from study inclusion to initiation was 1.0 (IQR: 0.0–0.4) in the ethanol group and 2.0 (IQR: 0.0–0.4) in the placebo group, without statistical differences. Once started, the mean duration of treatment was 19.7 (SD: 13.4) and 15.5 days (SD: 11.6), respectively, also without statistical significance. Equivalent doses of prednisone/day and the total equivalent doses of prednisone are shown in Table S13.

Antibiotics were prescribed in 15 (39.5%) and 9 (24.3%) patients in the ethanol and placebo group, respectively, during the study period. The time from inclusion to the start of treatment was 4.6 (SD: 3.0) days on average in the ethanol group, and 5.2 (SD: 3.5) days in the placebo group. Antimicrobials most frequently prescribed during the study were beta-lactams, 18.6% among the total number of participants. Differences between groups were not statistically significant.

### *3.4. Specific Safety Outcomes*

3.4.1. Determination of Systemic Absorption of Ethanol

Administration of inhaled ethanol was not associated with the presence of ethanol at a systemic level, as all patients tested negative for ethanol in blood.

3.4.2. Electrocardiogram and Ethanol toxicity Biomarkers

None of the subjects presented electrocardiogram abnormalities at baseline or after 5 days of treatment. Moreover, in terms of liver- or renal-function markers, no differences were found between groups at baseline and day 5 visits (Table S11) nor in the variation between visits (Table S12).

3.4.3. Occurrence of Adverse Effects

Neither during the administration of the experimental treatment nor in the subsequent follow-up period were adverse effects observed at the level of the respiratory system.



USC UNIVERSIDADE DE SANTIAGO DE COMPOSTELA

## 4. DISCUSSION

This randomized, triple-blind, placebo-controlled phase II clinical trial sought to assess the efficacy and safety of inhaled 65° ethanol to treat early stages SARS-CoV-2 infection in elderly patients.

In view of the risk of mass infection in nursing homes in the early stages of the pandemic, when a patient tested positive, a screening RT-PCR was performed on the rest of the residents, this was the reason why only half of the patients had symptoms at the beginning of the study. Regarding the general objective, both groups uniformly progress to more severe stages. Moreover, it is worth mentioning that numerous cases of "negative symptoms" were detected in both groups, despite not showing clear symptoms of COVID-19 progression. After more than two years of pandemic, it has already been described how elderly patients can appear "off" with SARS-CoV-2 infection, with symptoms such as fatigue, weakness, lethargy, delirium, loss of appetite, apathy, confusion, agitation or disorientation [29,30]. The modified WHO Clinical Progression Scale used in this clinical trial does not allow the appearance of these symptoms to be associated with clinical deterioration in the elderly population, which is one of the main limitations detected in the present study. When patients showed this negative symptomatology, clinicians proceeded to prescribe corticosteroids, which resulted in clinical improvement. Therefore, those prescriptions could have been used as an indirect measure of the appearance of negative symptoms, but the lack of differences obtained between groups did not allow us to draw conclusive results.

As for viral load, in both groups there was an increase in Ct values as the study progressed related to the decrease in viral load. Considering the three genes together, for most of the study visits Ct values were higher in the ethanol group, although statistical significance was not achieved. This trend was also observed considering only the N gene alone, and seems to suggest that our treatment hypothesis was fulfilled, in which ethanol may be exerting its antiseptic effect in the upper airways [17]. Even so, this reduction in viral load did not translate into a lower incidence of disease progression, as previously discussed. These results should also be interpreted with caution, since the loss of data was greater in the later study visits. However, it is important to note that with a Ct value above 33, the patient is considered not infectious for SARS-CoV-2 [23,31], a value that was only reached in the ethanol group at visit 14, both taking into account the three genes or the N gene alone. This would imply that the ethanol group would reach a non-infectious condition earlier than the placebo group. Patients with a Ct value above this value may receive an early discharge as preventive isolation is lifted to avoid new infections, thus favoring the return of patients to their nursing homes of origin without risk of infecting other residents. If we were to transfer this to the general



USC UNIVERSIDADE DE SANTIAGO DE COMPOSTELA

population, it could have much more relevant implications, associated with public health, sick leaves, reduction in isolation days, as well as cost savings. One of the limitations of the study is that viral viability was not known, as nasopharyngeal samples were not inoculated in cell culture. At the time of the clinical trial, all material and personnel resources were devoted to diagnostics, but viral culture is a very slow and complex process which cannot be used as a tool for clinical practice because it does not allow decision making. Therefore, transmissibility was monitored through Ct measurement by real-time PCR, from which infectivity can be inferred [32], which is the most sensitive method and endorsed by the Spanish Ministry of Health [24].

Regarding temperature, it should be noted that many patients had been treated with paracetamol or non-steroidal anti-inflammatory drugs (NSAIDs) prior to inclusion and during study as analgesics. This should be considered another limiting factor when it comes to detecting an association between fever and the use of antipyretics, since fever might have been masked.

In terms of the safety of the experimental treatment, it is very important to note that no adverse effects were observed during the administration or in the following weeks. Moreover, ethanol was not detected in the blood of patients in the experimental group. This means that it exerts its action at the respiratory-tract level without absorption, which could lead to the appearance of systemic effects or pharmacological interactions. This fact is further confirmed by the absence of electrocardiographic alterations, nor hepatic or renal toxicity at the end of treatment. It is important to bear in mind, as previously mentioned, that progression to more severe stages of infection could also be associated with alterations in these markers [25,26].

Ethanol inhalation has been previously used for acute respiratory distress syndrome and alcohol withdrawal, among others. However, ethyl alcohol had never been used to treat respiratory infections prior to the outbreak of the COVID-19 pandemic. To our knowledge, three other clinical trials with inhaled/nebulized ethanol for the treatment of SARS-CoV-2 have been conducted [33-35]. One of them showed that symptomatology and clinical status improved significantly in the ethanol group [33]. As in our work, differences were found in CRP but not in $SpO_2$. Even so, it should be noted that the study population, scale, and method of administration are not comparable with those used in our trial. In the other trial with published results, ethanol was administered together with dimethyl sulfoxide as an intranasal inhalation spray in volunteer health-care workers. Results showed that the incidence rates of COVID-19 in the control and intervention groups were 0.07 and 0.008, respectively [35]. As previously, important methodological differences make it difficult to establish direct comparisons with our work.



USC UNIVERSIDADE DE SANTIAGO DE COMPOSTELA

In the matter of the limitations of the present study, together with the selection of the progression scale, the most notable one was the small sample size. It is necessary to consider that the clinical trial took place in a center adapted to accommodate elderly patients with mild SARS-CoV-2 infection. After the initiation of vaccination, the number of positives in this population declined considerably in our area, forcing the closure of the center. For this reason, it was not possible to recruit the required number of subjects, a very important barrier to achieving statistical significance.

The present clinical trial demonstrates that the use of inhaled ethanol is safe for the treatment of early-stage SARS-CoV-2 infection in elderly patients. In addition, its non-specific mechanism of action would open the door to the evaluation of its use in other infectious respiratory pathologies. This trial represents an achievement in the field of hospital pharmacy, which has once again demonstrated its capacity for action with the implementation of an independent clinical trial in the early stages of the SARS-CoV-2 pandemic. This was possible thanks to the knowledge of pharmacology, and the mastery of compounding and drug repositioning. Further studies are required to obtain conclusive data and to evaluate the long-term efficacy and safety of inhaled ethanol for SARS-CoV-2 infection.

## 5. REFERENCES

1. Castro-Balado, A.; Varela-Rey, I.; Bandín-Vilar, E.J.; Busto-Iglesias, M.; García-Quintanilla, L.; Mondelo-García, C.; Fernández-Ferreiro, A. Clinical Research in Hospital Pharmacy during the Fight against COVID-19. *Farm. Hosp.* **2020**, *44*, 66–70.

2. Zheng, C.; Shao, W.; Chen, X.; Zhang, B.; Wang, G.; Zhang, W. Real-World Effectiveness of COVID-19 Vaccines: A Literature Review and Meta-Analysis. *Int. J. Infect. Dis.* **2022**, *114*, 252–260.

3. Chen, Y.; Klein, S.L.; Garibaldi, B.T.; Li, H.; Wu, C.; Osevala, N.M.; Li, T.; Margolick, J.B.; Pawelec, G.; Leng, S.X. Aging in COVID-19: Vulnerability, Immunity and Intervention. *Ageing Res. Rev.* **2021**, *65*, 101205.

4. de Labry-Lima, A.O.; Saez-de la Fuente, J.; Martin, L.A.-K.; Alegre-Del Rey, E.J.; García-Cabrera, E.; Sierra-Sánchez, J.F. Factors Associated with Mortality in Patients Hospitalized for COVID-19 in Spain. Data from the RERFAR Registry. *Farm. Hosp.* **2022**, *46*, 57–71.

5. Rothan, H.A.; Byrareddy, S.N. The Epidemiology and Pathogenesis of Coronavirus Disease (COVID-19) Outbreak. *J. Autoimmun.* **2020**, *109*, 102433.



USC UNIVERSIDADE DE SANTIAGO DE COMPOSTELA

6. Li, P.; Chen, L.; Liu, Z.; Pan, J.; Zhou, D.; Wang, H.; Gong, H.; Fu, Z.; Song, Q.; Min, Q.; et al. Clinical Features and Short-Term Outcomes of Elderly Patients with COVID-19. *Int. J. Infect. Dis.* **2020**, *97*, 245–250.

7. Yang, L.; Pei, R.-J.; Li, H.; Ma, X.-N.; Zhou, Y.; Zhu, F.-H.; He, P.-L.; Tang, W.; Zhang, Y.-C.; Xiong, J.; et al. Identification of SARS-CoV-2 Entry Inhibitors among Already Approved Drugs. *Acta Pharmacol. Sin.* **2021**, *42*, 1347–1353.

8. Mølhave, M.; Agergaard, J.; Wejse, C. Clinical Management of COVID-19 Patients—An Update. *Semin. Nucl. Med.* **2022**, *52*, 4–10.

9. Mishra, S.K.; Tripathi, T. One Year Update on the COVID-19 Pandemic: Where Are We Now? *Acta Trop.* **2021**, *214*, 105778.

10. Nomura, T.; Nazmul, T.; Yoshimoto, R.; Higashiura, A.; Oda, K.; Sakaguchi, T. Ethanol Susceptibility of SARS-CoV-2 and Other Enveloped Viruses. *Biocontrol Sci.* **2021**, *26*, 177–180.

11. Lo, C.-M.; Han, J.; Zuo, J.; Law, S.K.; Tang, K.-Y.; Lau, Y.-L.; Fung, Y.-H.; Chung, C.-H.; Leung, W.-T. Real-Time Measurement of Alcohol Vapours Released from Alcohol-Based Hand Disinfectants and User Habits Study of Hong Kong Residents in the Pandemic of COVID-19. *Biointerface Res. Appl. Chem.* **2022**, *13*, 272.

12. Kampf, G. Efficacy of Ethanol against Viruses in Hand Disinfection. *J. Hosp. Infect.* **2018**, *98*, 331–338.

13. Kampf, G.; Todt, D.; Pfaender, S.; Steinmann, E. Persistence of Coronaviruses on Inanimate Surfaces and Their Inactivation with Biocidal Agents. *J. Hosp. Infect.* **2020**, *104*, 246–251.

14. Laboratory Biosafety Guidance Related to Coronavirus Disease (COVID-19). Available online: https://www.who.int/publications-detail-redirect/laboratory-biosafety-guidance-related-to-coronavirus-disease-(COVID-19) (accessed on 21 June 2020).

15. Salvatori, P. The Rationale of Ethanol Inhalation for Disinfection of the Respiratory Tract in SARS-CoV-2-Positive Asymptomatic Subjects. *Pan Afr. Med. J.* **2021**, *40*, 201.

16. Jung, S.; Yeo, D.; Wang, Z.; Woo, S.; Seo, Y.; Hossain, M.I.; Choi, C. Viability of SARS-CoV-2 on Lettuce, Chicken, and Salmon and Its Inactivation by Peracetic Acid, Ethanol, and Chlorine Dioxide. *Food Microbiol.* **2023**, *110*, 104164.



USC UNIVERSIDADE DE SANTIAGO DE COMPOSTELA

17. Polak, S.B.; Van Gool, I.C.; Cohen, D.; von der Thüsen, J.H.; van Paassen, J. A Systematic Review of Pathological Findings in COVID-19: A Pathophysiological Timeline and Possible Mechanisms of Disease Progression. *Mod. Pathol.* **2020**, *33*, 2128-2183.

18. Castro-Balado, A.; Mondelo-García, C.; Barbosa-Pereira, L.; Varela-Rey, I.; Novo-Veleiro, I.; Vázquez-Agra, N.; Antúnez-López, J.R.; Bandín-Vilar, E.J.; Sendón-García, R.; Busto-Iglesias, M.; et al. Development and Characterization of Inhaled Ethanol as a Novel Pharmacological Strategy Currently Evaluated in a Phase II Clinical Trial for Early-Stage SARS-CoV-2 Infection. *Pharmaceutics* **2021**, *13*, 342.

19. European Union Clinical Trials Register. Phase II Clinical Trial to Evaluate the Efficacy and Safety of Inhaled Ethanol in the Treatment of Early-Stage COVID-19. Available online: https://www.clinicaltrialsregister.eu/ctr-search/trial/2020-001760-29/ES (accessed on 19 November 2022).

20. Centers for Disease Control and Prevention (CDC). CDC 2019-Novel Coronavirus (2019-NCoV) Real-Time RT-PCR Diagnostic Panel. Available online: https://www.fda.gov/media/134922/download (accessed on 7 October 2022).

21. Farfour, E.; Lesprit, P.; Visseaux, B.; Pascreau, T.; Jolly, E.; Houhou, N.; Mazaux, L.; Asso-Bonnet, M.; Vasse, M. The Allplex 2019-NCoV (Seegene) Assay: Which Performances Are for SARS-CoV-2 Infection Diagnosis? *Eur. J. Clin. Microbiol. Infect. Dis.* **2020**, *39*, 1997–2000.

22. Pfefferle, S.; Reucher, S.; Nörz, D.; Lütgehetmann, M. Evaluation of a Quantitative RT-PCR Assay for the Detection of the Emerging Coronavirus SARS-CoV-2 Using a High Throughput System. *Euro Surveill.* **2020**, *25*, 2000152.

23. Serrano-Cumplido, A.; Garcia, A.R.; Segura-Fragoso, A.; Olmo-Quintana, V.; Pérez, R.M.M.; Barquilla-García, A.; Morán-Bayón, A. Aplicación del valor umbral del número de ciclos (Ct) de PCR en la COVID-19. *Semergen* **2021**, *47*, 337–341.

24. Estrategia de Detección Precoz, Vigilancia y Control de COVID-19. Ministerio de Sanidad, Gobierno de España. Instituto de Salud Carlos III (ISCIII). Available online: https://www.sanidad.gob.es/profesionales/saludPublica/ccayes/alertasActual/nCov/documentos/COVID19_Estrategia_vigilancia_y_control_e_indicadores.pdf (accessed on 23 November 2022).



USC UNIVERSIDADE DE SANTIAGO DE COMPOSTELA

25. Ponti, G.; Maccaferri, M.; Ruini, C.; Tomasi, A.; Ozben, T. Biomarkers Associated with COVID-19 Disease Progression. *Crit. Rev. Clin. Lab. Sci.* **2020**, *57*, 389–399.

26. Wang, M.; Wu, D.; Liu, C.-H.; Li, Y.; Hu, J.; Wang, W.; Jiang, W.; Zhang, Q.; Huang, Z.; Bai, L.; et al. Predicting Progression to Severe COVID-19 Using the PAINT Score. *BMC Infect. Dis.* **2022**, *22*, 498.

27. Nicolaides, N.C.; Pavlaki, A.N.; Alexandra, M.A.M.; Chrousos, G.P. Glucocorticoid Equivalencies. National Library of Medicine. National Center for Biotechnology Information. Available online: https://www.ncbi.nlm.nih.gov/books/NBK279156/table/adrenal_glucocorticoid-therapy-and-adrenal-suppression.T./ (accessed on 29 October 2022).

28. Marshall, J.C.; Murthy, S.; Diaz, J.; Adhikari, N.K.; Angus, D.C.; Arabi, Y.M.; Baillie, K.; Bauer, M.; Berry, S.; Blackwood, B.; et al. A Minimal Common Outcome Measure Set for COVID-19 Clinical Research. *Lancet Infect. Dis.* **2020**, *20*, e192–e197.

29. Lozano-Montoya, I.; Quezada-Feijoo, M.; Jaramillo-Hidalgo, J.; Gómez-Pavón, F.J. Atypical symptoms of COVID-19 in hospitalised oldest old adults. *Rev. Esp. Geriatr. Gerontol.* **2021**, *56*, 120–121.

30. Meis-Pinheiro, U.; Lopez-Segui, F.; Walsh, S.; Ussi, A.; Santaeugenia, S.; Garcia-Navarro, J.A.; San-Jose, A.; Andreu, A.L.; Campins, M.; Almirante, B. Clinical Characteristics of COVID-19 in Older Adults. A Retrospective Study in Long-Term Nursing Homes in Catalonia. *PLoS ONE* **2021**, *16*, e0255141.

31. La Scola, B.; Le Bideau, M.; Andreani, J.; Hoang, V.T.; Grimaldier, C.; Colson, P.; Gautret, P.; Raoult, D. Viral RNA Load as Determined by Cell Culture as a Management Tool for Discharge of SARS-CoV-2 Patients from Infectious Disease Wards. *Eur. J. Clin. Microbiol. Infect. Dis.* **2020**, *39*, 1059–1061.

32. Berengua, C.; López, M.; Esteban, M.; Marín, P.; Ramos, P.; del Cuerpo, M.; Gich, I.; Navarro, F.; Miró, E.; Rabella, N. Viral Culture and Immunofluorescence for the Detection of SARS-CoV-2 Infectivity in RT-PCR Positive Respiratory Samples. *J. Clin. Virol.* **2022**, *152*, 105167.

33. Amoushahi, A.; Moazam, E.; Tabatabaei, A.R.; Ghasimi, G.; Grant-Whyte, I.; Salvatori, P.; Ezz, A.R. Efficacy and Safety of Inhalation of Nebulized Ethanol in COVID-19 Treatment: A Randomized Clinical Trial. *Cureus* **2022**, *14*, e32218.



USC UNIVERSIDADE DE SANTIAGO DE COMPOSTELA

34. Ezz, A.R.; Amoushahi, A.; Rashad, A. Disinfection of SARS-CoV-2 (COVID-19) in Human Respiratory Tract by Controlled Ethanol Vapor Inhalation Combined with Oral Asprin. *J. Vaccines Vaccin.* **2020**, *12*, 1000454.

35. Hosseinzadeh, A.; Tavakolian, A.; Kia, V.; Ebrahimi, H.; Sheibani, H.; Binesh, E.; Rahmati, M.; Yarmohammadi, M.; Aghayan, N.; Mirrezaie, S.M.; et al. Combined Application of Dimethyl Sulfoxide and Ethanol Nasal Spray during COVID-19 Pandemic May Protect Healthcare Workers: A Randomized Controlled Trial. *Iran. Red Crescent Med. J.* **2022**, *24*.



USC UNIVERSIDADE DE SANTIAGO DE COMPOSTELA

## 6. SUPPLEMENTARY MATERIAL

**Table S1.** Inclusion and exclusion criteria for of participants in the clinical trial.

| **Inclusion criteria** |
|---|
| Institutionalized men or women aged 65 or older at the time of signing the informed consent. |
| Patients able to understand the trial procedures and agree to participate. |
| Diagnosis of COVID-19 confirmed by RT-PCR. |
| Initial stage of the disease diagnosed by:<br>- Less than 7 days from the appearance of the first symptoms.<br>- Absence of dyspnea<br>- Absence of pneumonia<br>- Oxygen saturation >93% or $pO_2$ >70 mmHg<br>- Respiratory rate <25 $min^{-1}$ |
| Signature and date of the informed consent before any activity related to the study, including the evaluations necessary for the selection. |
| **Exclusion criteria** |
| Impaired renal function (creatinine > 2.5 times the normal limit), need for haemofiltration or impaired liver function (ALT or AST > 3 times the normal limits) or diagnosis of severe renal failure. |
| Hypersensitivity, allergy, or contraindications to study treatments. |
| Inability to administer oxygen therapy using Ventimask®. |
| Diagnosis of any other pathology that, in the investigator's opinion, may increase the risk of the subject or reduce the possibilities of obtaining satisfactory data to achieve the objectives of the study. |
| Consumption of any other drug that could incapacitate you, in the opinion of the investigator, to participate in the study. |
| Other circumstances or difficulties that, in the opinion of the investigator, may increase the risk of the subject or reduce the possibilities of obtaining satisfactory data to achieve the objectives of the study. |
| Participation in another clinical study where they have received an investigational drug in the 24 weeks prior to signing the informed consent. |
| Patients diagnosed with chronic broncho-pneumopathy. |
| Patients with a history of epilepsy. |
| Patients with a history of alcoholism. |
| Treatment with anticonvulsant drugs used to treat epilepsy and that have a higher degree of interaction with ethanol: topiramate, carbamazepine, perampanel and stiripentol |
| Treatment with drugs that, administered concomitantly with ethanol, can cause the so-called "disulfiram-like effect": disulfiram, metronidazole, tinidazole, chloramphenicol, levamisole, nitrofurantoin, isoniazid and griseofulvin. |

RT-PCR: reverse-transcriptase polymerase chain reaction; pO2: oxygen partial pressure; ALT: alanine aminotransferase; AST: aspartate aminotransferase.



USC UNIVERSIDADE DE SANTIAGO DE COMPOSTELA

**Table S2.** Modified WHO Clinical Progression Scale.

| Patient State | Descriptor |
|---|---|
| **Uninfected** | Uninfected, no clinical or virologic signs of infection |
| **Ambulatory mild disease** | Outpatient, without limitation of activities |
| | Outpatient, without limitation of activities |
| **Hospitalized: moderate disease** | Hospitalized, without oxygen therapy |
| | Hospitalized with oxygen therapy by mask or nasal prongs |
| **Hospitalized: severe diseases** | Hospitalized with non-invasive mechanical ventilation or high-flow oxygen therapy |
| | Hospitalized with invasive mechanical ventilation |
| | Hospitalized with mechanical ventilation + ECMO [1] + organic support |
| **Dead** | Dead |

[1] ECMO: extracorporeal membrane oxygenation.

**Table S3.** Classification of blood biomarkers as indicators of efficacy and/or safety.

| | Efficacy | Safety |
|---|---|---|
| **Basic biochemistry** | alanine aminotransferase (ALT), aspartate aminotransferase (AST), alkaline phosphatase (AP), gamma glutamyl transferase (GGT), bilirubin, albumin, creatinine, and urea | liver safety: alanine aminotransferase (ALT), aspartate aminotransferase (AST), alkaline phosphatase (AP), gamma glutamyl transferase (GGT), bilirubin and albumin renal safety: creatinine, and urea |
| **Complete blood count** | hemoglobin, platelets, leucocytes, lymphocytes | |
| | neutrophils, monocytes, basophils, eosinophils | |
| **Coagulation parameters** | prothrombin time (PT), activated partial thromboplastin time (aPTT), d-dimer, fibrinogen | |
| **Inflammatory parameters** | C-reactive protein (CRP), procalcitonin (PCT), creatine kinase (CK), lactate dehydrogenase (LHD), troponin-I (TnI) and interleukin-6 (IL-6) | |



USC UNIVERSIDADE DE SANTIAGO DE COMPOSTELA

**Table S4.** Chronic treatments grouped by therapeutic groups according to the Anatomical Therapeutic Chemical (ATC) Classification System at the beginning of the study in the intention-to-treat population. Fisher's exact test.

| Therapeutic group | Ethanol (N=38) | Placebo (N=37) | Overall (N=75) | p-value |
|---|---|---|---|---|
| | N (%) | N (%) | N (%) | |
| **Additives for IV solutions** | 1 (2.6%) | 0 (0.0%) | 1 (1.3%) | >0.9999 |
| **Adrenergic drugs for systemic use** | 1 (2.6%) | 0 (0.0%) | 1 (1.3%) | >0.9999 |
| **Inhaled Adrenergic agents** | 4 (10.5%) | 1 (2.7%) | 5 (6.7%) | 0.3580 |
| **Potassium sparing agents** | 4 (10.5%) | 1 (2.7%) | 5 (6.7%) | 0.3580 |
| **Anticholinergic agents** | 2 (5.3%) | 1 (2.7%) | 3 (4.0%) | >0.9999 |
| **Anti-inflammatory agents** | 0 (0.0%) | 1 (2.7%) | 1 (1.3%) | 0.4933 |
| **Antiparathyroid agents** | 1 (2.6%) | 0 (0.0%) | 1 (1.3%) | >0.9999 |
| **Antithrombotic agents** | 34 (89.5%) | 31 (83.8%) | 65 (86.7%) | 0.5161 |
| **Beta-blocking agents** | 10 (26.3%) | 6 (16.2%) | 16 (21.3%) | 0.2858 |
| **Agents against peptic ulcer and gastroesophageal reflux (GER/GORD)** | 35 (92.1%) | 34 (91.9%) | 69 (92.0%) | >0.9999 |
| **Agents against functional disorders of the stomach** | 1 (2.6%) | 0 (0.0%) | 1 (1.3%) | >0.9999 |
| **Dopaminergic agents** | 1 (2.6%) | 0 (0.0%) | 1 (1.3%) | >0.9999 |
| **Lipid-modifying agents** | 16 (42.1%) | 8 (21.6%) | 24 (32.0%) | 0.0573 |
| **Anxiolytics** | 12 (31.6%) | 10 (27.0%) | 22 (29.3%) | 0.6651 |
| **Hormone antagonists and related agents** | 0 (0.0%) | 1 (2.7%) | 1 (1.3%) | 0.4933 |
| **Angiotensin II receptor antagonists** | 14 (36.8%) | 12 (32.4%) | 26 (34.7%) | 0.6883 |
| **Antiandrogens** | 1 (2.6%) | 0 (0.0%) | 1 (1.3%) | >0.9999 |
| **Class I and III antiarrhythmics** | 0 (0.0%) | 1 (2.7%) | 1 (1.3%) | 0.4933 |
| **Beta-lactam antibiotics, penicillins** | 0 (0.0%) | 2 (5.4%) | 2 (2.7%) | 0.2400 |
| **Antidepressants** | 9 (23.7%) | 19 (51.4%) | 28 (37.3%) | 0.0133 |
| **Antiepileptics** | 5 (13.2%) | 9 (24.3%) | 14 (18.7%) | 0.2147 |
| **Antifungals for topical use** | 0 (0.0%) | 1 (2.7%) | 1 (1.3%) | 0.4933 |
| **Antipsychotics** | 11 (28.9%) | 13 (35.1%) | 24 (32.0%) | 0.5657 |
| **Direct-acting antivirals** | 0 (0.0%) | 1 (2.7%) | 1 (1.3%) | 0.4933 |
| **Belladonna and derivatives** | 0 (0.0%) | 1 (2.7%) | 1 (1.3%) | 0.4933 |
| **Selective calcium channel blockers with direct cardiac effects** | 0 (0.0%) | 1 (2.7%) | 1 (1.3%) | 0.4933 |
| **Selective calcium channel blockers with mainly vascular effects** | 7 (18.4%) | 10 (27.0%) | 17 (22.7%) | 0.3735 |
| **Corticosteroids for systemic use** | 16 (42.1%) | 15 (40.5%) | 31 (41.3%) | 0.8906 |
| **High ceiling diuretics** | 12 (31.6%) | 9 (24.3%) | 21 (28.0%) | 0.4842 |
| **Low ceiling diuretics** | 2 (5.3%) | 3 (8.1%) | 5 (6.7%) | 0.6745 |
| **Dopa and dopa derivatives** | 1 (2.6%) | 0 (0.0%) | 1 (1.3%) | >0.9999 |
| **Expectorants, excluding combinations with cough suppressants** | 1 (2.6%) | 0 (0.0%) | 1 (1.3%) | >0.9999 |
| **Anti-dementia drugs** | 0 (0.0%) | 4 (10.8%) | 4 (5.3%) | 0.0543 |
| **Hypoglycemic drugs excluding insulins** | 9 (23.7%) | 5 (13.5%) | 14 (18.7%) | 0.2584 |
| **Drugs for constipation** | 9 (23.7%) | 3 (8.1%) | 12 (16.0%) | 0.0658 |

USC UNIVERSIDADE DE SANTIAGO DE COMPOSTELA

| Therapeutic group | Ethanol (N=38) | Placebo (N=37) | Overall (N=75) | p-value |
|---|---|---|---|---|
| **Drugs used in benign prostatic hypertrophy** | 6 (15.8%) | 0 (0.0%) | 6 (8.0%) | 0.0253 |
| **Cardiac glycosides** | 2 (5.3%) | 4 (10.8%) | 6 (8.0%) | 0.4303 |
| **Hypnotics and sedatives** | 10 (26.3%) | 9 (24.3%) | 19 (25.3%) | 0.8428 |
| **ACE inhibitors** | 7 (18.4%) | 9 (24.3%) | 16 (21.3%) | 0.5327 |
| **Insulins and analogues** | 5 (13.2%) | 3 (8.1%) | 8 (10.7%) | 0.7110 |
| **Macrolides, lincosamides and streptogramins** | 4 (10.5%) | 3 (8.1%) | 7 (9.3%) | >0.9999 |
| **mydriatics and cycloplegics** | 0 (0.0%) | 1 (2.7%) | 1 (1.3%) | 0.4933 |
| **Nutritional modules** | 1 (2.6%) | 0 (0.0%) | 1 (1.3%) | >0.9999 |
| **Opioids** | 4 (10.5%) | 5 (13.5%) | 9 (12.0%) | 0.7361 |
| **Other inhaled agents for obstructive airway conditions** | 8 (21.1%) | 6 (16.2%) | 14 (18.7%) | 0.5910 |
| **Other diagnostic agents** | 0 (0.0%) | 3 (8.1%) | 3 (4.0%) | 0.1151 |
| **Other analgesics and antipyretics** | 7 (18.4%) | 7 (18.9%) | 14 (18.7%) | 0.9559 |
| **Beta-lactam antibacterials** | 8 (21.1%) | 4 (10.8%) | 12 (16.0%) | 0.2264 |
| **Other ophthalmological** | 1 (2.6%) | 1 (2.7%) | 2 (2.7%) | >0.9999 |
| **Other agents for the heart** | 1 (2.6%) | 0 (0.0%) | 1 (1.3%) | >0.9999 |
| **Other products for urological use, including antispasmodics** | 1 (2.6%) | 1 (2.7%) | 2 (2.7%) | >0.9999 |
| **Other mineral supplements** | 1 (2.6%) | 0 (0.0%) | 1 (1.3%) | >0.9999 |
| **Anti-gout agents** | 2 (5.3%) | 3 (8.1%) | 5 (6.7%) | 0.6745 |
| **Antithyroid agents** | 0 (0.0%) | 1 (2.7%) | 1 (1.3%) | 0.4933 |
| **Preparations with iron** | 8 (21.1%) | 4 (10.8%) | 12 (16.0%) | 0.2264 |
| **Anti-glaucoma and miotic agents** | 4 (10.5%) | 3 (8.1%) | 7 (9.3%) | >0.9999 |
| **Agents against vertigo** | 0 (0.0%) | 4 (10.8%) | 4 (5.3%) | 0.0543 |
| **Thyroid hormone agents** | 5 (13.2%) | 1 (2.7%) | 6 (8.0%) | 0.1997 |
| **Nonsteroidal anti-inflammatory and antirheumatic products** | 0 (0.0%) | 1 (2.7%) | 1 (1.3%) | 0.4933 |
| **Propellants** | 1 (2.6%) | 2 (5.4%) | 3 (4.0%) | 0.6148 |
| **Psychostimulants, agents used for ADHD, and nootropics** | 1 (2.6%) | 1 (2.7%) | 2 (2.7%) | >0.9999 |
| **Antibacterial quinolones** | 2 (5.3%) | 3 (8.1%) | 5 (6.7%) | 0.6745 |
| **IV Solutions** | 1 (2.6%) | 0 (0.0%) | 1 (1.3%) | >0.9999 |
| **Mineral supplements** | 4 (10.5%) | 3 (8.1%) | 7 (9.3%) | >0.9999 |
| **Cough suppressants, excluding combinations with expectorants** | 3 (7.9%) | 3 (8.1%) | 6 (8.0%) | >0.9999 |
| **Peripheral vasodilators** | 3 (7.9%) | 1 (2.7%) | 4 (5.3%) | 0.6148 |
| **Vasodilators used in heart disease** | 2 (5.3%) | 1 (2.7%) | 3 (4.0%) | >0.9999 |
| **Vitamin B1, alone and in combination with vitamins B6 and B12** | 1 (2.6%) | 0 (0.0%) | 1 (1.3%) | >0.9999 |
| **Vitamin B12 and folic acid** | 1 (2.6%) | 2 (5.4%) | 3 (4.0%) | 0.6148 |

ACE: Angiotensin-converting enzyme; ADHD: Attention deficit hyperactivity disorder; IV: intravenous; GER: gastroesophageal reflux; GORD: Gastro-oesophageal reflux disease



USC UNIVERSIDADE DE SANTIAGO DE COMPOSTELA

**Table S5.** Classification of patients per visit according to the modified WHO Clinical Progression Scale.

| | Ethanol (N=38) | | Placebo (N=37) | | Total (N=75) | |
|---|---|---|---|---|---|---|
| **Modified WHO Clinical Progression Scale** | **N** | **%** | **N** | **%** | **N** | **%** |
| **Baseline** | | | | | | |
| **Not infected, no clinical or virological signs of infection.** | 0 | 0.0 | 0 | 0.0 | 0 | 0.0 |
| **Ambulatory, without limitation of activities** | 32 | 84.2 | 32 | 86.5 | 64 | 85.3 |
| **Ambulatory with activity limitation** | 6 | 15.8 | 5 | 13.5 | 11 | 14.7 |
| **Hospitalized, without oxygen therapy** | 0 | 0.0 | 0 | 0.0 | 0 | 0.0 |
| **Hospitalized with oxygen therapy by mask or nasal goggles** | 0 | 0.0 | 0 | 0.0 | 0 | 0.0 |
| **Hospitalized with noninvasive mechanical ventilation or high-flow oxygen therapy** | 0 | 0.0 | 0 | 0.0 | 0 | 0.0 |
| **Hospitalized with invasive mechanical ventilation** | 0 | 0.0 | 0 | 0.0 | 0 | 0.0 |
| **Hospitalized with mechanical ventilation + ECMO + organ support** | 0 | 0.0 | 0 | 0.0 | 0 | 0.0 |
| **Death** | 0 | 0.0 | 0 | 0.0 | 0 | 0.0 |
| **Day 5** | | | | | | |
| **Not infected, no clinical or virological signs of infection.** | 0 | 0.0 | 0 | 0.0 | 0 | 0.0 |
| **Ambulatory, without limitation of activities** | 32 | 84.2 | 29 | 78.4 | 61 | 81.3 |
| **Ambulatory with activity limitation** | 1 | 2.6 | 3 | 8.1 | 4 | 5.3 |
| **Hospitalized, without oxygen therapy** | 0 | 0.0 | 1 | 2.7 | 1 | 1.3 |
| **Hospitalized with oxygen therapy by mask or nasal goggles** | 5 | 13.2 | 4 | 10.8 | 9 | 12.0 |
| **Hospitalized with noninvasive mechanical ventilation or high-flow oxygen therapy** | 0 | 0.0 | 0 | 0.0 | 0 | 0.0 |
| **Hospitalized with invasive mechanical ventilation** | 0 | 0.0 | 0 | 0.0 | 0 | 0.0 |
| **Hospitalized with mechanical ventilation + ECMO + organ support** | 0 | 0.0 | 0 | 0.0 | 0 | 0.0 |
| **Death** | 0 | 0.0 | 0 | 0.0 | 0 | 0.0 |
| **Day 14** | | | | | | |
| **Not infected, no clinical or virological signs of infection.** | 12 | 31.6 | 15 | 40.5 | 27 | 36.0 |
| **Ambulatory, without limitation of activities** | 18 | 47.4 | 15 | 40.5 | 33 | 44.0 |
| **Ambulatory with activity limitation** | 0 | 0.0 | 3 | 8.1 | 3 | 4.0 |
| **Hospitalized, without oxygen therapy** | 3 | 7.9 | 0 | 0.0 | 3 | 4.0 |
| **Hospitalized with oxygen therapy by mask or nasal goggles** | 2 | 5.3 | 4 | 10.8 | 6 | 8.0 |
| **Hospitalized with noninvasive mechanical ventilation or high-flow oxygen therapy** | 1 | 2.6 | 0 | 0.0 | 1 | 1.3 |
| **Hospitalized with invasive mechanical ventilation** | 0 | 0.0 | 0 | 0.0 | 0 | 0.0 |
| **Hospitalized with mechanical ventilation + ECMO + organ support** | 0 | 0.0 | 0 | 0.0 | 0 | 0.0 |
| **Death** | 2 | 5.3 | 0 | 0.0 | 2 | 2.7 |



USC UNIVERSIDADE DE SANTIAGO DE COMPOSTELA

| | Ethanol (N=38) | | Placebo (N=37) | | Total (N=75) | |
|---|---|---|---|---|---|---|
| **Modified WHO Clinical Progression Scale** | **N** | **%** | **N** | **%** | **N** | **%** |
| **Day 28** | | | | | | |
| **Not infected, no clinical or virological signs of infection.** | 35 | 94.6 | 31 | 83.8 | 66 | 89.2 |
| **Ambulatory, without limitation of activities** | 0 | 0.0 | 3 | 8.1 | 3 | 4.1 |
| **Ambulatory with activity limitation** | 0 | 0.0 | 0 | 0.0 | 0 | 0.0 |
| **Hospitalized, without oxygen therapy** | 0 | 0.0 | 0 | 0.0 | 0 | 0.0 |
| **Hospitalized with oxygen therapy by mask or nasal goggles** | 1 | 2.7 | 1 | 2.7 | 2 | 2.7 |
| **Hospitalized with noninvasive mechanical ventilation or high-flow oxygen therapy** | 0 | 0.0 | 0 | 0.0 | 0 | 0.0 |
| **Hospitalized with invasive mechanical ventilation** | 0 | 0.0 | 0 | 0.0 | 0 | 0.0 |
| **Hospitalized with mechanical ventilation + ECMO + organ support** | 0 | 0.0 | 0 | 0.0 | 0 | 0.0 |
| **Death** | 2 | 5.3 | 2 | 5.4 | 4 | 5.3 |

[1] ECMO: extracorporeal membrane oxygenation.

**Table S6.** Number of patients who progressed and/or died per visit with respect to the previous visit. Fisher's exact test.

| Visit | Ethanol (N=38) | Placebo (N=37) | p |
|---|---|---|---|
| **Day 5, N (%)** | 5 (13.2) | 6 (16.2) | 0.7543 |
| **Day 14, N (%)** | 8 (21.1) | 8 (21.6) | >0.9999 |
| **Day 28, N (%)** | 8 (21.1) | 8 (21.6) | >0.9999 |

**Table S7.** Oxygen saturation (%) throughout the study in the intention-to-treat population. U Mann–Whitney test.

| Visit | Group | Median | IQR | Range | p |
|---|---|---|---|---|---|
| **Baseline** | **Ethanol (N=38)** | 95.0 | 95.0-96.0 | 91.0-97.0 | 0.4482 |
| | **Placebo (N=37)** | 96.0 | 95.0-96.0 | 91.0-98.0 | |
| **Day 5** | **Ethanol (N=38)** | 95.5 | 95.0-96.0 | 86.0-96.0 | 0.7318 |
| | **Placebo (N=37)** | 96.0 | 95.0-96.0 | 85.0-98.0 | |
| **Day 10** | **Ethanol (N=37)** | 96.0 | 95.0-96.0 | 90.0-96.0 | 0.5433 |
| | **Placebo (N=37)** | 95.0 | 95.0-96.0 | 88.0-97.0 | |
| **Day 14** | **Ethanol (N=37)** | 96.0 | 95.0-96.0 | 88.0-98.0 | 0.4300 |
| | **Placebo (N=37)** | 95.0 | 95.0-96.0 | 85.0-97.0 | |
| **Day 21** | **Ethanol (N=36)** | 96.0 | 95.0-96.0 | 92.0-97.0 | 0.4182 |
| | **Placebo (N=35)** | 96.0 | 95.0-96.0 | 91.0-97.0 | |
| **Day 28** | **Ethanol (N=36)** | 96.0 | 95.0-96.0 | 93.0-97.0 | 0.8489 |
| | **Placebo (N=35)** | 96.0 | 95.0-96.0 | 89.0-96.0 | |



USC UNIVERSIDADE DE SANTIAGO DE COMPOSTELA

**Table S8.** Patients who presented hypoxia (defined as oxygen saturation <91%) throughout the study according to each visit in the intention-to-treat population. Fisher's test.

| Visit | Ethanol (N=38) | Placebo (N=37) | p |
|---|---|---|---|
| **Basal, N (%)** | 0 (0) | 0 (0) | - |
| **Day 5, N (%)** | 2 (5.3) | 2 (5.4) | >0.9999 |
| **Day 10, N (%)** | 2 (5.4) | 1 (2.7) | >0.9999 |
| **Day 14, N (%)** | 1 (2.7) | 3 (8.1) | 0.6145 |
| **Day 21, N (%)** | 0 (0) | 0 (0) | - |
| **Day 28, N (%)** | 0 (0) | 1 (2.9) | 0.4930 |

**Table S9.** Temperature (°C) throughout the study in the intention-to-treat population. U Mann–Whitney test.

| Visit | Group | Median | IQR | Range | p |
|---|---|---|---|---|---|
| **Baseline** | **Ethanol (N=38)** | 36.2 | 36.1-36.4 | 35.7-37.6 | 0.2894 |
| | **Placebo (N=37)** | 36.3 | 36.2-36.5 | 35.7-38.0 | |
| **Day 2** | **Ethanol (N=38)** | 36.2 | 36.0-36.3 | 35.0-38.0 | 0.1125 |
| | **Placebo (N=36)** | 36.2 | 36.1-36.4 | 35.6-38.0 | |
| **Day 3** | **Ethanol (N=38)** | 36.2 | 36.0-36.3 | 35.7-38.5 | 0.6251 |
| | **Placebo (N=35)** | 36.2 | 36.0-36.3 | 35.7-37.0 | |
| **Day 5** | **Ethanol (N=38)** | 36.2 | 36.0-36.4 | 35.5-38.1 | 0.5482 |
| | **Placebo (N=37)** | 36.2 | 36.0-36.3 | 35.7-38.0 | |

**Table S10.** Administration of antipyretics in the different study visits in the intention-to-treat population. Fisher's test.

| Visit | Ethanol (N=38) | Placebo (N=37) | p |
|---|---|---|---|
| **Baseline, N (%)** | 7 (18.4) | 4 (10.8) | 0.5161 |
| **Day 2, N (%)** | 5 (13.2) | 5 (13.5) | >0.9999 |
| **Day 3, N (%)** | 4 (10.5) | 5 (13.5) | 0.7361 |
| **Day 5, N (%)** | 6 (15.8) | 6 (16.2) | >0.9999 |

**Table S11.** Analytical parameters collected at the baseline study visit and at the end-of-treatment visit (day 5) expressed as median and interquartile ranges. U Mann–Whitney test.

| Parameter | Visit | Ethanol | Placebo | p |
|---|---|---|---|---|
| **Basic biochemistry** | | | | |
| **Glucose (mg/dL)** | **Baseline** | 90.5 (80.0-112.0) | 88.0 (79.5-107.0) | 0.7653 |
| | **Day 5** | 96.0 (79.0-111.0) | 85.5 (76.0-97.5) | 0.1815 |
| **Urea (mg/dl)** | **Baseline** | 54.5 (38.5-80.0) | 41.0 (39.0-61.5) | 0.1572 |
| | **Day 5** | 59.0 (43.0-82.0) | 48.5 (35.5-73.0) | 0.1564 |
| **Creatinine (mg/dl)** | **Baseline** | 1.0 (0.7-1.1) | 0.8 (0.7-1.0) | 0.2437 |
| | **Day 5** | 0.9 (0.7-1.1) | 0.8 (0.7-0.8) | 0.1676 |
| **Bilirubin (mg/dl)** | **Baseline** | 0.5 (0.3-0.6) | 0.5 (0.4-0.6) | 0.8731 |
| | **Day 5** | 0.4 (0.4-0.6) | 0.4 (0.3-0.6) | 0.9034 |



USC UNIVERSIDADE DE SANTIAGO DE COMPOSTELA

| Parameter | Visit | Ethanol | Placebo | p |
|---|---|---|---|---|
| **AST (GOT) (U/l)** | **Baseline** | 23.0 (18.5-30.5) | 23.0 (20.0-29.0) | 0.6742 |
| | **Day 5** | 24.0 (21.0-29.0) | 29.5 (20.0-47.0) | 0.1380 |
| **ALT (GPT) (U/l)** | **Baseline** | 20.5 (13.5-30.0) | 18.0 (14.0-30.0) | 0.8790 |
| | **Day 5** | 24.0 (17.0-31.0) | 30.0 (17.0-53.5) | 0.3573 |
| **Gamma GT (GGT) (U/l)** | **Baseline** | 22.5 (14.0-38.0) | 25.0 (16.0-44.5) | 0.4777 |
| | **Day 5** | 27.5 (14.0-41.0) | 27.5 (18.0-69.0) | 0.4392 |
| **Albumin (g/dl)** | **Baseline** | 3.8 (3.6-4.0) | 3.9 (3.6-4.0) | 0.2869 |
| | **Day 5** | 3.8 (3.6-4.0) | 3.8 (3.5-3.9) | 0.6554 |
| **Calcium (mEq/l)** | **Baseline** | 8.8 (8.4-9.0) | 8.7 (8.5-9.1) | 0.5799 |
| | **Day 5** | 8.8 (8.4-9.0) | 8.7 (8.4-9.1) | 0.7862 |
| **Inorganic phosphate (mEq/l)** | **Baseline** | 3.2 (2.8-3.8) | 3.3 (3.0-3.5) | 0.6041 |
| | **Day 5** | 3.1 (2.9-3.4) | 3.2 (2.8-3.5) | 0.6041 |
| **Complete blood count** | | | | |
| **Hemoglobin (g/dl)** | **Baseline** | 12.6 (11.6-13.6) | 12.9 (12.4-13.7) | 0.1259 |
| | **Day 5** | 12.6 (11.4-13.5) | 12.8 (11.9-13.9) | 0.4121 |
| **Platelets (x10³/µL)** | **Baseline** | 190.5 (152.5-229.5) | 178.0 (144.0-217.0) | 0.2384 |
| | **Day 5** | 218.5 (173.0-273.0) | 186.5 (153.5-249.5) | 0.1679 |
| **Leucocytes (x10³/µL)** | **Baseline** | 4.5 (3.4-6.5) | 4.8 (3.7-6.1) | 0.9551 |
| | **Day 5** | 5.7 (4.5-7.1) | 5.0 (4.3-7.1) | 0.4019 |
| **Lymphocytes (x10³/µL)** | **Baseline** | 1.2 (0.8-1.7) | 1.5 (1.0-2.0) | 0.3384 |
| | **Day 5** | 1.3 (0.9-1.8) | 1.3 (0.9-1.8) | 0.7333 |
| **Neutrophils (x10³/µL)** | **Baseline** | 2.6 (1.9-3.3) | 2.5 (2.0-3.3) | 0.7227 |
| | **Day 5** | 3.4 (2.5-5.1) | 3.0 (2.2-4.6) | 0.2494 |
| **Monocytes (x10³/µL)** | **Baseline** | 0.430 (0.330-0.490) | 0.420 (0.310-0.580) | 0.7226 |
| | **Day 5** | 0.430 (0.350-0.540) | 0.420 (0.320-0.525) | 0.5960 |
| **Basophils (x10³/µL)** | **Baseline** | 0.020 (0.010-0.030) | 0.020 (0.010-0.020) | 0.5920 |
| | **Day 5** | 0.020 (0.010-0.030) | 0.020 (0.010-0.030) | 0.8839 |
| **Eosinophils (x10³/µL)** | **Baseline** | 0.04 (0.01-0.12) | 0.03 (0.01-0.11) | 0.8960 |
| | **Day 5** | 0.06 (0.02-0.17) | 0.04 (0.01-0.12) | 0.3541 |
| **Coagulation parameters** | | | | |
| **Prothrombin time (s)** | **Baseline** | 11.9 (11.6-12.5) | 12.1 (11.6-12.6) | 0.9706 |
| | **Day 5** | 12.2 (11.6-12.9) | 12.1 (11.6-12.9) | 0.9678 |
| **aPTT (s)** | **Baseline** | 29.3 (27.3-32.9) | 30.0 (28.3-32.5) | 0.2667 |
| | **Day 5** | 29.3 (25.8-30.6) | 28.5 (27.6-31.3) | 0.3746 |
| **Fibrinogen (mg/dL)** | **Baseline** | 388.0 (324.0-449.0) | 384.5 (319.0-446.0) | 0.8291 |
| | **Day 5** | 410.0 (368.0-494.0) | 483.0 (412.0-555.0) | 0.0939 |
| **D-dimer (ng/mL)** | **Baseline** | 714.0 (437.0-1126.0) | 559.0 (410.0-918.0) | 0.3384 |
| | **Day 5** | 575.0 (433.0-1212.0) | 669.0 (460.0-1159.0) | 0.9214 |
| **Inflammatory parameters** | | | | |
| **Troponin-I (ng/mL)** | **Baseline** | 0.04 (0.02-0.06) | 0.03 (0.00-0.04) | 0.2360 |
| | **Day 5** | 0.02 (0.00-0.03) | 0.02 (0.00-0.03) | 0.5476 |
| **Creatinine Kinase (U/L)** | **Baseline** | 70.0 (48.0-104.0) | 59.5 (33.0-110.5) | 0.2057 |
| | **Day 5** | 40.5 (27.0-60.0) | 48.0 (34.0-85.0) | 0.3310 |
| **Lactate Dehydrogenase (UI/l)** | **Baseline** | 328.0 (297.0-386.0) | 352.0 (294.0-420.0) | 0.4270 |
| | **Day 5** | 348.0 (299.0-401.0) | 389.0 (309.5-432.5) | 0.2584 |
| **C-reactive protein (mg/dL)** | **Baseline** | 0.81 (0.22-1.48) | 0.73 (0.23-1.67) | 0.9820 |
| | **Day 5** | 0.46 (0.14-1.48) | 1.11 (0.41-3.02) | 0.0529 |
| **Procalcitonin (ng/mL)** | **Baseline** | 0.06 (0.05-0.11) | 0.05 (0.04-0.08) | 0.0306 |
| | **Day 5** | 0.06 (0.04-0.08) | 0.05 (0.04-0.08) | 0.8825 |
| **IL-6 (pg/mL)** | **Baseline** | 0.9 (0.6-1.3) | 1.1 (0.8-1.9) | 0.0990 |
| | **Day 5** | 0.8 (0.5-1.4) | 1.2 (0.7-1.9) | 0.0540 |

ALT: alanine aminotransferase; aPTT: activated Partial Thromboplastin Time; AST: aspartate aminotransferase; GOT: Glutamic-oxaloacetic transaminase; GPT: Glutamic-pyruvic transaminase; IL-6: interleukin-6



USC UNIVERSIDADE DE SANTIAGO DE COMPOSTELA

**Table S12.** Percentage change in analytical parameters between baseline visit and end-of-treatment visit (day 5). U Mann–Whitney test.

| Parameter | Ethanol (% median) | Placebo (% median) | p |
|---|---|---|---|
| **Basic biochemistry** | | | |
| **Glucose (mg/dL)** | 1.98 | 0.00 | 0.6008 |
| **Urea (mg/dl)** | 1.22 | 6.06 | 0.4900 |
| **Creatinine (mg/dl)** | -2.97 | -3.57 | 0.9345 |
| **Bilirubin (mg/dl)** | 0.00 | 0.00 | 0.8606 |
| **AST (GOT) (U/I)** | 0.00 | 4.86 | 0.5028 |
| **ALT (GPT) (U/I)** | 15.00 | 9.09 | 0.6999 |
| **Gamma GT (GGT) (U/I)** | 8.63 | 6.67 | 0.6086 |
| **Albumin (g/dl)** | 0.00 | -2.50 | 0.0408 |
| **Calcium (mEq/l)** | 0.00 | 0.00 | 0.5684 |
| **Inorganic phosphate (mEq/l)** | -3.33 | -3.97 | 0.8051 |
| **Complete blood count** | | | |
| **Hemoglobin (g/dl)** | 0.00 | 0.00 | 0.1327 |
| **Platelets (x10$^3$/µL)** | 11.13 | 8.67 | 0.7377 |
| **Leucocytes (x10$^3$/µL)** | 14.41 | 0.00 | 0.1364 |
| **Lymphocytes (x10$^3$/µL)** | -1.96 | 0.00 | 0.7561 |
| **Neutrophils (x10$^3$/µL)** | 22.08 | 4.70 | 0.1425 |
| **Monocytes (x10 µ$^3$/L)** | 3.08 | 0.00 | 0.6331 |
| **Basophils (x10$^3$/µL)** | 0.00 | 0.00 | 0.7962 |
| **Eosinophils (x10$^3$/µL)** | 0.00 | 0.00 | 0.3131 |
| **Coagulation parameters** | | | |
| **Prothrombin time (s)** | 0.84 | 0.74 | 0.9678 |
| **aPTT (s)** | -2.39 | -4.41 | 0.8193 |
| **Fibrinogen (mg/dL)** | 13.58 | 15.42 | 0.3361 |
| **D-dimer (ng/mL)** | -8.66 | 0.00 | 0.2432 |
| **Inflammatory parameters** | | | |
| **Troponin-I (ng/mL)** | -38.54 | -1.28 | 0.0772 |
| **Creatinine Kinase (U/L)** | -36.08 | -11.65 | 0.0020 |
| **Lactate Dehydrogenase (UI/I)** | 1.56 | 5.59 | 0.3083 |
| **C-reactive protein (mg/dL)** | 0.66 | 50.56 | 0.0379 |
| **Procalcitonin (ng/mL)** | -14.29 | 0.00 | 0.1257 |
| **IL-6 (pg/mL)** | 0.00 | 0.00 | 0.6411 |

ALT: alanine aminotransferase; aPTT: activated Partial Thromboplastin Time; AST: aspartate aminotransferase; GOT: Glutamic-oxaloacetic transaminase; GPT: Glutamic-pyruvic transaminase; IL-6: interleukin-6

**Table S13.** Equivalent doses of prednisone/day and the total equivalent doses of prednisone administered in both groups.

| | Daily prednisone dose prescribed | | | Total prednisone administered | | | |
|---|---|---|---|---|---|---|---|
| | **Median** | **IQR** | **p** | **Mean** | **SD** | **p** | **n** |
| **Ethanol** | 48.1 | 39.9-56.2 | 0.4912 | 919.2 | 752.9 | 0.2104 | 19 |
| **Placebo** | 51.7 | 37.0-66.4 | | 657.8 | 481.6 | | 19 |



USC UNIVERSIDADE DE SANTIAGO DE COMPOSTELA

USC
UNIVERSIDADE
DE SANTIAGO
DE COMPOSTELA

# CONCLUSIONS

USC
UNIVERSIDADE
DE SANTIAGO
DE COMPOSTELA

USC
UNIVERSIDADE
DE SANTIAGO
DE COMPOSTELA

# CONCLUSIONS

In this Doctoral Thesis we have searched for therapeutic alternatives based on pharmaceutical compounding and drug repositioning to respond to situations of therapeutic gaps such as ocular cystinosis and SARS-CoV-2 infection, which has allowed us to draw the following conclusions:

1. In the **first part**, an ophthalmic magistral formulation of cysteamine in hyaluronic acid packaged in novel single-dose containers for the treatment of ocular cystinosis has been successfully developed and characterized.

   1.1. Molecular imaging techniques make it possible to visualize, localize, characterize and quantify radiolabeled compounds in real time after administration in a reliable, safe and non-invasive manner. None of them has both high sensitivity and specificity, although the combination of these techniques makes it possible to successfully study the biological processes associated with ocular drug administration.

   1.2. The development of new cysteamine delivery systems is limited due to its poor stability in the presence of oxygen, light and high temperatures, although different alternatives have been recently proposed, such as hydrogels, nanowafers and contact lenses. Its complex analytical determination is evidenced by the absence of a gold standard, so several techniques have been described, such as high-performance liquid chromatography (HPLC), high voltage electrophoresis, enzymatic assay and gas chromatography with flame ionization and photometric detection, among others.

   1.3. The 0.55% cysteamine formulation developed is physicochemically and microbiologically stable for 30 days at −20 °C, while storage at 2-8 °C is possible without exceeding 7 days in any case. Moreover, each single dose container can be used at room temperature for a total of 16 hours once opened. Saturation with nitrogen does not provide additional stability.

      1.3.1. The pH and osmolarity values of the formulation cysteamine 0.55% in hyaluronic acid, as well as the mechanical resistance of the single-dose containers after storage for 30 days in the freezer remain within a range suitable for topical ophthalmic administration. In contrast, the viscosity



USC UNIVERSIDADE DE SANTIAGO DE COMPOSTELA

of the formulation is reduced after freezer storage, although it is maintained in the refrigerator.

1.3.2. *In vivo* ocular permanence PET studies show a high ocular biopermanence of the 0.55% cysteamine formulation in hyaluronic acid, with a half-life twice as long as that of the classic vehicle used in compounded formulation, 0.9% sodium chloride. Thus, it is shown that the drop in viscosity observed after freezing does not influence the ocular residence time.

1.3.3. The preparation and packaging of the compounded formulation of cysteamine 0.55% in hyaluronic acid enables its preparation in Hospital Pharmacy Departments, allowing it to be dispensed for long periods of time and reducing patients' visits to the hospital. This makes it a very attractive alternative for translation to clinical practice, where access to some of the orphan drugs is complex.

2. In the **second part** of this Doctoral Thesis, a master formulation of inhaled ethanol has been developed for the treatment of patients infected with SARS-CoV-2 in early stages.

2.1. The 65° ethanol formulation is stable at room temperature for 15 days protected from light, maintaining its physicochemical and microbiological properties. The oxygen flow rate of 2 L/min is the most suitable, with higher and more stable concentrations during daily administration than at 3 L/min. Despite this, and taking into account the ventilatory parameters in humans, the estimated mean amount of ethanol inhaled at 2 L/min is 33.6 ± 3.6 mg/min, lower than the 40.0 ± 5.7 mg/min at 3 L/min.

2.1.1. The inhaled formulation of 65° ethanol at 2 L/min is safe based on preclinical histology studies of the respiratory tract and lungs. PET images show that radiolabeled ethanol is localized in the lungs in early stages, with subsequent disposition in the liver.

2.2. The phase II clinical trial with inhaled ethanol shows that the progression of the disease according to the WHO scale is similar in the ethanol group and in the placebo group.

2.2.1. The viral load is reduced over time in the ethanol group and in the placebo group. Mean Ct values are higher than 33 on day 14 only in the placebo group, a value above which patients are considered non-infectious, and may therefore be an alternative that favors early epidemiological discharge.

2.2.2. In terms of efficacy, there are no significant differences between the ethanol and placebo groups in the evolution of body temperature, use



USC UNIVERSIDADE DE SANTIAGO DE COMPOSTELA

of antipyretics, oxygen saturation, and the use of antibiotics or corticosteroids. Regarding inflammatory parameters, creatinine kinase decreased to a greater extent in the ethanol group, while C-reactive protein increased only in the placebo group.

2.2.3. Regarding safety, inhaled ethanol proved to be a safe treatment, since no respiratory or analytical changes were observed, no ethanol was detected in plasma, and no electrocardiographic changes were produced.



USC UNIVERSIDADE DE SANTIAGO DE COMPOSTELA

USC
UNIVERSIDADE
DE SANTIAGO
DE COMPOSTELA

# CONCLUSIONES

En esta Tesis Doctoral se han buscado alternativas terapéuticas basadas en la formulación magistral y en el reposicionamiento terapéutico para para dar respuesta a situaciones de vacío terapéutico como la cistinosis ocular y la infección por SARS-CoV-2, lo que ha permitido extraer las siguientes conclusiones:

1. En la **primera parte**, se ha desarrollado y caracterizado exitosamente una formulación magistral oftálmica de cisteamina en ácido hialurónico envasada en novedosos envases monodosis para el tratamiento de la cistinosis ocular.

   1.1. Las técnicas de imagen molecular permiten visualizar, localizar, caracterizar y cuantificar en tiempo real los compuestos radiomarcados tras su administración de forma fiable, segura y no invasiva. Ninguna de ellas presenta a la vez una alta sensibilidad y especificidad, aunque la combinación de estas permite estudiar adecuadamente los procesos biológicos asociados a la administración ocular de fármacos.

   1.2. El desarrollo de nuevos sistemas de administración de cisteamina es limitado debido a la escasa estabilidad de esta ante la presencia de oxígeno, luz y altas temperaturas, aunque diferentes alternativas se han propuesto recientemente, como los hidrogeles, nanowafers y lentes de contacto. Su compleja determinación analítica se evidencia con la ausencia de un *gold standard*, por lo que diversas técnicas han sido descritas, como la cromatografía líquida de alta resolución (HPLC), la electroforesis de alto voltaje, el ensayo enzimático y la cromatografía de gases con ionización de llama y detección fotométrica, entre otros.

   1.3. La formulación de cisteamina al 0,55% desarrollada es estable fisicoquímica y microbiológicamente durante 30 días a −20 °C, mientras que su almacenamiento a 2-8 °C es posible sin superarse en ningún caso los 7 días. Además, cada monodosis puede ser empleado a temperatura ambiente durante un total de 16 horas una vez abierto. La saturación con nitrógeno no proporciona estabilidad adicional.

      1.3.1. Los valores de pH y osmolaridad de la formulación cisteamina 0.55% en ácido hialurónico, así como la resistencia mecánica de los envases monodosis tras su conservación durante 30 días en congelador se mantienen dentro de un rango adecuado para su administración



USC UNIVERSIDADE DE SANTIAGO DE COMPOSTELA

oftálmica tópica. En cambio, la viscosidad de la formulación se reduce tras el almacenamiento en congelador, aunque se mantiene en el frigorífico.

1.3.2. Los estudios PET de permanencia ocular *in vivo* muestran una alta biopermanencia ocular de la formulación de cisteamina 0.55% en ácido hialurónico, con una vida media dos veces superior a la del vehículo clásico utilizado en formulación magistral, cloruro sódico al 0,9%. De este modo, se muestra que la caída de viscosidad observada tras la congelación no influye en el tiempo de residencia ocular.

1.3.3. La elaboración y envasado de la formulación magistral de cisteamina 0.55% en ácido hialurónico es un proceso que posibilita su preparación en las secciones de farmacotecnia, permitiendo su dispensación para largos periodos de tiempo y reduciendo las visitas al hospital de los pacientes. Esto la convierte en una alternativa muy atractiva para su traslación a la práctica clínica, en la cual el acceso a algunos de los medicamentos huérfanos resulta complejo.

2. En la **segunda parte** de esta Tesis doctoral se ha desarrollado una formulación magistral de etanol inhalado para el tratamiento de pacientes infectados por SARS-CoV-2 en estadios iniciales.

2.1. La formulación de etanol 65° es estable a temperatura ambiente durante 15 días protegida de la luz, manteniendo sus propiedades fisicoquímicas y microbiológicas. El flujo de oxígeno de 2 L/min es el más adecuado, con concentraciones mayores y más estables durante la administración diaria que a 3 L/min. A pesar de ello, y teniendo en cuenta los parámetros ventilatorios en humanos, la cantidad media estimada de etanol inhalado a 2 L/min es de 33,6 ± 3,6 mg/min, menor que los 40,0 ± 5,7 mg/min a 3 L/min.

2.1.1. La formulación inhalada de etanol 65° a 2 L/min es segura en base a los estudios histológicos preclínicos de vías respiratorias y pulmones. Las imágenes PET muestran que el etanol radiomarcado se localiza en los pulmones en fases tempranas, con una disposición posterior a nivel hepático.

2.2. El ensayo clínico fase II con etanol inhalado muestra que la progresión de la enfermedad según la escala de la OMS es similar en el grupo etanol y en el grupo placebo.

2.2.1. La carga viral se reduce con el tiempo en el grupo etanol y en el grupo placebo. Los valores medios de Ct son superiores a 33 en el día 14 únicamente en el grupo placebo, valor por encima del cual los pacientes



USC UNIVERSIDADE DE SANTIAGO DE COMPOSTELA

se consideran no infecciosos, pudiendo por lo tanto ser una alternativa que favorezca el alta epidemiológica temprana.

2.2.2. En términos de eficacia, no existen diferencias significativas entre los grupos etanol y placebo en la evolución de la temperatura corporal, uso de antipiréticos, saturación de oxígeno, y el uso de antibióticos o corticoides. En lo relativo a parámetros inflamatorios, la creatinina quinasa se reduce en mayor medida en el grupo etanol, mientras que la proteína C reactiva se incrementa únicamente en el grupo placebo.

2.2.3. En relación a la seguridad, el etanol inhalado mostró ser un tratamiento seguro, ya que no se observaron alteraciones a nivel respiratorio ni analítico, no se detectó etanol en plasma y no se produjeron cambios electrocardiográficos.



USC UNIVERSIDADE DE SANTIAGO DE COMPOSTELA

USC
UNIVERSIDADE
DE SANTIAGO
DE COMPOSTELA

# CONCLUSIÓNS

Nesta Tese Doutoral buscáronse alternativas terapéuticas baseadas na formulación maxistral e no reposicionamento terapéutico para dar resposta a situacións de baleiro terapéutico como a cistinose ocular e a infección por SARS-CoV-2, o que permitiu extraer as seguintes conclusións:

1. Na **primeira parte**, desenvolveuse e caracterizouse exitosamente unha formulación maxistral oftálmica de cisteamina en ácido hialurónico envasada en novidosos envases monodosis para o tratamento da cistinose ocular.

   1.1. As técnicas de imaxe molecular permiten visualizar, localizar, caracterizar e cuantificar en tempo real os compostos radiomarcados tras a súa administración de forma fiable, segura e non invasiva. Ningunha delas presenta á vez unha alta sensibilidade e especificidade, aínda que a combinación das mesmas permite estudar adecuadamente os procesos biolóxicos asociados á administración ocular de fármacos.

   1.2. O desenvolvemento de novos sistemas de administración de cisteamina é limitado debido á escasa estabilidade de esta ante a presenza de osíxeno, luz e altas temperaturas, aínda que diferentes alternativas propuxéronse recentemente, como os hidroxeis, nanowafers e lentes de contacto. A súa complexa determinación analítica evidénciase coa ausencia dun *gold standard*, polo que diversas técnicas foron descritas, como a cromatografía líquida de alta resolución (HPLC), a electroforesis de alta voltaxe, o ensaio encimático e a cromatografía de gases con ionización de chama e detección fotométrica, entre outros.

   1.3. A formulación de cisteamina ao 0,55% desenvolvida é estable fisicoquímica e microbiolóxicamente durante 30 días a −20 °C, mentres que o seu almacenamento a 2-8 °C é posible sen superarse en ningún caso os 7 días. Ademais, cada monodose pode ser empregado a temperatura ambiente durante un total de 16 horas unha vez aberto. A saturación con nitróxeno non proporciona estabilidade adicional.

      1.3.1. Os valores de pH e osmolaridade da formulación cisteamina 0.55% en ácido hialurónico, así como a resistencia mecánica dos envases monodosis tras a súa conservación durante 30 días en conxelador mantéñense dentro dun rango adecuado para a súa administración



USC UNIVERSIDADE DE SANTIAGO DE COMPOSTELA

oftálmica tópica. En cambio, a viscosidade da formulación redúcese tras o almacenamento en conxelador, aínda que se mantén no frigorífico.

1.3.2. Os estudos PET de permanencia ocular *in vivo* mostran unha alta biopermanencia ocular da formulación de cisteamina 0.55% en ácido hialurónico, cunha vida media dúas veces superior á do vehículo clásico utilizado en formulación maxistral, cloruro sódico ao 0,9%. Deste xeito, móstrase que a caída de viscosidade observada tras a conxelación non inflúe no tempo de residencia ocular.

1.3.3. A elaboración e envasado da formulación maxistral de cisteamina 0.55% en ácido hialurónico é un proceso que posibilita a súa preparación nas seccións de farmacotecnia, permitindo a súa dispensación para longos períodos de tempo e reducindo as visitas ao hospital dos pacientes. Isto convértea nunha alternativa moi atractiva para a súa translación á práctica clínica, na cal o acceso a algúns dos medicamentos orfos resulta complexo.

2. Na **segunda parte** desta Tese Doutoral desenvolveuse unha formulación maxistral de etanol inhalado para o tratamento de pacientes infectados por SARS-CoV-2 en estadios iniciais.

2.1. A formulación de etanol 65° é estable a temperatura ambiente durante 15 días protexida da luz, mantendo as súas propiedades fisicoquímicas e microbiolóxicas. O fluxo de osíxeno de 2 L/min é o máis adecuado, con concentracións maiores e máis estables durante a administración diaria que a 3 L/min. A pesar diso, e tendo en conta os parámetros ventilatorios en humanos, a cantidade media estimada de etanol inhalado a 2 L/min é de 33,6 ± 3,6 mg/min, menor que os 40,0 ± 5,7 mg/min a 3 L/min.

2.1.1. A formulación inhalada de etanol 65° a 2 L/min é segura en base aos estudos histolóxicos preclínicos de vías respiratorias e pulmóns. As imaxes PET mostran que o etanol radiomarcado localízase nos pulmóns en fases temperás, cunha disposición posterior a nivel hepático.

2.2. O ensaio clínico fase II con etanol inhalado mostra que a progresión da enfermidade segundo a escala da OMS é similar no grupo etanol e no grupo placebo.

2.2.1. A carga viral redúcese co tempo no grupo etanol e no grupo placebo. Os valores medios de Ct son superiores a 33 no día 14 unicamente no grupo placebo, valor por encima do cal os pacientes se consideran non infecciosos, podendo por tanto ser unha alternativa que favoreza o alta epidemiolóxica temperá.



USC UNIVERSIDADE DE SANTIAGO DE COMPOSTELA

2.2.2. En termos de eficacia, non existen diferenzas significativas entre os grupos etanol e placebo na evolución da temperatura corporal, uso de antipiréticos, saturación de osíxeno, e o uso de antibióticos ou corticoides. No relativo a parámetros inflamatorios, a creatinina quinasa redúcese en maior medida no grupo etanol, mentres que a proteína C reactiva increméntase unicamente no grupo placebo.

2.2.3. En relación á seguridade, o etanol inhalado mostrou ser un tratamento seguro, xa que non se observaron alteracións a nivel respiratorio nin analítico, non se detectou etanol en plasma e non se produciron cambios electrocardiográficos.



USC UNIVERSIDADE DE SANTIAGO DE COMPOSTELA

USC
UNIVERSIDADE
DE SANTIAGO
DE COMPOSTELA

# APPENDIX

USC
UNIVERSIDADE
DE SANTIAGO
DE COMPOSTELA

USC
UNIVERSIDADE
DE SANTIAGO
DE COMPOSTELA

# APPENDIX

## CONFLICT OF INTEREST

The doctoral student declares that there is no conflict of interest regarding the Doctoral Thesis.

## ANIMAL EXPERIMENTS

In the present Thesis, male adult Sprague-Dawley rats with a 200-300 g average weight were used, supplied by the animal facility of the University of Santiago de Compostela (Santiago de Compostela, Spain). During the experiments, the animals were kept in individual cages with free access to food and water in a room under controlled temperature (22 ± 1°C) and humidity (60 ± 5%) and with day–night cycles regulated by artificial light (12/12 hours). The animals were treated according to the guidelines for the care and use of laboratory animals. Animal experiments complied with the ARRIVE guidelines (Kilkenny C, Browne WJ, Cuthill IC, Emerson M, Altman DG. Improving bioscience research reporting: the ARRIVE guidelines for reporting animal research. PLoS Biol. 2010 Jun 29;8(6):e1000412.). Experiments were performed at the Preclinical Imaging Service of the Experimental Biomedicine Center (CEBEGA) (REGA number: ES150780292901).

Experiments were approved by the Consellería de Medio Rural da Xunta de Galicia (15010/2019/006) and were authorized by the Animal Research Committee of the Health Research Institute of Santiago de Compostela (IDIS). They followed the Spanish and European Union (EU) regulations for animal experimentation (86/609/CEE, 2003/ 65/CE, 2010/63/EU, and RD53/2013).

## CLINICAL STUDY

In the present Thesis, the phase II clinical trial was performed in 75 patients with SARS-CoV-2 infection. This was performed at the nursing home CEGADI, intended for the treatment of institutionalized elderly patients in the second wave of the pandemic. The clinical trial is registered in the European Union Drug Regulating Authorities Clinical Trials Database (EudraCT: 2020-001760-29). The study is adhered to the tenets of the Declaration of Helsinki and was approved by the



USC UNIVERSIDADE DE SANTIAGO DE COMPOSTELA

Institutional Review Board/Ethics Committee of the Ethical Committee of Clinical Research of Galicia and the Consellería de Sanidade da Xunta de Galicia (2020/218) and by the Agencia Española de Medicamentos y Productos Sanitarios (AEMPS). The committee complies with current legal requirements applicable to Research Ethics Committee, following the Standards of Good Clinical Practice (CPMP/ICH/135/95).

## FUNDING AND ACKNOWLEDGEMENTS

This Thesis has been partially funded by Fundación Española de Farmacia Hospitalaria (FEFH 18-19), Fundación Mutua Madrileña (XVI Convocatoria de Ayudas a la Investigación en Salud), Fundación Mutua Madrileña (XIX Convocatoria de Ayudas a la Investigación en Salud 2022), "Asociación La Lucha de Iker", Axencia Galega de Coñecemento en Saúde (ACIS) through the project SA 304 C by Programa Traslaciona-COVID19 (CT850A-4), Fundación Española de Farmacia Hospitalaria and Axencia Galega Innovación (Grupos de Potencial Crecimiento IN607B2020/11.

The doctoral student acknowledges the financial support of Instuto de Salud Carlos III (ISCIII) for the personnel contract (CM21/00114).

## ARTICLES DERIVED FROM THIS THESIS

In compliance with the rules of doctoral studies at Universidade de Santiago de Compostela in Regulamento dos estudos de doutoramento na USC, DOG de 16 de Setembro de 2020, it was provided some information regarding the articles on which this work is based and the journals that published those articles. In particular, it was given the names of the authors, the title of the journals, the year each article was published, the publisher, the DOI-type link, the Journal Impact Factor and the quartile from the Journal Citation Reports, some relevant information regarding copyright and use of the articles and the author contribution.

⇒ **Chapter 1**

**TITLE:** *Ocular Biodistribution Studies using Molecular Imaging*

**AUTHORS:** *Castro-Balado A, Mondelo-García C, González-Barcia M, Zarra-Ferro I, Otero-Espinar FJ, Ruibal-Morell Á, Aguiar-Fernández P, Fernández-Ferreiro A.*



USC UNIVERSIDADE DE SANTIAGO DE COMPOSTELA

**JOURNAL:** *Pharmaceutics*

**YEAR:** *2019*

**PUBLISHER**: *MDPI*

**LINK:** https://doi.org/10.3390/pharmaceutics11050237

**JOURNAL IMPACT FACTOR:** *6.525 (Q1; 39/279)*

**INFORMATION REGARDING COPYRIGHT AND USE:** Information about permissions can be found on the website: https://www.mdpi.com/authors/rights where the following statement is placed:

"For all articles published in MDPI journals, copyright is retained by the authors. Articles are licensed under an open access Creative Commons CC BY 4.0 license, meaning that anyone may download and read the paper for free. The article may be reused and quoted provided that the original published version is cited."

**AUTHOR CONTRIBUTION:** The contributions of the Ph.D. candidate were essential in all the included articles. The candidate contributed to the information research and analysis, and the writing of the manuscript.

⇒ **Chapter 2**

**TITLE:** *Recent Research in Ocular Cystinosis: Drug Delivery Systems, Cysteamine Detection Methods and Future Perspectives*

**AUTHORS:** *Castro-Balado A, Mondelo-García C, Varela-Rey I, Moreda-Vizcaíno B, Sierra-Sánchez JF, Rodríguez-Ares MT, Hermelo-Vidal G, Zarra-Ferro I, González-Barcia M, Yebra-Pimentel E, Giráldez-Fernández MJ, Otero-Espinar FJ, Fernández-Ferreiro A.*

**JOURNAL:** *Pharmaceutics*

**YEAR:** *2020*

**PUBLISHER**: *MDPI*

**LINK:** https://doi.org/10.3390/pharmaceutics12121177

**JOURNAL IMPACT FACTOR:** *6.525 (Q1; 39/279)*



USC UNIVERSIDADE DE SANTIAGO DE COMPOSTELA

**INFORMATION REGARDING COPYRIGHT AND USE:** Information about permissions can be found on the website: https://www.mdpi.com/authors/rights where the following statement is placed:

"For all articles published in MDPI journals, copyright is retained by the authors. Articles are licensed under an open access Creative Commons CC BY 4.0 license, meaning that anyone may download and read the paper for free. The article may be reused and quoted provided that the original published version is cited."

**AUTHOR CONTRIBUTION:** The contributions of the Ph.D. candidate were essential in all the included articles. The candidate contributed to the information research and analysis, and the writing of the manuscript.

⇒ **Chapter 3**

**TITLE:** *Cysteamine Eye Drops in Hyaluronic Acid Packaged in Innovative Single-Dose Systems: Stability and Ocular Biopermanence*

**AUTHORS:** *Castro-Balado A, Bandín-Vilar E, Cuartero-Martínez A, García-Quintanilla L, Hermelo-Vidal G, García-Otero X, Rodríguez-Martínez L, Mateos J, Hernández-Blanco M, Aguiar P, Zarra-Ferro I, González-Barcia M, Mondelo-García C, Otero-Espinar FJ, Fernández-Ferreiro A.*

**JOURNAL:** *Pharmaceutics*

**YEAR:** *2022*

**PUBLISHER:** *MDPI*

**LINK:** https://doi.org/10.3390/pharmaceutics14102194

**JOURNAL IMPACT FACTOR:** *6.525 (Q1; 39/279)*

**INFORMATION REGARDING COPYRIGHT AND USE:** Information about permissions can be found on the website: https://www.mdpi.com/authors/rights where the following statement is placed:

"For all articles published in MDPI journals, copyright is retained by the authors. Articles are licensed under an open access Creative Commons CC BY 4.0 license, meaning that anyone may download and read the paper for free. The article may be reused and quoted provided that the original published version is cited."



USC UNIVERSIDADE DE SANTIAGO DE COMPOSTELA

**AUTHOR CONTRIBUTION:** The contributions of the Ph.D. candidate were essential in all the included articles. The candidate contributed to the design of the research and proofs, to the analysis of the results and to the writing of the manuscript.

⇒ **Chapter 4**

**TITLE:** *Development and Characterization of Inhaled Ethanol as a Novel Pharmacological Strategy Currently Evaluated in a Phase II Clinical Trial for Early-Stage SARS-CoV-2 Infection.*

**AUTHORS:** *Castro-Balado A, Mondelo-García C, Barbosa-Pereira L, Varela-Rey I, Novo-Veleiro I, Vázquez-Agra N, Antúnez-López JR, Bandín-Vilar EJ, Sendón-García R, Busto-Iglesias M, Rodríguez-Bernaldo de Quirós A, García-Quintanilla L, González-Barcia M, Zarra-Ferro I, Otero-Espinar FJ, Rey-Bretal D, Lago-Quinteiro JR, Valdés-Cuadrado L, Rábade-Castedo C, Del Río-Garma MC, Crespo-Diz C, Delgado-Sánchez O, Aguiar P, Barbeito-Castiñeiras G, Pérez Del Molino-Bernal ML, Trastoy-Pena R, Passannante R, Llop J, Pose-Reino A, Fernández-Ferreiro A.*

**JOURNAL:** *Pharmaceutics*

**YEAR:** *2021*

**PUBLISHER**: *MDPI*

**LINK:** https://doi.org/10.3390/pharmaceutics13030342

**JOURNAL IMPACT FACTOR:** *6.525 (Q1; 39/279)*

**INFORMATION REGARDING COPYRIGHT AND USE:** Information about permissions can be found on the website: https://www.mdpi.com/authors/rights where the following statement is placed:

"For all articles published in MDPI journals, copyright is retained by the authors. Articles are licensed under an open access Creative Commons CC BY 4.0 license, meaning that anyone may download and read the paper for free. The article may be reused and quoted provided that the original published version is cited."

**AUTHOR CONTRIBUTION:** The contributions of the Ph.D. candidate were essential in all the included articles. The candidate contributed to the design of the research and proofs, to the analysis of the results and to the writing of the manuscript.



USC UNIVERSIDADE DE SANTIAGO DE COMPOSTELA

⇒ **Chapter 5**

**TITLE:** *Efficacy and safety of inhaled ethanol in early-stage SARS-CoV-2 infection in older adults: a phase II randomized clinical trial*

**AUTHORS:** *Castro-Balado A, Novo-Veleiro I, Vázquez-Agra N, Barbeito-Castiñeiras G, Estany-Gestal A, Trastoy-Pena R, González-Barcia M, Zarra-Ferro I, Del Río-Garma MC, Crespo-Diz C, Delgado-Sánchez O, Otero-Espinar FJ, Mondelo-García C, Pose-Reino A, Fernández-Ferreiro A.*

**JOURNAL:** *Pharmaceutics*

**YEAR:** *2023*

**PUBLISHER:** *MDPI*

**LINK:** https://doi.org/10.3390/pharmaceutics15020667

**JOURNAL IMPACT FACTOR:** *6.525 (Q1; 39/279)*

**INFORMATION REGARDING COPYRIGHT AND USE:** Information about permissions can be found on the website: https://www.mdpi.com/authors/rights where the following statement is placed:

"For all articles published in MDPI journals, copyright is retained by the authors. Articles are licensed under an open access Creative Commons CC BY 4.0 license, meaning that anyone may download and read the paper for free. The article may be reused and quoted provided that the original published version is cited."

**AUTHOR CONTRIBUTION:** The contributions of the Ph.D. candidate were essential in all the included articles. The candidate contributed to the design of the research and proofs, to the analysis of the results and to the writing of the manuscripts.

**FIGURES AUTHORSHIP**

The author declares that all unreferenced figures of this Thesis are of his authorship and created with BioRender.com.



USC UNIVERSIDADE DE SANTIAGO DE COMPOSTELA

# RESOLUCIÓN DE AUTORIZACIÓN DE PROXECTOS DE EXPERIMENTACIÓN ANIMAL

XUNTA DE GALICIA
CONSELLERÍA DO MEDIO RURAL

Departamento Territorial
Edificio Administrativo de Servizos Múltiples
Vicente Ferrer, 2
15071 – A Coruña

RESOLUCIÓN DE AUTORIZACIÓN DE PROXECTOS DE EXPERIMENTACIÓN ANIMAL

**Expediente núm.:** 15010/2019/005 **Data de inicio:** 12.08.2019
**Persona interesada:** Asteria Mª Luzardo Álvarez **Procedemento:** resolución de autorización
**Forma de inicio:** solicitude da persoa interesada

ANTECEDENTES

A persoa interesada, como representante do centro CIMUS (Universidade de Santiago de Compostela), presentou con data 08.082.2019 unha solicitude para a realización do proxecto de experimentación animal (entrada no Rexistro Electrónico da Xunta de Galicia 2019/1688969), cuxos datos se detallan a continuación:

**Denominación do proxecto:** *Novas formulacións para o tratamento de enfermidades de depósito lisosomal (mucopolisacaridose)*
**Nome do centro usuario:** Animalario do CIMUS
**Persoa responsable do proxecto:** Asteria Mª Luzardo Álvarez
**Establecemento onde se realizarán os procedementos do proxecto (ou lugar xeográfico no caso de traballos de campo):** Animalario do CIMUS
**Clasificación do proxecto :** Tipo I ☐ Tipo II ☒ Tipo III ☐

CONSIDERACIÓNS LEGAIS E TÉCNICAS

1 O Real decreto 53/2013, de 1 de febreiro (BOE 34, do 8 de febreiro), polo que se establecen as normas básicas aplicables para a protección dos animais utilizados en experimentación e outros fins científicos, incluíndo a docencia, establece no seu artigo 33 as condicións de autorizacións dos proxectos con animais de experimentación.

2 O artigo 88 da Lei 39/2015, de 1 de outubro, do procedemento administrativo común das administracións públicas (BOE 236, do 2 de outubro de 2015) establece que a resolución que poña fin o procedemento decidirá todas as cuestións expostas polos interesados e aquelas outras derivadas deste.

3 O Servizo de Gandaría da Coruña revisou a documentación achegada na solicitude e o resultado favorable da avaliación do proxecto, realizada polo órgano habilitado da Sección de Experimentación Animal do Comité de Bioética da Universidade de Santiago de Compostela.

CVE: MQgxerIGQ2
Verificación: https://sede.xunta.gal/cve



USC UNIVERSIDADE DE SANTIAGO DE COMPOSTELA

XUNTA DE GALICIA
CONSELLERÍA DO MEDIO RURAL

Departamento Territorial
Edificio Administrativo de Servizos Múltiples
Vicente Ferrer, 2
15071 – A Coruña

Esta xefatura territorial é competente para ditar unha resolución, de conformidade co Decreto 149/2018, do 5 de decembro, polo que se establece a estrutura orgánica da Consellería do Medio Rural e se modifica parcialmente o Decreto 177/2016, do 15 de decembro, polo que se fixa a estrutura orgánica da Vicepresidencia e das consellerías da Xunta de Galicia (DOG 235, do 11 de novembro).

De acordo con todo o indicado, RESOLVO:

1 Autorizar o proxecto solicitado.
2 O mencionado proxecto non precisa someterse a unha avaliación retrospectiva.
3 A autorización deste proxecto terá unha duración de 60 meses e unha vez transcorrido este tempo deberá ser autorizado de novo.

A citada autorización é unicamente válida nas condicións que figuran no expediente. Ante calquera cambio significativo no proxecto que poida ter efectos negativos sobre o benestar dos animais, deberá solicitar a confirmación da autorización ao Servizo Provincial de Gandaría.

Esta autorización poderá ser suspendida, no caso de que o proxecto non se leve a cabo de acordo coas condicións de autorización e retirala, previo expediente tramitado ao que se lle dará audiencia.

Contra a presente resolución, que non lle pon fin á vía administrativa, poderá interpoñer un recurso de alzada ante o conselleiro de Medio Rural. O prazo comezará a contar dende o día seguinte ao da recepción desta resolución. Todo isto, segundo o disposto nos artigos 121 e 122 da citada Lei 39/2015.

Mediante este escrito notifícaselle ao CIMUS da USC esta resolución segundo o esixido no artigo 40.1 da antedita Lei 39/2015.

**Asinado por:** LOPEZ LOPEZ, MONICA
**Cargo:** Xefa Territorial
**Data e hora:** 12/08/2019 13:32:05

**CVE:** MOgxeifGQ2
**Verificación:** https://sede.xunta.gal/cve



USC UNIVERSIDADE DE SANTIAGO DE COMPOSTELA

# DICTAMEN DEL COMITÉ DE ÉTICA DE LA INVESTIGACIÓN CON MEDICAMENTOS DE GALICIA

XUNTA DE GALICIA
CONSELLERÍA DE SANIDADE

SERVIZO GALEGO de SAÚDE | Xerencia do Servizo Galego de Saúde

galicia

**2020/218**

**DICTAMEN DEL Comité de ética de la investigación con medicamentos de Galicia (CEIm-G)**

Paula M. López Vázquez, Secretaria del Comité de ética de la investigación con medicamentos de Galicia (CEIm-G)

**CERTIFICA:**

Que este Comité evaluó la propuesta del ensayo clínico:

> Nº **EudraCT**: 2020-001760-29
> **Título:** Ensayo clínico fase III para evaluar la eficacia y seguridad de etanol inhalado en el tratamiento de la COVID-19 en estadio inicial.
> **Código del promotor**: ALCOVID-19
> **Código de Registro**: 2020/218
> **Promotor: Sociedad Española de Farmacia Hospitalaria (SEFH)**
> **Versión/fecha del protocolo y Hoja de Información al Paciente**: Versión 02 del 15 de Mayo de 2020 y HIP/CI versión 02 del 15 de Mayo de 2020

Que este Comité ha realizado la evaluación de la parte I de la solicitud de autorización del ensayo, ha valorado las respuestas del promotor a las aclaraciones solicitadas (si las hubiera) y ha transmitido a la Agencia Española de medicamentos su opinión final sobre la parte I.

Que este Comité ha realizado la evaluación de la parte II de la solicitud de autorización del ensayo, de acuerdo con lo previsto en el Real Decreto 1090/2015 y en el art 7 del reglamento (UE) 536/2014 y considera que:

1. El procedimiento para obtener el consentimiento informado (incluyendo las hojas de información al sujeto de ensayo y consentimientos informados mencionados en el encabezamiento), y el plan de reclutamiento de sujetos previsto son adecuados y cumplen con los requisitos para la obtención del consentimiento informado previstos en el capítulo II del Real Decreto 1090/2015. Podrán realizarse versiones lingüísticas de los documentos aprobados mencionados, siendo responsabilidad del promotor garantizar al CEIm que se trata de una traducción fiel de los documentos aprobados por el CEIm.
2. Las compensaciones previstas a los participantes son adecuadas, así como las previsiones de indemnización por daños y perjuicios que pueda sufrir el participante.
3. El procedimiento previsto para el manejo de datos personales es adecuado.
4. El uso futuro de las muestras biológicas obtenidas durante el ensayo se adecua a lo previsto en el Real Decreto 1716/2011.
5. Para la realización del ensayo se consideran adecuados los centros e investigadores previstos en el anexo II a este dictamen, teniendo en cuenta las declaraciones de idoneidad emitidas por el promotor y por los responsables de las instituciones correspondientes.

Documento asinado dixitalmente por:
Paula López Vázquez (16/06/2020 13:50)
https://sede.xunta.gal/cve?idcve=SAOC-L4G4-BOAH-OF4O-TJC2-L159-2308-2338-90

Xacobeo 2021

CEIm de Galicia
Edificio Administrativo San Lázaro
15703 SANTIAGO DE COMPOSTELA
Teléfono: 881546425
ceic@sergas.es



USC UNIVERSIDADE DE SANTIAGO DE COMPOSTELA

XUNTA DE GALICIA
CONSELLERÍA DE SANIDADE

SERVIZO GALEGO de SAÚDE | Xerencia do Servizo Galego de Saúde

galicia

Que este Comité decidió emitir **DICTAMEN FAVORABLE condicionado** a que remitan el certificado del seguro para el ensayo clínico (de acuerdo al art. 9.3 del RD 1090/2015 que regula los ensayos clínicos en España, el promotor al tratarse de una investigación clínica sin ánimo comercial tiene un plazo de treinta días naturales para presentar el citado certificado, no pudiendo iniciarse el estudio hasta que este considere que se cuenta con el seguro o garantía financiera exigidos) en la reunión celebrada el día 11/06/20 (acta n.º 298)

Que en dicha reunión se cumplieron los requisitos establecidos en la legislación vigente – Real Decreto 1090/2015 – para que la decisión del citado CEIm sea válida.

Que el Comité tanto en su composición como en sus procedimientos, cumple con las normas de BPC (CPMP/ICH/135/95) y con la legislación vigente que regula su funcionamiento, y que la composición del mismo es la indicada en el anexo I, teniendo en cuenta que en el caso de que algún miembro participe en el ensayo o declare algún conflicto de interés, se ausentará durante la evaluación.

En Santiago de Compostela

XUNTA DE GALICIA · SECRETARÍA XERAL TÉCNICA · COMITÉ DE ÉTICA DE LA INVESTIGACIÓN DE GALICIA · CONSELLERÍA DE SANIDADE

*Nota: Incluir la opción de consentimiento oral ante testigos, especialmente importante para la situación de enfermos de COVID19 por razones de bioseguridad se puede aceptar la firma oral ante testigo, y que firme definitivamente el documento una vez se resuelva y sea negativo.*

Documento asinado dixitalmente por:
Paula López Vázquez (16/06/2020 13:50)
https://sede.xunta.gal/cve?idcve=SAOC-L4G4-BOAH-OF4O-TJC2-L159-2308-2338-90

Xacobeo 2021

CEIm de Galicia
Edificio Administrativo San Lázaro
15703 SANTIAGO DE COMPOSTELA
Teléfono: 881546425
ceic@sergas.es



USC UNIVERSIDADE DE SANTIAGO DE COMPOSTELA

XUNTA DE GALICIA
CONSELLERÍA DE SANIDADE

SERVIZO GALEGO de SAÚDE | Xerencia do Servizo Galego de Saúde

galicia

**Anexo I : Composición del Comité de ética de la investigación con medicamentos de Galicia (CEIm-G)**

Susana María Romero Yuste (Presidenta). Médico Especialista en Reumatología.
* Irene Zarra Ferro. (Vicepresidenta). Farmacéutica de Atención Especializada.
Paula Mª López Vázquez, (Secretaria). Médico Especialista en Farmacología Clínica.
Belen Pérez Marcos (Vicesecretaria). Farmacéutica de Atención Especializada
Rosendo Bugarín González. Médico Especialista en Medicina Familiar y Comunitaria.
Juan Casariego Rosón. Médico Especialista en Cardiología.
Nuria Carballeda Feijóo. Miembro lego. Representante de los intereses de los pacientes.
Juana Mª Cruz del Río. Trabajadora Social.
Rafael Álvaro Millán Calenti. Licenciado en Derecho. Asesor jurídico.
Juan Fernando Cueva Bañuelos. Médico Especialista en Oncología Médica.
José Álvaro Fernández Rial. Médico Especialista en Medicina Interna.
José Luis Fernández Trisac. Médico Especialista en Pediatría.
Mª José Ferreira Díaz. Diplomada Universitaria de Enfermería.
Agustín Pía Morandeira. Farmacéutico de Atención Primaria
Jorge Prado Casal. Licenciado en CC. Físicas. Experto en Protección de Datos.
Carmen Rodríguez-Tenreiro Sánchez. Licenciada en Farmacia.
Diego Santos García. Médico Especialista en Neurología.
Juan Vázquez Lago. Médico Especialista en Medicina Preventiva y Salud Pública.
Mª Asunción Verdejo González. Médico Especialista en Farmacología Clínica..

***** La miembro Irene Zarra no estuvo presente ni participó en la evaluación del estudio.

**Anexo II: Centros e investigadores principales participantes en España**

CÓDIGO: ALCOVID-19 NÚMERO EUDRACT: 2020-001760-29
TÍTULO: Ensayo clínico fase III para evaluar la eficacia y seguridad de etanol inhalado en el tratamiento de la COVID-19 en estadio inicial.
PROMOTOR: Sociedad Española de Farmacia Hospitalaria (SEFH)

**FECHA ACTUALIZACIÓN ANEXO II:** 11/06/20

| Centros (Investigador Principal) |
|---|
| C.H. Universitario de Santiago (Anxo Fernández Ferreiro) |
| C.H. de Pontevedra (Carlos Crespo Diz) |

Documento asinado dixitalmente por:
Paula López Vázquez (16/06/2020 13:50)
https://sede.xunta.gal/cve?dcve=SAOC-L4G4-BOAH-OF4O-TJC2-L159-2308-2338-90

Xacobeo 2021

CEIm de Galicia
Edificio Administrativo San Lázaro
15703 SANTIAGO DE COMPOSTELA
Teléfono: 881546425
ceic@sergas.es



USC UNIVERSIDADE DE SANTIAGO DE COMPOSTELA

USC
UNIVERSIDADE
DE SANTIAGO
DE COMPOSTELA

# RESOLUCIÓN DE LA SOLICITUD DE AUTORIZACIÓN DE UN ENSAYO CLÍNICO







DEPARTAMENTO
DE MEDICAMENTOS
DE USO HUMANO
Área de Ensayos Clínicos

**Referencia: MUH/CLIN/EC**

**ASUNTO:** RESOLUCIÓN DE LA SOLICITUD DE AUTORIZACIÓN DE UN ENSAYO CLÍNICO

**DESTINATARIO:** C.R.O. Delos Clinical
Editor José Manuel Lara, 28, 1B
41013 Sevilla (España)

**DATOS DE LA SOLICITUD**

Solicitud de autorizacion del Ensayo clinico Nº EudraCT **2020-001760-29** y título **Ensayo clínico fase II para evaluar la eficacia y seguridad de etanol inhalado en el tratamiento de la COVID-19 en estadio inicial.**.

**Promotor:** Sociedad Española de Farmacia Hospitalaria
Calle Serrano, número 40, planta 2, puerta derecha
28001 Madrid (España)

**Fecha de solicitud válida:** 09/06/2020

Una vez evaluada la solicitud de autorización de ensayo clínico previamente indicada, se considera que cumple con los requisitos indicados en el Real Decreto 1090/2015, de 4 de diciembre, por el que se regulan los ensayos clínicos con medicamentos, los Comités de Ética de la Investigación con medicamentos y el Registro Español de Estudios Clínicos y demás legislación aplicable*.

Por todo lo anteriormente expuesto la Directora de la Agencia de Medicamentos y Productos Sanitarios en el ejercicio de sus competencias **RESUELVE:**

AUTORIZAR el ensayo clínico solicitado y al Servicio de Farmacia Hospitalaria del Complejo Hospitalario Universitario de Pontevedra, que dispone de las condiciones mínimas en cuanto a instalaciones, medios personales y sistema de gestión de la calidad, para cumplir con las Normas de Correcta Fabricación aplicables, para la fabricación de etanol de 65º inhalado y su placebo, como medicamentos en investigación, en el ámbito del ensayo clínico Nº EudraCT 2020-001760-29.

* Texto refundido de la Ley de Garantías y Uso Racional de los medicamentos y productos sanitarios, aprobado por Real Decreto Legislativo 1/2015, de 24 de julio.
Real Decreto 1275/2011, de 16 de septiembre, por el que se crea la Agencia estatal "Agencia Española de Medicamentos y Productos Sanitarios y se aprueba su Estatuto".

**Agencia Española de Medicamentos y Productos Sanitarios (AEMPS)**
**Fecha de la firma: 09/09/2020**
*Puede comprobar la autenticidad del documento en la sede de la AEMPS:https://localizador.aemps.es*
**CSV: N V 2 4 9 2 8 B F 7**





USC UNIVERSIDADE DE SANTIAGO DE COMPOSTELA

COMENTARIOS A LA AUTORIZACIÓN:
En aras de la salud pública es imprescindible trasladar lo más rápidamente posible a la práctica clínica la evidencia científica que generen las investigaciones sobre el COVID-19. Por ello, le rogamos encarecidamente que comunique a la AEMPS los resultados preliminares de este estudio en cuanto estén disponibles, independientemente de su ulterior publicación en revistas científicas.
(*) NOTA DEL CEIm: Deben tomar en consideración la CONDICIÓN que el CEIm impuso en su DICTAMEN del 07/09/2020.

Contra esta Resolución, que pone fin a la vía administrativa, puede interponerse potestativamente Recurso de Reposición ante el/la Director/a de la Agencia Española de Medicamentos y Productos Sanitarios en el plazo de un mes, conforme a lo dispuesto en los artículos 123 y 124 de la Ley 39/2015, de 1 de octubre, del Procedimiento Administrativo Común de las Administraciones Públicas, o interponerse Recurso Contencioso-Administrativo ante el Juzgado Central de lo Contencioso-Administrativo de Madrid, en el plazo de dos meses a contar desde el día siguiente a la recepción de la presente notificación, conforme a lo dispuesto en la Ley Reguladora de la Jurisdicción Contencioso-Administrativa de 13 de julio de 1998, y sin perjuicio de cualquier otro recurso que pudiera interponerse.

DIRECTORA DE LA AGENCIA ESPAÑOLA DE MEDICAMENTOS Y PRODUCTOS SANITARIOS

agencia española de medicamentos y productos sanitarios

Fdo. Mª Jesús Lamas Díaz

This doctoral thesis focuses on offering therapeutic alternatives through pharmaceutical compounding and drug repositioning from the hospital pharmacy to cover therapeutic gaps. An ophthalmic compounded formulation of cysteamine in hyaluronic acid packaged in novel single-dose containers was developed for the treatment of ocular cystinosis. On the other hand, an inhaled compounded formulation of ethanol was developed for the treatment of SARS-CoV-2 infection, and subsequently studied for efficacy and safety in the Phase II clinical trial ALCOVID-19. In both cases, appropriate galenic development and characterisation has been performed in conjunction with preclinical pharmacokinetic studies prior to appropriate translation into clinical practice.